FORMULATION OF

IMMUNOMODULATORY AGENTS

MOHAMMED IQBAL

Doctor of Philosophy

THE UNIVERSITY OF ASTON IN BIRMINGHAM

January 1990

THE UNIVERSITY OF ASTON IN BIRMINGHAM

FORMULATION OF IMMUNOMODULATORY AGENTS

MOHAMMED IQBAL

DOCTOR OF PHILOSOPHY

1989

SUMMARY

Reversed-phase high-performance liquid chromatography procedures were developed for the analysis of pyrimidine-based drugs bropirimine and its derivatives (2-N-acetyl- and 2-N-propanoyl-) and for pyrimethamine and its 2/4- substituted derivatives (2,N- propanoyl and 2,4-N,N-dipropanoyl-) and its 6- substituted (methyl-, ethyl-, propyl- and isopropyl- carboxylates) analogues. Stability studies indicated that these derivatives were not sufficiently labile to act as potential prodrugs. Solubility-pH profiles were constructed from which the dissociation constants were calculated.

The physicochemical properties of these compounds were studied and attempts were made to increase the poor aqueous solubility of bropirimine (~35µg/mL) by prodrug synthesis, solvate formation (acetic acid, N,N-dimethylformamide and N-methylformamide) and the use of co-solvents and additives. The first two methods proved to be fruitless whereas the latter method resulted in an intravenous formulation incorporating 32mg/mL of bropirimine. An *in-vitro* method for the detection of precipitation was developed and the results suggested that by using low injection rates (<0.24mL/min) and high mobile phase flow rates (>500mL/hr) precipitation could be minimised. Differential scanning calorimetry showed that bropirimine debrominates in the presence of a number of additives commonly used in formulation work but the temperature at which this occurred were usually >200°C. *In-vitro* work gave encouraging results for the possibility of rectal delivery of bropirimine but *in-vivo* work on rabbits showed considerable variations in the resulting plasma levels and pharmacokinetic parameters.

KEYWORDS:

Bropirimine
Bropirimine prodrugs
Differential Scanning Calorimetry
High-performance liquid-chromatography
Stability
Suppository

DEDICATION

To my mother and late father . . .

. . . fountains of wisdom and inspiration

ACKNOWLEDGEMENTS

I wish to thank my supervisor and a friend, Dr W.J. Irwin, for his valuable guidance, inspiring comments and constant encouragement throughout the course of this thesis. I owe thanks also to Dr H.O. Alpar for her continued interest, help and support.

I am grateful to Dr R.J. Griffin and Dr G. Baig for all synthetic work, Mel Gamble for help with the *in-vivo* work, and Professor M.F.G Stevens for making available to me the facilities of the Department of Pharmaceutical Sciences. Gratitude is extended to the technical staff and to Sheila and Ian Eden for labouring away in typing this thesis.

I acknowledge and appreciate the generous award of a post-graduate research studentship offered to me by the University of Aston.

Finally, I would like to thank my family for their support, patience and encouragement in very difficult circumstances.

LIST OF CONTENTS

Thesis summary 2

Dedication 3

Acknowledgements 4

List of contents 5

List of tables 11

List of figures 15

1.0 INTRODUCTION 23

1.1 Interferon 23

1.1.1 Interferon nomenclature 23

1.1.2 Interferon assay 25

1.1.3 Units 25

1.1.4 Uses of interferons 26

1.1.5 Routes of administration of interferon 27

1.1.6 Mechanisms of action of interferons 28

1.1.7 Biosynthesis of interferon 30

1.2 Interferon inducers 31

1.2.1 Structure-activity relationships (SAR) of synthetic interferon inducers 31

1.3 The pyrimidinone interferon inducers 33

1.3.1 Interferon response 34

1.3.2 Antiviral activity 38

1.3.3 Antineoplastic activity 38

1.3.4 Immunomodulatory effects 41

1.3.5 Other bioactivities of pyrimidinones 42

1.4 Mechanism of action of interferon inducers 42

1.4.1 Hypo-responsiveness 43

1.4.2 Structure-activity relationships (SAR) of pyrimidinones... 45

1.4.3 Pharmacokinetics of ABPP 46
1.4.4 Clinical studies on ABPP 53
1.4.5 Toxicity of ABPP 56
1.5 Aims of the thesis 56
2.0 HIGH PERFORMANCE LIQUID CHROMATOGRAPHY OF THE IMMUNOMODULATORY AGENTS 58
2.1 Introduction 58
2.2 Instrumentation, materials and methods 61
2.3 Results and discussion 62
2.3.1 HPLC system for bropirimine, AB and PB 62
2.3.2 HPLC system for MPP and DPP 72
2.3.3. HPLC system for Py, MDPC, EDPC,PDPC and iPDPC . 78
2.3.4 Internal standards 83
2.3.5 Construction of calibration curves 84
3.0 KINETICS OF DEGRADATION 89
3.1 Introduction 89
3.2 Materials and methods 91
3.2.1 Chemical degradation of bropirimine prodrugs 91
3.2.2 Degradation of 2/4 substituted pyrimethamine 92
3.2.2.1 Degradation of 2-N-propanoylpyrimethamine (MPP) 92
3.2.2.2 Degradation of 2, 4-N, N-dipropanoyl pyrimethamine (DPP) 93
3.2.3 Degradation of 6-carboxylate ester analogues of pyrimethamine 94
3.3 Results and discussion 96
3.3.1 Degradation of bropirimine derivatives 96
3.3.1.1 Effect of temperature 96
3.3.1.2 Effect of pH on the aqueous degradation of AB .. 99

3.3.2 Degradation of pyrimethamine derivatives 107
3.3.2.1 Degradation of 2/4-N-substituted pyrimethamines 107
3.3.2.2 Degradation of 6-carboxylate ester analogues of pyrimethamine 112
3.3.2.2.1 Effect of temperature on degradation 112
3.3.2.2.2 Effect of pH on the degradation of EDPC 117
4.0 THE USE OF DIFFERENTIAL SCANNING CALORIMETRY IN THE ASSESSMENT OF PHYSICAL INTERACTIONS 120
4.1 Introduction 120
4.1.1 Aims 120
4.2 Experimental 121
4.2.1 Apparatus 121
4.3 Results and discussion 124
4.3.1 The effect of additives on the thermal behaviour of bropirimine and structurally related compounds 124
4.3.2 The use of DSC variable heating rate for solid state stability predictions. 140
4.3.3. The use of DSC in the evaluation of physical changes upon mechanical treatment of compounds 147
5.0 PHYSICO-CHEMICAL PROPERTIES OF THE IMMUNOMODULARATORY AGENTS 165
5.1 Introduction 165
5.2 Materials and methods 165
5.2.1 Solubility determination 165
5.2.1.1 Solubility in Britton-Robinson (B-R) buffers 165
5.2.1.2 Solubility of bropirimine in sodium carbonate 167
5.2.1.3 Solubility of bropirimine in acetic acid 167

5.2.1.4 Solubility of bropirimine in dimethylacetamide (DMA), propylene glycol (PG) and polyethylene glycols (PEGs) 168
5.2.1.5 Solubility of bropirimine in cyclodextrins 168
5.2.1.6 Solubility of bropirimine in N-methyl-D-glucamine (meglumine) 168
5.2.2 Partition coefficent (PC) determination 168
5.2.2.1 Assay of octanol layer 169
5.2.2.2 Assay of aqueous layer 170
5.3 Results and discussion 170
5.3.1 Estimation of dissociation constant (Ka) from solubility data 170
5.3.2 Aqueous solubility 175
5.3.3 Partition coefficient (PC) 182
5.3.4 Solubility of bropirimine in co-solvents and additives 190
5.3.4.1 Solubility in acids and bases 190
5.3.4.2 Solubility in co-solvents 192
5.3.4.3 Solubility of bropirimine in cyclodextrins 201
5.3.4.4 Solubility in meglumine 204
5.3.4.5 Solubility in mixed solvents 206
5.3.4.5.1 Stability of the formulation 206
6.0 DISSOLUTION STUDIES ON BROPIRIMINE 208
6.1 Introduction 208
6.2 Experimental 213
6.2.1 Particle size analysis 213
6.2.2 Measurement of intrinsic dissolution 213
6.2.2.1 Preparation of physical mixes and compressed discs 215
6.2.3 Dissolution of powders 216

6.3 Results and discussion 216
6.3.1 Dissolution of powders 218
6.3.2 Intrinsic dissolution of bropirimine 225
7.0 STUDIES ON PARENTERAL FORMULATION OF BROPIRIMINE 231
7.1 Introduction 231
7.2 Materials and method 233
7.2.1 Preparation of bropirimine injections 234
7.2.2 Calculation of buffering capacity 236
7.2.3 Solubility measurements of bropirimine 237
7.3 Results and discussions 237
8.0 THE SUPPOSITORY AS A DOSAGE FORM FOR BROPIRIMINE 254
8.1 Introduction 254
8.1.1 Rectal Anatomy 255
8.1.2 Factors affecting rectal absorption 255
8.1.3 Aim 257
8.2 Materials and methods 257
8.2.1 Preparation of suppositories 258
8.2.2 In-vitro dissolution testing of suppositories 259
8.2.3 In-vivo Testing of bropirimine suppositories 261
8.3 Results and discussion 262
8.3.1 In-vitro dissolution testing of bropirimine suppositories... 263
8.3.1.1 Effect of suppository base on the release of bropirimine 263
8.3.1.2 The effect of stirring speed on the release of bropirimine 266
8.3.1.3 The effect of surfactants on the release of bropirimine 266
8.3.1.4 Effect of pH of the dissolution media on the release of bropirimine 270

8.3.1.5 Effect of meglumine on the release of bropirimine 271

8.3.2 In-Vivo testing of bropirimine suppositories. 275

9.0 CONCLUSION 280

Appendices..... 283

References 290

LIST OF TABLES

1.1	Properties of type I and type II interferons	24
1.2	Nomenclature of human interferons	24
1.3	Some properties of marketed interferons	26
1.4	Immunological actions of interferon	30
1.5	Classification of interferon inducer	32
1.6	Murine serum interferon levels in mice receiving a single dose of ABPP	37
1.7	Serum interferon response induced by ABPP in various animal species	37
1.8	Spectrum of *in-vivo* antiviral activity of ABPP in various animal models	39
1.9	Summary of immune modulating activities of ABPP	41
1.10	Other bioactivities of the pyrimidinones	42
2.1	Bropirimine and its derivatives	59
2.2	Pyrimethamine and its 2/4 substituted derivatives	59
2.3	Pyrimethamine and its 6-substituted derivatives	60
2.4	Working wavelengths and molar extinction coefficients of bropirimine and its prodrugs and pyrimethamine and its prodrugs	68
2.5	Effect of acetonitrile in the mobile phase on the HPLC parameters of bropirimine, AB and PB	69
2.6	Effect of diethylamine concentration in the mobile phase on the HPLC parameters of MPP and DPP	69
2.7	Effect of acetonitrile concentration in the mobile phase on the HPLC parameters of MPP and DPP (with 0.1%v/v diethylamine in the mobile phase and adjusted to pH 2.0)	76

2.8 Effect of diethylamine concentration in the mobile phase on the HPLC parameters of MPP and DPP (mobile phase consisted of 55%v/v acetonitrile and adjusted to pH 2.0)..... 76

2.9 Effect of acetonitrile concentration on the HPLC parameters of Py, MDPC, EDPC, PDPC and iPDPC (0.1%v/v diethylamine added to the mobile phase and pH adjusted to 2.0)..... 82

2.10 Effect of diethylamine concentration on the HPLC parameters of Py, MDPC, EDPC, PDPC and iPDPC (40%v/v acetonitrile added to the mobile phase and pH adjusted to 2.0)..... 82

2.11 HPLC parameters of some compounds suitable as internal standards..... 83

2.12 Statistical parameters for the calibration graphs of the three compounds..... 85

3.1 First order rate constants for the degradation of acetyl- and propanoylbropirimine at different temperatures..... 98

3.2 Half-lives of acetylbropirimine and propanoyl bropirimine at various temperatures in Britton-Robinson buffer pH10.0..... 101

3.3 Half-lives of acetylbropirimine and propanoyl bropirimine at various pHs in aqueoues solutions at 60°C..... 106

3.4 Half-lives for DPP at different temperatures (a) and pH values (b)..... 110

3.5 A list of various Arrhenius parameters for MDPC, EDPC, PDPC and iPDPC..... 117

4.1 DSC onset transitions of 5-halogenouracils alone and in 1:1 admixture with PEG 20M..... 136

4.2 DSC onset transitions of bropirimine on 1:1 admixture with various excipients..... 137

4.3 Kinetic parameters of bropirimine on admixture with various excipients..... 141

4.4 Models used for solid state decomposition [adapted from ref 850] 154

4.5 Rate constants and correlation coefficients for the degradation of MPAA under various conditions 155

4.6 Rate constants and correlation coefficients for the degradation of MPAA on admixture with lactose 164

5.1 Composition of standard solutions and the internal standards and mobile phases used in solubility studies 167

5.2 List of pK_a values and aqueous solubilities of the immunomodulatory agents 174

5.3 Estimation of solubilities of the immunomodulatory agents in blood (brackets indicate percent ionised) 182

5.4 A list of P_u, P_i and correlation coefficients for bropirimine, AP and PB calculated from equation 5.8 186

5.5 Estimation of amounts of bropirimine and its derivatives (AB, PB) and pyrimethamine and its derivatives (MPP, DPP, EDPC, PDPC and iPDPC) absorbed from the stomach using equations 5.9 and 5.10 189

5.6 Comparison of pKa values obtained by either using solubility data or by partition data for bropirimine, AB and PB 190

5.7 Solubilising power, S, of some co-solvents 200

5.8 Some physico-chemical properties of α-, β-, γ- and hydroxypropyl β-cyclodextrin 203

5.9 Solubility of bropirimine in various solubilising systems 207

6.1 A list of cube-root dissolution-rate constants for three fractions of bropirimine powder 221

6.2 A list of cube-root dissolution-rate constants for bropirimine and acetic acid, N-methylformamide and N,N-dimethylformamide solvates of bropirimine 223

6.3 Intrinsic dissolution rates for bropirimine and admixtures with PEG 20M..... 225

6.4 Intrinsic dissolution rates for bropirimine/PVP 44M from compressed discs..... 227

7.1 Buffering capacities of Tris buffer..... 239

8.1 Factors influencing drug availability from suppositories 257

8.2 Pharmacokinetic parameters of rabbits 1, 2, 3 and 4 using 90 mg/kg bropirimine and PEG 1M:4M as the suppository base..... 277

8.3 Pharmacokinetic parameters of rabbits 1, 2, 3 and 4 using 90 mg/kg bropirimine and Suppocire L as the suppository base..... 278

8.4 Pharmacokinetic parameters of rabbits 1, 2, 3 and 4 using 90 mg/kg bropirimine and Witespol H15 as the suppository base..... 279

LIST OF FIGURES

1.1 A view of the antiviral action of interferon 29

1.2 Maximum interferon levels induced by increasing concentration of ABMP, ABPP and AIPP injected (a) sc (b) ip (c) po 35

1.3 *In-vitro* system to determine the ability of compounds to induce interferon or antiviral resistance in human cells as a predictive tool for future evaluations in humans 36

1.4 Relationship between the dose of ABPP and the serum levels of drug at 2 hours post-treatment when ABPP was given ip or po at 25-1000mg/kg to mice 47

1.5 Serum interferon response of mice following (a) sc, (b) ip or (c) po administration of 1000mg/kg ABMP, ABPP or AIPP 48

1.6 Murine serum interferon response to ABMP, ABPP and AIPP administered (a) po, (b) ip or (c) sc 50

1.7 Comparison of the serum levels of ABPP and interferon induced by the drug in cats dosed once with 25mg/kg at 0 hr or 5 times (0, 2, 4, 6, 8 hr) with 10mg/kg 51

1.8 Comparison of the serum levels of ABPP and the interferon titres induced in cats by the drug (25mg/kg) given in gelatin capsules or as suspension in an aqueous vehicle 52

1.9 Bovine interferon response to ABPP 54

1.10 ABPP rabbit pharmacokinetics from a 25mg/kg iv bolus injection..... 55

2.1 Ultraviolet spectra of bropirimine (a), AB (b) and PB (c) 63

2.2 Ultraviolet spectra of pyrimethamine (1), MPP (2) and DPP (3) 64

2.3 Ultraviolet spectra of MDPC (4), EDPC (5), PDPC (6) and iPDPC (7)... 65

2.4 The effect of acetonitrile concentration on the retention times of bropirimine, AB and PB 66

2.5 The effect of diethylamine concentration on the retention times of bropirimine, AB and PB (30%v/v acetonitrile) 66

2.6 Chromatograms to show the effect of diethylamine on the separation of bropirimine (1), AB (2) and PB (3) 70

2.7 The effect of pH of the mobile phase on the retention times of bropirimine, AB and PB 71

2.8 The effect of acetonitrile concentration on the retention times of MPP and DPP (0.1%v/v diethylamine) 74

2.9 The effect of diethylamine concentration on the retention times of bropirimine, AB and PB (55%v/v acetonitrile) 74

2.10 Chromatograms to show the effect of diethylamine on the separation of MPP (1) and DPP (2) 75

2.11 The effect of pH of the mobile phase on the retention times of MPP and DPP 77

2.12 The effect of acetonitrile concentration on the retention times of Py, MDPC, PDPC and iPDPC (0.1%v/v diethylamine) 79

2.13 The effect of diethylamine concentration on the retention times of Py, MDPC, PDPC and iPDPC (40%v/v acetonitrile) 79

2.14 HPLC chromatograms to show the effect of diethylamine on the separation of Py (1), MDPC (2) EDPC (3), PDPC (4) and iPDPC (5) 80

2.15 The effect of pH of the mobile phase on the retention times of Py, MDPC, PDPC and iPDPC 81

2.16 Calibration curves for bropirimine, AB and PB 86

2.17 Calibration curves for MDPC, PDPC and iPDPC 87

2.18 Calibration curves for Py, MPP and DPP 88

3.1 Temperature dependent hydrolysis of acetylbropirimine in Britton-Robinson buffer pH 10.0 97

3.2 Temperature dependent hydrolysis of propanoylbropirimine in Britton-Robinson buffer pH 10.0 97
3.3 Arrhenius plots for acetyl- and propanoylbropirimine at pH 10.0..... 100
3.4 The effect of pH on first-order degradation of acetylbropirimine at 60°C.. 102
3.5 Rate constant-pH profile of acetylbropirimine at 60°C (μ=0.5) in aqueous buffered solutions..... 104
3.6 Hydrolysis of monopropanoylpyrimethamine at 60°C and pH 2.0 in aqueous buffered solution (μ=0.5)..... 108
3.7 Temperature-dependent hydrolysis of dipropanoylpyrimethamine (DPP) in aqueous buffered solution pH 11.2 108
3.8 Arrhenius plot for dipropanoylpyrimethamine in aqueous buffer pH 11.2
3.9 The effect of pH on the first-order degradation of dipropanoylpyrimethamine (DPP) at 60°C 109
3.10 Rate constant-pH profile of dipropanoylpyrimethamine at 60°C in aqueous buffered solutions 111
3.11 Degradation of dipropanoylpyrimethamine (DPP) in aqueous buffer pH 2.62 at 50°C and the formation of monopropanoylpyrimethamine (MPP) and pyrimethamine (Py) 111
3.12 HPLC chromatograms to show the degradation of 2.4-N,N-dipropanoyl pyrimethamine 113
3.13 Temperature-dependent hydrolysis of MDPC in aqueous buffered solution pH 11.2 114
3.14 Temperature-dependent hydrolysis of EDPC in aqueous buffered solution pH 11.2 114
3.15 Temperature-dependent hydrolysis of PDPC in aqueous buffered solution pH 11.2 115
3.16 Temperature-dependent hydrolysis of iPDPC in aqueous buffered solution pH 11.2 115
3.17 Arrhenius plots for MDPC, EDPC, PDPC and iPDPC..... 116

3.18 pH-dependent hydrolysis of EDPC in aqueous buffers at 60°C 118

3.19 Rate constant-pH profile of EDPC in aqueous buffered solution at 60°C.. 118

4.1 Thermograms from differential scanning calorimetry of PEG 20M, bropirimine and a 4:1 physical mixture 125

4.2 DSC trace of the co-crystallised mixture 2-amino-5-(4-chlorophenyl)-6-ethyl pyrimidine-4(3H)-one and the corresponding 4-amino-2-one, both alone and crystallised and also the dimer in admixture with PEG 20M 128

4.3 DSC thermograms of N-acetyl, N-propanoyl and N-chloroacetyl derivatives of bropirimine alone and in admixture with PEG 20M 130

4.4 DSC thermograms of 5-bromo-1-methyluracil; 5-bromocytosine and 5-iodocytosine 131

4.5 HPLC traces showing:

(A) 2-amino-6-phenylpyrimidin-4(3H)-one(a)

(B) Bropirimine (b)

(C) a mixture of each obtained from partial thermal degradation of 5mg bropirimine-PEG 20M mixture (10:1) at 210°C for 5 minutes and dissolved in methanol

(D) a standard mixture of each component in (1) 20%v/v methanol in the mobile phase and (2) 20%v/v acetonitrile in the mobile phase 133

4.6 DSC thermograms of 2-amino-4(N-hydroxy ethyl) amino-5-bromo-6-phenylpyrimidine, an analogue of bropirimine, alone and upon admixture with PEG 20M, showing the independence of the degradation exotherm at 267-268°C once melting has been effected 139

4.7 Plots of ln (β/T^2) against 1/T for various admixtures of bropirimine with additives 142

4.8 Degradation of bropirimine at various temperatures using the isothermal method 144

4.9 Plots of ln k against 1/T for an admixture of 10% PEG bropirimine using the variable heating rate (VHR) and isothermal method (IM) 146

4.10 DSC thermograms of acetic acid solvate of bropirimine ground for 1. 0 mins, 2. 1 min, 3. 3 min, 4. 4 min and 5. 5 min 149

4.11 DSC thermograms of 4-Methoxyphenyl aminoacetate hydrochloride (MPAA) 150

4.12 DSC thermograms of 1:1 admixtures of 4-Methoxyphenyl aminoacetate hydrochloride (MPAA) and acetic acid solvate of bropirimine 150

4.13 HPLC traces showing:

A. 4-hydroxyanisole (a)

B. 4-Methoxyphenyl aminoacetate hydrochloride (MPAA) (b)

C. a mixture of each obtained from partial degradation by grinding with acetic acid solvate of bropirimine (1:1)

D. standard mixture of each component 152

4.14 Photomicrograph of 4-Methoxyphenyl aminoacetate hydrochloride (MPAA) 153

4.15 Decomposition of MPAA alone and with admixtures of acetic acid solvate of bropirimine 156

4.16 DSC thermograms of

1. α-lactose monohydrate

2. Ground for 2 mins

3. Ground for 5 mins

4. Ground for 10 mins 158

4.17 DSC thermograms of 4-Methoxyphenyl aminoacetate hydrochloride (MPAA) and lactose monohydrate admixtures (1:4) 160

4.18 Plots to illlustrate the disappearance of MPAA and the appearance of 4-hydroxyanisole (OHA). Both MPAA and lactose ground together for 10 min 162

4.19 Degradation of MPAA on admixture with lactose 163

5.1 A plot of S against $[H_3O^+]$ for bropirimine to show the validity of equation 5.1 172

5.2 A plot of S against $\frac{1}{[H_3O^+]}$ for bropirimine to show the validity of equation 5.2 172
5.3 Solubility-pH profile of bropirimine 176
5.4 Solubility-pH profile of acetylbropirimine 176
5.5 Solubility-pH profile of propanoylbropirimine 177
5.6 Solubility-pH profile of monopropanoyl pyrimethamine (MPP) 178
5.7 Solubility-pH profile of DPP 178
5.8 Solubility -pH profile of MDPC 180
5.9 Solubility-pH profile of EDPC 180
5.10 Solubility-pH profile of PDPC 181
5.11 Solubility-pH profile of iPDPC 181
5.12 Apparent partition coefficient-pH profiles for bropirimine, AB and PB.... 185
5.13 A plot of degree of ionisation, α, against pH for bropirimine, AB and PB 185
5.14 The linear relationship of equation 5.8 for the partition of bropirimine in octanol/buffer at different pH values 187
5.15 The linear relationship of equation 5.12 for bropirimine 191
5.16 Solubility of bropirimine in sodium carbonate 193
5.17 Solubility of bropirimine in acetic acid at 6°C and 60°C 193
5.18 Solubility of bropirimine in dimethyl-acetamide 196
5.19 Solubility of dimethylacetamide in accordance with equation 5.18 196
5.20 Solubility of bropirimine in polyethylene glycols 197
5.21 Solubility of bropirimine in polyethylene glycols in accordance with equation 5.18 197
5.22 Solubility of bropirimine in propylene glycol 199
5.23 Solubility of some sedative hypnotics/antiepileptics in propylene glycol-water mixtures 199
5.24 Solubility of bropirimine in α-, β- and γ- cyclodextrins 202
5.25 Solubility of bropirimine in hydroxypropyl β-cyclodextrin 205

5.26 Solubility of bropirimine in meglumine .....

6.1 Diagramatic representation of the diffusion layer model .....

6.2 Block diagram of dissolution equipment .....

6.3 Particle size distribution of bropirimine powder .....

6.4 Cumulative undersize distribution curve for bropirimine .....

6.5 Log-normal plot for bropirimine .....

6.6 Dissolution profiles of bropirimine in Britton-Robinson buffer at pH 2.0 at 37°C .....

6.7 Dissolution of bropirimine powder in accordance with equation 6.10 ....

6.8 Dissolution profiles of bropirimine and acetic acid (AcOH), N-methylformamide (NMF), N,N-dimethylformamide (DMF) solvates of bropirimine in Britton-Robinson buffer at pH 7.4 .....

6.9 Data from Fig 6.8 plotted in accordance with equation 6.10 .....

6.10 A log-log plot for three sieve fractions of bropirimine .....

6.11 Intrinsic dissolution of bropirimine from compressed discs containing PEG .....

6.12 Intrinsic dissolution of bropirimine from compressed discs containing PVP .....

6.13 Appearance of a disc containing 60:40 mixture of bropirimine/PEG 20M (a). before and (b). after dissolution .....

7.1 The *in-vitro* set up for the detection of precipitation on injection .....

7.2 The effect of wavelength on the noise level of the vehicle.....

7.3 The effect of injection rate on precipitation .....

7.4

7.5 The effect of flow rate on precipitation .....

7.6 The effect of infusion rate on precipitation .....

7.7 The effect of infusion rate on precipitation .....

7.8 Effect of bropirimine concentration on precipitation.....

7.9 Effect of tube length (x) on precipitation 246
7.10 The effect of DMA composition and pH on the solubility of bropirimine 247
7.11 Effect of formulation pH (vehicle A) on the solubility of bropirimine at two temperatures 248
7.12 Effect of formulation pH (vehicle A) on the solubility of bropirimine at different temperatures 248
7.13 The effect of phenytoin and diazepam injections on precipitation..... 250
7.14 The effect of injection rate on the pH change of Tris double strength buffer by several formulations 252
8.1 Detailed diagram of the venous drainage of the human rectum 256
8.2 Processes involved in the release from fatty suspension suppositories ... 264
8.3 Release of bropirimine from different suppository bases in distilled water at 37°C 267
8.4 The effect of stirring speed on the release of bropirimine in distilled water at 37°C using Witepsol H15 as the base 268
8.5 A plot to show the linear relationship between the release rate and the stirring speed 269
8.6 A plot of total amount of bropirimine released after 50 minutes against stirring speed 269
8.7 The effect of surfactants on the release of bropirimine in distilled water at 37°C (50 rpm) 272
8.8 The effect of pH on the release of bropirimine in Britton-Robinson buffers at 37°C (50 rpm) 273
8.9 The effect of meglumine in the suppository on the release of bropirimine in distilled water at 37°C (50 rpm) 274
8.10 A plot release rate against concentration of meglumine in the suppository 276

1.0 INTRODUCTION

1.1 Interferon

In 1957, while attempting to show that nucleic acid escaped from the virus and entered the host cell, Isaac and Lindenmann[1] unexpectedly discovered that the treated host cells were producing a virus-inhibiting substance which they called 'interferon'. This has since been shown to be glycoprotein in nature, containing the oligosaccharide sequence sialic acid-galactose, which is broken down by proteolytic enzymes such as trypsin[2]. Mogensen and Cantell[3] demonstrated that at least one disulphide bond is important for biological activity. The activity was lost following reduction by mercaptoethanol but completely recovered when the molecule was treated with either guanidine hydrochloride or urea and allowed to oxidise in air. Shortly after the discovery, Tyrrell[4] introduced the concept of species specifity when he showed that interferon prepared in chicken had no detectable antiviral activity on infected calf cells.

1.1.1 Interferon nomenclature

Younger *et.al.* [5], working on mice, broadly categorised interferons into two types; type I (or 'classical') interferons and type II (or 'immune') interferons. They differ in a number of ways as shown in table 1.1.

In order to standardise nomenclature, human interferons have been re-named according to their source. They are listed in table 1.2 along with the trivial names and sources.

Type I	Type II
Induced in a variety of cells including lymphocytes	Only produced by lymphocytes (T or B)
Stable at pH 2	Unstable at pH 2
Unstable at 56°C †	Stable at 56°C †
Active in guinea pig kidney cells ††	Inactive in primary guinea pig kidney cells ††
Neutralised by type I interferon antibodies	Not neutralised by antibodies raised against type I interferon

† This criterion cannot be extrapolated to human interferon
†† May be interpreted to mean that type II interferon is more species specific in its antiviral activity than type I interferon

Table 1.1: Properties of type I and type II interferons

Designation	Previous Designation	Source
Interferon – α	Leucocyte (Le)	Human peripheral blood leucocytes
	Type I, pH 2 stable	Lymphoblastoid cells
Interferon – β	Fibroplast (F) Type I pH stable	Human fibroblasts
Interferon – γ	Immune Type II pH stable antigen or mitogen induced	Human peripheral blood leucocytes

Table 1.2: Nomenclature of human interferons

1.1.2 Interferon assay

Interferon estimation is by biological assay whereby the ability of the interferon to inhibit virus replication is detected. Although there are several methods[6], the most commonly used is the plaque reduction assay. Monolayers of cells are treated with a range of dilutions of the interferon preparation and are incubated at 37°C for approximately 12 hours. The interferon is then removed and about 50-80 plaque-forming units of the sensitive virus are inoculated onto each dish. After a period of absorption of the virus, the monolayers are overlaid with nutrient agar and incubated until plaques begin to appear. The titre of the interferon is usually taken as the reciprocal of the dilution which decreases the number of plaques per dish by 50%. Other methods that have been used include yield-reduction assay, cytopathic affect, inhibition assay, radiochemicial assays and non-viral assays[6].

1.1.3 Units

Because of the species specificities inherent in interferons, there is no way of inter-relating units of different interferons. However, the term unit can be used in one of two ways in relation to interferon assay[87]. Firstly, the end point is obtained at a certain dilution of the interferon for a given assay method and the reciprocal of this gives the potency of that prepartion in arbitrary end point 'units'. The second way is where a unit is the amount of biological activity in a designated amount of reference preparation. For example, in order to assess the murine serum interferon levels, the workers used the murine leukocyte international interferon standard G-002-902-026 having a titre of 6800 units/mL.

1.1.4 Uses of interferons

Since its discovery in 1957, the number of papers published on interferon have increased dramatically. Most of the tumour systems has been studied with respect to interferon as well as a great number of common viruses. However, it was not until 1986 that the first of the interferons was marketed under the trade name of 'Wellferon' (Wellcome Foundation Ltd). This was followed by two other interferons; Roche's 'Roferon-A' and Kirby-Warwick's 'Intron-A'. All three are the α-type or type I interferons[7]. Table 1.3 gives some of their properties.

Trade Name	Manufacturer	Method of production	Uses
Wellfron	Wellcome	Produced by human lymphoblastoid cells after viral stimulation	- Hairy cell leukaemia
Roferon-A	Roche	Genetically engineered	- AIDS† related Kaposi's sarcoma
Intron-A	Kirby-Warwick	Genetically engineered	- Hairy cell leukaemia - Chronic myelogeneou leukaemia - Genital warts

† Acquired Immune Deficiency Syndrome

Table 1.3 Some properties of the marketed interferons

The most serious consequence of administering exogeneous protein is the production of antibodies against the protein rendering the treatment ineffective. In a recent study it was found that the incidence of antibody formation with 'Roferon-A' was more than 25%[10]. The incidence of antibody formation with 'Welferon' and 'Intron-A' appears

to be much less[11]. The differences in the antigenic responses may be a reflection of the manufacturing processes involved and hence the purity of the final product.

Interferon has also been used in other conditions of supposed or proven viral aetiology without much success, e.g. arthritis[8] and severe psychiatric disease[9]. However, these studies are all difficult to interpret because of the relatively small dosages that were administered and the small number of patients involved.

1.1.5 Routes of administration of interferon

Cantell and Pyhala used human leucocyte interferon ($3x10^6$ units) and administered it to rabbits via the oral (p.o.), intravenous (i.v.), intramuscular (i.m.) and subcutaneous (s.c.) routes[88].

Intravenous administration resulted in high inital clearance ($t_{1/2}$ = 13 mins) but the clearance rate was greatly reduced after 1 hour ($t_{1/2}$ = 73 mins), followed by complete removal of interferon from the circulation in 6 hours. I.m. injection maintained a relatively stable interferon level (200 units/mL) in the serum for up to 12 hours. S.c. administration resulted in similar levels but the effect was further prolonged (approx. 20 hours) indicating possible depot effect via these two routes. In both instances, higher doses raised the serum levels and prolonged the persistance of the circulating interferon.

The serum interferon levels appear to be a reflection of the relative bioavailabilities from each of the routes, with the i.v. route having 100% bioavailability and giving high serum levels in contrast to no absorption from the p.o., rectal or intradermal routes[12].

The high molecular weight of the interferon, like any other protein, may be a contributing factor with regards to the poor bioavailability. Molecular weights in the 20,000 to 30,000 range are

common although values as high as 160,000 have also been reported[89]. However, there is evidence to suggest that the larger molecules are made up of smaller sub-units such as the sub-units of human interferon having molecular weights of 12,000 and 24,000[90].

Clearance of interferons from the circulation involves either renal clearance (2-20%) or by the removal of the carbohydrate moeity and subsequent sequestration by the liver[6].

1.1.6 Mechanisms of action of interferons

Three decades after its discovery, the mechanism of action of interferon is still not well understood. However, the possible mechanisms may be considered in two categories. These are (a) direct action on cells and (b) immunological action. Both of these may be involved to affect antiviral or antitumour activity.

(a) Direct Action. There is divided opinion as to how the interferons act on the offending cells[6]. It is fairly well understood that a number of changes take place within the cell as a result of interferon. However, this could be as a result of a single unifying mechanism (translation inhibition) or as a result of multiple mechanisms of interferon action but no coherent theory to prove all these actions as yet exists. All of these mechanisms have been comprehensively reviewed[6] and are shown schematically in Fig. 1.1. It can be seen that not only is translation inhibited but virus attachment, penetration, uncoating, transcription and maturation and release are also affected.

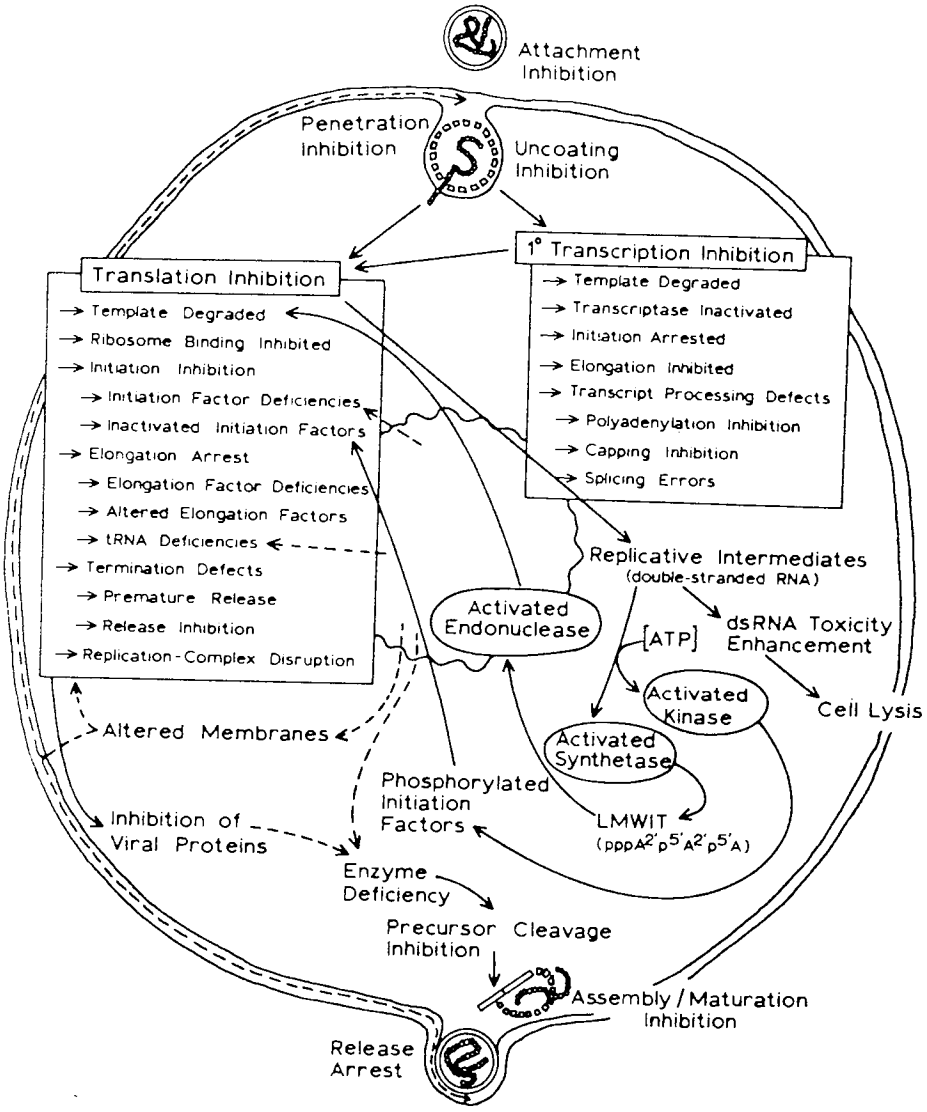

Fig. 1.1: A view of the antiviral action of interferon (reproduced from ref 6.)

(b) Immunological Actions. Interferon has an effect on several immunological mechanisms through which it exerts an action. These are summarized in Table 1.4 below.

Action	Reference
Enhanced cytotoxicity of T-lymphocyctes	15 , 16
Enhanced cytotoxicity of NK cells	17 , 18
Antibody formation	19
Increased phagocytic potential of macrophages	20
Increased production of lysosomal enzymes by macrophages	21

Table 1.4 Immunological actions of interferon

1.1.7 Biosynthesis of interferon

It has been shown that interferon is commonly made at the site of maximum multiplication of the invading cells[91] and that the cells of the reticuloendothelial system are involved[92]. RNA synthesis and in particular messenger RNA is required for the interferon protein[93]. Subsequent work by Tan *et. al.* [94] revealed that human chromosomes 2 and 5 are required for interferon production.

Induction may involve a combination between a specific cellular receptor site and the inducer with the induction extent being proportional to the amount of this complex formed[95]. Detailed account of interferon biosynthesis is available[6].

1.2 Interferon inducers

Since the discovery of interferon[1], interest has shifted towards substances that would stimulate the body to produce its own interferon. Although viruses were implicated in the original discovery, it soon became apparent that these organisms were not the sole inducers of interferon. Non-viral micro-organisms[22], bacterial endotoxins[23], synthetic anionic polymers[24], mitogen[25], specific antigens[26] and low molecular weight compounds such as tilorone[27,28] have all shown to induce interferon production. However, probably the most important discovery was made when Lampson *et.al.*[29] demonstrated that the active component of helenine, a substance extracted from *Penicillin funiculosum*, which was known to induce interferon synthesis, was a double stranded (ds) ribonucleic acid (RNA) species. It was further demonstrated that ds-RNA, whether of viral origin or synthetic, were not only very effective interferon inducers but also induced interferon in most cell types[30-32].

As with the interferons, interferon inducers may also be classified into Type I and Type II[5]. Type I is split into four sub-types depending on the origin of the inducer. The low molecular weight synthetic interferon inducers fall into the sub-type IV of the Type I interferon inducers (Table 1.5).

1.2.1 Structure-activity relationships (SAR) of synthetic interferon inducers

Interferon inducers have enjoyed much publicity since the discovery of interferon. In particular, interest has shifted towards synthetic interferon inducers. Despite the discovery of a large number of agents, no structural relationship appears to exist between the type of molecule and its ability to induce interferon[33,34]. However, structural modifications to a particular molecule may lead to some structure-activity relationship within the series[34]. For example, in a study using the polyribonucleotide duplex polyinosinic acid•polycitidylic acid

Type I interferon inducers

I Microorganisms
Viruses (including animal, bacterial, fungal, mycoplasmatal, insect and plant viruses)
Chlamydiae (Trachoma, Psittacosis)
Rickettsiae (e.g. *Coxiella burneti*)
Mycoplasmas
Bacteria (e.g. *Brucella abortus*)
Protozoa (e.g. *Toxoplasma gondii*)

II Microbial components
Double-stranded RNA (from viruses, e.g. reovirus, or virus-infected cells, e.g. mouse L-cells infected with mengovirus)
Surface glycoproteins (from enveloped viruses, e.g. hemagglutinin from Sendai virus)
Endotoxin, lipopolysaccharide (from bacteria, e.g. *Escherichia coli*, *Brucella abortus*)
Glutarimide antibiotics, e.g. cycloheximide, 9-methylstreptimidone (from Streptomyces)

III Synthetic high molecular weight compounds (polyanions)
Polycarboxylates, e.g. pyran (maleic anhydride divinyl ether) copolymer
Polysulphates (polyvinylsulphate)
Polyphosphates (dextran phosphate)
Polynucleotides:homopolyribonucleotide duplexes, e.g. (I)n.(C)n:polyinosinic acid.polycytidylic acid

IV Synthetic low molecular weight compounds
Flourene and fluorenone derivatives, e.g. tilorene
Anthraquinone derivatives
Pyrazolo (3,4-b)quinoline derivatives
Acridine derivatives
Propanediamine derivatives
Pyrimidine derivatives

Type II interferon inducers
T or B lymphocyte-stimulating agents
Mitogens (phytohemagglutinin, concavalin A, pokeweed mitogen)
Mixed lymphocyte cultures
Antilymphocyte antibody
Specific antigens, e.g. tuberculin (or PDD, purified protein derivative), Staphylococcal anterotoxin A, Streptolysin-O, tetanus toxoid, diphtheria toxoid

Table 1.5 Classification of interferon inducers[5]

$[(I)_n.(C)_n]$, a molecular weight of $1.5x10^5$ was found to be inactive, whereas the compound with a molecular weight of $2.7x10^5$ or higher was found to be active[96]. Structure-activity relationships specifically for the pyrimidinones are discussed in section 1.4.2.

1.3 The pyrimidinone interferon inducers

In 1976, one compound in a series of pyrimidine derivatives, 2-amino-5-bromo-6-methyl-4(3H)-pyrimidinone (ABMP,I), was found to stimulate the endogenous production of interferon and protected mice against lethal virus infections in rodents[36,37]. However, further investigation revealed that ABMP caused a dose-related crystal formation in the renal pelvis and urinary bladder, possibly due to the low solubility of the compound[38]. ABMP analogues were synthesised in the hope of eliminating renal toxicity yet having comparable or even increased interferon induction or anti-viral activity. Two such compounds were 2-amino-5-iodo-6-phenyl-4(3H)-pyrimidinone (AIPP,II) and 2-amino-5-bromo-6-phenyl-4(3H)-pyrimidinone (ABPP,III, bropirimine).

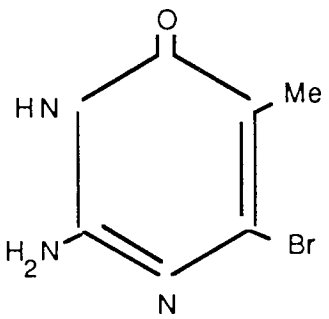

(I)

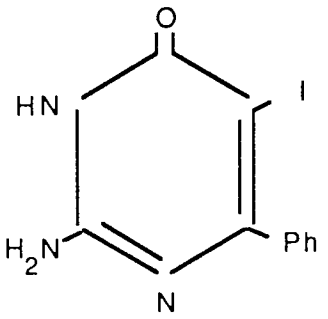

(II)

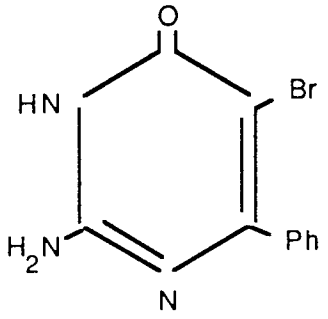

(III)

These were found to have reduced incidence of crystal formation compared to ABMP[38], improved interferon induction in a variety of animals[39] and were effective antiviral agents.

1.3.1 Interferon response

Fig 1.2 shows a dose-related response to ABMP, ABPP and AIPP in mice[39]. It can be seen that at lower doses ABPP is much more potent interferon inducer than either ABMP or AIPP. For example, ABPP was found to be 10 times more potent than either ABMP or AIPP at 50 mg/kg via the intraperitoneal (i.p.) route . Above this dose the interferon levels exhibited were relatively linear. Poor responses were obtained when the drugs were administered either subcutaneously (s.c.) or orally (p.o.) particularly at low doses (Table 1.6). The differences in the responses via the various routes employed are most likely to be due to the poor bioavailablities exhibited from the s.c. and p.o. routes[44].

The spectrum of species which respond to ABPP was expanded to cats, cattle, dogs and monkeys[39,41-44]. All demonstrated the ability to produce interferon when ABPP was administered either i.p., s.c. or p.o. routes in the dose range 1-500 mg/kg body weight (Table 1.7). A rank order can thus be obtained for the greatest sensitivity for interferon induction by ABPP in the order mice>cats>dogs>cattle>rabbits. Similar rank orders were observed with other pyrimidinones (ABMP and AIPP) although the levels of interferon induced were not as high as bropirimine and the animal species were restricted to mice, cats and cattle[39].

An *in-vitro* model was developed by Stringfellow[34] to determine whether ABPP was active in human tissues (Fig 1.3). Human tonsillar tissue was co-cultivated with confluent mono-layers of human amnion cells. After incubation with the drug, this system was challenged with Vesicular Stomatitis Virus (V.S.V.). Concentrations as low as 10μg/ml protected human amnion cells against virus infection whereas a higher concentration of 100 μg/ml induced 90 units/mL of interferon. This system may also be used to determine anti-viral resistance.

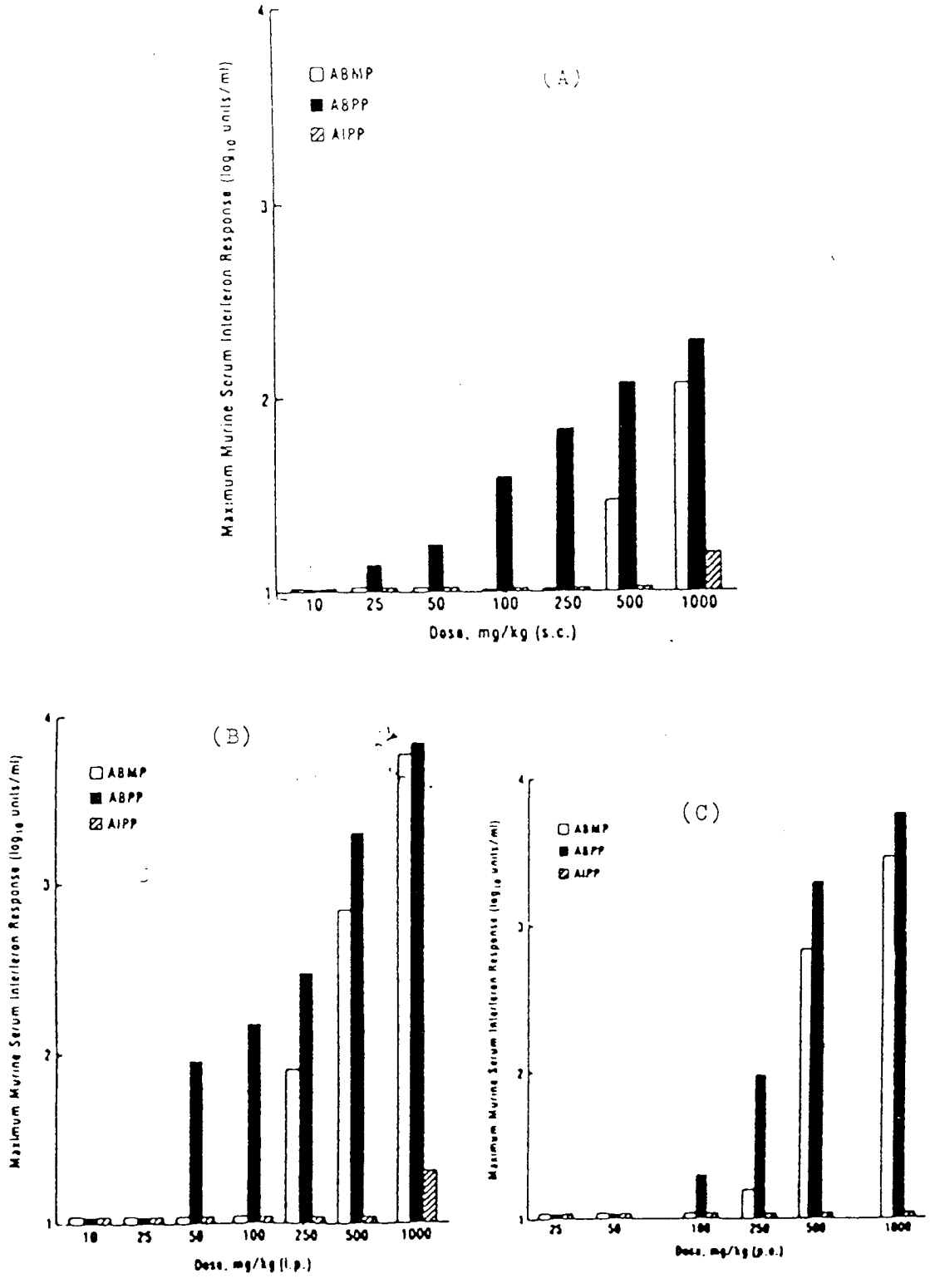

Fig. 1.2: Maximum interferon levels induced by increasing concentration of ABMP, ABPP and AIPP injected (a) sc (b) ip (c) po[39]

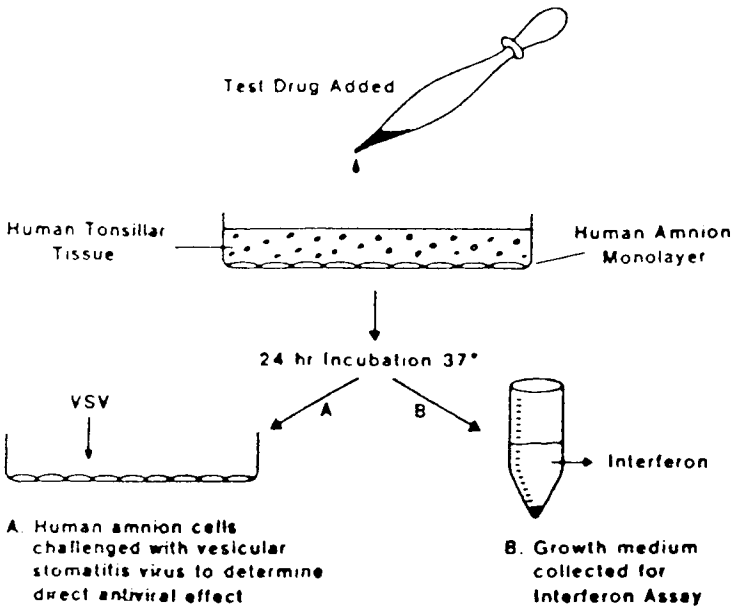

Fig. 1.3: In-vitro *system to determine the ability of compounds to induce interferon or antiviral resistance in human cells as a predictive tool for future evaluations in humans*[34]

Dose of ABPP (mg/kg)	Interferon (Units/mL of serum)		
	i.p.	p.o.	s.c.
500	5,000	400	650
250	3,500	4,000	380
100	980	1,100	100
50	230	60	<10

Table 1.6: Murine serum interferon levels in mice receiving a single dose of ABPP (39)

Animal species	Maximum serum response	
	p.o.	s.c.
Monkey	500	ND
Feline	12 000	1 300
Canine	450	ND
Bovine	3 200	450
Murine	6 300	200

ND = Not done

Table 1.7: Serum interferon response induced by ABPP in various animal species (39,41-44)

To document which organs were responsible for producing interferon in response to ABPP in mice, it was found that as the interferon response rose, the concentration of interferon in the spleen and thymus simultaneously increased suggesting that the serum interferon response may have originated in the spleen and thymus(39,41,43). Neither ABPP nor AIPP inhibited virus replication in murine L929 cells or mouse embryo fibroblast cells in-vitro nor did they

induce interferon in these systems, These data, in combination with the fact that antilymphocyte serum did not affect the interferon response, whereas X-radiation did, suggest that a radiosensitive cell population other than lymphocytes might be responsible for the observed anti-viral activity.

1.3.2 Antiviral activity

Any agent that induces interferon and/or augments the body's own immune response is expected to have a broad spectrum of anti-viral activity. This, indeed, is the case with ABPP which has been demonstrated to have activity in both RNA and DNA viruses. Table 1.8 lists the anti-viral activity of ABPP and the routes of administration of both the viruses and the drug.

1.3.3 Antineoplastic activity

Stringfellow demonstrated that the antineoplastic activity of ABPP depended upon the tumour load when using the B16 malignant melanoma[40,43]. Little anti-tumour activity was evident with a $2x10^6$ initial tumour burden, but when this was reduced to 10^5 and 10^4 there was an increase in the number of survivors from 30% to 50% at doses of 100-400 mg/kg/day of ABPP.

Milas *et. al.*[50] showed that ABPP had a dramatic effect on pulmonary metastasis. Three tumours of varying immunogenicity and metastatic capacity, namely spontaneous fibrosarcoma, methyl-cholanthrene-induced fibrosarcoma and spontaneous mammary carcinoma were treated. ABPP administered at 250 mg/kg/injection (3 in total), either prior to or after the removal of the tumour, reduced metastatic incidence from 82% to 9%. Comparison with cyclophosphamide (which has similar anti-tumour activity as ABPP but

Virus	Route of administration of virus	Route of administration of ABPP	Species	Reference(s)
Semliki Forest (SLF)	ip	ip, sc, po	Mouse	42
West Nile	ip	ip	Mouse	42
Vesicular stomatitis (VSV)	ip	ip	Mouse	42
Friend leukaemia	ip	ip	Mouse	42
Encephalomyocarditis	ip, in	ip, in, po, sc	Mouse	45
Herpes Simplex-1 (HSV-1)	ip	ip	Mouse	42, 46, 48
	ivag	ivag	Mouse	47
Herpes Simplex-2 (HSV-2)	ip	ip	Mouse	46, 48
	ivag	ivag	Mouse	47
	ivag	ivag	G. Pig	47
	ivag	ivag	Cebus monkey	47
Cytomeglavirus	ip	ip	Mouse	49
Pseudorabies	ip	ip	Mouse	48
Influenza-A	in	in	Hamster	48
Parainfluenza-3	in	ip	Hamster	48
Infectious bovine rhinotracheaitis	in	in	Calf	46

Table 1.8 Spectrum of in-vivo antiviral activity of ABPP in various animal models (for abbreviations see Appendix III)

different interferon induction properties) lead to the conclusion that the reduction in the rate of metastatic incidence was not due to interferon induction[50].

ABPP and other pyrimidinones have also shown to be effective against a number of other tumours[51,52].

Treatment of cancers with a number of agents is now common in the hope of reaping the benefit of each while reducing the toxic effects by lowering the dose of each. ABPP combined with tamoxifen was shown to result in an additive effect of anti-tumour activity[53]. Similarly, a combination therapy of ABPP and cyclophosphamide also showed an additive anti-tumour activity in the P388 tumour model[54]. However, adjustment to the dose, namely lowering the cyclophosphamide dose with a concomitant increase in the ABPP dose led to a synergistic activity between the two agents, at times increases in the life span of 45% above the sum effect of the two were observed. Li *et. al.*[55,56] demonstrated that this synergistic activity depended on the dosing intervals between the drugs. The simultaneous administration of the two did not produce the best therapeutic effect, whereas the pyrimidinone administered 1, 2 or 4 days after cyclophosphamide gave the best results. However, the synergistic effect diminished as the interval between the administration of the two agents increased such that after eight days no synergism was seen.

Concomitant administration of ABPP with γ-interferon showed no additive synergistic effect[57]. However, when the γ-interferon was used as a primer prior to ABPP administration, a synergistic anti-tumour effect was observed. It is possible that this may be due to the exogeneous γ-interferon rendering the α/β interferon receptors more sensitive to the ABPP-induced interferons.

It therefore appears that the synergistic activity is dependent upon the fine adjustments to the dose of the constituents, type of tumour model, tumour load and dose regime.

1.3.4 Immunomodulatory effects

To determine the action of ABPP and other pyrimidinones, studies were carried out to investigate the ability of these compounds to potentiate various immune functions. The results from these studies are summarised in Table 1.9. ABPP increased the natural killer (NK) cell

Response	Effect	Reference(s)
1. Murine NK cells *in-vivo*	Increased†	58, 62, 63
2. Murine microphage mediated cytotoxicity after *in-vivo* or *in-vitro* addition	Increased†	59
3. *In-vivo* antibody formation in immunised and unimmunised mice	Increased†	59, 60
4. Bone marrow colony-forming units	Increased	61
5. *In-vitro* spleen cell response to sheep erythrocytes	Decreased	60, 61
6. T-Killer cell cytotoxicity *in-vitro*	Decreased	61
7. *In-vitro* compounds not mitogenic nor did they effect mitogen response	No effect	61

†Also observed with interferon

Table 1.9 Summary of immune modulating activities of ABPP

activity, macrophage mediated cytotoxicity after *in-vivo* or *in-vitro* treatment, antibody response *in-vivo* in un-immunised and immunised and bone marrow colony-forming units in treated animals. The compound did not appear to have an effect on *in-vitro* mitogenic

response nor did it affect the mitogen response of lymphocytes when added *in-vitro*. These results indicate that ABPP is an immune modulator which might exert some of the *in-vivo* antiviral activity through the above mechanisms.

1.3.5 Other bioactivities of pyrimidinones

A number of other bioactivities have been reported with the pyrimidinones. Some of these may be as an indirect result of the immuno-modulatory actions of these compounds but the mechanism is not understood. Table 1.10 summarisies these bioactivities.

	Reference(s)
1. Suppression of experimental atherosclerosis	63
2. Hypertensive/diuretic effect	66
3. Depression of murine cytochrome P-450	65
4. Inhibition of delayed hypersensitivity	59
5. Anti-inflammatory action (Reverse Passive Arthus Reaction)	66

Table 1.10 Other bioactivities of the pyrimidinones

1.4 Mechanism of action of interferon inducers

Although most of the work regarding the mechanism of action has been centred around the poly(I):poly(C), the same mechanism(s) may well apply to other interferon inducers including the low molecular weight pyrimidinones. The processes occuring during interferon induction have been the subject of several comprehensive reviews[36,67,68]. These mechanisms are summarised below:

(a) possible sequence of results

I Interaction of interferon inducer with specific cellular receptor site (may be located at the cell-plasma membrane).

II Transfer of message from cell plasma membrane to cell genome, followed by de-repression of interferon gene.

III Transcription and translation of interferon mRNA.

IV Glycosylation and release of interferon.

(b) alternative possibilities

1 Interferon inducer binds directly to repressor of the interferon gene, thereby allowing transcription of the interferon gene to interferon mRNA.

2 Interferon inducer binds directly to repressor of interferon mRNA, thereby allowing translation of the interferon mRNA to interferon protein.

3 Two repressor systems are involved, a first one at the transcription level and a second one at the translational level.

4 Interferon acts as its own repressor.

The majority of biological effects observed with the interferon inducers may be as a result of the interferon induced[33]. However, several important immunological responses are seen with the interferon inducers which are not seen with interferon alone[58-63]. These are highlighted in Table 1.9.

1.4.1 Hypo-responsiveness

This is also termed hyporeactivity, refractoriness or tolerance and is a decreased response to interferon induction which develops following repeated injections of the interferon inducer and appears to be interferon inducer-dependent[34]. This could have serious implications in the clinical use of the interferon inducer, i.e. treatment ceasing to be effective. This phenomenon has been observed with a number of

pyrimidinones including ABPP[39]. Various methods have been employed to overcome this problem.

1. Increasing the duration of injections[69]. When a pyrimidinone interferon inducer (ABMP) was given to cats on a once every week basis, normal interferon response was maintained for as long as 18 weeks.
2. Alternating between injections of different interferon inducers[70]. Animals developing hypo-responsiveness to pyrimidinones maintained their ability to respond to tilorone or anthraquinone and vice-versa. This may be due to the compounds stimulating separate cell populations.
3. Prostaglandins were found to restore the ability of hypo-reactive virus infected animals to respond to interferon inducers[71]. Administration of prostaglandins PGE_1, $PGF_{1\alpha}$ and PGA_1 restored the cell's ability to respond to the interferon inducer. Hypo-reactivity due to encaphalomyocarditis virus was associated with a factor in the serum of mice which suppressed the normal interferon response of murine cells *in-vitro*[73]. This transferable factor was called *serum hyporeactive factor*. The only apparent difference found between hypo-reactive and normal cells was that hypo-reactive cells had low intracellular cAMP and membrance associated adenylcyclase levels than normal interferon responsive cells. However, addition of cAMP to the system did not restore the response, whereas the addition of prostaglandins did. Some of these prostaglandins have the ability to stimulate cAMP. It therefore appears that the presence of certain prostaglandins is essential to interferon induction.
4. Priming of the tissue by the injection of 10,000 iu or more of interferon 3 hours prior to administration of ABPP[72].

1.4.2 Structure-activity relationships (SAR) of pyrimidinones

Skulnick *et.al.*[74] have produced a study incorporating an exhaustive list of analogues based upon 2-amino-5-substituted-6-arylpyrimidinone. Antiviral and interferon induction were determined.

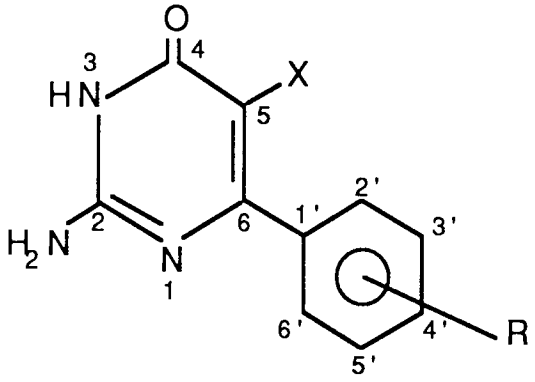

It was concluded that:-

1. Nitrogen was essential at positions 1 and 3, a free amine at the 2 position, and an oxygen at the 4 position.
2. The most potent interferon inducers and antiviral agents were mono- and difluorophenyl analogues at the 2',3' or 5' positions.
3. There was no apparent trend in antiviral activity or interferon induction with the selection of the halogen at C-5.
4. There exists a corresponding lack of selectivity with 4'-substitution on the 6-phenyl ring.
5. The optimum activities were found in the 2'- and 3'-monosubstituted series with secondary preference for disubstituted phenyl analogues.

A secondary study showed that even the smallest structural changes greatly influenced the diuretic/antiinflammatory actions of these compounds[66]. ABPP has diuretic effect of the same order as furosemide. Some of the diuretic activity was retained when the amine

at position-2 was replaced with oxygen and the hydrogen on the nitrogen at position-3 replaced with a methyl group. Addition of any larger group rendered the molecule inactive. No trend was apparent with the halogens at position-5. Similarly, the antiinflammatory activity appeared to be governed by the spatial/steric configuration of the molecule. ABPP only had a mild antiinflammatory effect whereas the 2-methylamino analogue was found to be much more potent. Substitution of the 2-amino group with oxygen and addition of a methyl group to the 6-phenyl ring retained the antiinflammatory action. Any other changes rendered the molecule inactive or of weak activity.

1.4.3 Pharmacokinetics of ABPP

The data so far on the pharmacokinetics and pharmacology of ABPP has been obtained from a variety of animals such as mice, cats, cattle, rabbits and monkeys. Different animals respond differently to the drug e.g. the circulating drug levels associated with detectable interferon response were 10-15 μg/mL in mice, 15-30 μg/mL in cats and dogs and 30-50 μg/mL in cattle[44].

Fig. 1.4 shows the results of studies in mice to determine the relationship between the dose of ABPP and the serum drug levels when ABPP was given either intraperitoneally (i.p.) or orally (p.o.)[44]. It was found that the minimum interferon-inducing dose for ABPP given p.o. was twice that of the drug administered i.p; doses being 100μg/mL and 50μg/mL respectively.

The kinetics of interferon response of mice at or near the maximum tolerated dose by p.o., i.p. or s.c. routes is shown in Fig. 1.5[43,76]. As a comparison, mice received either ABMP, AIPP or

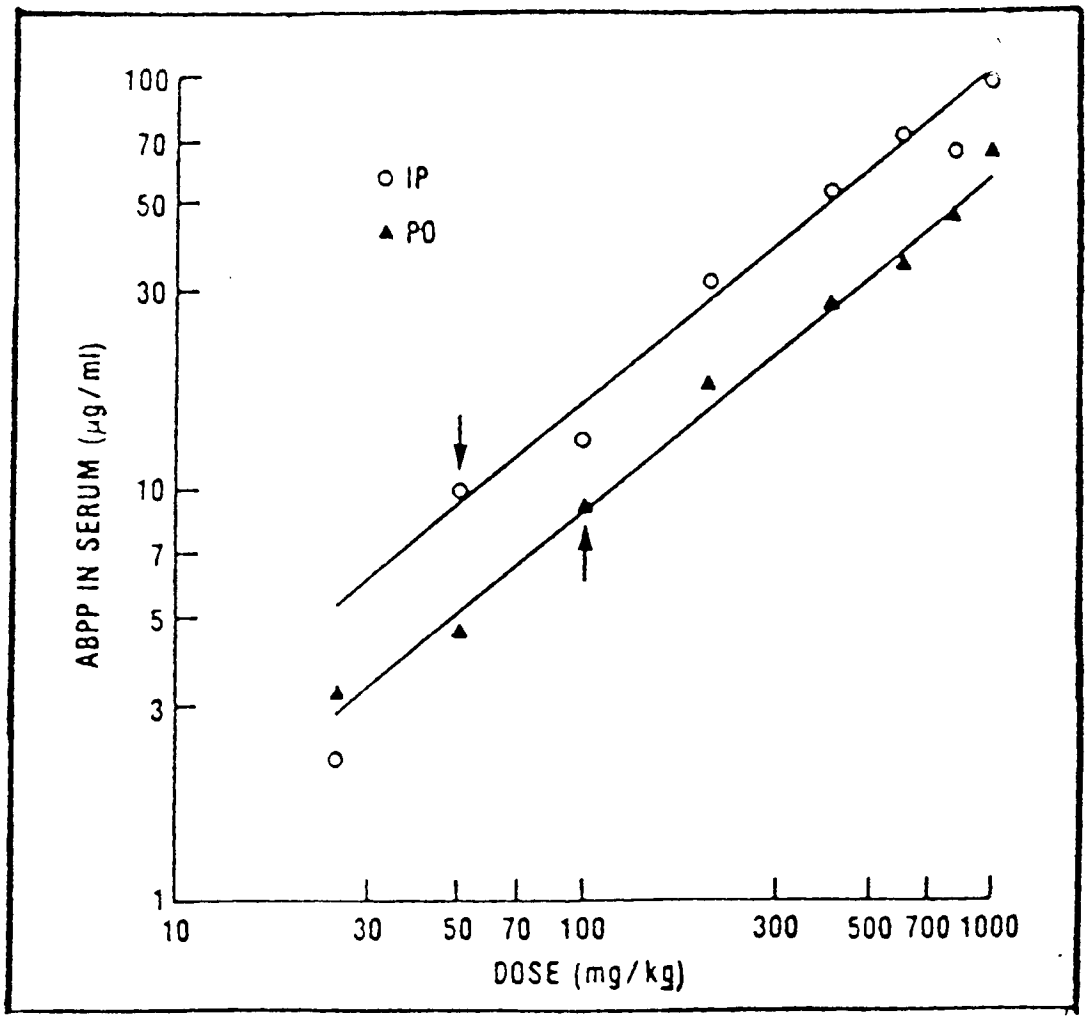

Fig. 1.4: Relationship between the dose of ABPP and the serum levels of drug at 2 hours post-treatment when ABPP was given ip or po at 25-1000mg/kg to mice. Arrows point to the minimum interferon inducing dose for ip and po administration of ABPP[44]

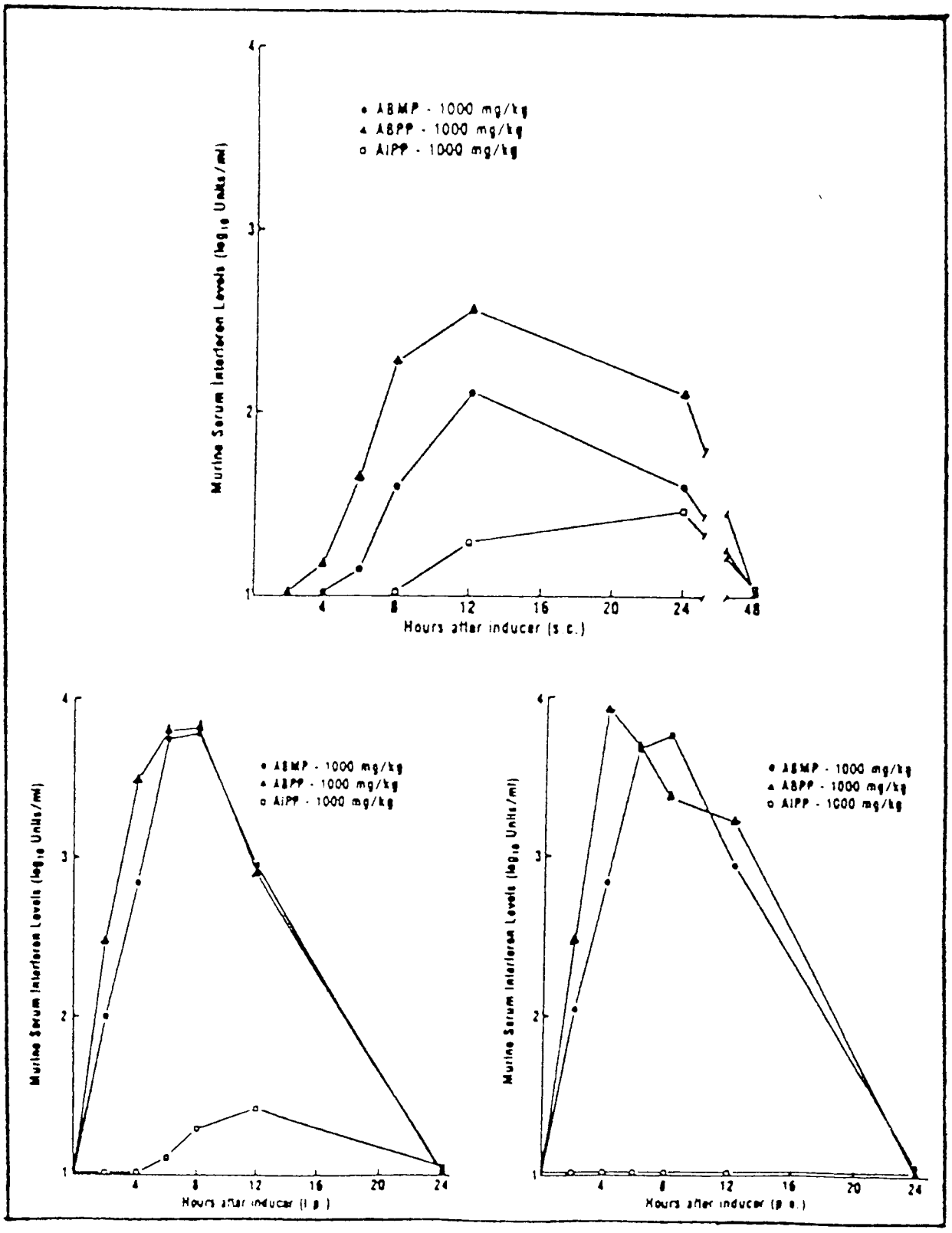

Fig. 1.5: Serum interferon response of mice following (a) sc, (b) ip or (c) po administration of 1000mg/kg ABMP, ABPP or AIPP[43,76]

ABPP at a dose of 1000mg/kg and the serum collected and assayed for interferon over fixed intervals of time. For ABPP, the peak interferon levels were achieved in 6-8 hours after i.p. injection or oral administration and approximately 12 hours after s.c. injection. However, whereas AIPP induced low levels of interferon via all three routes, ABPP was seen to be a superior interferon inducer to both AIPP and ABMP by any route.

Fig. 1.6 shows the response in mice when the drug was given at different dosages via the i.p., s.c. or p.o. routes[42,76]. Subcutaneously there is a relatively linear response and interferon was detected at doses as low as 10 mg/kg. However, no interferon was detected at low levels of the drug when administered intraperitoneally or orally. At higher doses, the amount of interferon detected by these two routes exceeded that from the s.c. route. Again of the three inducers, ABPP was more potent giving higher levels of serum interferon at all doses.

Fig. 1.7 compares serum concentration and circulating interferon levels in cats dosed orally with ABPP in capsule form[44]. At oral doses of 50 mg/kg, ABPP was sometimes lethal for cats. This was possibly as a result of conversion of ABPP in the cats to phenolic metabolites[44,105] which are favoured in this species. Maximum serum interferon levels were achieved 6 to 9 hours after drug administration.

Fig. 1.8 demonstrates that the bioavailability of ABPP is similar whether administered either in a capsule or given as a suspension[44]. However, the interferon induction from capsule was greater than with the suspension, albeit slight.

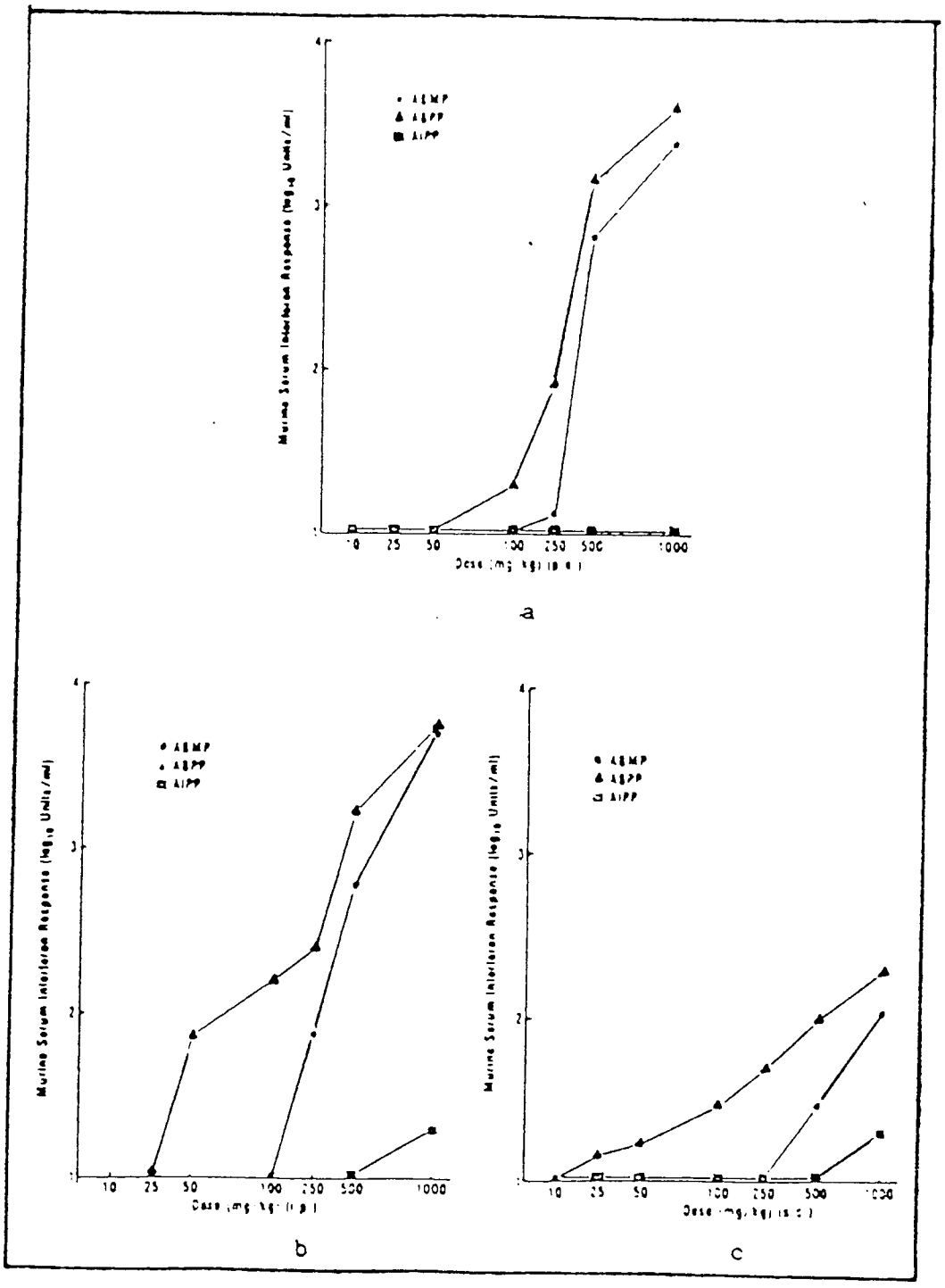

Fig. 1.6: Murine serum interferon response to ABMP, ABPP and AIPP administered (a) po, (b) ip or (c) sc [76]

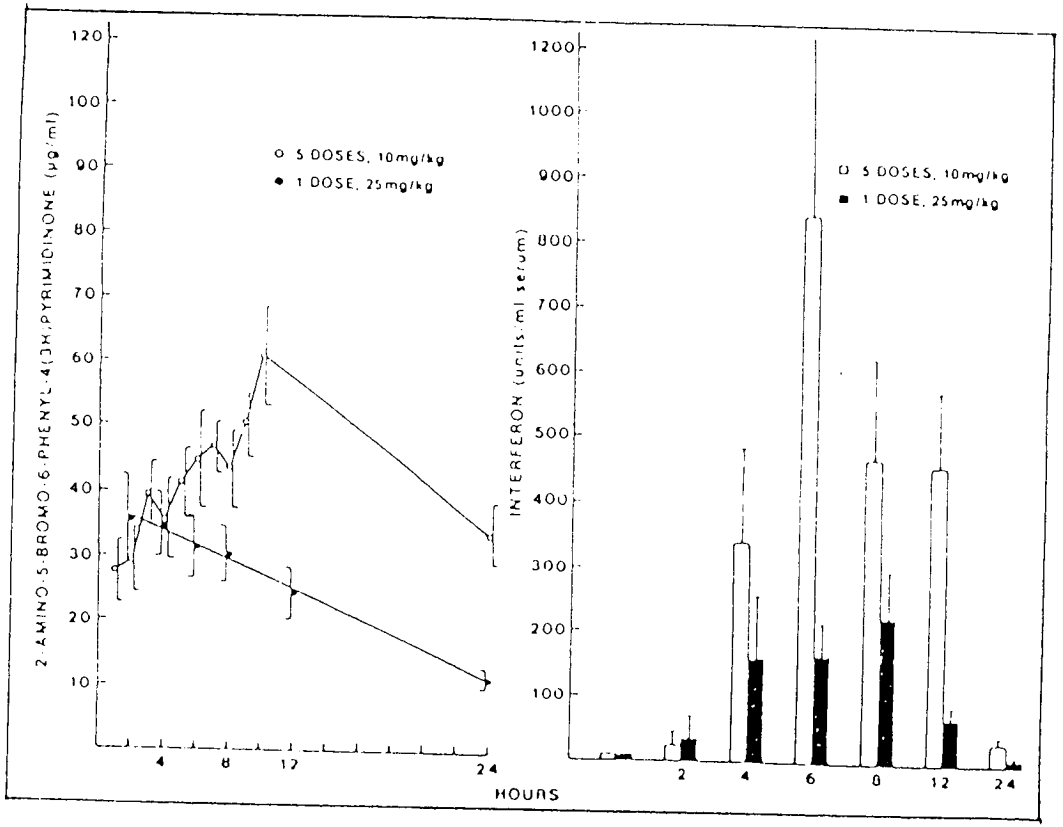

Fig. 1.7: Comparison of the serum levels of ABPP and interferon induced by the drug in cats dosed once with 25mg/kg at 0 hr or 5 times (0, 2, 4, 6, 8 hr) with 10mg/kg. Drug and interferon concentrations were determined after the single or multiple doses given orally in gelatin capsules[44]

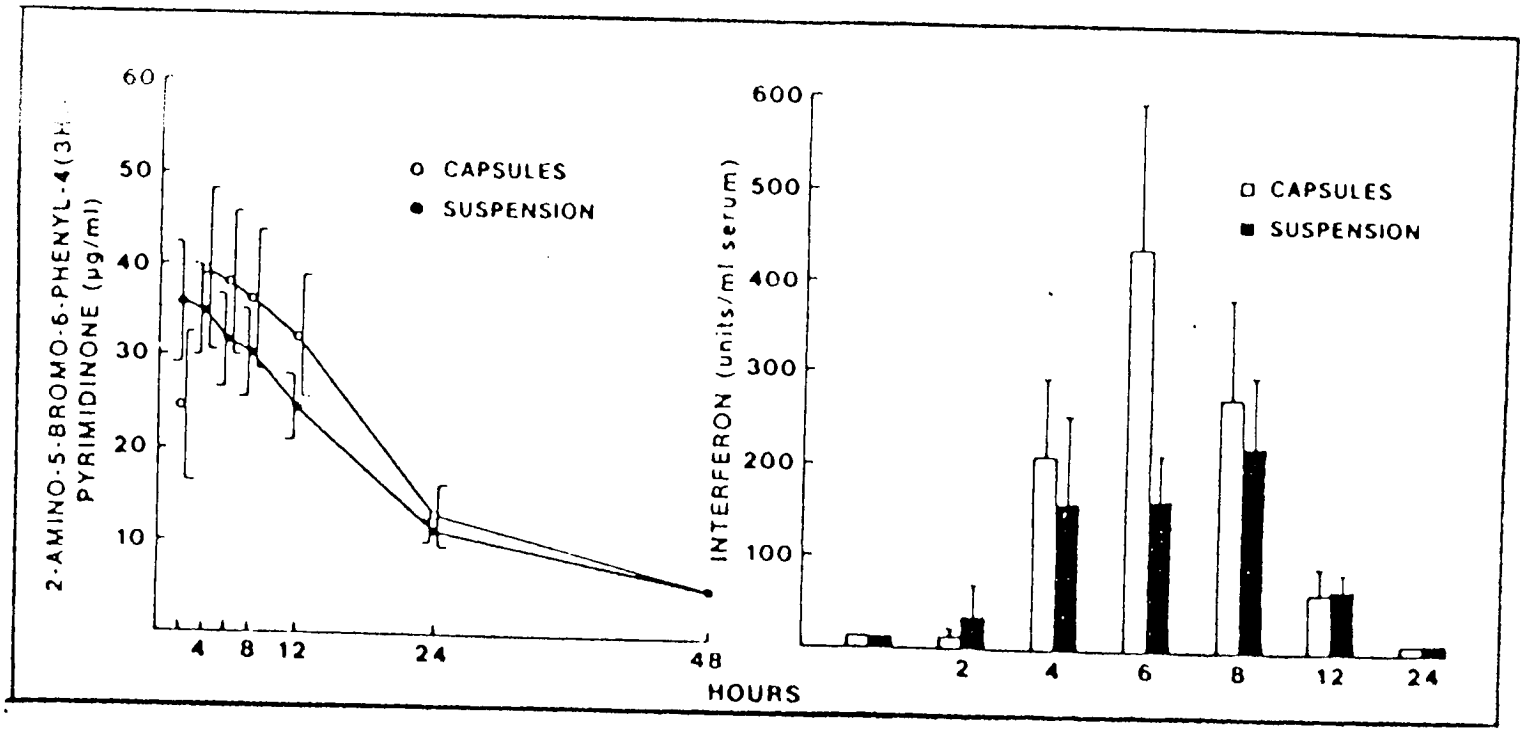

Fig. 1.8: *Comparison of the serum levels of ABPP and the interferon titres induced in cats by the drug (25mg/kg) given in gelatin capsules or as suspension in an aqueous vehicle. Drug and interferon titres were determined in serum after single oral dose*[44]

Interferon response was compared, for different routes of administration to ABPP in calves (Fig. 1.9)[41,44]. Similar responses were obtained with both s.c. and i.m. injections; the responses being low but prolonged. The oral route appeared to be the most beneficial giving interferon levels (1000 i.u./mL) after 3 hours and falling to zero after 48 hours. The intranasal (i.n.) route offered a good alternative, using a nasal spray, giving peak interferon levels (500 i.u./mL nasal interferon) after 3 hours. However, the response was somewhat short lived and the interferon levels fell to zero after 24 hours. The intranasal route of administration may, therefore, be the route of choice for superficial naso-pharangeal infection where direct application would deliver a high concentration.

The intravenous route of administration of ABPP to rabbits gave high but short-lived peaks[77] (Fig. 1.10). The apparent elimination half-life of ABPP (0.8 h) appeared not to be dose related but a straight line relationship between the area under the curve and dose and also between $C_{p_{max}}$ and dose was obtained.

No conclusive work has been carried out regarding the metabolism of pyrimidinones.

1.4.4 Clinical studies on ABPP

Clinical studies on oral ABPP in humans (Phase I cancer) have been carried out in two phases[78]. In the first phase, the drug was administered as a single oral dose. In the second phase, the highest tolerated dose was used. The dose in the first instance was 25-200 mg/m^2 and in the second the patients were treated weekly with the starting dose of 2 g/m^2 and increased to 3, 4 and 5 g/m^2 each week. No cardiac, haematological, hepatic or renal toxicity was observed.

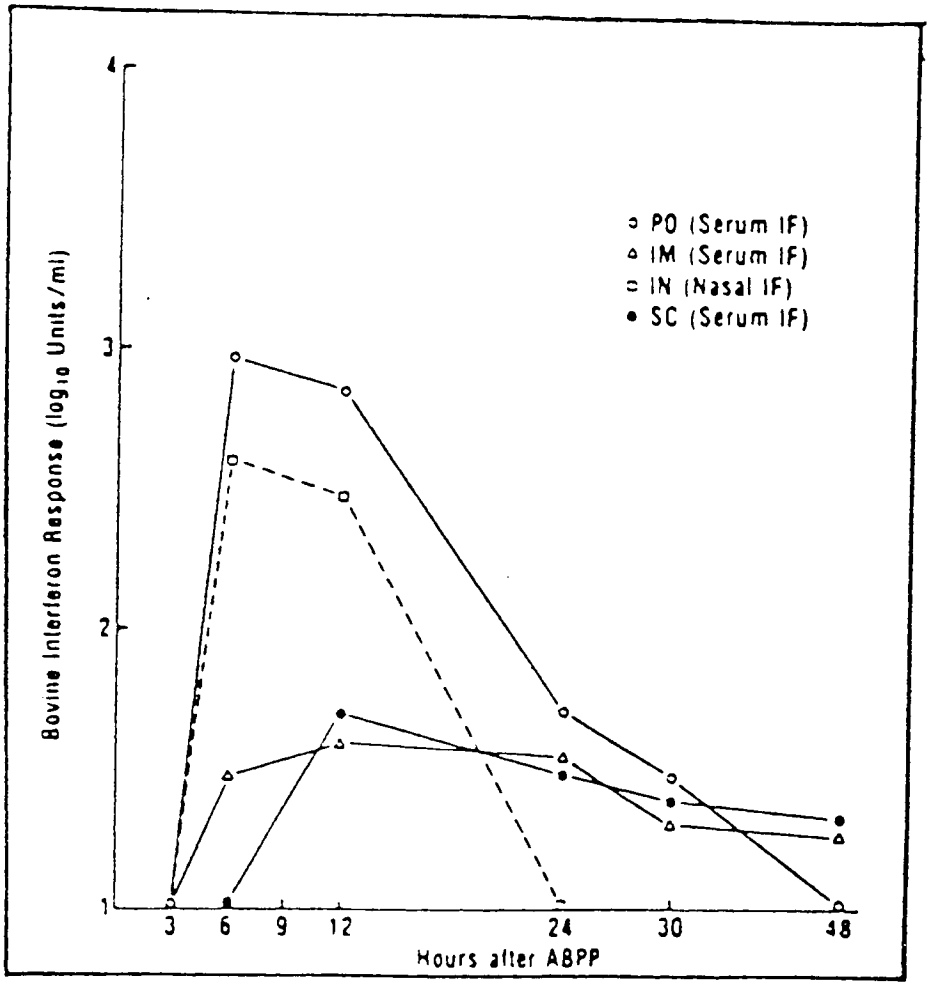

Fig. 1.9: Bovine interferon response to ABPP (100mg/kg po, im and sc; 1g/calf in)[41,44]

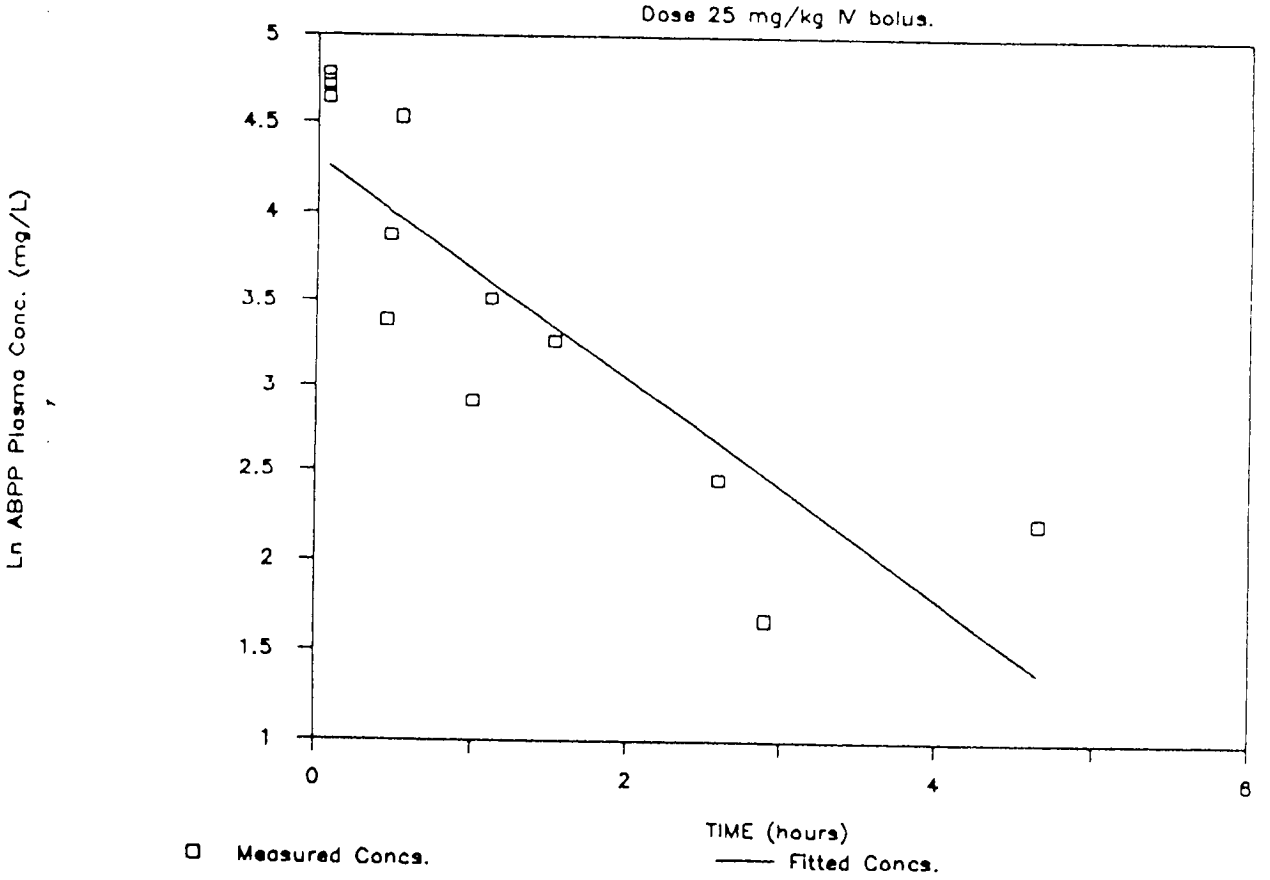

Fig. 1.10: ABPP rabbit pharmacokinetics from a 25mg/kg iv blus injection[77]

The second study was conducted in 16 solid tumour patients[79]. It was found that after eight 1g oral doses, mild orthostatic hypotension was observed in some patients. Duration of peak ABPP, area under the curve, serum concentration and total urinary ABPP increased with dose. No other serious side effects were observed.

1.4.5 Toxicity of ABPP

Toxicological data obtained from studies carried out by the Upjohn Company are shown in Appendix IV - VII.

1.5 Aims of the thesis

Although broprimine (ABPP) is an extremely potent interferon inducer, its poor aqueous solubility of 30-40 μg/mL[77] has hindered progress towards an intravenous formulation suitable for clinical use. Furthermore, no comprehensive study has been made regarding the physico-chemical properties. In light of this, the aim of the thesis will be to study these parameters and attempt to formulate bropirimine incorporating sufficient drug so that high blood levels could be achieved following administration. Attempts will also be made to deliver bropirimine rectally using the suppository as the dosage form. Possible methods for increasing the aqueous solubility will include prodrug synthesis, solvate formation and the use of co-solvents and additives. A method for predicting the behaviour of the formulation following administration will be sought and the conditions optimised. Differential scanning calorimetry (DSC) will be used to evaluate any interactions with possible excipients.

Psoriasis is a disease of the skin characterised by the appearance of sharply defined erythematous patches covered with distinctive scales caused by hyperproliferation of keratinocytes. It can be caused by a number of factors such as infection, trauma or drugs[80]. Although there is no cure at present, the disease disappears spontaneously in almost one third of the affected

population[81]. Treatment may take a number of forms such as topical therapy, phytotherapy and phytochemotherapy[83,84], retinoids[82], dialysis[85] and even hypothermia[86].

The use of dihydrofolate reductions (DHFR) inhibitors such as methotrexate has been a considerable advance in management of severe psoriasis[97-99,100]. The 2, 4-diaminopyrimidines such as pyrimethamine have also shown encouraging results[101] and intensive efforts are underway to find potent analogues[102].

2.0 HIGH-PERFORMANCE LIQUID CHROMATOGRAPHY OF THE IMMUNOMODULATORY AGENTS

2.1 Introduction

Formulation and stability studies require a method of assay which is able to detect simultaneously the parent compound and the breakdown products. High-performance liquid chromotography (HPLC) is a method by which such objectives may be achieved. It is relatively cheap, quick, versatile and, most importantly, it can be extremely accurate when used correctly, even at low drug levels. It is also a technique that is sensitive, specific, and precise.

The optimum HPLC conditions may be arrived at by considering the variables which contribute to the overall efficiency of the system. There is no certainty that one set of conditions will work for two different drugs, and therefore these parameters have to be established for each drug. However, for a series of related compounds, such as esters of the same compound, optimum conditions may be obtained by minor modifications to the original component of the mobile phase as the ester chain length increases.

The aim here was to establish HPLC conditions that would separate the following groups of drugs, namely bropirimine and its acetyl- and propanoyl derivatives (Table 2.1) and pyrimethamine and its derivatives (Tables 2.2 and 2.3).

Group 1

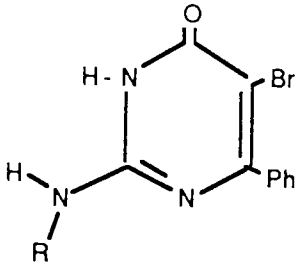

R	Compound
H -	Bropirimine (III)
$CH_3C(=O)-$	2-acetylbropirimine (AB, IV)
$CH_3CH_2C(=O)-$	2-propanoylbropirimine (PB, V)

Table 2.1: Bropirimine and its derivatives

Group 2

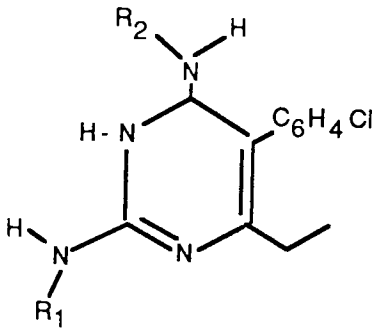

R_1	R_2	Compound
H -	H -	Pyrimethamine (Py, VI)
$CH_3CH_2C(=O)-$	H -	2-propanoylpyrimethamine (MPP, VII)
$CH_3CH_2C(=O)-$	$CH_3CH_2C(=O)-$	2,4-Dipropanoylpyrimethamine (DPP,VIII)

Table 2.2: Pyrimethamine and its 2/4 substituted derivatives

Group 3

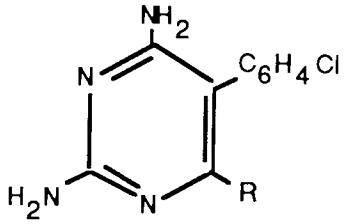

R	Compound
- CH_2CH_3	Pyrimethamine (Py, VI)
- $COOCH_3$	Methyl-5-(p-chlorophenyl)-2,4-diaminopyrimidine-6-carboxylate (MDPC, IX)
- $COOC_2H_5$	Ethyl-5-(p-chlorophenyl)-2,4-diaminopyrimidine-6-carboxylate (EDPC, X)
- $COOC_3H_7$	Propyl-5-(p-chlorophenyl)-2,4-diaminopyrimidine-6-carboxylate (PDPC, XI)
- $COO{\cdot}CH(CH_3)_2$	Isopropyl-5-(p-chlorophenyl)-2,4-diaminopyrimidine-6-carboxylate (iPDPC, XII)

Table 2.3 Pyrimethamine and its 6-substituted derivatives

2.2 Instrumentation, materials and methods

The high-performance liquid chromatograph consisted of an Altex 100A constant flow solvent metering pump, a Rheodyne 7120 injector valve fitted with a 20μL loop, a PYE Unicam LC3 variable wavelength detector, equipped with an 8μL flow cell, operated at sensitivity of 0.08-0.64 AUFS and a J J chart recorder (J J Instruments). Shandon stainless steel columns (10cmx4.6mm ID) were used, which were packed in the laboratory using a Shandon column packer with 5μm particle size Hypersil-ODS (Shandon) used as the packing material.

The ultraviolet (UV) spectra were recorded on a Unicam SP8000 spectrophotometer using 1cm path length matching quartz cells. pH measurements were made on a Radiometer PHM64 Research pH meter and calibrated using colour coded standards (BDH).

The compounds were dissolved in methanol (Fisons plc) with the aid of a Whirlmixer (Fisons plc) and an ultrasonic water bath (Kerry, Pulsatron 125) which was also used to remove any gases in the mobile phases. The acetonitrile (Fisons) and the diethylamine (BDH) were used as received. Unless otherwise stated, the pH of the mobile phase was adjusted to 2.0 using orthophosphoric acid (BDH). All solutions were freshly prepared prior to use.

2.3 Results and discussion

Before any HPLC analysis is carried out, it is important to establish the working wavelength (λ_{max}) for each compound, especially when sensitivity is of paramount importance. Fig. 2.1 to 2.3 show the uv spectra of the compounds listed in Tables 2.1 to 2.3 using methanol as the solvent. The λ_{max} was measured for each compound and the molar extinction coefficient, E, calculated from:

$$A = \varepsilon c l \qquad \ldots 2.1$$

Where A is the absorbance at λ_{max}

c is the molar concentration of the compound

l is the path length of the solution (in cm).

The results are summarised in Table 2.4. Where there are two peaks the higher one should be used for λ_{max} in order to avoid possible interference by the solvent at lower λ_{max} values. Hence, rows in Table 2.4 effectively represent the recommended wavelengths to be used for experimental work. The spectra were recorded at different molar concentrations but at the same strength of 10 µg/mL except bropirimine, AB and PB which were recorded at concentration of 2 µg/mL.

2.3.1 HPLC system for bropirimine, AB and PB

Fig. 2.4 shows the effect of variation of acetonitrile concentration in the mobile phase on the retention time of bropirimine, AB and PB. A decrease in acetonitrile concentration leads to increased analysis time and poor chromatography. At levels of acetonitrile below 20%$^{v}/_{v}$ the retention time becomes so long as to be impractical. Several

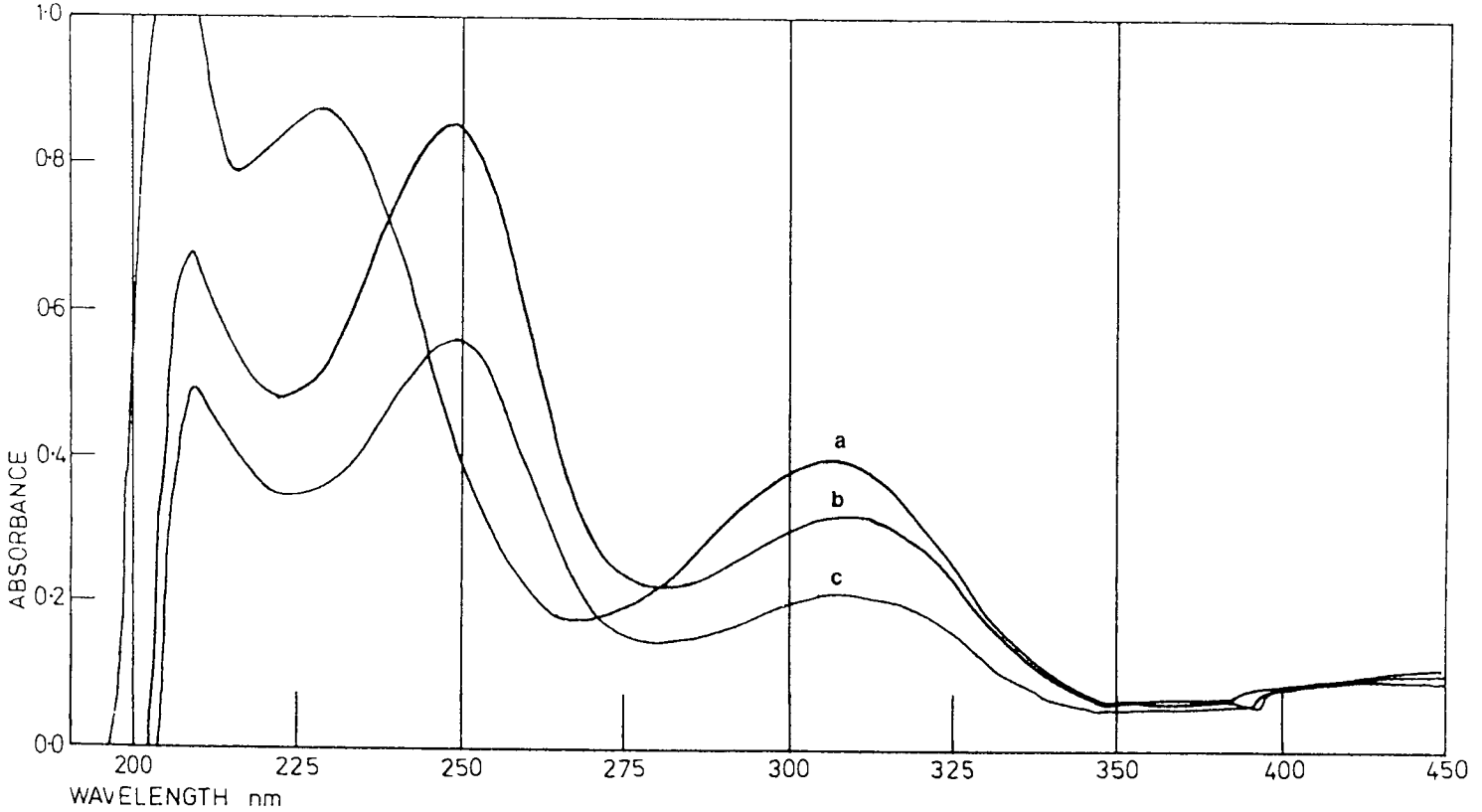

Fig. 2.1: Ultraviolet spectra of bropirimine (a), AB (b) and PB (c)

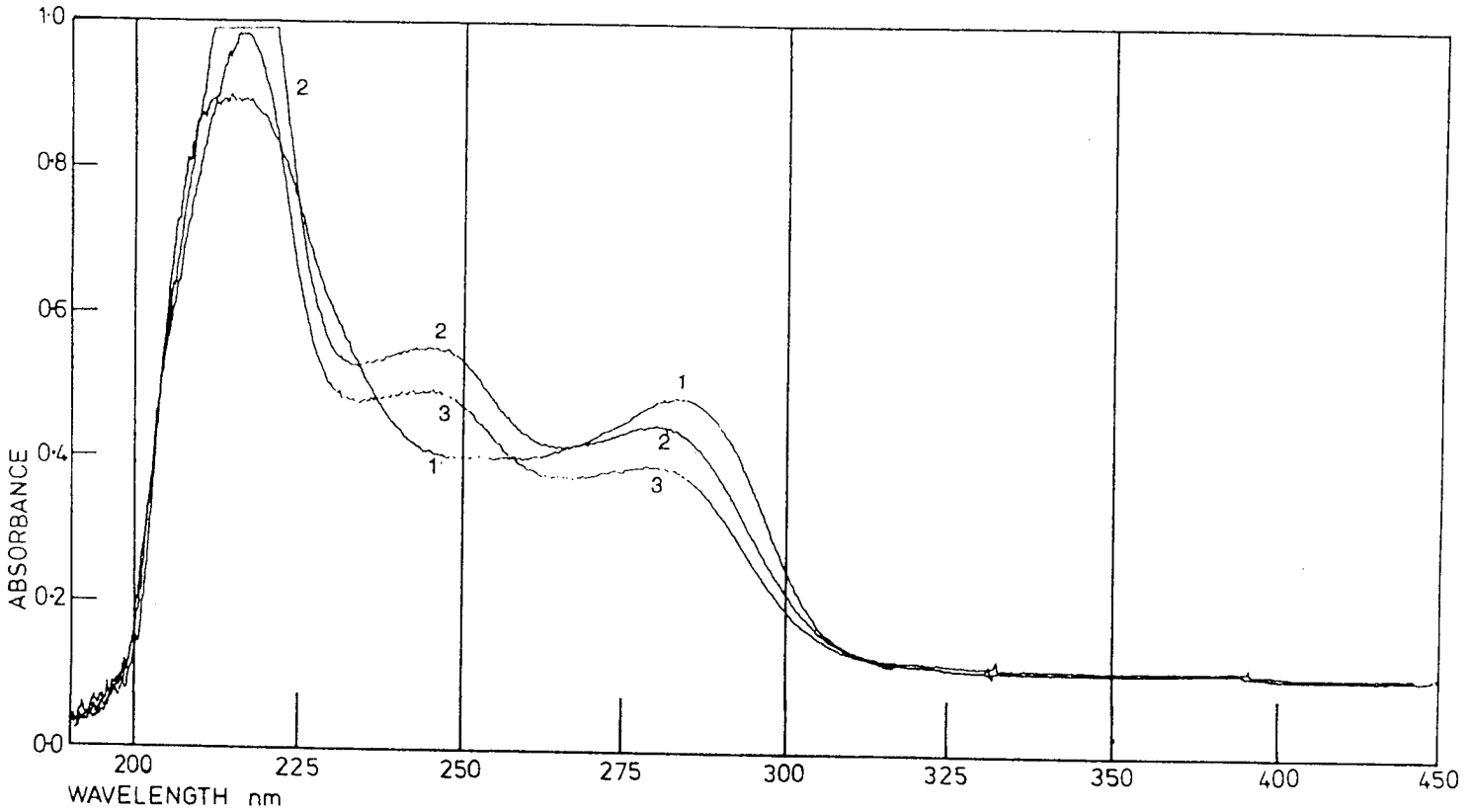

Fig. 2.2: Ultraviolet spectra of pyrimethamine (1), MPP (2) and DPP (3)

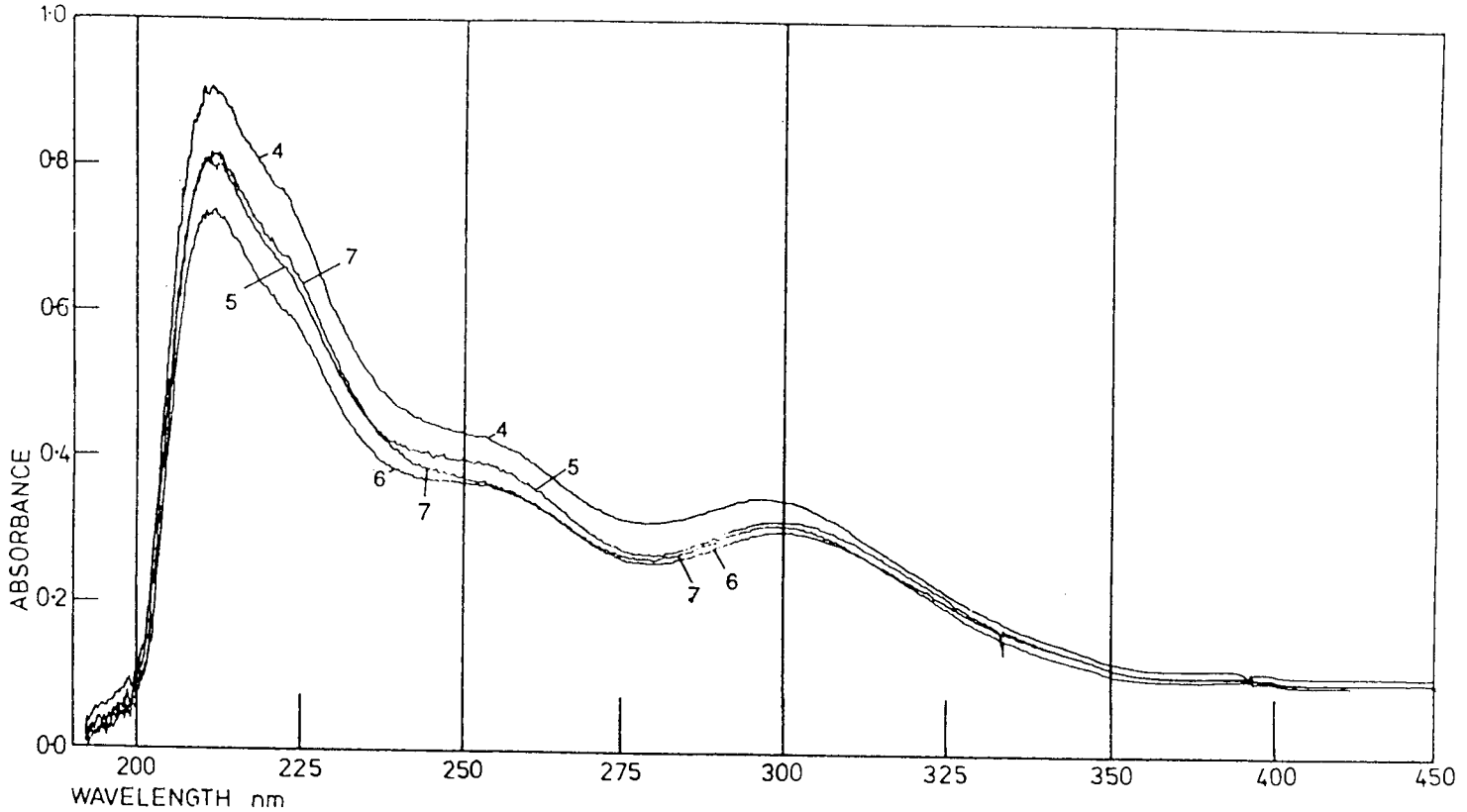

Fig. 2.3: Ultraviolet spectra of MDPC (4), EDPC (5), PDPC (6) and iPDPC (7)

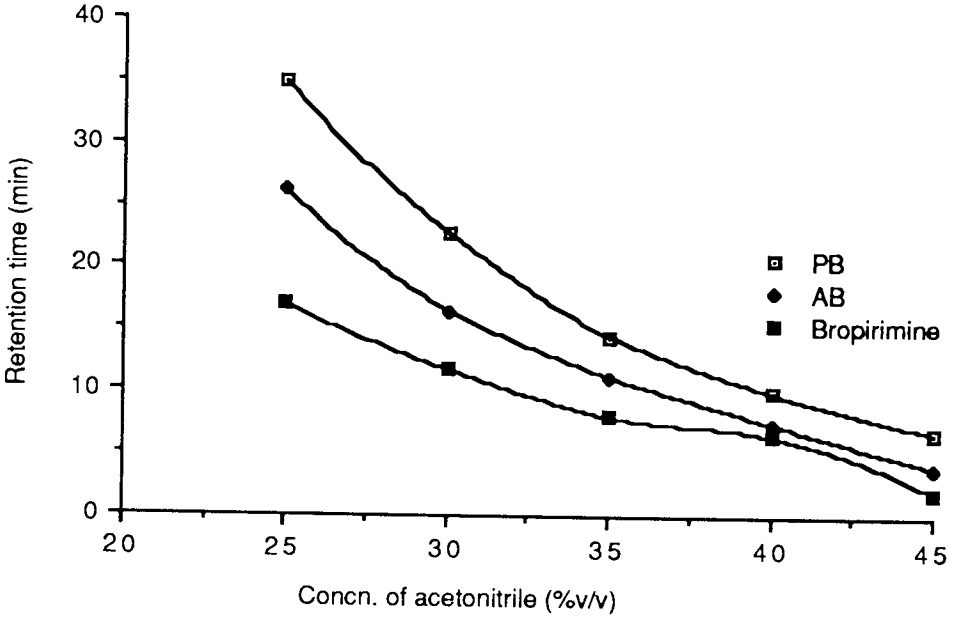

Fig. 2.4: The effect of acetonitrile concentration on the retention times of bropirimine, AB and PB

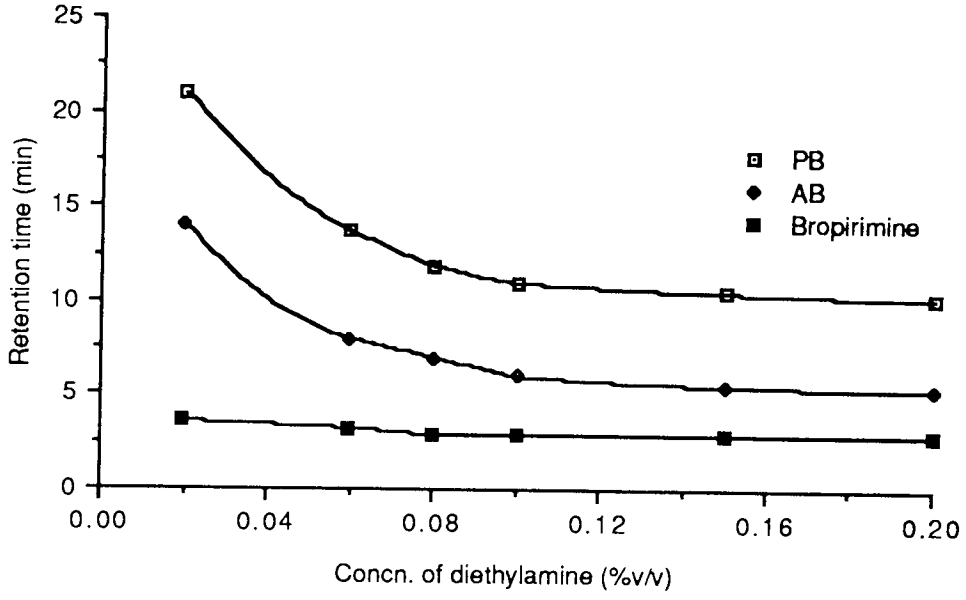

Fig. 2.5: The effect of diethylamine concentration on the retention times of bropirimine, AB and PB

mathematical parameters may be calculated which give an indication of the performance of the systems. These parameters are:

1. Capacity ratio/factor, K', where

$$K' = \frac{(t_A - t_O)}{t_A} \qquad \ldots 2.2$$

Optimum K' values range from 1-10 (K'=0 for unretained solutes). Very small K' values indicate interference with solvent and other early peaks whereas large values of K' show peak broadening and therefore lengthy analysis times[103].

2. Number of theoretical plates, N, where

$$N = 16 \left(\frac{t_A}{W_A}\right)^2 \quad \text{or} \quad 5.54 \left(\frac{t_A}{W_{1/2A}}\right)^2 \qquad \ldots 2.3$$

Typical values for N usually lie within the range N = 2500 - 10 000[103].

3. Resolution, R_S, where

$$R_S = \frac{2(t_B - t_A)}{W_A + W_B} \qquad \ldots 2.4$$

A value of R_S=1.5 indicates almost total separation of the bands[103,106]. Symmetrical peaks will be at R_S=1.0, but for values R_S<0.8 only partial separation is obtained and chromatographic conditions may have to be changed[103,106].

Peak	λ_{max}									
	Bropirimine	AB	PB	Py	MPP	DPP	MDPC	EDPC	PDPC	iPDPC
1	230	250	250	-	248	248	255	255	255	255
2	305	305	305	283	286	284	300	300	300	300

Peak	ε									
1	20480	23304	15456	-	14024	14440	8521	7936	7521	7918
2	8597	7670	4946	8707	11890	10830	6265	5820	5710	6452

Table 2.4: Working wavelengths and molar extinction coefficients of bropirimine and its prodrugs and pyrimethamine and its prodrugs

Concⁿ. of acetonitrile (%v/v)	Capacity Factors, K			Theoretical plates, N			Resolution R_s	
	Bropirimine	AB	PB	Bropirimine	AB	PB	Bropirimine + AB	AB + PB
25	14.18	22.48	30.25	15231	17292	13611	1.38	0.87
30	9.45	13.73	19.27	9873	10310	10179	0.86	0.80
35	6.14	9.00	11.95	6400	6635	5980	0.67	0.51
40	4.80	5.70	7.93	5518	5625	4444	0.27	0.50
45	0.79	1.77	5.07	3600	2090	2959	0.43	0.66

Table 2.5: Effect of acetonitrile concentration in the mobile phase on the HPLC parameters of bropirimine, AB and PB

Concⁿ. of diethylamine (%v/v)	Capacity Factors, K			Theoretical plates, N			Resolution R_s	
	Bropirimine	AB	PB	Bropirimine	AB	PB	Bropirimine + AB	AB + PB
0.02	2.63	11.00	17.00	1282	7423	9766	1.99	0.93
0.06	1.74	5.86	10.71	1820	3385	5339	1.13	0.87
0.08	1.49	5.00	9.20	3364	3136	4624	1.17	0.82
0.10	1.46	4.14	8.43	5857	2844	4582	1.04	0.91
0.15	1.46	3.71	8.00	5857	2390	4175	0.88	0.91
0.20	1.45	3.54	7.74	5817	2220	3940	0.89	0.89

Table 2.6: Effect of diethylamine concentration in the mobile phase on the HPLC parameters of bropirimine AB and PB (Mobile phase consisted of 55%v/v acetonitrile adjusted to pH 2.0)

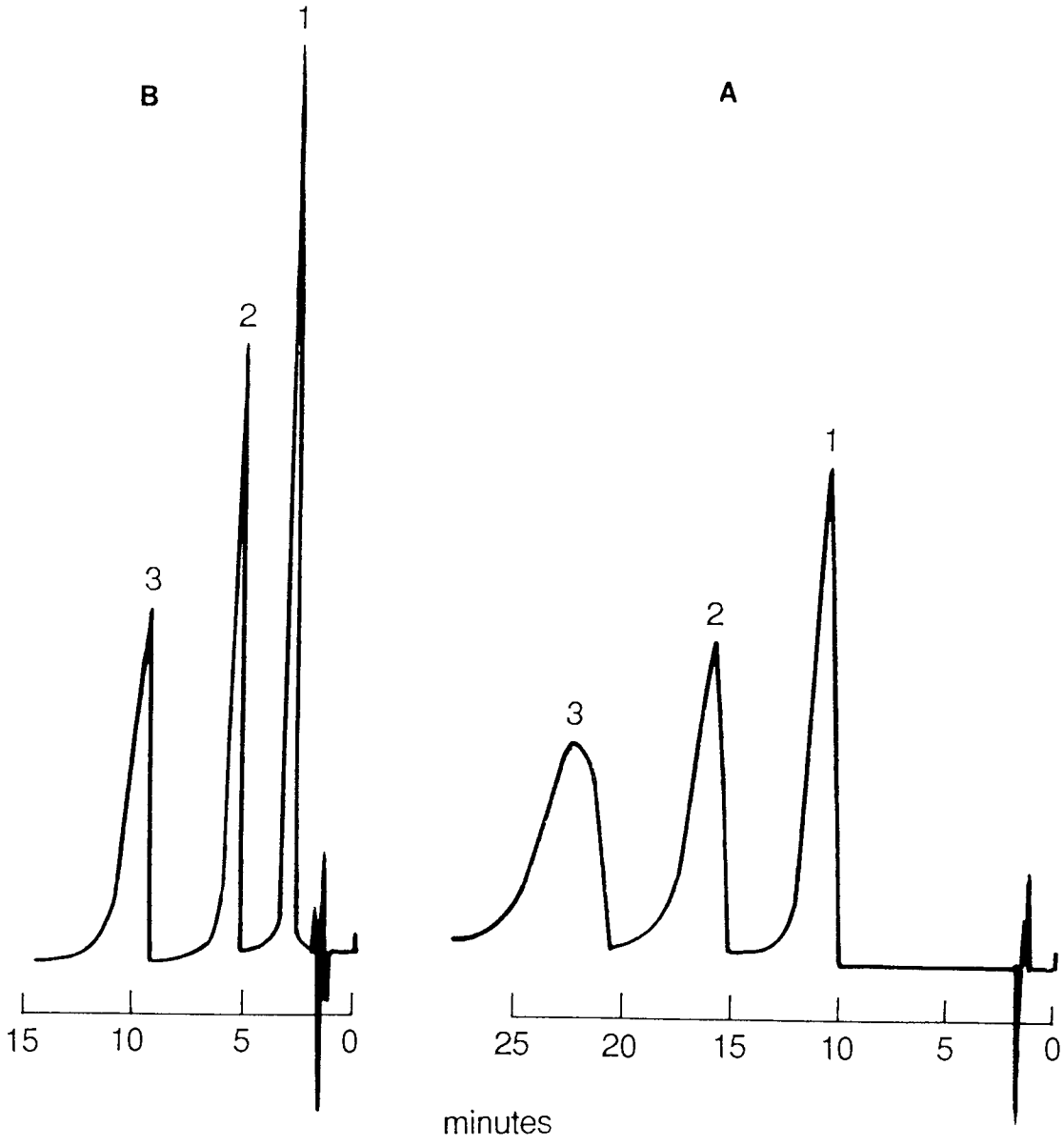

Fig. 2.6: *Chromatograms to show the effect of diethylamine on the separation of bropirimine (1), AB (2) and PB (3).*
A 30%v/v acetonitrile and NO diethylamine
B 30%v/v acetonitrile and 0.1%v/v diethylamine

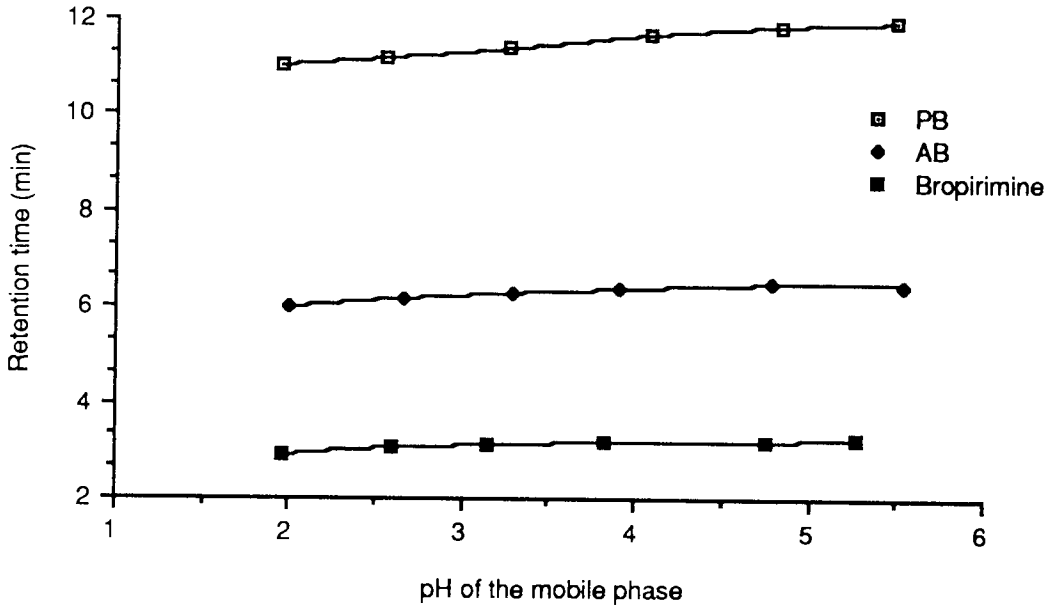

Fig. 2.7: The effect of pH of the mobile phase on the retention times of bropirimine, AB and PB

In the above equations,

t_O = the retention time of the unretained compound
t_A, t_B = the retention times of compounds A and B respectively
W_A, W_B = the peak width of compounds A and B respectively
$W_{1/2A}$ = the peak width at half of the peak height.

Fig. 2.5 shows how the concentration of diethylamine affects the retention times of bropirimine, AB and PB. The retention times of each component are reduced dramatically upon the addition of diethylamine. The peaks become sharper and the capacity factor is reduced.

Fig. 2.6 shows the improvement in the chromatogram when diethylamine is added. This is a basic compound added as a moderator for the following reason. The surface silanol groups in the column packing material are acidic and often interact very strongly with basic compounds resulting in broadening and poor resolution of peaks. Addition of small amounts of diethylamine prevents interaction of these groups with the eluting compound[104]. Concentrations of diethylamine greater than 0.1% $^{v}/_{v}$ have little effect on the chromatography of bropirimine, AB and PB. The HPLC parameters for these compounds in the absence and presence of diethylamine are shown in Tables 2.5 and 2.6, respectively. pH has little effect on the retention times of bropirimine, AB and PB (Fig. 2.7).

2.3.2 HPLC system for MPP and DPP

Using acetonitrile concentration in the mobile phase between 30 - 60%$^{v}/_{v}$, in the absence of diethylamine, resulted in extremely long retention times. Therefore, in order to study the effect of acetonitrile concentration on the retention times, a fixed amount of diethylamine (0.1%$^{v}/_{v}$) was added to reduce the analysis times and sharpen the peaks.

Fig. 2.8 shows the variation in the retention times of MPP and DPP with the composition of acetonitrile in the mobile phase. Low concentrations (<50%$^{v}/_{v}$) resulted in unacceptably long retention times and high capacity ratios.

Using 55%$^{v}/_{v}$ acetonitrile in the mobile phase at pH 2.0, the effect of diethylamine was studied (Fig. 2.9). It is apparent that the addition of diethylamine as a moderator has a significant effect on the resolution of the compounds as well as the retention times and capacity ratios. Increasing the diethylamine concentration from 0.02%$^{v}/_{v}$ (Fig. 2.10(A)) to 0.10%$^{v}/_{v}$ (Fig.2.10(B)) dramatically improves the chromatography and reduces both the retention times and the capacity ratios.

Changing the pH of the mobile phase also has considerable effect on the chromatographic parameters. Since both MPP and DPP are weakly basic compounds (having pK_a values of 4.40 and 2.89 respectively), decreasing the pH leads to increased amount of the ionised form and this is reflected in shorter retention times of the compounds at lower pHs (Fig. 2.11). The HPLC parameters of these compounds are listed in Tables 2.7 and 2.8.

The following mobile phase thus satisfactorily eluted both MPP and DPP:

Acetonitrile	55%$^{v}/_{v}$
Diethylamine	0.1%$^{v}/_{v}$

pH adjusted to 2.0 with orthophosphoric acid

Possible internal standards for use with MPP and DPP are listed in Table 2.11.

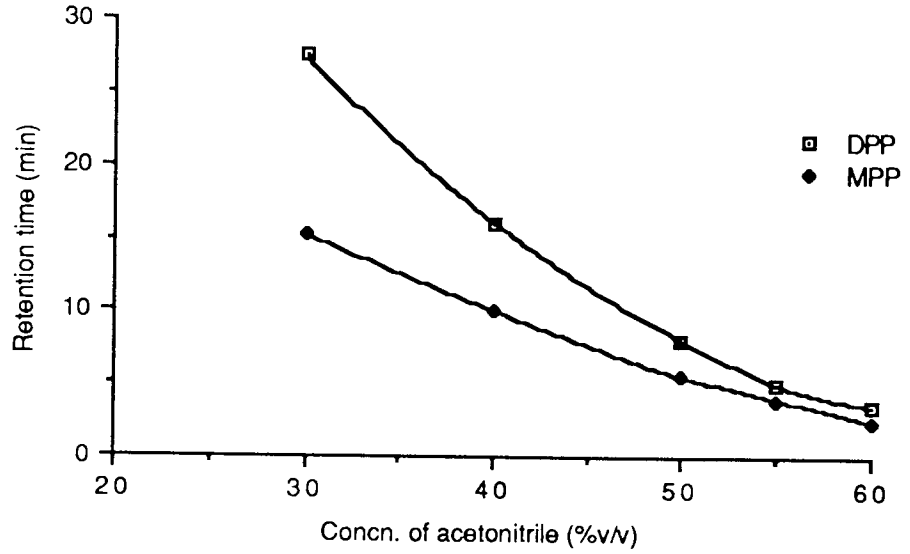

Fig. 2.8: The effect of acetonitrile on the retention times of MPP and DPP

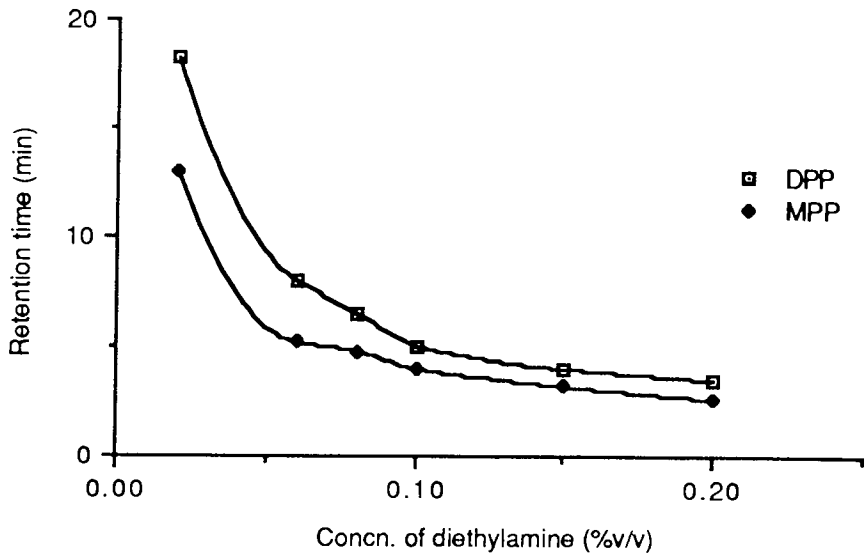

Fig. 2.9: The effect of diethylamine on the retention times of MPP and DPP (55%v/v acetonitrile)

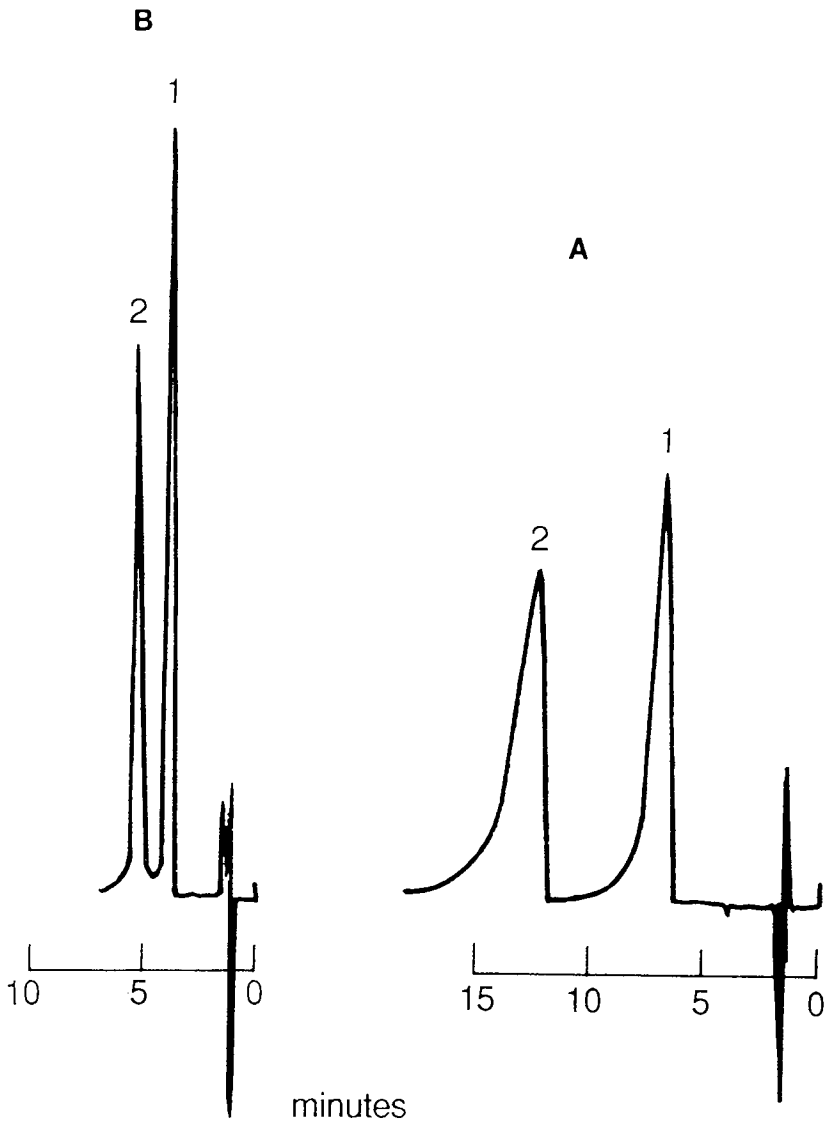

Fig. 2.10: *Chromatograms to show the effect of diethylamine on the separation of MPP (1) and DPP (2).*
A. 55%v/v acetonitrile + 0.02%v/v diethylamine
B. 55%v/v acetonitrile + 0.10%v/v diethylamine

Conc^{n}. of acetonitrile (% v/v)	Capacity Factors, K'		Theoretical plates, N		Resolution R_s
	MPP	DPP	MPP	DPP	
30	13.1	24.0	3229	3025	0.93
40	8.1	13.6	1975	2090	0.83
50	4.0	6.3	3951	1264	0.94
55	2.6	3.6	6400	3265	0.98
60	1.3	2.2	4444	2178	0.94

Table 2.7: Effect of acetonitrile composition in the mobile phase on the HPLC parameters of MPP and DPP (With 0.1%v/v diethythamine in the mobile phase and adjusted to pH 2.0)

Conc^{n}. of diethylamine (% v/v)	Capacity Ratio		Theoretical plates, N	
	MPP	DPP	MPP	DPP
0.02	10.8	15.6	4333	4807
0.06	3.7	6.3	4807	3385
0.08	3.4	4.9	5898	4225
0.10	2.6	3.6	6400	3265
0.15	1.9	2.6	7282	2844
0.20	1.4	2.7	4807	3136

Table 2.8: Effect of diethylamine composition in the mobile phase on the HPLC parameters of MPP and DPP (Mobile phase consisted of 55%v/v acetonitrile and adjusted to pH 2.0)

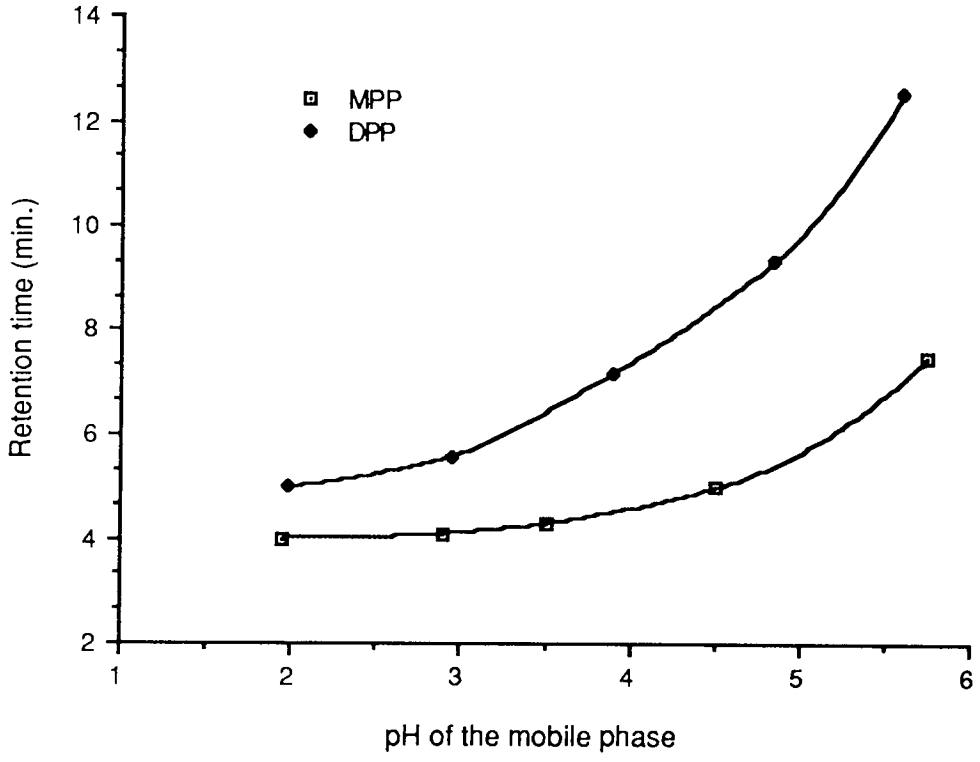

Fig. 2.11: The effect of pH of the mobile phase on the retention times of MPP and DPP

2.3.3. HPLC system for Pyrimethamine and the 6-carboxylate esters

As the length of the side chain increases, the lipophilicity of the molecule increases requiring greater concentrations of acetonitrile in the mobile phase for elution.

Concentration of acetonitrile ranging from 30%$^{v}/_{v}$ to 55%$^{v}/_{v}$ were prepared and adjusted to pH 2.0. Again, in order to reduce the lengthy assay times, 0.10%$^{v}/_{v}$ diethylamine was added to each concentration of acetonitrile.

Fig. 2.12 shows how acetonitrile concentration affects the retention times of Py, MDPC, EDPC, PDPC and iPDPC. At low levels of acetonitrile (<40%$^{v}/_{v}$) the retention times of iPDPC became very long whereas concentrations greater than 45%$^{v}/_{v}$ resulted in interference of pyrimethamine peak with the solvent front.

At 40%$^{v}/_{v}$ acetonitrile, the retention times and capacity ratios are high when the concentration of diethylamine is below 0.06%$^{v}/_{v}$ (Fig. 2.13 and Table 2.11). There is only marginal improvement in the chromatography when the diethylamine concentration is in excess of 0.1%$^{v}/_{v}$. Fig. 2.14 displays chromatograms at low (A) and high (B) concentrations of diethylamine and the improvement in the chromatogram at the higher concentration.

As with MPP and DPP, these compounds are also affected by the pH of the mobile phase (Fig. 2.15). Again these are weakly basic compounds and decreases in pH leads to ionisation and a consequent decrease in the retention times. The HPLC parameters are listed in Tables 2.9 and 2.10 and the internal standards listed in Table 2.11.

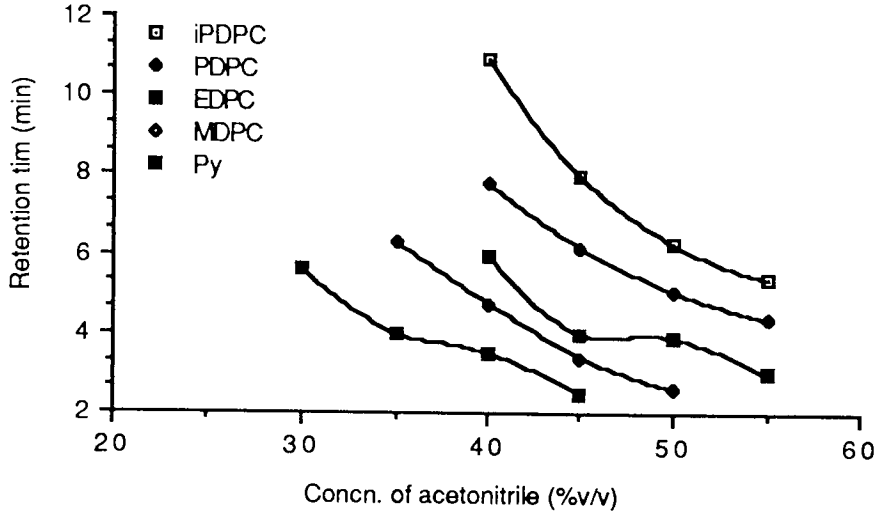

Fig. 2.12: The effect of acetonitrile on the retention timesof Py, MDPC, EDPC, PDPC and iPDPC (0.1%v/v diethylamine)

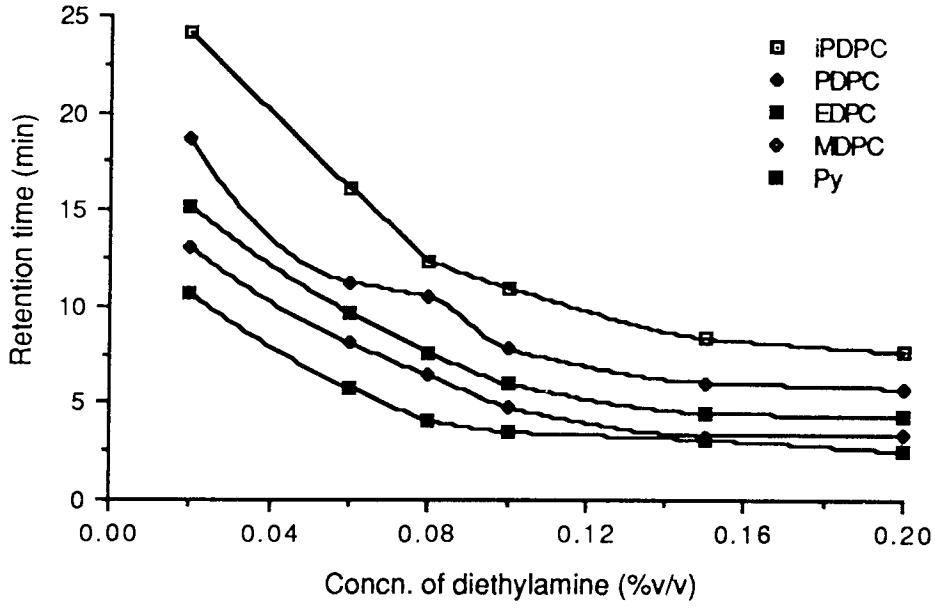

Fig. 2.13: The effect of diethylamine concentration on the retention times of Py, MDPC, EDPC, PDPC and iPDPC (40%v/v acetonitrile)

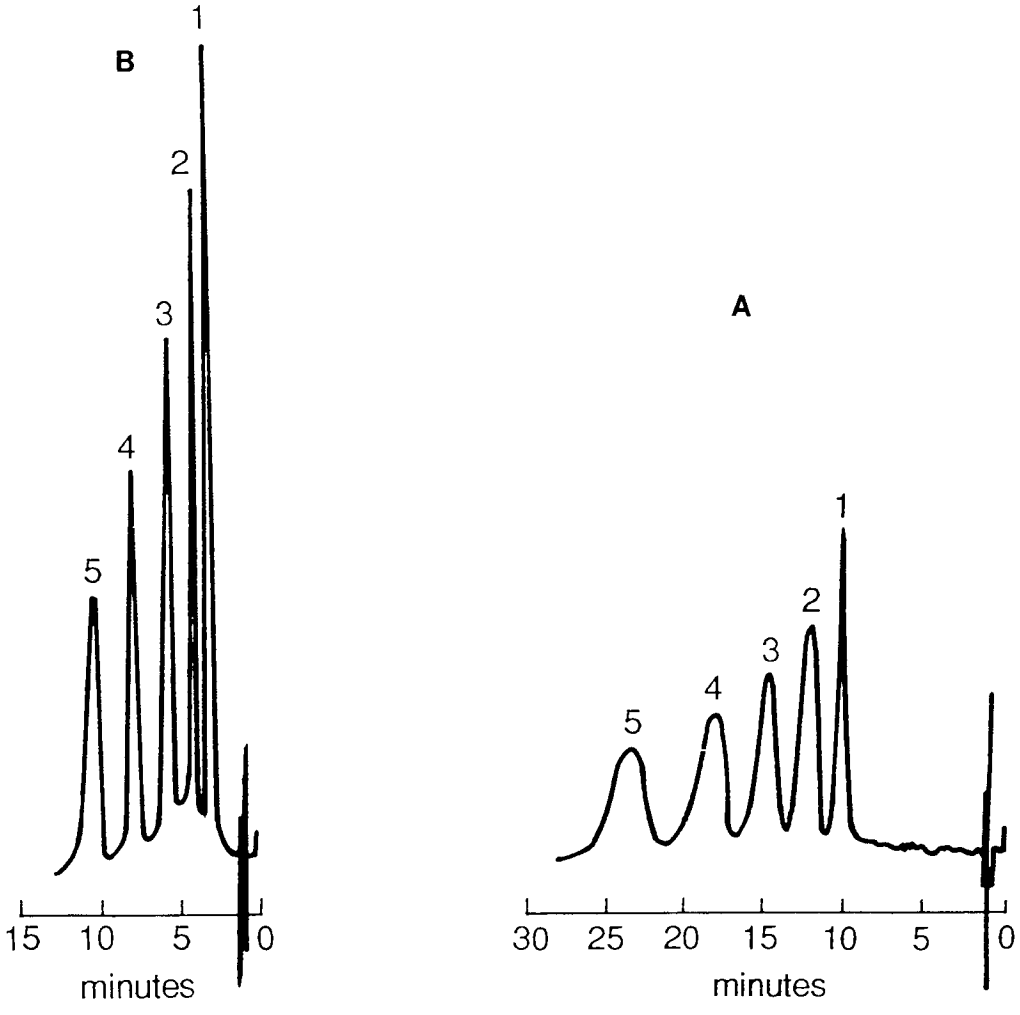

Fig. 2.14: HPLC chromatograms to show the effect of diethylamine on the separation of Py (1), MDPC (2) EDPC (3), PDPC (4) and iPDPC (5).
A. 40%v/v acetonitrile + 0.02%v/v diethylamine
B. 40%v/v acetonitrile + 0.10%v/v diethylamine

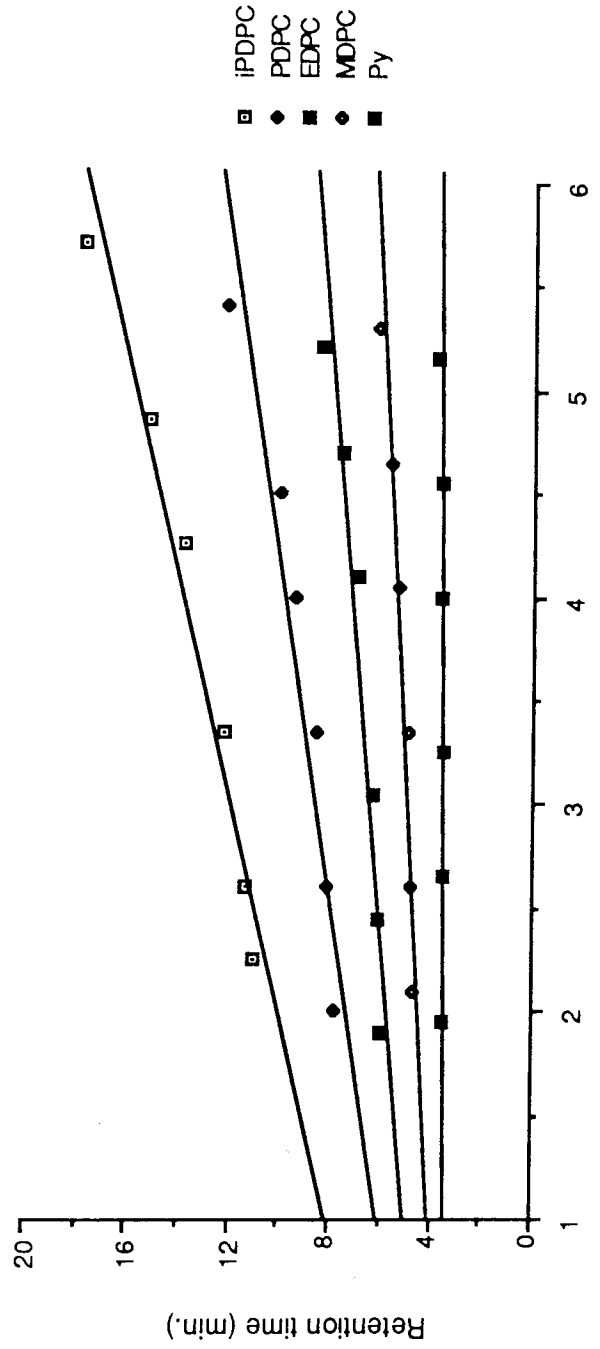

Fig. 2.15: The effect of pH on the retention times of Py, MDPC, EDPC, PDPC and iPDPC

Conc^{n}. of acetonitrile (%^{v}/v)	Capacity Ratio, K'					Theoretical plates, N					Resolution, R_S			
	Py	MDPC	EDPC	PDPC	iPDPC	Py	MDPC	EDPC	PDPC	iPDPC	Py+MDPC	MDPC+EDPC	EDPC+PDPC	PDPC+iPDPC
30	2.73	-	-	-	-	8028	-	-	-	-	-	-	-	-
35	1.67	3.20	-	-	-	11378	7056	-	-	-	1.02	-	-	-
40	1.33	2.17	3.00	4.20	6.33	19600	9025	4702	4807	3025	0.83	0.92	0.95	0.89
45	0.67	1.27	2.29	3.13	4.33	10000	8220	4444	5021	4096	0.36	0.88	0.89	0.77
50	-	0.73	1.60	2.40	3.20	-	10816	6084	4624	5184	-	0.87	0.88	0.67
55	-	-	1.00	1.93	2.60	-	-	3600	7744	5184	-	-	0.80	0.40

Table 2.9: The effect of acetonitrile concentration on the HPLC parameters of Py, MDPC, EDPC, PDPC and iPDPC (0.1% v/v diethylamine added to the mobile phase and the pH adjusted to 2.0)

Conc^{n}. of diethylamine (%^{v}/$_{v}$)	Capacity Ratio, K'					Theoretical plates, N				
	Py	MDPC	EDPC	PDPC	iPDPC	Py	MDPC	EDPC	PDPC	iPDPC
0.02	6.13	7.73	9.13	11.47	15.13	7327	6499	5116	5595	5997
0.06	2087	4.40	5.47	6.53	9.80	8612	5184	4182	4170	4653
0.08	1.73	3.27	4.07	6.00	7.27	6724	7282	4564	4900	3405
0.10	1.33	2.17	3.00	4.20	6.33	8711	9025	4702	4807	3025
0.15	1.07	1.20	2.00	3.07	4.60	6834	7744	5184	4860	3732
0.20	0.67	1.27	1.87	2.87	4.13	10000	8269	7396	5980	4685

Table 2.10: The effect of diethylamine concentration on the HPLC parameters of Py, MDPC, EDPC, PDPC and iPDPC (40% v/v acetonitrile added to the mobile phase and the pH adjusted to 2.0)

2.3.4 Internal standards

The use of 2-amino-5-bromo-6-(3-fluorophenyl)-4(3H)-pyrimidinone (ABmFPP) has been suggested perviously by Alpar *et.al.* for use as an internal standard for bropirimine[77]. The parabens are frequently used in internal standards. Table 2.11 gives some chromatographic details of these compounds for use as internal standards in the mobile phases listed.

Compound	Mobile Phase	Retention time (Mins)	Capacity factor K'
ABmFPP	1	3.75	2.47
Methylparaben	2	2.51	1.32
Ethylparaben	3	2.75	1.56
Propylparaben	3	3.27	2.03

Table 2.11: HPLC parameters of some compounds suitable as internal standards

HPLC conditions

Flow rate = 1 mL/min

Detection = 300 nm

Sensitivity = 0.64 AUFS

Mobile phase 1	Mobile phase 2	Mobile phase 3
30%$^{v}/_{v}$ acetonitrile	40%$^{v}/_{v}$ acetonitrile	50%$^{v}/_{v}$ acetonitrile
0.1%$^{v}/_{v}$ diethylamine	0.1%$^{v}/_{v}$ diethylamine	0.1%$^{v}/_{v}$ diethylamine
pH 2.0	pH 2.0	pH 2.0

Although the recommended mobile phases are quoted for each set of compounds, minor adjustments were made according to the experiments. Similarly, the internal standard was chosen according to the mobile phase used and the experiment in question.

2.3.5 Construction of calibration curves

Stock solutions of 0.20mg/mL in methanol were prepared of each compound. A series of dilutions were then prepared from these, using methanol, so that calibration curves could be constructed. 1mL of each of the dilution was then added to 1mL of internal standard, thoroughly vortexed and 20μL injected into the HPLC.

For Py, MPP and DPP, stock solutions of 1.0 mMoles were prepared in methanol, and these were then serially diluted.

Fig. 2.16 to 2.18 show the linearity of the calibration curves for each of the compounds, constructed by plotting the peak heights against concentration. The statistical parameters for each of the lines were calculated by linear line regression analysis programme using a CASIO fx 180p scientific calculator, and the results recorded in Table 2.12.

Good linearity is obtained for each of the compounds using methanol as the solvent.

Compound	Intercept, C	Gradient, M	Correlation coefficient, r
Bropirimine	7×10^{-3}	10.14	0.9999
AB	-0.028	6.72	0.9998
PB	0.040	12.69	0.9995
MDPC	0.037	9.05	0.9996
EDPC	0.042	8.54	0.9997
PDPC	0.234	6.46	0.9993
iPDPC	0.070	5.57	0.9996
MPP	0.777	9.04	0.9969
DPP	0.864	10.37	0.9963
Pyrimethamine	0.260	9.82	0.9999

Table 2.12: Statistical parameters for the calibration graphs of the three groups of compounds

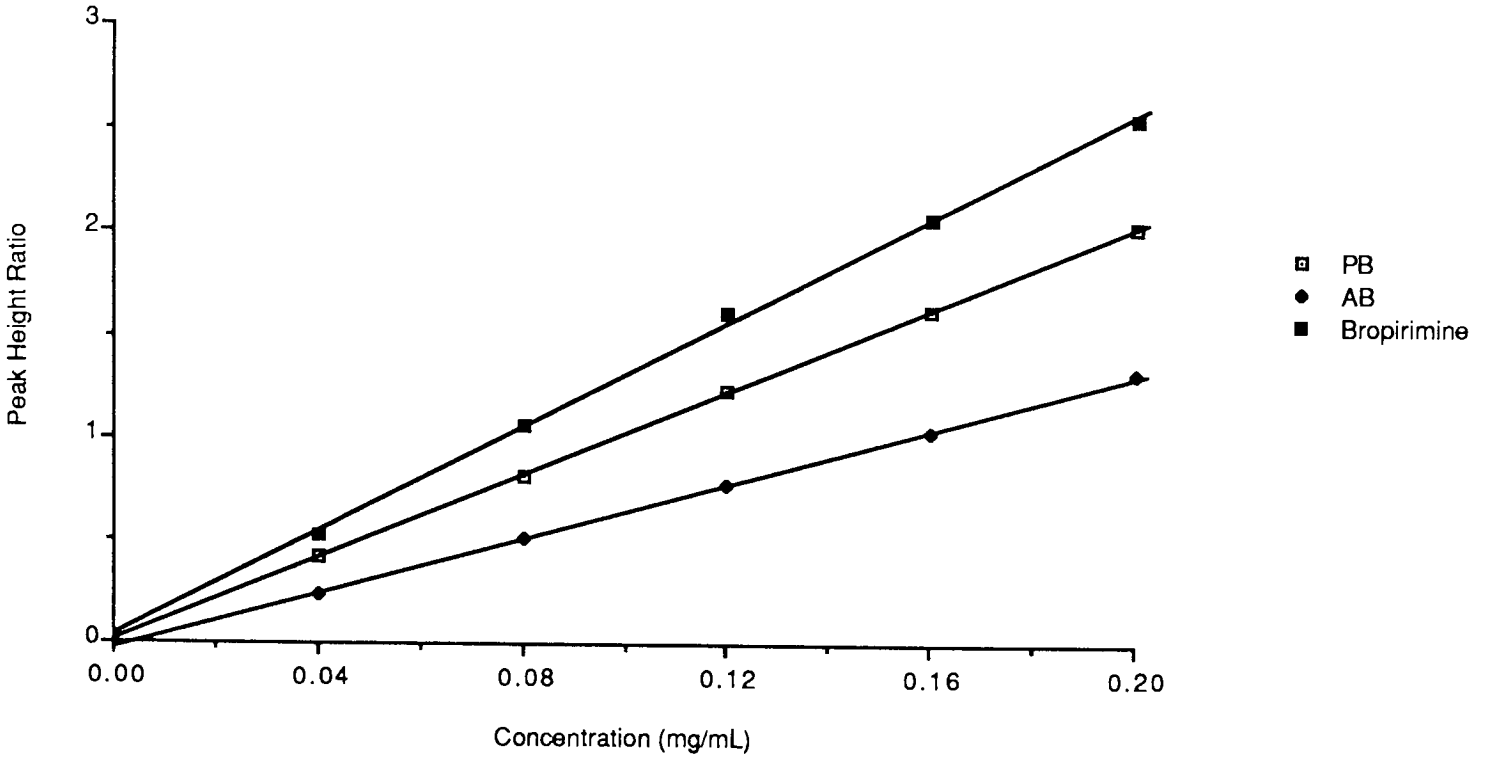

Fig. 2.16: Calibration curves of bropirimine, AB and PB

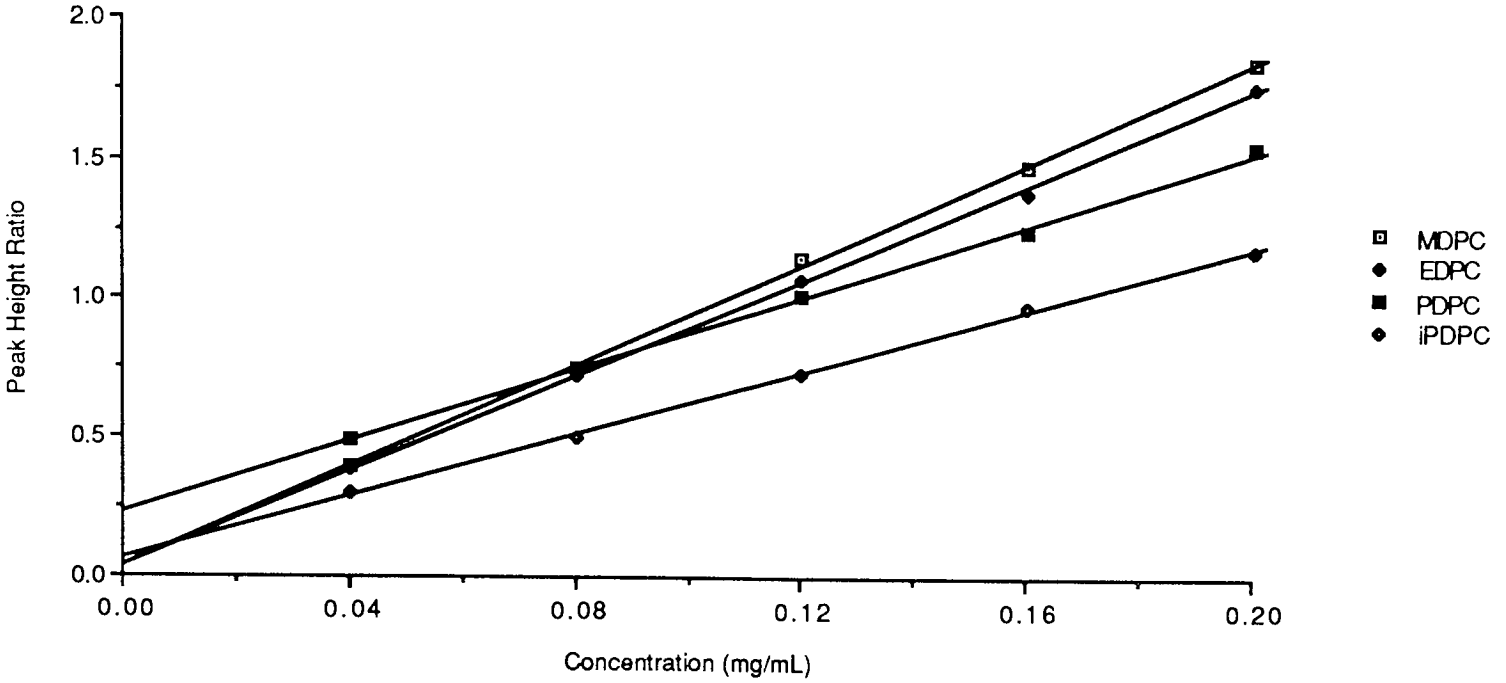

Fig 2.17: Calibration curves for MDPC, EDPC, PDPC and iPDPC

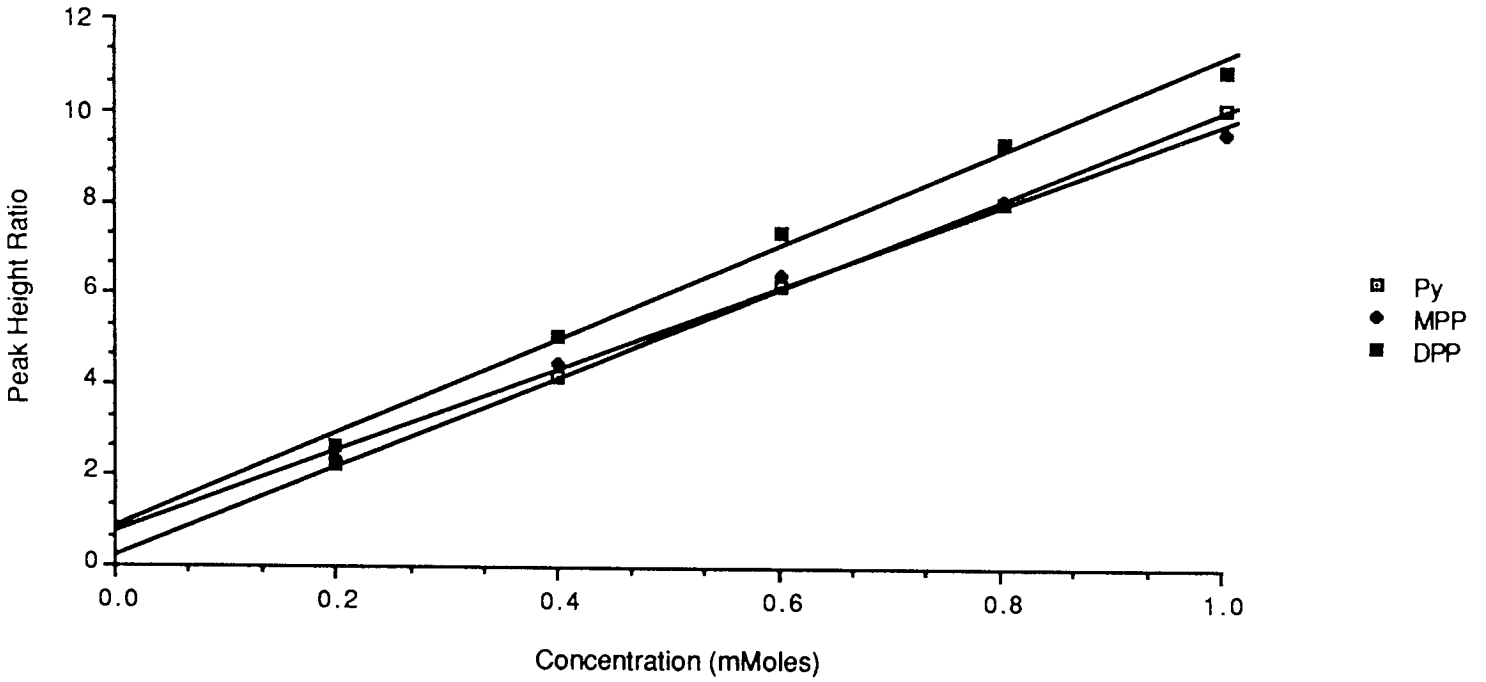

Fig 2.18: Calibration curves for Py, MPP and DPP

3.0 KINETICS OF DEGRADATION

3.1 Introduction

Stability prediction is of paramount importance when considering formulation of labile drugs. A prodrug may be defined as a chemical entity, usually inactive, which breaks down to yield the parent (active) drug. The prodrug can be tailor-made depending on the requirement, e.g. increased solubility, altered stability and lipophilicity[227]. This approach thus takes on added importance when considering stability in that the limiting step for pharmacological activity may be the breakdown of the prodrug to the parent compound.

The most common degradative pathway exhibited by drugs in aqueous solution is hydrolysis. This can be catalysed by hydrogen ions (specific acid catalysed reaction) or hydroxyl ions (specific base catalysed reaction). Non-ionised water molecules may also be responsible for the breakdown of a drug in which case the reaction is solvent catalysed.

Depending on the type of compound in question, the overall velocity of degradation, in most cases, may be obtained from one or more of the following schemes:

$$D + H_2O \xrightarrow{k_1} \text{Products} \qquad \text{scheme 3.1}$$

$$D + H^+ \xrightarrow{k_2} \text{Products} \qquad \text{scheme 3.2}$$

$$D + OH^- \xrightarrow{k_3} \text{Products} \qquad \text{scheme 3.3}$$

Schemes 3.2 and 3.3 refer to specific acid or base catalyed hydrolysis respectively. The overall observed rate constant, k_{obs}, will be a function of k_1, k_2 and k_3. If the reaction involved all the above three schemes , i.e. if the

solvent catalysis had a role to play in the overall hydrolysis, then the rate expression for the reaction would be:

$$\frac{-dD}{dt} = \left[k_1 + k_2[H^+] + k_3[OH^-] \right] \times [D] \qquad \ldots 3.1$$

Where: $\frac{-dD}{dt}$ is the rate of disappearance of the drug.

[D] is the concentration of the drug.

In the absence of solvent catalysis, equation 3.1 reduces to:

$$\frac{-dD}{dt} = \left[k_2[H^+] + k_3[OH^-] \right] \times [D] \qquad \ldots 3.2$$

And $$k_{obs} = k_2 \left[H^+\right] + k_3 \left[OH^-\right] \qquad \ldots 3.3$$

A plot of log k_{obs} against pH generally yields a 'V' type plot from which the pH of maximum stability can be estimated.

For monobasic and acidic drugs, the above relationship is complicated due to ionisation and can be represented by equation 3.4:

$$k_{obs} = \left\{ k_1 + k_2[H^+] + k_3[OH^+] \right\} \frac{K_a}{K_a + H^+} + \left\{ k_4 + k_5[H^+] + k_6[OH^-] \right\} \frac{H^+}{K_a + H^+} \qquad \ldots 3.4$$

Where: k_4, k_5 and k_6 are rate constants of the ionised species,

K_a is the dissociation constant.

The aim of this chapter was to study the chemical degradation of both bropirimine derivatives (2-N-acetyl and 2-N-propanoyl) and the pyrimethamine (2 and 4-acyl and 6-carboxylates) derivatives.

3.2 Materials and methods

3.2.1 Chemical degradation of bropirimine prodrugs: Britton - Robinson (B-R) buffers were prepared as described in Appendix I and the ionic strength of each adjusted to 0.5M with potassium chloride.

A 2mg/mL solution of either 2-N-acetyl bropirimine (AB) or 2-N-propanoylbropirimine (PB) was prepared in dimethylacetamide (DMA, Fisons). 1mL of this solution was then transferred to a 100mL flask and made up to volume with pre-heated (37-80°C) buffer of the required pH (2.1-11.2). The contents were vigorously shaken, a small magnetic flea inserted, and the flask mounted on an underwater stirrer in a constant-temperature water-bath equilibrated at the desired temperature (37-80°C), and the clock started. 1mL samples were then withdrawn at various time intervals and added to 1mL of the internal standard (5μg/mL ABmFPP in DMA). The analytes were well mixed using a vortex mixer and 20μL injected into the HPLC.

The standard solutions were prepared in the same manner as the test and in the same concentration range. 1mL of a 2mg/mL solution of the drug (AB or PB), prepared in DMA, was transferred to a 100mL flask and made up to volume with B-R buffer pH 7.0 pre-heated to the appropriate temperature. This was then serially diluted with 1%$^{v}/_{v}$ DMA in B-R buffer pH 7.0, pre-heated as above, to give a concentration range between 20μg/mL and 2μg/mL. Again 1mL of this solution was added to 1mL of the internal standard, thoroughly mixed and 20μL injected into HPLC once steady state-conditions had been reached.

HPLC Conditions

Mobile phase	:	30%$^{v}/_{v}$ acetonitrile
		0.1%$^{v}/_{v}$ diethylamine
		adjusted to pH 2.0 with orthophosphoric acid
Flow rate	:	1 mL/min
Chart speed	:	2mm/min
Wavelength	:	300nm
Sensitivity	:	0.04 AUFS

3.2.2 Degradation of 2/4 substituted pyrimethamine

3.2.2.1 Degradation of 2-N-propanoylpyrimethamine (MPP)

40 mg of MPP were accurately weighed and dissolved in 20mL of dimethylacetamide (DMA) with the aid of a sonic bath (≡ 2 mg/mL). 10 mL of this solution were then transferred to a 100 mL flask and made up to volume with B-R buffer pH 2.0 pre-heated to 60°C (final concentration of MPP ≡ 200µg/mL). The contents were thoroughly shaken, a magnetic flea added to the flask and then mounted on an underwater stirrer in a constant temperature water bath, pre-equilibrated at 60°C such that the content was constantly stirred at the desired temperature. At various time intervals, 1mL samples were withdrawn and added to 1mL of internal standard (4µg/mL ethyl paraben) prepared in equimixture of methanol and distilled water. The two components were well mixed with a vortex mixer and 20µL injected into the HPLC once steady state conditions had been reached.

The calibration solutions were prepared in a similar way. 20mg of MPP were dissolved in 10mL of DMA and thoroughly mixed. 1mL of this solution was then transferred to a 10mL flask and made up to volume with B-R buffer pH 2.0 pre-heated to 60°C. This was serially

diluted with 10%$^{v}/_{v}$ DMA in B-R buffer pH 2.0, at the same temperature, to give a concentration range 200µg/mL to 20µg/mL. 1mL of the calibration solution was finally added to 1mL of the internal standard and treated as above (3.2.1).

HPLC Conditions

Mobile phase	:	55%$^{v}/_{v}$ acetonitrile
		0.1%$^{v}/_{v}$ diethylamine
		adjusted to pH 2.0 with orthophosphoric acid
Flow rate	:	1mL/min
Chart speed	:	2mm/min
Wavelength	:	272nm
Sensitivity	:	0.16 AUFS

3.2.2.2 Degradation of 2, 4-N, N-dipropanoylpyrimethamine (DPP)

Britton-Robinson buffers were prepared as shown in Appendix I. A stock solution of DPP (0.4mg/mL) was prepared in DMA. 5mL of this solution was transferred to a 100mL flask and further 10mL of DMA added to ensure that DPP stayed in solution (due to its poor solubility in alkaline environment). The volume was made up to 100mL with B-R buffer of the required temperature and pH. Again, the contents were vigorously shaken and analysis undertaken as described in section 3.2.2.1. The standard solutions were also prepared as in section 3.2.2.1., except that serial dilutions were carried out using 15%$^{v}/_{v}$ DMA.

Experiments to ascertain the pH dependency were conducted at 60°C whereas the temperature dependent degradation was carried out at a pH of 11.2.

HPLC Conditions

Mobile phase : 55%$^{v}/_{v}$ acetonitrile

0.1%$^{v}/_{v}$ diethylamine

adjusted to pH 2.0 with orthophosphoric acid

Flow rate : 1mL/min

Chart speed : 2mm/min

Wavelength : 300nm

Sensitivity : 0.02 AUFS

3.2.3 Degradation of 6-carboxylate ester analogues of pyrimethamine

Degradation of these compounds was followed using a similar method to that described in Section 3.2.2.1.

Solutions (0.4mg/mL) of each of the carboxylates (methyl, ethyl, propyl and isopropyl) were accurately prepared in DMA. 5mL of this solution was transferred to a 100mL flask and made up to volume with the B-R buffer at the required temperature and pH (final concentration of each = 20µg/mL). A magnetic flea was then added to the flask and mounted on an underwater stirrer. 1mL samples were withdrawn at different time intervals and added to 1mL of internal standard. The contents were thoroughly mixed and treated as in Section 3.2.2.1.

Standard solutions of each of the drugs were prepared by dissolving 200mg in 50mL of DMA (= 0.4mg/mL). 1mL of this was then transferred to a 20mL volumetric flask and made up to volume with B-R buffer. Serial dilutions were prepared by using 5%$^{v}/_{v}$ DMA in B-R buffer to give a concentration range 20µg/mL to 2µg/mL. These were subsequently treated as described above (3.2.1).

HPLC Conditions

Mobile phase	:	40%$^{v}/_{v}$ acetonitrile
		0.1%$^{v}/_{v}$ diethylamine
		adjusted to pH 2.0 with orthophosphoric acid
Flow rate	:	1mL/min
Chart speed	:	2mm/min
Wavelength	:	296nm
Sensitivity	:	0.01 AUFS

Internal standards

The internal standards were prepared in equimixture of methanol and water to give a concentration of 0.5mg/mL.

Carboxylic ester	Internal standard
Methyl	Ethyl paraben
Ethyl Propyl i-propyl	Methyl paraben

3.3 Results and discussion

3.3.1 Degradation of bropirimine derivatives

3.3.1.1 Effect of temperature

The parent compound, bropirimine, appears to be very stable under both acidic and basic conditions. Even under extreme conditions, such as refluxing in Britton-Robinson buffers pH 2.0 and 10.0 for over 2 hours, HPLC analysis did not indicate a reduction in the bropirimine peak nor the appearance of any extra peaks. Under similar conditions, both acetylbropirimine (AB) and propanoylbropirimine (PB) showed evidence of breakdown and these were subjected to further study.

Fig. 3.1 and 3.2 show the progress of hydrolysis, plotted as first-order reactions, of AB and PB in Britton-Robinson buffer pH 10.0 at various temperatures (37-80°C).

Linear plots are obtained at each temperature when ln (% remaining) is plotted against time. It is also apparent that the order of the degradation process is unaffected by temperature. The high pH of the experiment ensured, firstly that no solubility problems arose, and secondly, to increase the rate of degradation and hence shorten the experimental time. Table 3.1 shows the first order rate constants for acetyl- and propanoylbropirimine obtained from the slopes of the plots in Fig. 3.1 and 3.2.

HPLC analysis showed that each of the compounds hydrolysed to yield a product which co-eluted with a standard solution of bropirimine.

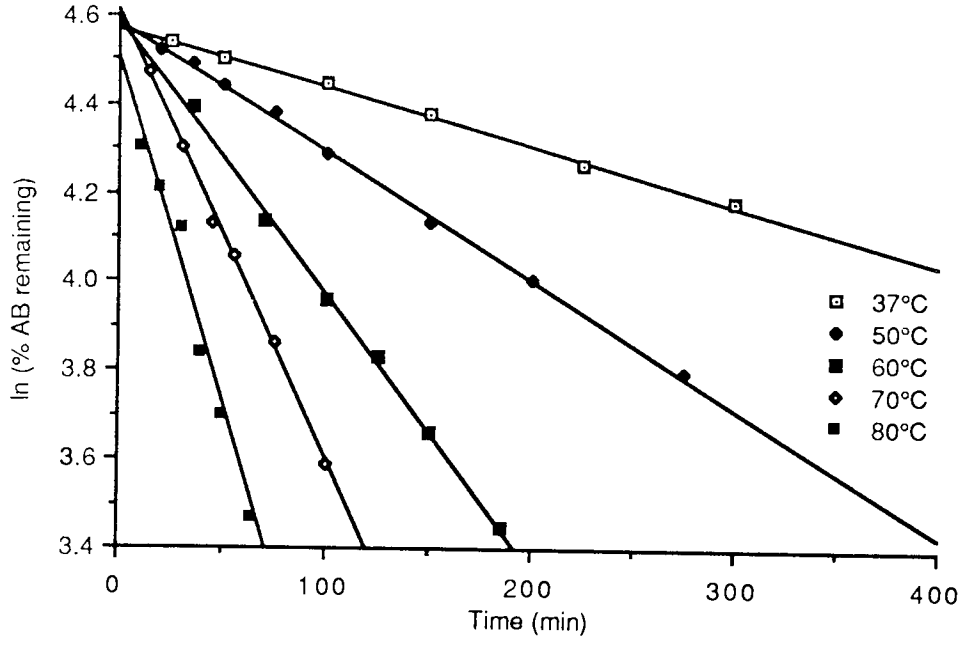

Fig. 3.1: Temperature-dependent hydrolysis of acetylbropirimine (AB) in B-R buffer pH 10.0

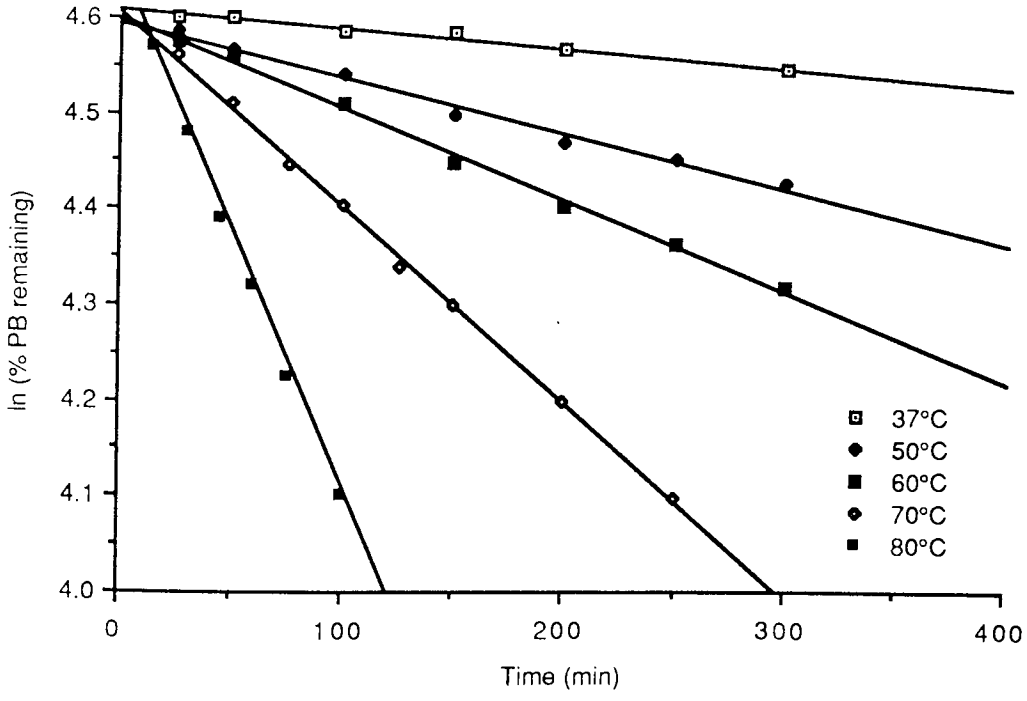

Fig. 3.2: Temperature-dependent hydrolysis of propanoylbropirimine (PB) in B-R buffer pH 10.0

Applying the Arrhenius equation to the hydrolysis of AB and PB:

$$k_{obs} = A.e^{-\frac{E_a}{RT}} \qquad \ldots 3.5$$

where: A is the frequency factor

E_a is the energy of activation

R is the molar gas constant

T is the temperature (in K)

Logarithmic transformation gives the linear form:

$$\ln k_{obs} = \ln A - \frac{E_a}{RT} \qquad \ldots 3.6$$

A plot of ln k_{obs} against $^1/_T$ should yield a straight line having a slope of Ea/R and an intercept of ln A. Such plots are invaluable for obtaining stability data at a particular temperature and may be extrapolated to obtain the stability at, say, room temperature.

Temperature (°C)		k x 10^{-3} (/min)	
		Acetylbropirimine	Propanoylbropirimine
37	(310K)	1.30	0.17
50	(323K)	2.95	0.60
60	(333K)	8.00	0.95
70	(343K)	9.87	2.37
80	(353K)	24.50	5.20

Table 3.1: First order rate constants for the degradation of acetyl- and propanoylbropirimine at different temperatures

Fig. 3.3 shows plots according to equation 3.6 for the two derivatives of bropirimine. At each of the temperatures in the range investigated, PB consistently shows a lower rate of degradation compared to AB. Calculation of the activation energies, from the slope in equation 3.6, gives values for AB as 6.08×10^4 J/Mol (A = 2.24×10^7/min) and 7.06×10^4 J/Mol (A = 1.40×10^8/min) for PB.

The half-life, $t_{1/2}$, values were calculated from the k_{obs} and the results listed in Table 3.2. Comparison of half-lives of the two compounds show considerable difference at all temperatures. These results clearly indicate that a larger side chain length at the C-2 position of bropirimine leads to a more stable compound. This could possibly be due to an inductive reduction in carbonyl reactivity and to steric hindrance to the approaching nucleophile. No further compounds having longer chain lengths were synthesised on the basis of the long half-lives of AB and PB (Table 3.2).

3.3.1.2 Effect of pH on the aqueous degradation of AB

Rate constant-pH profiles afford information that facilitates the optimum formulation of the drug with respect to stability. These profiles also yield information which can be used to predict the degradative fate of the drug on oral administration.

Fig. 3.4 shows the effect of pH on the hydrolysis of AB in Britton-Robinson buffers (ionic strength 0.5M) conducted at 60°C. As with the temperature-dependent hydrolysis of AB (Fig. 3.1), first order degradation is also displayed in the pH range 2.1 to 11.2. The observed rate constant, k_{obs}, at each pH value was calculated from the slopes of the plots in Fig. 3.4 by statistical regression analysis using a CASIO fx-3600p Scientific calculator. The correlation coefficients for all the pH values were greater than 0.98.

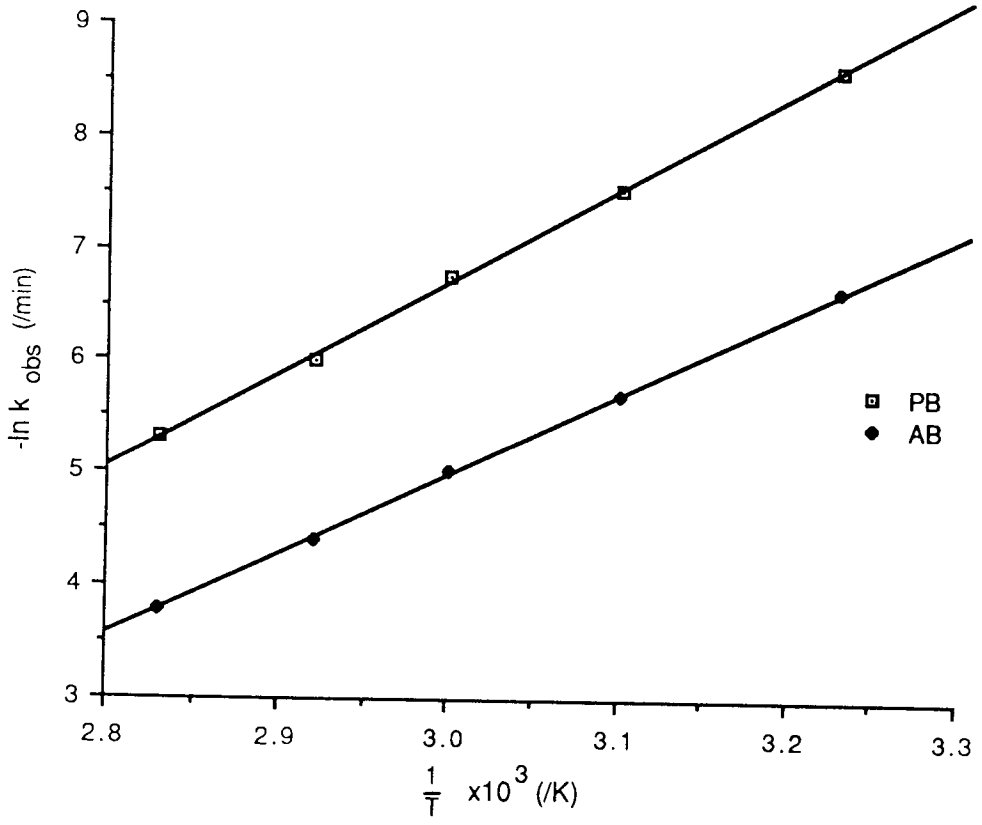

Fig. 3.3: Arrhenius plots for acetyl- and propanoylbropirimine at pH 10.0.

Temperature (°C)	$t_{1/2}$ (min)	
	Acetylbropirimine	Propanoylbropirimine
37 (310K)	533	4077
50 (323K)	235	1155
60 (333K)	87	707
70 (343K)	70	293
80 (353K)	28	133

Table 3.2: Half-lifes of acetylbropirimine and propanoyl bropirimine at various temperatures in Britten-Robinson buffer pH 10.0

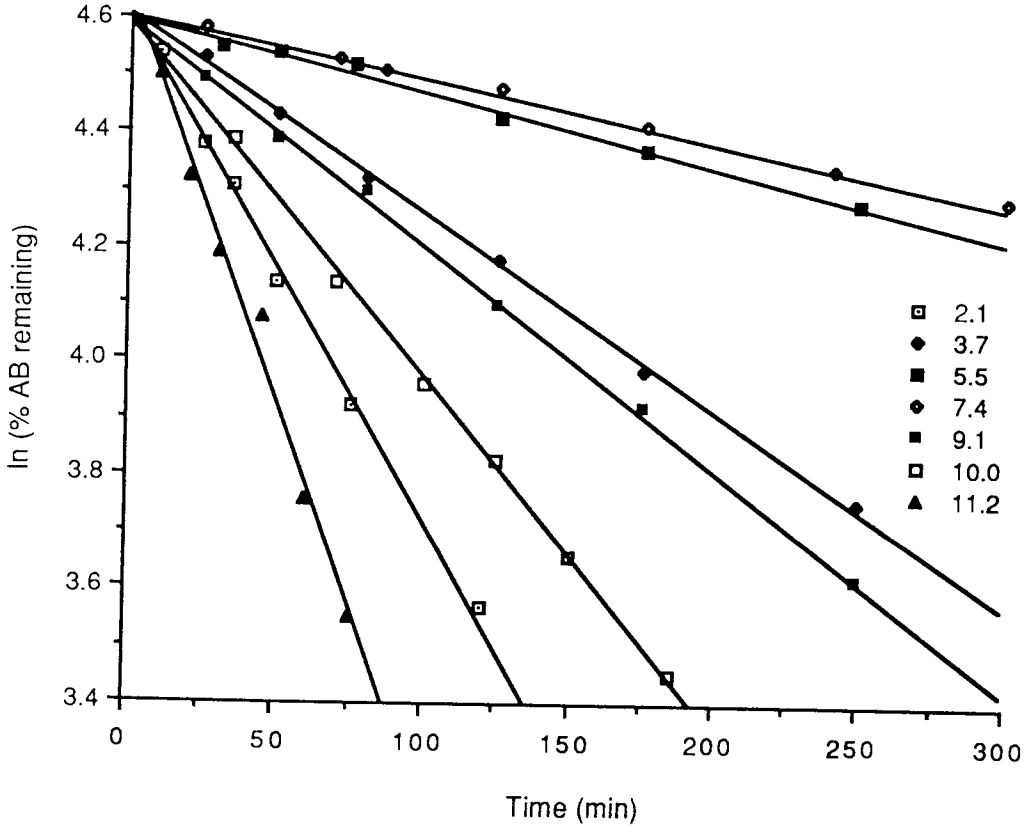

Fig. 3.4: The effect of pH on first-order degradation of acetylbropirimine at 60°C

At low pH values, the acetylbropirimine is mostly present in the undissociated form. The hydrogen ion concentration will predominate over the hydroxyl ion concentration and under such conditions, the hydrolysis will predominently be due to hydrogen ion catalysis. Thus equation 3.3 will reduce to:

$$k_{obs} = k_2[H^+] \quad \ldots 3.7$$

or $$\log k_{obs} = \log k_2 - pH \quad \ldots 3.8$$

Also, $$k_{obs} = k_2 a_H \quad \ldots 3.9$$

Where: a_H is the hydrogen ion activity.

A plot of k_{obs} against pH should therefore yield a linear relationship and Fig. 3.5 proves that this indeed is so, having a correlation coefficient of 0.999. Below pH 5, the rate of hydrolysis increases with decreasing pH in accordance with equation 3.8. From the intercept the acid catalysed rate constant, k_2, was calculated as 3.07×10^{-2}/M/min. The slope had a value of 0.26 indicating that the reaction is not a straight forward specific acid catalysed hydrolysis but may also involve some contribution from other reactions (equation 3.4).

Extrapolation of the pH region 5-7 shows very low rate of degradation, possibly independent of pH, and resulting predominantly from water catalysed hydrolysis. Above pH 7, the rate of hydrolysis once again begins to increase as the pH increases.

At higher pH values, hydroxyl ions predominate and thus dictate the hydrolytic reaction. Equation 3.3 thus reduces to:

$$k_{obs} = k_3 [OH^-] \quad \ldots 3.10$$

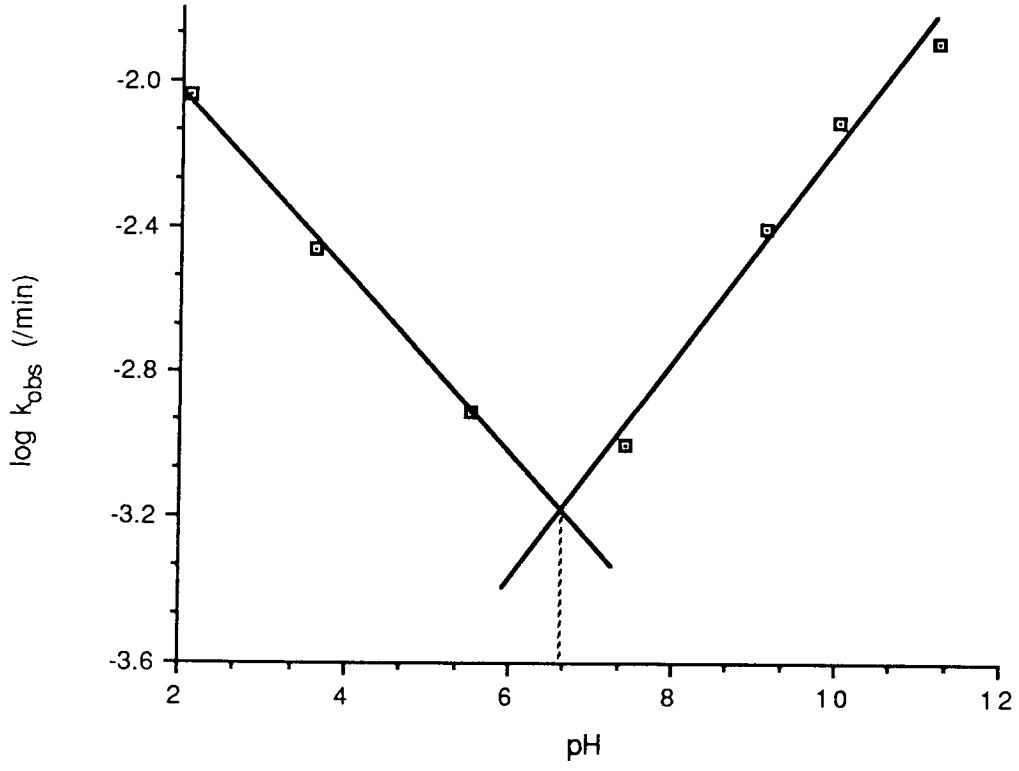

Fig. 3.5: Rate constant-pH profile of acetylbropirimine at 60°C (μ=0.5) in aqueous buffered solutions.

or, $k_{obs} = k_3 a_{OH}$ . . . 3.11

where a_{OH} is the hydroxyl ion activity.

And, $\log k_{obs} = \log k_3 + \log a_{OH}$ . . . 3.12

At 60°C, the hydroxyl ion activity may be calculated from the following equation[224]:

$$\log a_{OH} = pH - 13.02 \quad \ldots 3.13$$

The linear relationship is again seen in Fig. 3.5 ($r = 0.991$) for the basic region. A slope of 0.302 indicates that AB does not follow a simple specific base catalysed hydrolysis. The base catalysed rate constant, k_3, was estimated from the equation 3.12 as 5.58×10^{-2} /M/min.

Profiles such as these are not unique to AB but are displayed frequently by many compounds which do not share a common chemical structure [228-231].

Extrapolation of the lines in Fig. 3.5 gives the pH value at which AB is most stable (= 6.70). However, it is also possible to calculate this point as below. At this pH:

$$k_2 [H^+] = \frac{k_3 K_W}{[H^+]} \quad \ldots 3.14$$

where K_W = ionic product of water

Hence $$[H^+] = \sqrt{\frac{k_3 k_W}{k_2}} \quad \ldots 3.15$$

Using the values for k_2 and k_3 obtained from the above plots, the pH of maximum stability was calculated as 6.87. Hence the measured value agrees well with the calculated value.

The $t_{1/2}$ value of AB at each of the pH is calculated and displayed in Table 3.3. At the temperature of the experiment the $t_{1/2}$ of AB at pH 2.1 was 75 minutes. The most stable region for AB appears to be between pH 5 and pH 7 (Fig. 3.5).

Depending on the physical and emotional state of an individual, the gastric pH is within the range 1-2, with an average gastric emptying rate of about 50 minutes[233]. Under such conditions the conversion of AB to bropirimine would be slow resulting in poor oral bioavailability.

pH	$t_{1/2}$ of acetylbropirimine (/min)
2.1	75
3.7	201
5.5	564
7.4	693
9.1	173
10.0	87
11.2	52

Table 3.3: Half-lifes of acetylbropirimine and propanoyl bropirimine at various pHs in aqueous solutions at 60°C

3.3.2 Degradation of pyrimethamine derivatives

3.3.2.1 Degradation of 2/4-N-substituted pyrimethamines

The two 2-N-substituted pyrimethamine derivatives were 2-N-propanoylpyrimethamine (MPP, VII) and 2,4-N,N-dipropanoylpyrimethamine (DPP, VIII). The pK_a values of these compounds are 4.40 and 2.89 respectively (Chapter 5).

These weakly basic compounds have limited solubility in the alkaline region (Chapter 5). As an indication of the ease of hydrolysis of MPP, degradation was studied at pH 2.0 at 60°C in Britton-Robinson buffer (μ=0.5). Degradation under these conditions displayed a first order reaction, showing good linear relationship (r=0.9997) when ln(% MPP remaining) was plotted against time (Fig 3.6). The stable nature of MPP is apparent, having $k_{obs} = 4.34x10^{-3}$/h and a $t_{1/2}$ of 160h.

Temperature-dependent degradation of DPP follows a first order reaction over several half-lives giving linear plots (Fig. 3.7). DPP appears to be a much more thermo-labile molecule than the mono-substituted derivative MPP. This is reflected in the $t_{1/2}$ values (Table 3.4) which range from 5 minutes (80°C) to 99 minutes at 37°C. Application of the Arrhenius equation to DPP at these temperatures gives a linear plot (Fig. 3.8) having a correlation coefficient of 0.99. The activation energy, calculated from the slope of Fig. 3.8, gives a value of 62.5 kJ/Mol ($A=3.01x10^8$) which is somewhat lower than that for propanoylbropirimine (70.6 kJ/Mol) but compares well with acetylbropirimine (60.8 kJ/Mol).

Fig. 3.9 shows the dependence of the first order degradation on the pH of the aqueous environment for DPP. Hydroylsis occurs both in acidic and basic regions suggesting both acid and base catalysed degradation.

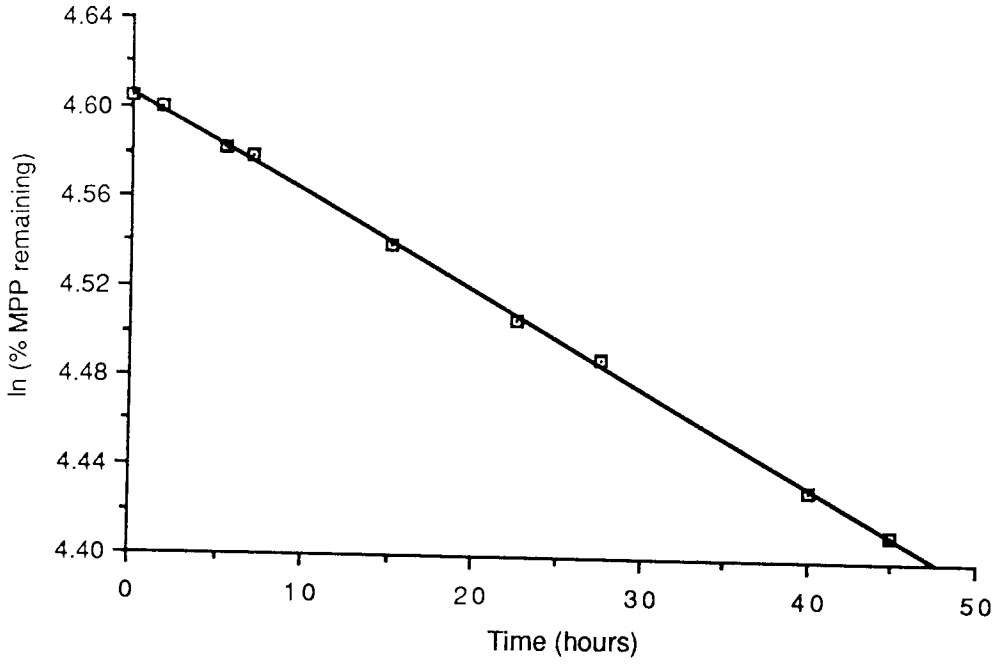

Fig. 3.6: Hydrolysis of monopropanoylpyrimethamine at 60°C and pH 2.0 in aqueous buffered solution (μ=0.5).

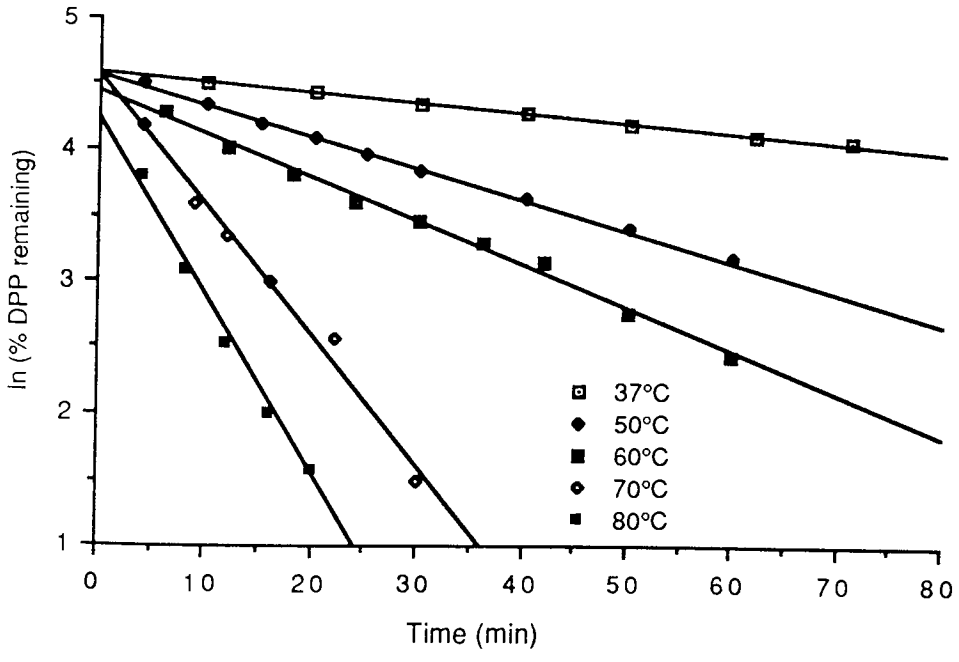

Fig. 3.7: Temperature-dependent hydrolysis of dipropanoylpyrimethamine (DPP) in aqueous buffered solution pH 11.2.

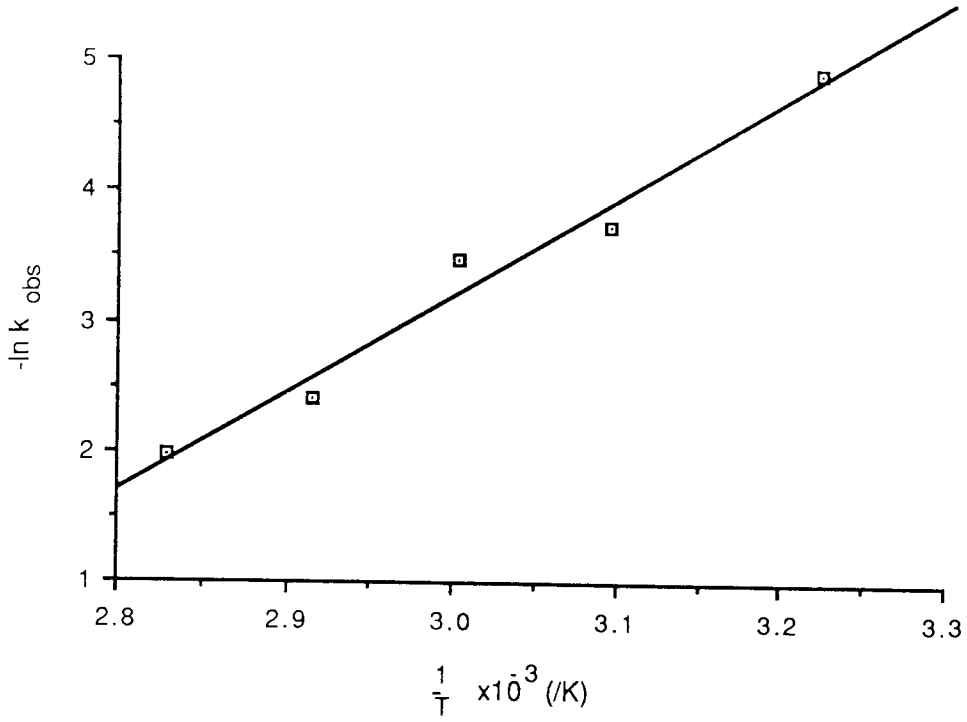

Fig. 3.8: Arrhenius plot for dipropanoylpyrimethamine in aqueous buffer pH 11.2.

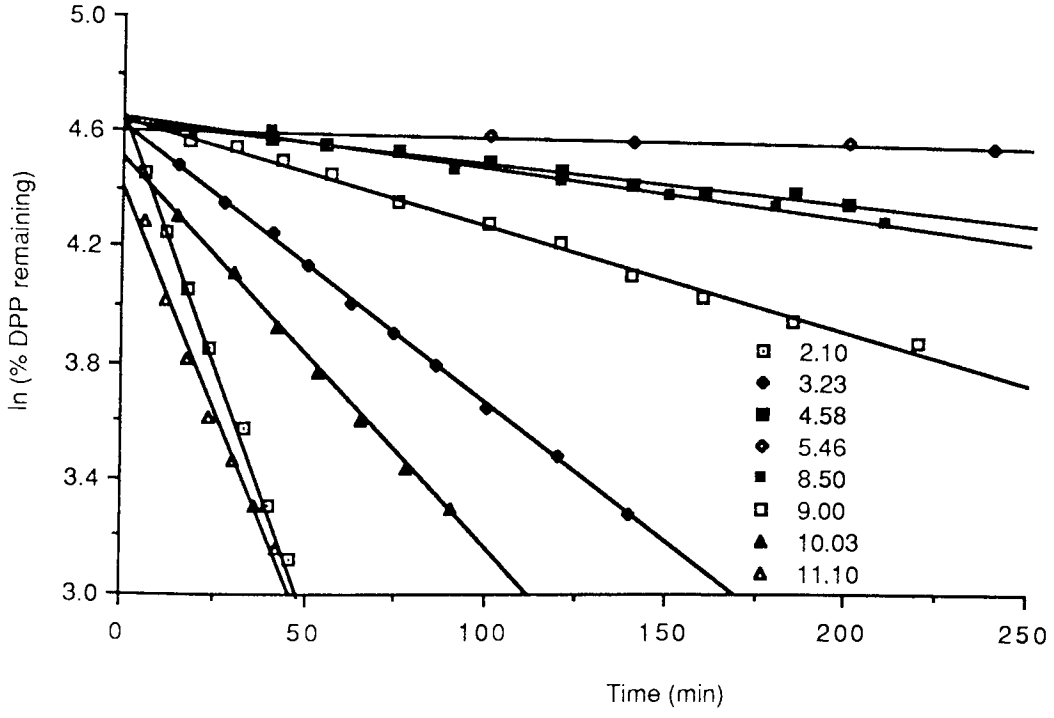

Fig. 3.9: The effect of pH on the first order degradation of dipropanoylpyrimethamine (DPP) at 60°C.

Temperature (°C)	$t_{1/2}$ (/min)
37	99.0
50	29.6
60	22.4
70	7.8
80	5.0

(a) at pH 11.1

pH	$t_{1/2}$ (/min)
2.1	21.1
3.23	72.7
4.58	550.0
5.46	3648.0
8.50	478.0
9.00	189.0
10.03	48.2
11.10	22.4

(b) at 60°C

Table 3.4: Half-lifes for DPP at different temperatures (a) and pH values (b)

Decreasing the pH leads to an increase in the rate of degradation (Fig. 3.10) giving a linear plot for $\log(k_{obs})$ against pH. Similarly increasing the pH in the basic region also leads to an increase in the rate of hydrolysis. From pH 4.5 to about 8.5 there appears to be little degradation and represents the most stable part of the profile. The respective rate constants were calculated as 1.01 /M/min for the acid-catalysed hydrolysis and 0.29 /M/min for the base-catalysed hydrolysis. Values for the slopes were 0.66 and 0.49 respectively indicating other possible contributions. The half-lives ranged from 21.1 minutes (pH 2.1) up to 3648 minutes (pH 5.46) as listed in Table 3.4. By extrapolation, the pH of maximum stability was estimated as 6.30 as compared with a value of 7.26 for the calculated value (from equation 3.15). The difference in the calculated and measured values may be due to the complex hydrolysis of the compound.

Fig. 3.11 shows the breakdown of DPP and the formation of MPP and pyrimethamine.

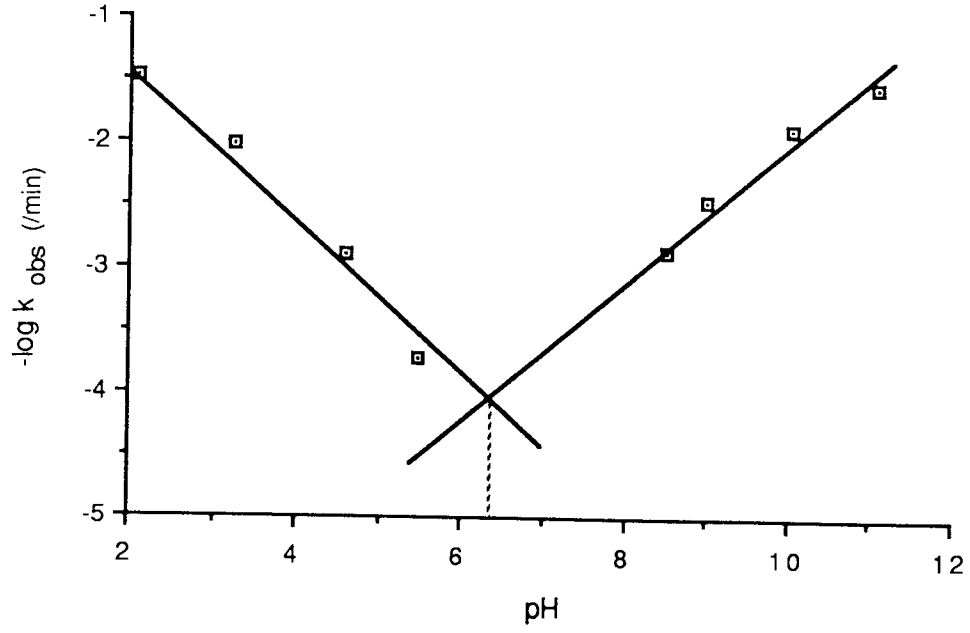

Fig. 3.10: Rate constant-pH profile of dipropanoylpyrimethamine at 60℃ in aqueous buffered solutions.

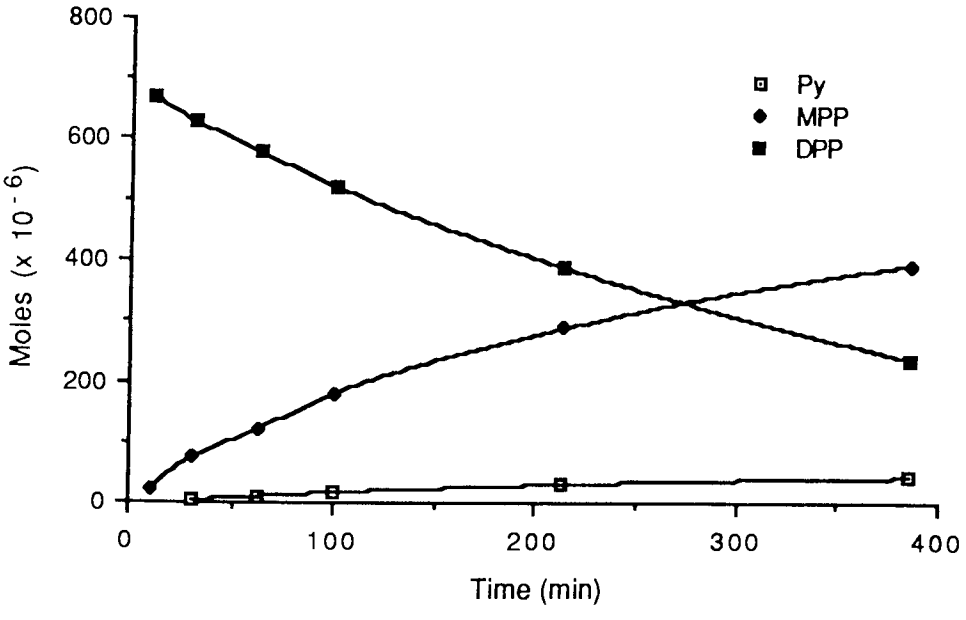

Fig. 3.11: Degradation of dipropanoylpyrimethamine (DPP) in aqueous buffer pH 2.62 at 50℃ and the formation of monopropanoyl-pyrimethamine (MPP) and pyrimethamine (Py).

For the reaction:

$$A \xrightarrow{k_a} B \xrightarrow{k_b} C$$

$$A_t = A_o\, e^{-k_a t} \qquad \ldots 3.16$$

$$B_t = \frac{A_o\, k_a}{k_b - k_a} \cdot \left[e^{-k_a t} - e^{-k_b t} \right] \qquad \ldots 3.17$$

$$C_t = A_o \left[1 - \frac{k_b e^{-k_a t} - k_a e^{-k_b t}}{k_b - k_a} \right] \qquad \ldots 3.18$$

These models were used for the theoretical lines in Fig. 3.11. Fig. 3.12 shows the HPLC chromatograms to confirm the presence of MPP and pyrimethamine using 55% $^{V}/_{V}$ acetonitrile in the mobile phase.

3.3.2.2 Degradation of 6-carboxylate ester analogues of pyrimethamine

3.3.2.2.1 Effect of temperature on degradation: These were synthesised by esterification of the 6-carboxylic acid and the general structure is shown in Chapter 2.

Fig. 3.13 to 3.16 show degradation of MDPC, EDPC, PDDC and iPDPC in aqueous buffered solutions pH 11.2 at a number of different temperatures. Also the esters consistently demonstrated first order reactions at all temperatures at the aforementioned pH.

As expected an increase in the side-chain length invariably led to more stable compounds, as with bropirimine (section 3.3.1), possibly due to steric hindrance. Using equation 3.6, the Arrhenius plots for these compounds show good linearity (Fig. 3.17). From these plots, the energy of activation, E_a, and the frequency factor, A, were calculated

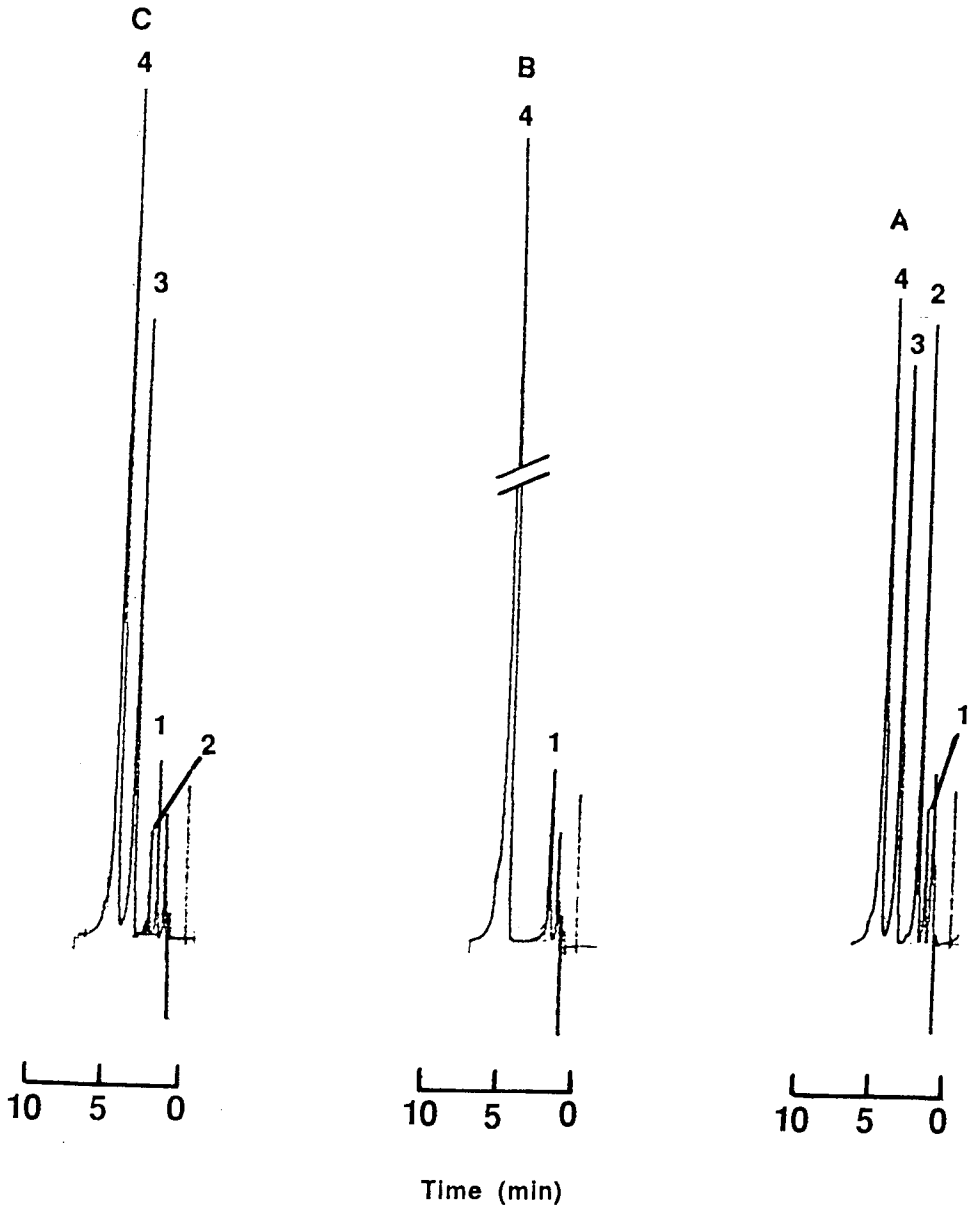

Fig. 3.12: HPLC chromatagrams to show the degradation of 2.4-N,N-dipropanoyl pyrimethamine.
1. Internal standard (ethyl paraben)
2. Pyrimethamine
3. R,N-Proponoyl pyrimethamine
4. 2,4 -N,N-Dipropanyl pyrimethamine
A = 0.4mμ standard solutions, B = 0 mins, C = 213 mins
Mobile Phase = 55%v/v acetonitrile

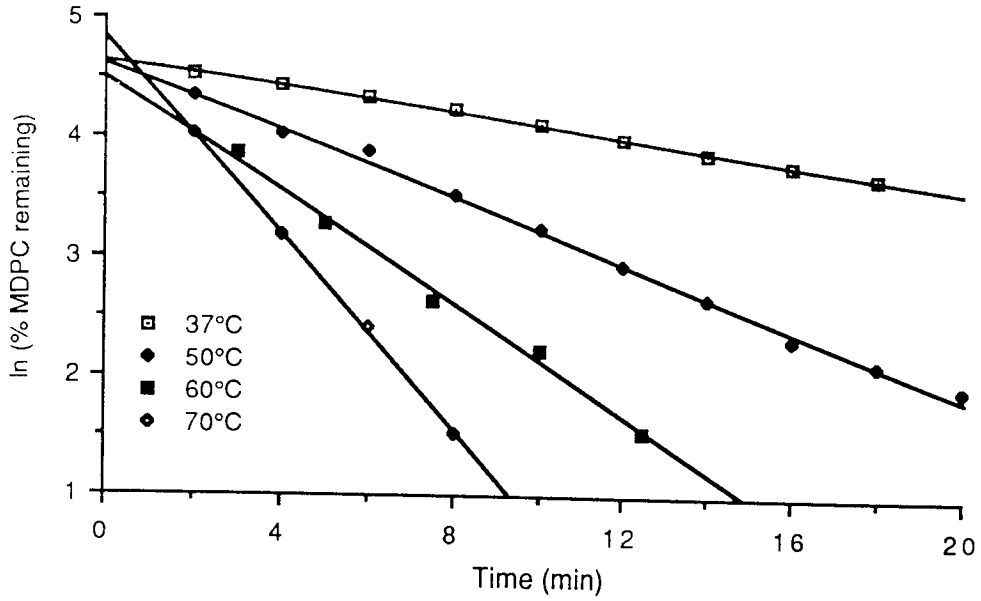

Fig. 3.13: Temperature-dependent hydrolysis of MDPC in aqueous buffered solution pH 11.2.

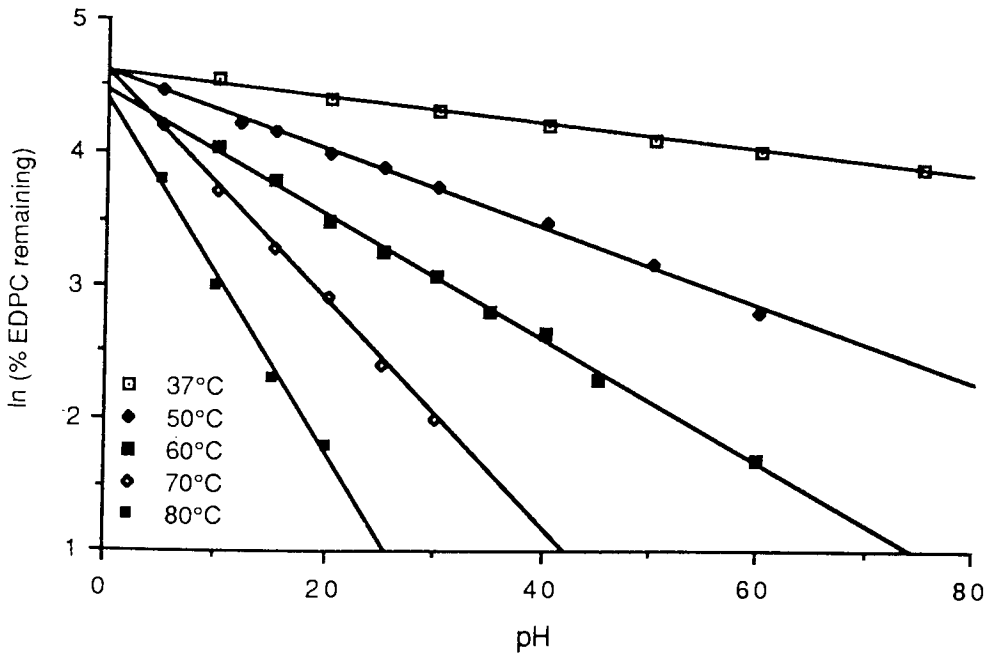

Fig. 3.14: Temperature-dependent hydrolysis of EDPC in aqueous buffered solution pH 11.2.

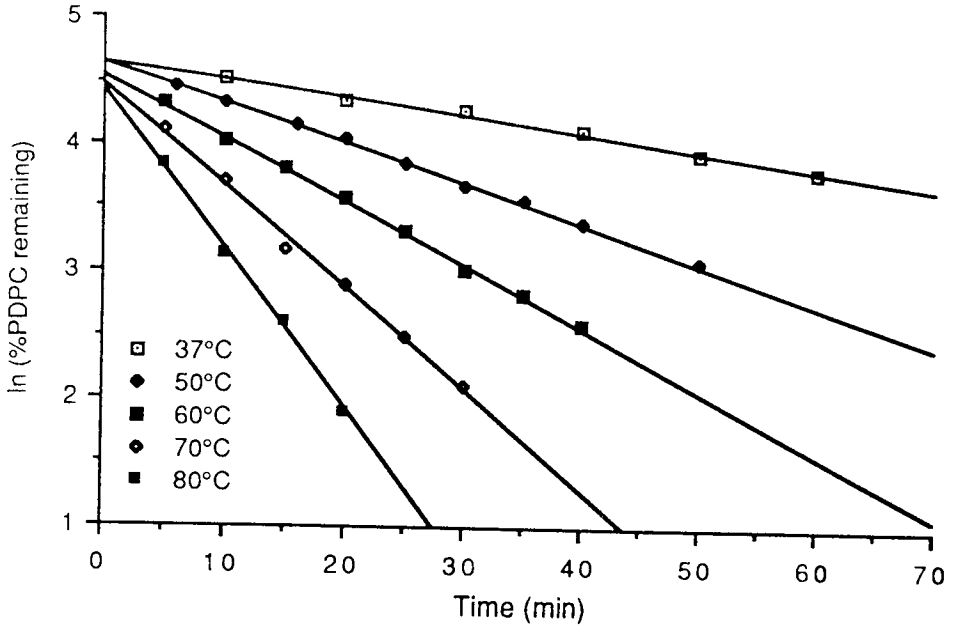

Fig. 3.15: Temperature-dependent hydrolysis of PDPC in aqueous buffered solution pH 11.2.

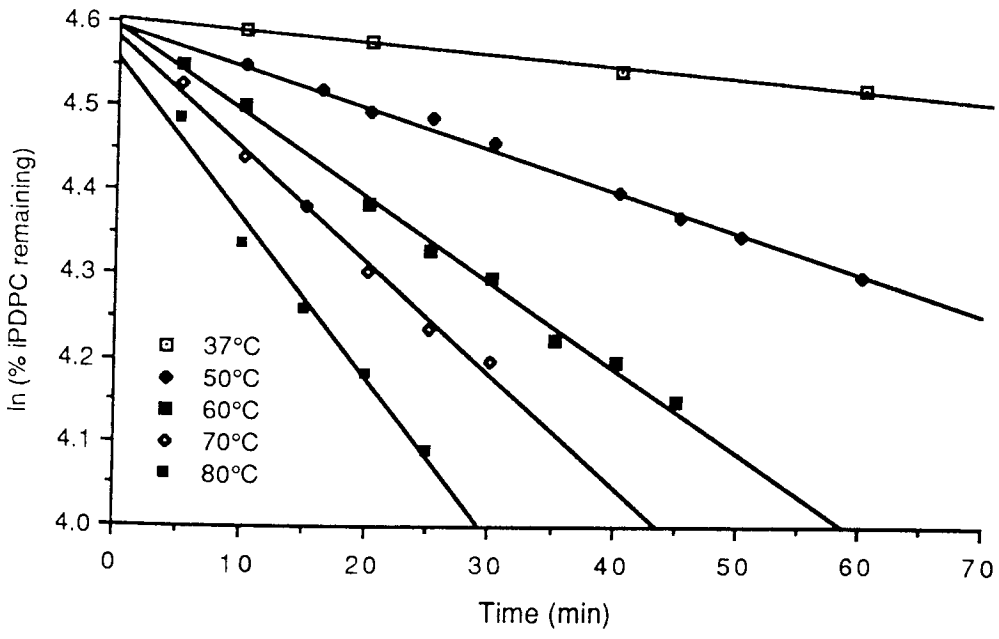

Fig. 3.16: Temperature-dependent hydrolysis of iPDPC in aqueous buffered solution pH 11.2

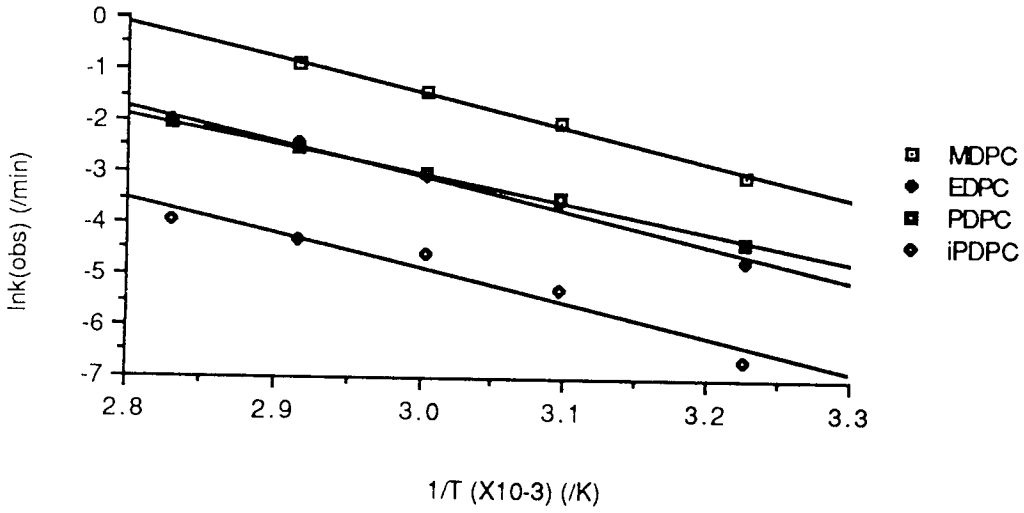

Fig. 3.17: Arrhenius plots for MDPC, EDPC, PDPC and iPDPC.

for each compound and listed in Table 3.5 together with the half-lives of the compounds at each of the temperatures. A general trend is observed within the series *viz*. an increase in the side chain length leads to increased $t_{1/2}$ values. These range from 1.68 minutes for MDPC at 70°C to $t_{1/2}$ values exceeding 500 minutes for iPDPC at 37°C. With the exception of PDPC, the energies of activation do not vary a great deal and indeed, if these were used as indicators of stability then little difference would be seen between this series of compounds. However, the frequency factor decreases as the series progresses, again with the exception of PDPC, and possibly gives a better reflection of the stability.

Temperature (°C)	Half-life, $t_{1/2}$ (/min)			
	MDPC	EDPC	PDPC	iPDPC
80	-	5.2	5.5	36.7
70	1.68	7.9	8.7	52.1
60	2.94	14.5	14.2	68.6
50	5.04	24.0	22.5	135.9
37	13.59	73.2	52.5	533.2
E_a (J/Mol)	5.58×10^4	5.56×10^4	4.72×10^4	5.54×10^4
A (/min)	1.37×10^8	2.52×10^7	1.25×10^6	3.77×10^6

Table 3.5: A list of various Arrhenius parameters for MDPC, EDPC, PDPC and iPDPC

3.3.2.2.2 Effect of pH on the degradation of EDPC: Hydrolysis of EDPC was undertaken in Britton-Robinson buffers (μ=0.5) at 60°C. First order degradation was seen at all the pH values for the base catalysed hydrolysis of EDPC (Fig. 3.18).

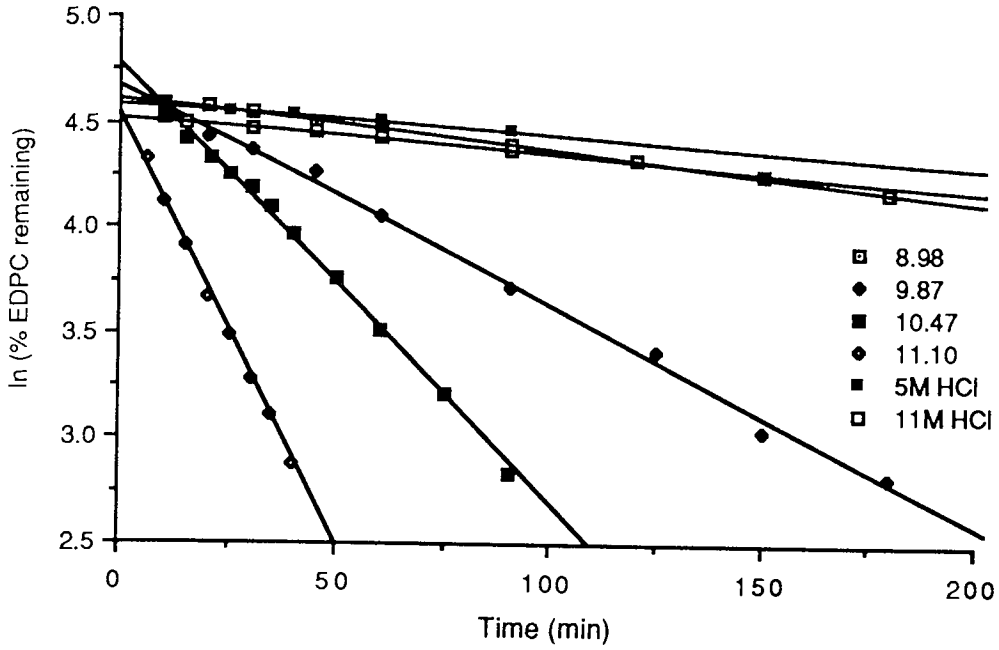

Fig. 3.18: pH-dependent hydrolysis of EDPC in aqueous buffers at 60°C.

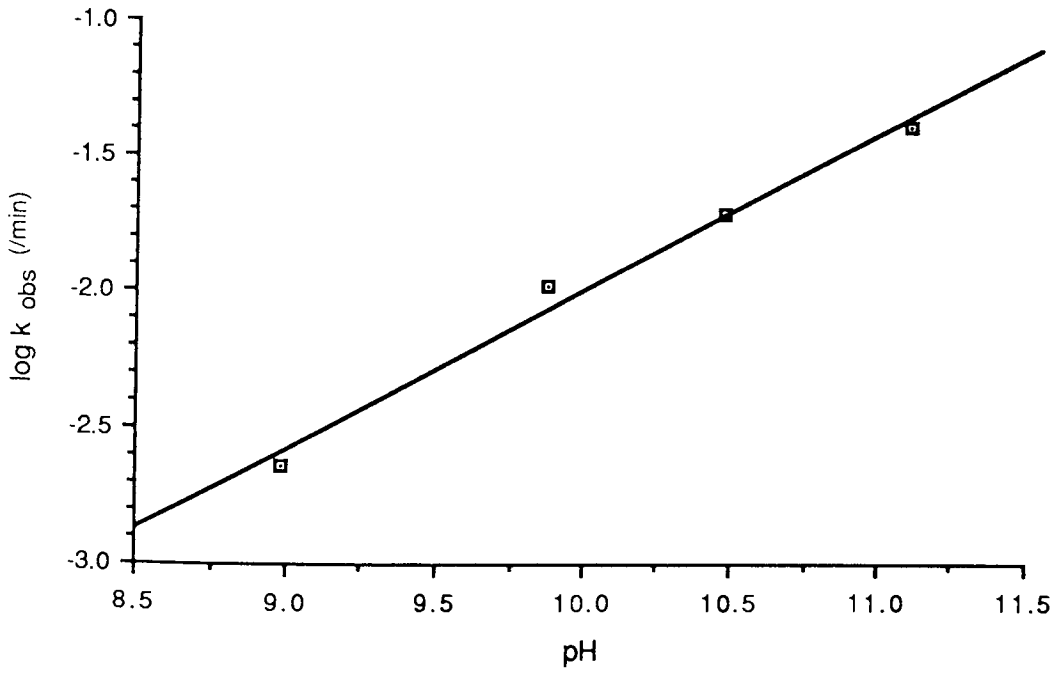

Fig. 3.19: Rate constant-pH profile of EDPC in aqueous buffered solution at 60°C.

4.0 THE USE OF DIFFERENTIAL SCANNING CALORIMETRY IN THE ASSESSMENT OF PHYSICAL INTERACTIONS

4.1 Introduction

Although references to the use of differential scanning calorimetry (DSC) in the pharmaceutical industry are legion, this technique is now successfully being applied to the biochemical field on a routine basis. Examples include whole blood and blood constituents[107], protein denaturation studies [108,109] and lipid-drug interactions[110] amongst others. Excellent reviews by Giron[111] and Fairbrother[112] outline further uses.

It is common practice in the pharmaceutical industry to use exicipients in order to produce pharmaceutically satisfactory dosage forms. The diversity and flexibility of the DSC as a tool in determining interactions is well accepted[112]. Contributions from Botha *et.al.*[115,116] showed interactions occuring between compounds commonly used in cold and flu remedies, although no attempt was made to elucidate the nature of the interactions. It is in this context that the DSC plays an invaluable role.

4.1.1 Aims

The thermal behaviour of bropirimine in combination with possible excipients was examined by DSC to study potential interactions. The work was further extended to study solid state degradation using model compounds.

A plot of log(k_{obs}) against pH yields a straight line (r=0.993) as shown in Fig. 3.19. From this plot, the value of the base catalysed rate constant, k_{OH},was calculated to be 0.61 /M/min.

When low pH buffers were used, no degradation was apparent. Even under extremely hostile acidic environment such as strong hydrochloric acid solution (5M and 11.3 M) very little breakdown occurred. Under these conditions the k_{obs} values were calculated as 1.32×10^{-3} /min in the 5M HCl solution and 1.77×10^{-3} /min in the 11.3M solution (Fig. 3.18). EDPC (pK_a=3.86) is predominantly unionised in the basic region. Hence this phenomenon can be ascribed to different reactivities of the protonated and free base forms of the compound[208, 283, 234, 235]. The ionised form of EDPC thus represents a very stable moeity towards acid-catalysed hydrolysis.

The half-lives of EDPC varied from 303 minutes at pH 5.95 to 6.5 minutes at pH 11.1.

4.2 Experimental

The materials were either used as received from the manufacturers or synthesised at the University of Aston.

4.2.1 Apparatus

Differential scanning calorimetry (DSC) was undertaken with a Perkin Elmer DSC-4 instrument using the Thermal Analysis Data Station (TADS) for data collection and plotted on a Perkin-Elmer Graphic Plotter 2.

The ^{1}H-NMR spectra were recorded in a d_6-dimethylsulphoxide solution (Sigma), with tetra-methylsilane (Sigma) as the internal standard at 360MHz by means of a Bruker Spectrospin spectrometer. Mass spectra were obtained with a VG Micromass MM12 mass spectrometer using a direct insertion probe with a inlet temperature of 250°C, an ionisation energy of 70eV, an accelerating voltage of 3kV and a trap current of 100μA.

Physical mixtures of drug and additive were prepared by trituration on a glass tile or ball milling as described in Section 5.2.2.1.

Samples for thermal analysis were accurately weighed (1-4mg) into an aluminium pan, covered with an aluminium lid and crimped into position using a hand press. The pan was placed in the DSC oven together with a blank, prepared in exactly the same way but without the sample. Both the sample and the blank were continuously purged with nitrogen gas at a flow rate of 25cm^3/min and a pressure of 20psi (1.4kg/cm^{-2}). Thermograms were recorded over a temperature range of 35-350°C with various programmed heating rates, usually 10 K/min. Changes to the sample are recorded as either an endotherm or an exotherm depending on the nature of the change. Temperature

calibration was made with an indium standard (onset termperature 156.6°C).

For the isothermal degradation of bropirimine in the presence of polyethylene glycol (PEG) 20M, a 1:9 admixture was prepared by trituration. 2-3mg of the mixture was then accurately weighed into an aluminium pan and the unsealed pan placed in the DSC oven at a loading temperature of 50°C and a heating rate of 100°C/min up to the maximum desired temperature. Samples were left in the oven for fixed periods of time after which the contents were extracted in 10mL methanol (Fisons). 1mL of this solution was added to 1mL internal standard (50μg/mL ABmFPP in methanol) and injected into the HPLC as discussed below.

For the mechanical treatment of lactose monohydrate (BDH), the following experiments were carried out to complement the DSC thermograms. The model compound used was 4-methoxyphenyl aminoacetate hydrochloride (MPAA), a prodrug of 4-hydroxyanisole, synthesised at Aston University.

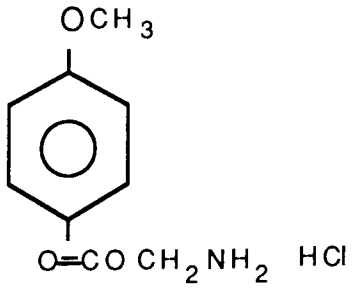

4-methoxyphenyl aminoacetate hydrochloride (MPAA, XIII)

Three samples were prepared in the ratio 10%$^{w}/_{w}$ MPAA and 90%$^{w}/_{w}$ lactose monohydrate, both sieved and the sieve fraction 150-212μm collected and both components triturated.

Sample 1 Gentle mixing of both lactose monohydrate and MPAA in a vial. No grinding.

Sample 2 Lactose monohydrate ground for 10 minutes using an agate pestle and mortar, gently mixed with unground MPAA.

Sample 3 Both lactose monohydrate and MPAA ground together for 10 minutes using a pestle and mortar.

Acetic solvate of bropirimine Either a 1:1 mixture of MPAA and the solvate ground together for 5 minutes or MPAA ground individually and then gently mixed with the solvate.

Each sample was separated into 20mg aliquots (5mg for acetic acid solvate) into individual plastic vials and the vials placed in a glass desiccator above a saturated solution of ammonium sulphate (relative humidity of 80% at 37°C)[144]. This in turn was placed in an oven pre-equilibrated at 37°C. After fixed intervals of time, the pertinent vials were removed and the powder dissolved in 5mL methanol. The contents were thoroughly mixed by shaking and subsequent sonication and the suspension finally filtered through a 0.20μm Millipore filter. 1mL of the filtrate was added to 1mL of internal standard (0.1mg/mL ABmFPP), thoroughly mixed and 20μL injected into the HPLC once steady conditions had been achieved.

HPLC Conditions

Mobile phase : 20%$^{v}/_{v}$ acetonitrile

0.1%$^{v}/_{v}$ diethylamine

adjusted to pH 2.0 using orthophosphoric acid

Flow rate : 1 mL/min

Chart speed : 2mm/min

Sensitivity : 0.08-0.16 AUFS

Wavelength : 300nm

4.3 Results and discussion

4.3.1. The effect of additives on the thermal behaviour of bropirimine and structurally related compounds.

Fig. 4.1 shows thermograms obtained for PEG 20M and bropirimine, recorded at a heating rate of 10 K/min over a temperature range of 35°C to 330°C. The themogram for PEG 20M shows a single sharp peak with a melting endotherm near 63°C. The thermogram for bropirimine shows a peak at 289.3°C (onset 284.5°C) which develops into peaks showing irregular variations characteristic of thermal degradation as evident from the dark deposits of the breakdown product on the oven lid. The exact temperature range over which the transformation occurs varies somewhat with the origin of the sample, sample weight and the heating rate employed, although all show similar profiles[113,114].

Mixtures of the drug with excipients were prepared either by dry mixing, by evaporation or by melting. The enhanced rate of dissolution obtained by using mixed systems (PEG, PVP) can be clearly seen from the dissolution profiles in Section 6.3. Fig. 4.1 also shows thermograms obtained from a mixture of bropirimine and PEG 20M. It is apparent that the PEG 20M endotherm is retained in the same place in the mixture but that corresponding to the melting of the bropirimine has been lost and in its place a new, exothermic transition is observed at a lower onset temperature of 247.9°C. Provided that the ratio of the

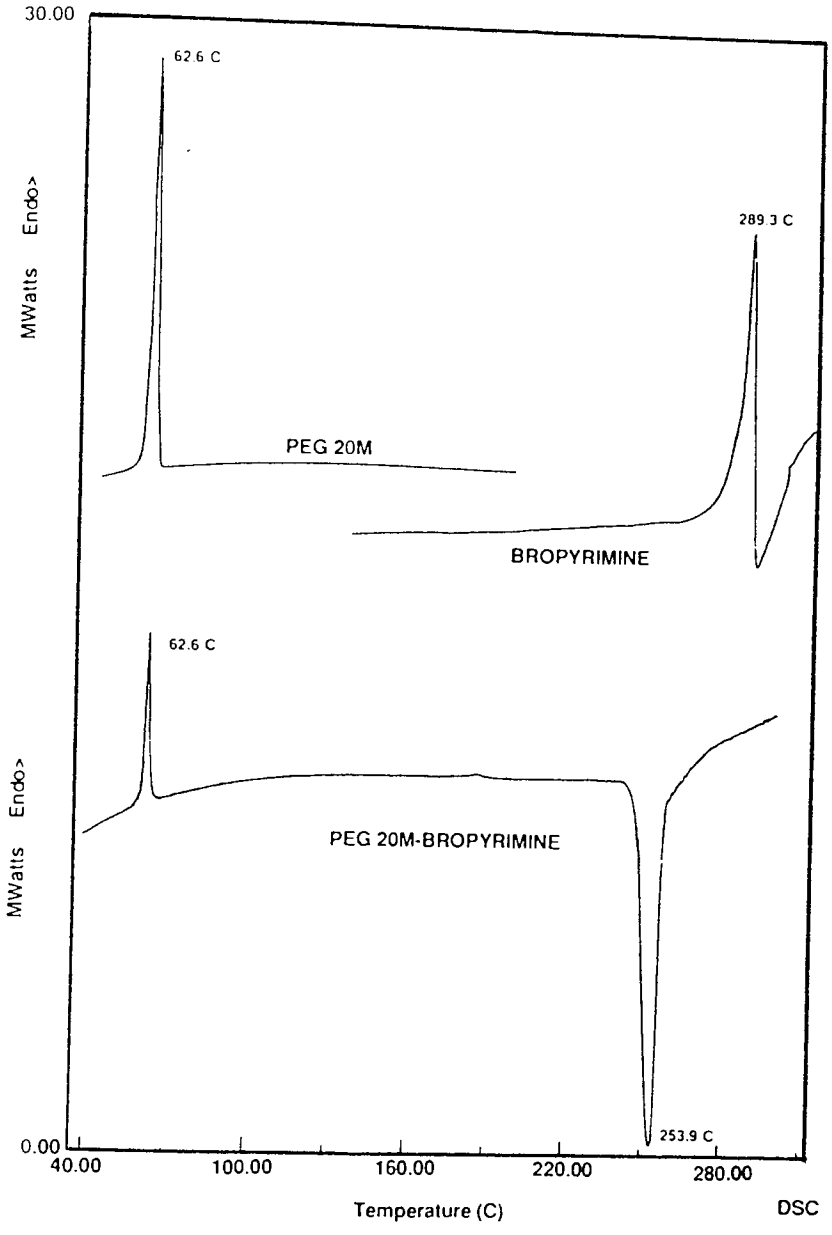

Fig. 4.1: Thermograms from differential scanning calorimetry of PEG 20M, bropirimine and a 4:1 physical mixture

mixture remained the same, the onset temperature was independent of the method of mixture. Furthermore, no trend was observed between the ratios of the PEG 20M and bropirimine mixture and the onset temperature; the exothermic event occurring in the onset temperature range of 230 - 250°C. These exothermic events may be as a consequence of one of the following:

1. Dissolution of bropirimine in the PEG 20M melt.
2. Crystallisation/recrystallisation phenomena.
3. Degradation of bropirimine.

In order to test the above possibilities, DSC thermograms of bropirimine and related compounds, both alone and in admixtures with a number of additives, were determined.

Crystallographic studies of bropirimine have shown it to exist in a dimeric conformation with a strong Watson-Crick type association[117] and the correspondingly low aqueous solubility has been attributed to this dimerisation[77]. In order to assess whether this phenomenon contributed to the aforementioned behaviour, molecules having similar conformations were used.

The acid hydrolysis of pyrimethamine under controlled conditions gives rise to a mixture of 2-amino-5-(4-chlorophenyl)-6-ethylpirimidine-4(3H)-one(XIV) and the corresponding 4-aminopyrimidin-2(1H)-one(XV) as shown in scheme 4.1[119]. These compounds co-crystallise as a paired dimer which also shows strong Watson-Crick type association[119] (XVI). For comparative purposes, the dimeric conformation of bropirimine (XVII) is also shown in scheme 4.1.

Fig. 4.2 shows the DSC thermograms of (XIV), (XV) and (XVI) alone and in admixture with PEG 20M. The 2-amino-4-one (XIV)

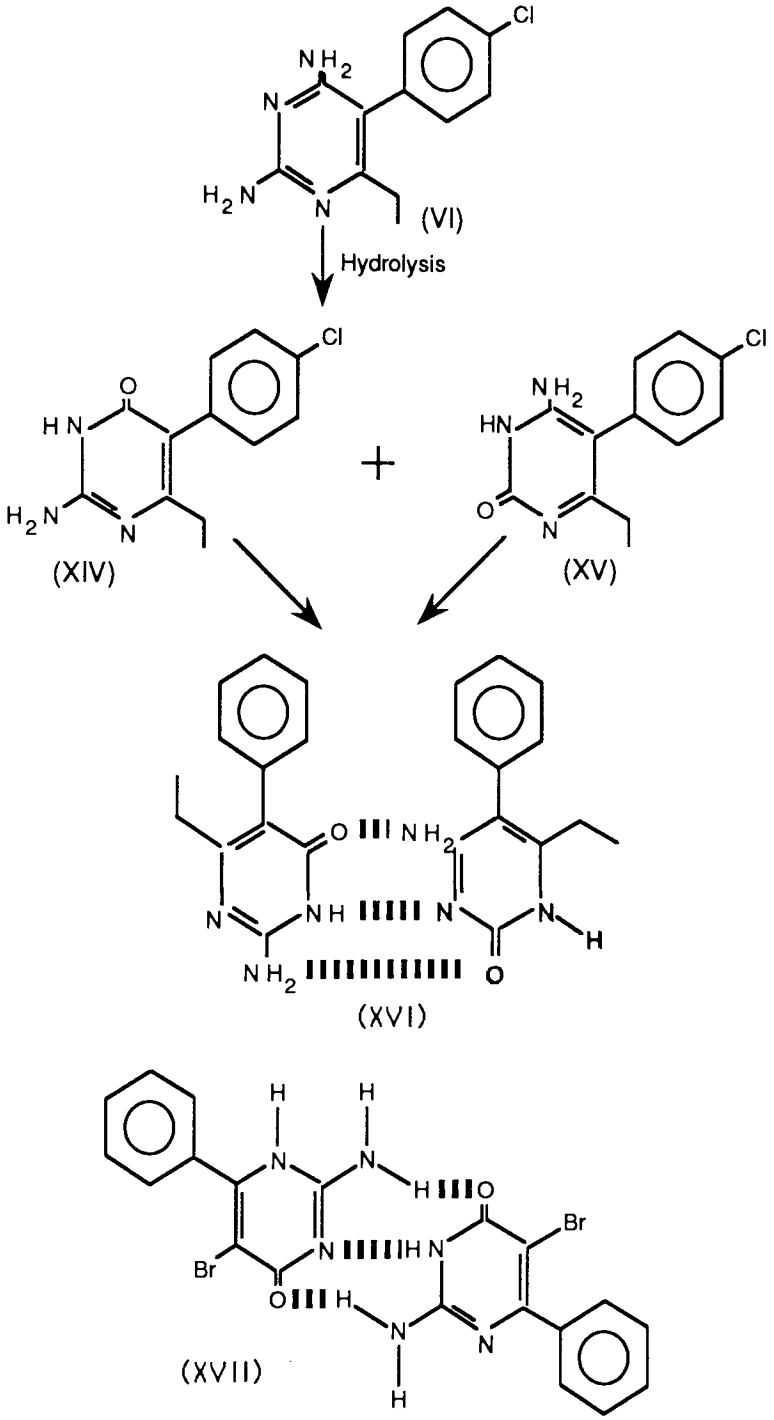

VI = Pyrimethamine

XIV = 2-amino-5-(4-chlorophenyl)-6-ethylpyrimidin-4(3H)-one

XV = 4-amino-5-(4-chlorophenyl)-6-ethylpyrimidin-2(1H)-one

XVI = Mixed dimer of II and II

XVII = Bropirimine dimer

Scheme 4.1

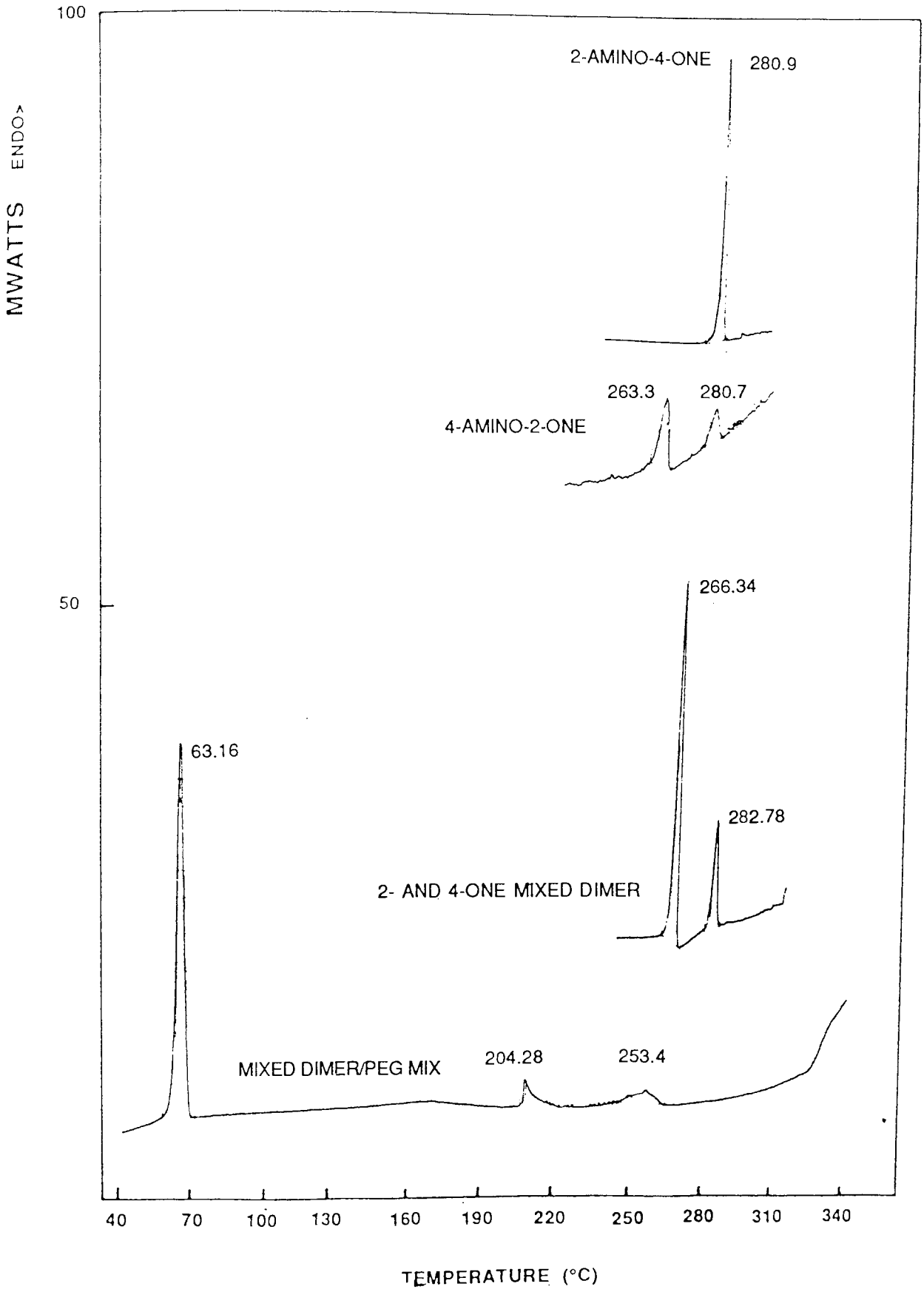

Fig. 4.2: *DSC trace of the co-crystallised mixture 2-amino-5-(4-chlorophenyl)-6-ethyl pyrimidine-4(3H)-one and the corresponding 4-amino-2-one, both alone and crystallised and also the dimer in admixture with PEG 20M*

displays a single sharp endotherm with a peak temperature of 280.9°C indicating one component only. In contrast, the 4-amino-2-one (XV) simply yields two peaks at peak temperatures of 263.3°C and 280.7°C indicating the presence of both isomers with similar peak temperatures to the mixed dimer (266.3°C and 282.8°C). Although a rather complex thermal profile is obtained for the PEG 20M dimer mix, there is no indication that any exothermic events, characteristic of the bropirimine-PEG 20M mixture, are initiated on admixture. Addition of PEG 20M to the mixed dimer leads to progressive dilution and consequently the major effect appears to be a large reduction in the intensity of the endotherms.

Amide modifications to the 2-amino group of the bropirimine through acetyl, propanoyl and chloroacetyl derivatisation followed by treatment with PEG 20M shows that the exotherm is retained in all instances, and at lower temperatures, following admixture (Fig.4.3). The depression in the temperature of the new event with these close derivatives of bropirimine does not appear to be as marked as the bropirimine itself. These results indicate that the 2-amino group is not implicated in the exothermic event.

When other pyrimidine derivatives containing bromine at the 5-position were subjected to DSC analysis, it was immediately apparent that it was this substitution which was the cause of the anomalous thermal behaviour of the mixtures, although the exact behaviour of bropirimine was not duplicated (Fig.4.4). In the case of 5-bromo-1-methyl uracil, a sharp endotherm (peak temperature 273.3C) was immediately followed by an exothermic transition (peak temperature 278.5°C). In contrast to this, only a strong exotherm was recorded for 5-bromocytosine, at a peak temperature of 252.8°C. A similar thermogram, with a maximum at 250.9°C was obtained for the 5-iodo

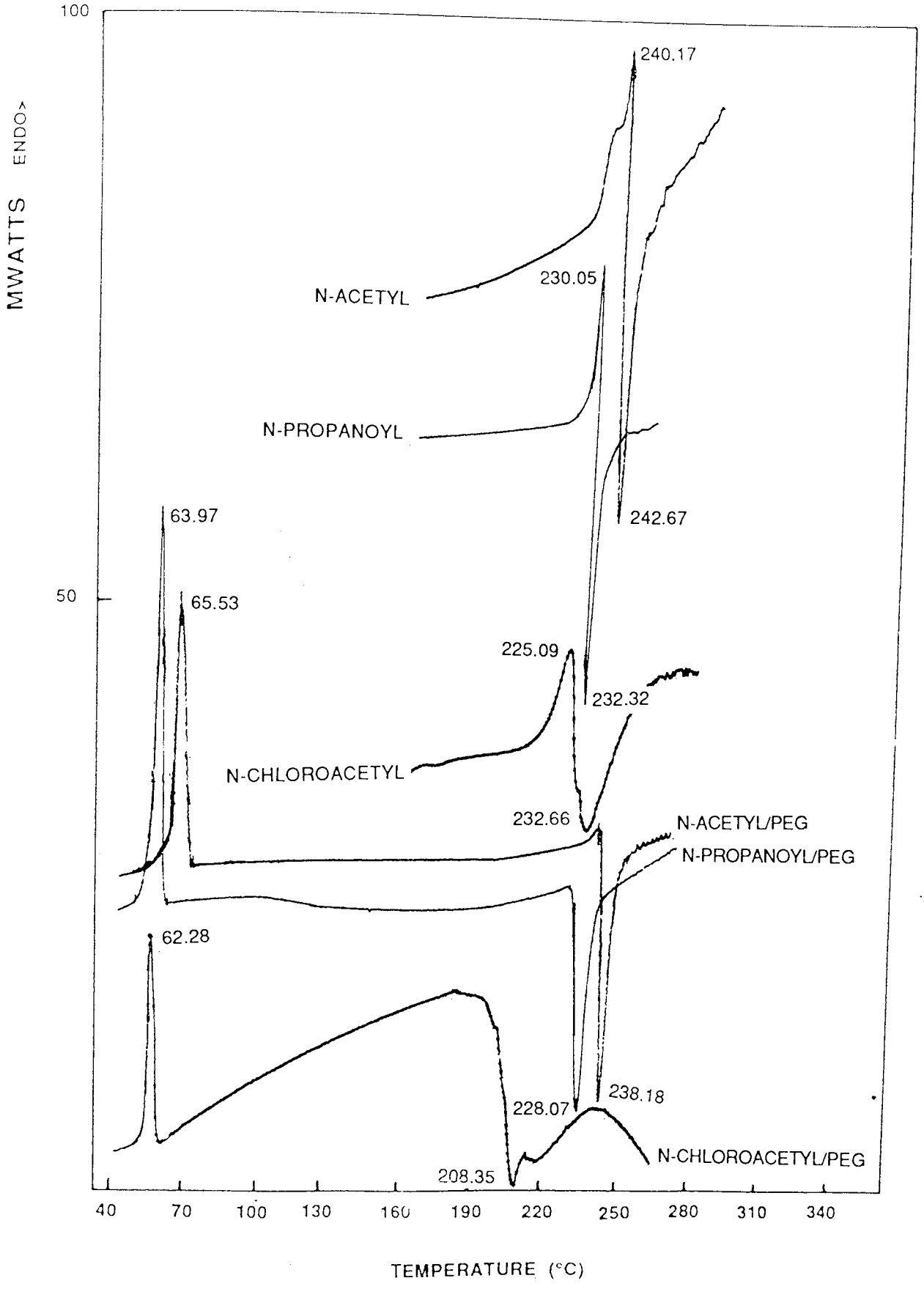

Fig. 4.3: DSC thermograms of N-acetyl, N-propanoyl and N-chloroacetyl derivatives of bropirimine alone and in admixture with PEG 20M

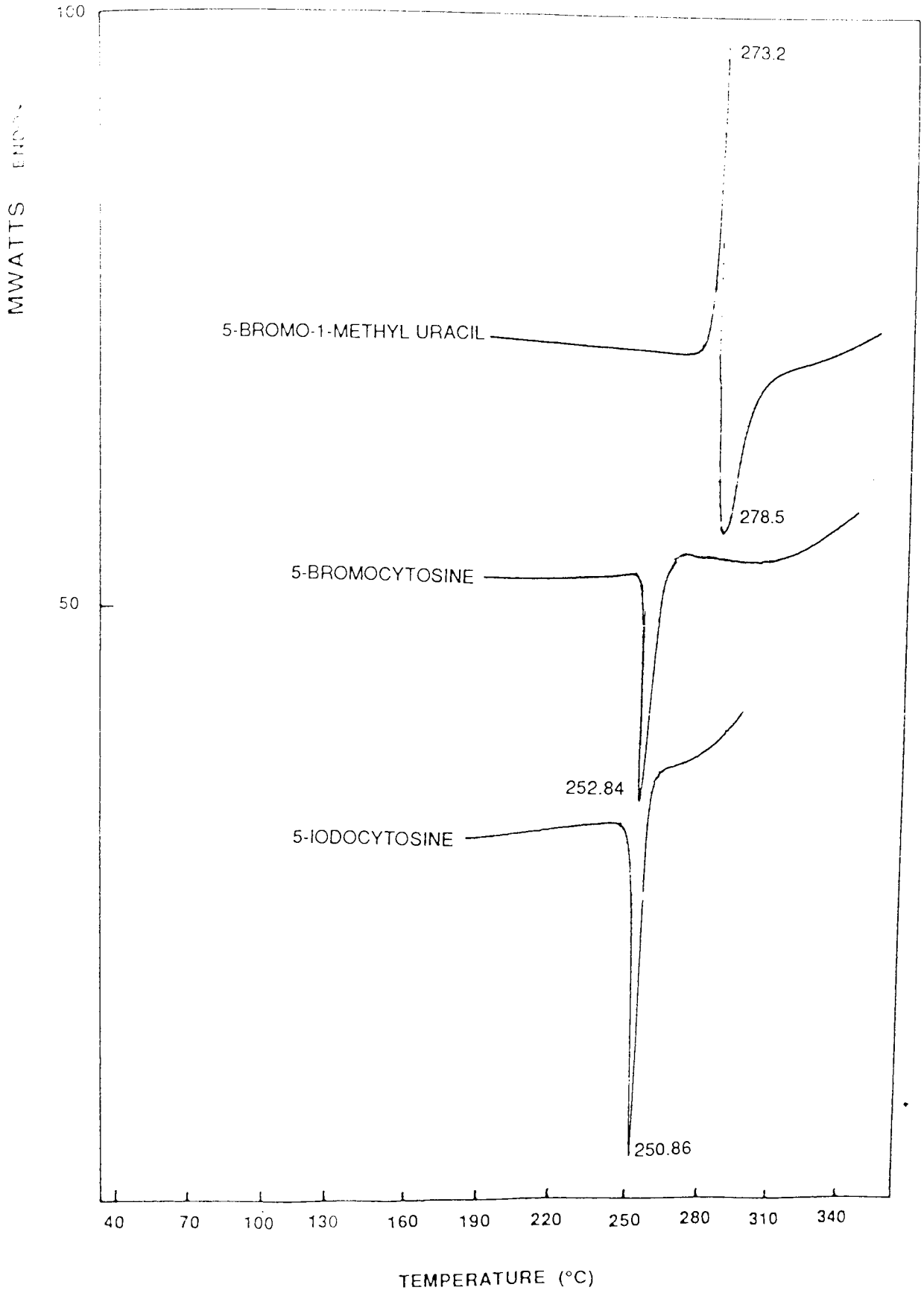

Fig. 4.4: DSC thermograms of 5-bromo-1-methyluracil; 5-bromocytosine and 5-iodocytosine

analogue. It seems plausible to suggest, therefore, that the exotherm in the bropirimine mixture is due to degradation caused by the incorporation of a labile C-Br bond on the molecule. Consideration of the average bond dissociation energies for =C-H (460 kJ/mol) and =C-Br (335 kJ/mol)[120] gives added weight to this theory. In an attempt to confirm this and to identify the degradation product(s), a 4:1 bropirimine-PEG mixture was heated in a DSC pan until the exotherm was just completed. The mixture, showing signs of a white sublimate, was extracted from the pan and analysed by chromatography, by mass spectrometry and by ^{1}H-NMR spectroscopy.

HPLC analysis was carried out using two mobile phases. The first mobile phase consisted of 20%$^{v}/_{v}$ acetonitrile (section 4.2.1) and in the second mobile phase, the acetonitrile was replaced with 20%$^{v}/_{v}$ methanol.

Fig. 4.5 shows the HPLC traces obtained with both of these mobile phases for 2-amino-6-phenylpirimidin-4(3H)-one (APP) and bropirimine. Both confirm the presence of one major component only which, in both systems, co-eluted with APP; the product derived from bropirimine by substitution of the hydrogen for the bromine atom. The elution times for bropirimine and APP in 20%$^{v}/_{v}$ acetonitrile were 5.8 and 2.7 minutes respectively and 20 minutes and 6.5 minutes respectively in 20%$^{v}/_{v}$ methanol.

^{1}H-NMR spectroscopic analysis further supported the above rationale with the presence of an absorption band at δ 6.11 ppm due to the new proton at the 5-position of the pyrimidine ring.

The final confirmation of the assignment was provided by mass spectrometry which revealed a molecular ion at m/z 187 together with the absence of the ^{79}Br:^{81}Br doublets characteristic of the bromine-containing ions in the starting material (Scheme 4.2). The iodo analogue

(1)

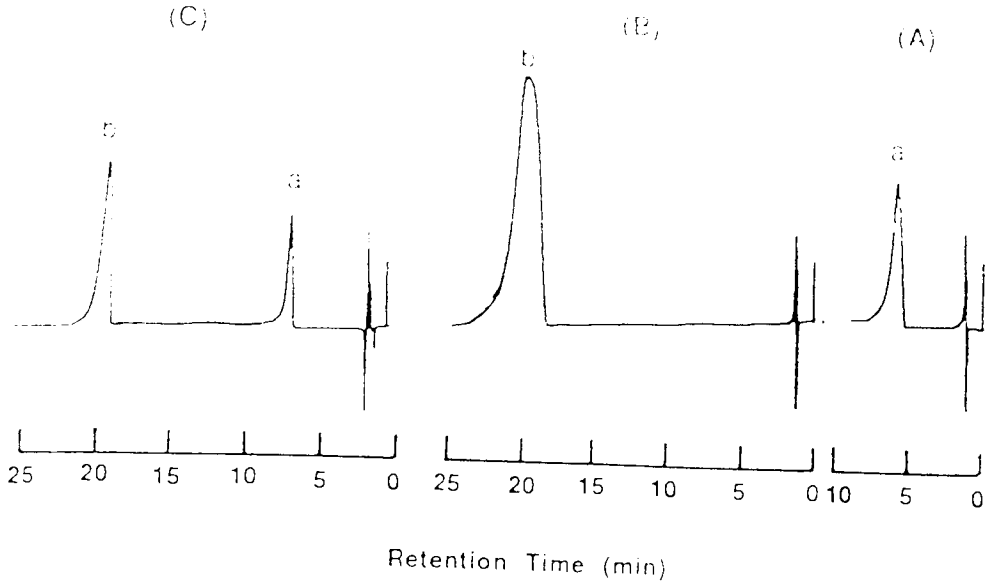

(2)

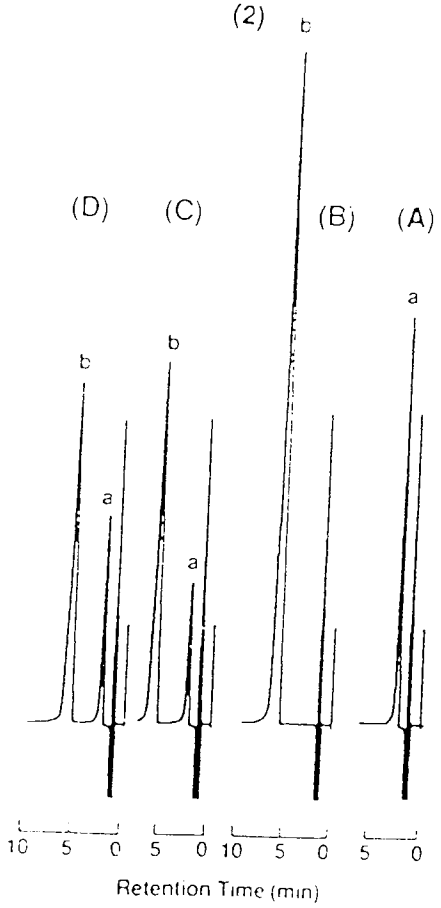

Fig.4.5: *HPLC traces showing:*
(A) 2-amino-6-phenylpyrimidin-4(3H)-one(a)
(B) Broprimine (b)
(C) a mixture of each obtained from partial thermal degradation of 5mg bropirimine-PEG 20M mixture (10:1) at 210°C for 5 minutes and dissolved in methanol
(D) a standard mixture of each component in (1) 20%v/v methanol in the mobile phase and (2) 20%v/v acetonitrile in the mobile phase

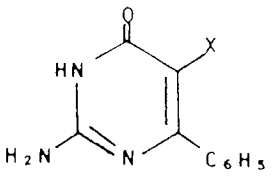

I. X=Br, Bropirimine; M+· 267(97%), 265(100%)
II. X=H, M+· 187(100%)

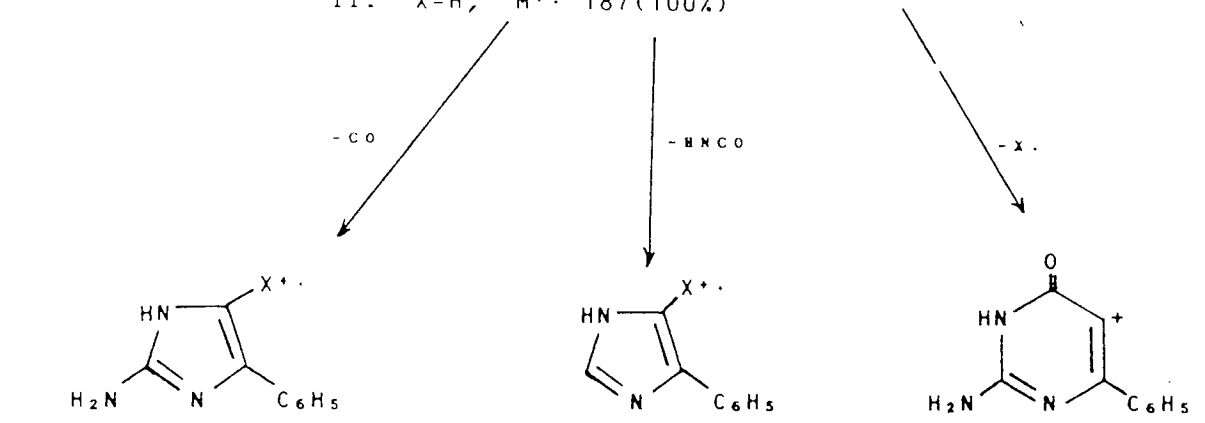

X=Br, m/z 239(17%), 237(17%)
X=H, m/z 159(28%)

X=Br, m/z 226(15%), 224(15%)
X=H, m/z 146(22%)

X=Br, m/z 186(83%)
X=H, m/z 186(88%)

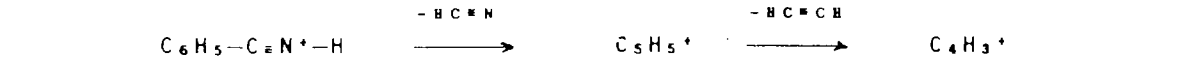

$C_6H_5-C\equiv N^+-H$ → $C_5H_5^+$ → $C_4H_3^+$

X=Br, m/z 104(80%)
X=H, m/z 104(30%)

X=Br, m/z 77(50%)
X=H, m/z 77(15%)

X=Br, m/z 51(33%)
X=H, m/z 51(10%)

$HNCO^{+\cdot}$

X=Br, m/z 43(60%)
X=H, m/z 43(20%)

Scheme 4.2: Mass spectral assignments of bropirimine and 2-amino-6-phenylpyrimidin-4(3H)-one, its debrominated product

of bropirimine, 2-amino-5-iodo-6-phenylpyrimidin-4(3H)-one (AIPP), reveals similar behaviour. Pure AIPP shows an endotherm at 285.6°C followed by an exotherm at 288.9°C, whereas on admixture with PEG 20M both transitions are replaced by a single exothermic event at a lower temperature of 257.6°C due to de-iodination.

No trace of products incorporating oxyethylene chains, expected if the reaction involved nucleophilic displacement of bromine by PEG hydroxyl groups, was detected. It is thus possible that the thermal dissociation of the C-Br bond is followed by a hydrogen abstraction reaction involving the molten PEG 20M.

Using a range of 5-halogeno-uracils the generality of this interaction may be demonstrated. DSC analysis of these compounds show that the fluoro-, chloro- and bromo compounds are characterised by a single endothermic transition (Table 4.1). This endotherm also begins to develop in the 5-iodo-analogue but degradation overtakes melting and a strong exotherm immediately follows the initial transition. The DSC curves of these compounds have been reported previously [121,122] but thermograms with multiple transitions were observed due to impurities in the samples. Using pure samples, only single endothermic transition was apparent for each compound except the 5-iodo-analogue (Table 4.1). When each of the uracils was mixed with PEG 20M and the DSC analysis repeated, the 5-fluoro- and 5-chloro- derivatives appeared as physical mixtures of the individual components. Although some broadening of the endotherm was observed, the onset temperature remained relatively constant. No disappearance was observed nor was there introduction of any new peaks. In contrast, both 5-bromo- and 5-iodo- analogues revealed strong exothermic bands on admixture, due to the corresonding substitution reactions as detailed in Table 4.1.

URACIL	Onset temperature (°C)	
	Pure	Admixture
5 - F	281.9	282.8
5 - Cl	319.9	317.1
5 - Br	310.4	296.5*
5 - I	285.3	266.5*
	292.6*	

* signifies exothermic transitions

Table 4.1: DSC onset transitions of 5-halogenouricals alone and in 1:1 admixture with PEG 20M

The behaviour of this series is in accordance with the predictions based on the bond energies with the weakest bond (C-I) initiating reaction at the lowest temperature and parallels degradation. To support this view, thin layer chromatography indicated the presence of uracil as a thermolysis product of 5-bromo-2^1-deoxyuridine and the exothermic transition at 345°C has been attributed to this reaction[121].

In order to investigate whether the induction of this reaction is specific to PEG 20M, the interaction of bropirimine with a series of compounds, which may be of use as additives to influence solubility profiles, were examined. The results are recorded in Table 4.2 which shows that several excipients share the potential exhibited by PEG 20M to facilitate thermal degradation of this type. Dehalogenation of bropirimine has also been shown to occur in strongly alkaline aqueous solutions over a period of time[151]. With the exception of urea, no melting endotherms were observed and all showed a single exotherm for bropirimine degradation. Urea shows a melting endotherm (133.6°C) but on further heating a large endotherm develops from 188°C onwards. This signals the thermal degradation of urea (H_2N-CO-NH_2) to biuret

(H_2N-CO-NH-CO-NH_2) with the evolution of ammonia[123]. On admixture with bropirimine, the melting profile broadens and is depressed (116°C) while the degradation begins at 160°C and obscures bropirimine transitions. Confirmation of the reaction may be demonstrated by extraction of the melt from the DSC pan, as described above, isolated after heating to:

i) 200°C and

ii) 250°C

HPLC analysis of the extracts gave traces similar to Fig. 4.5 thus confirming that debromination is occuring over this range. At 200°C, little of the debrominated product is observed, whereas at 250°C, considerable reduction in the intensity of the bropirimine peak, with a corresponding increase in that due to 2-amino-6-phenyl-pyrimidin-4(3H)-one is apparent.

Additives	Onset temperature of transition (°C)
β -cyclodextrin	225.7*
Hydroxypropyl- β -cyclodextrin	215.6*
N-methyl-D-glucamine (Meglumine)	241.4*
Polyethylene glycol 1000	250.5*
Polyvinylpyrrolidone (PVP)	253.2*
Urea	
Urea melting	133.6
Biuret formation	188.0*

* signifies exothermic transitions

Table 4.2: DSC onset transitions of bropirimine on 1:1 admixture with various excipients

It is possible that the catalytic effect afforded by these additives is a consequence of the increased proportion of the aromatic halogeno compound in the liquid state at any fixed temperature. This may be due to the presence of the molten additive phase causing total or partial dissolution or else, for those additives such as PVP, which does not show a melting endotherm, depression of melting point of the halogeno compound may occur which will similarly increase the proportion in the liquid state. It is well recognised that such factors significantly enhance the rates of reaction in the solid state[124-127]. Evidence for this interpretation may be gained from examination of a compound which clearly melts prior to degradation. Such a compound is 2-amino-4(N-hydroxyethyl)amino-5-bromo-6-phenylpyrimidine, an analogue of bropirimine. The thermograms of this compound, alone and in admixture are displayed in Fig. 4.6. The pure component shows successive melting (192.5°C) and degradation (268.4°C) behaviour. On admixture with PEG 20M, the profile is retained. The melting transition is rather broader with a range of 173.9-197,3°C in the presence of PEG 20M, compared to 177.6-197.3°C observed for the pure compound, which may be perhaps due to competing dissolution of the pyrimidine in the PEG melt. The degradation exotherm, however, is virtually unchanged showing a reaction range of 226.6-276.3°C. This compares well with the range of 235.4-276.3°C found in the pure state and confirms that degradation is largely unaffected by the low amounts of the excipient in the liquid phase.

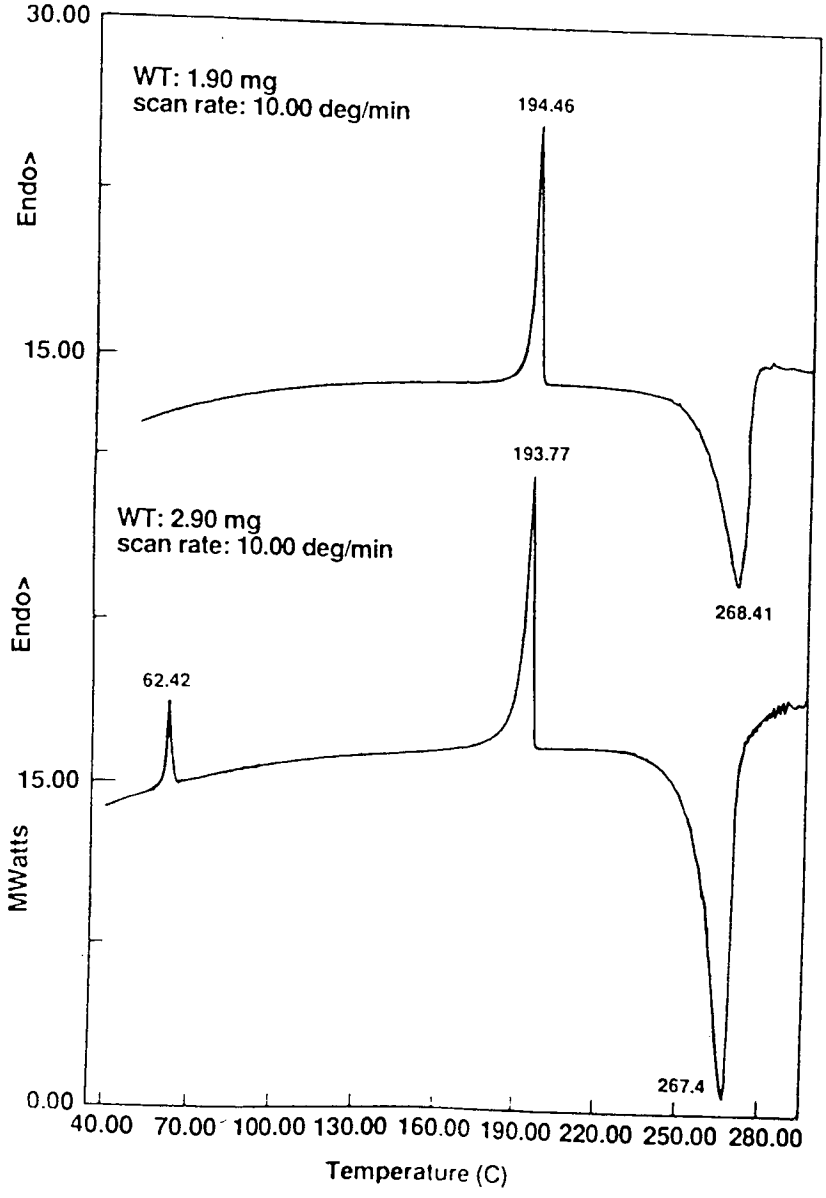

Fig. 4.6: *DSC thermograms of 2-amino-4(N-hydroxy ethyl) amino-5-bromo-6-phenylpyrimidine, an analogue of bropirimine, alone and upon admixture with PEG 20M, showing the independence of the degradation exotherm at 267-268°C once melting has been effected*

4.3.2 The use of DSC variable heating rate for solid state stability predictions.

The standard method for carrying out accelerated stability testing is to degrade the sample isothermally at a number of discrete temperatures with variables, e..g. humidity, kept constant. However, this process is usually time consuming.

Using the expressions derived by Ozawa[128], the ASTM E698 method[129] has embodied an alternative method whereby DSC may be used for solid state stability testing. This is done by recording the peak maximum temperatures for several different heating ratios and plotting $\ln\left(\frac{\beta}{T^2}\right)$ against $\frac{1}{T}$, where β is the heating rate in K/min and T is the corrected peak maximum temperature[129] in K. This should yield a straight line from which the activation energy, E, and Arrhenius pre-exponential factor, Z, may be derived from:

$$E = R \frac{d - \ln \frac{\beta}{T^2}}{d\left(\frac{1}{T}\right)} \qquad \ldots 4.1$$

where R = Molar gas constant

$$E = R \times \text{slope} \qquad \ldots 4.2$$

And,

$$Z = \frac{\beta E e^{-E/RT}}{RT^2} \qquad \ldots 4.3$$

where β = heating rate in the middle of the range.

The rate constant, k, may also be calculated from:

$$k = Z e^{-E/RT} \qquad \ldots 4.4$$

where T is in K.

Fig. 4.7 shows plots of $\ln\frac{\beta}{T^2}$ against $\frac{1}{T}$, for admixtures of bropirimine with various additives. All of these have been shown to promote decomposition of bropirimine by substitution reaction (Section 4.3.1). As can be seen from equation 4.2, the slope of each of these is directly proportional to the activation energy and is a measure of the ease of a reaction.

No relationship appeared to exist between the amount of PEG 20M in the mixture and the peak maximum temperature of the exothermic event (Section 4.3.1). However, Fig. 4.7 shows that as the amount of PEG 20M is increased from 10%$^{w}/_{w}$ to 50%$^{w}/_{w}$, there is a corresponding increase in Z and a corresponding decrease in the activation energy, albeit a small change. Table 4.3 lists the activation energies and the pre-exponential factors for these admixtures.

Excipient	Amount added (%v/v)	E x 10^{-5} (J/Mol)	Z x 10^{-17} (/min)	Correlation coefficient, r
PEG 20M	50	1.59	9.54	0.998
PEG 20M	10	1.88	8.96	0.998
PVP	10	1.69	3.16	0.990
HPBCD	10	1.59	6.74	0.998

PEG Polyethylene glycol
PVP Polyvinylpyrrolidone
HPBCD Hydroxypropyl- β- cyclodextrin

Table 4.3: Kinetic parameters of bropirimine on admixture with various excipients

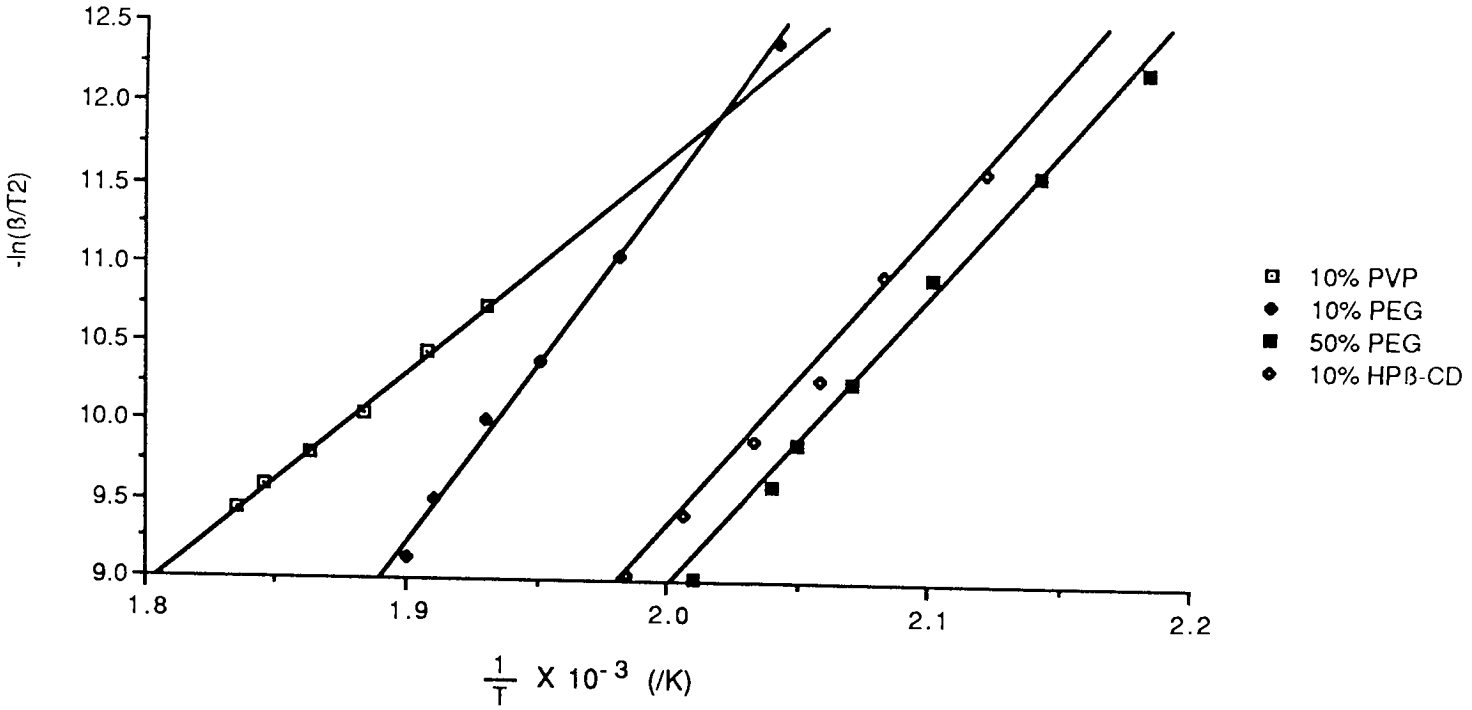

Fig. 4.7: Plots of $ln(\beta/T^2)$ against $\frac{1}{T}$ for various admixtures of bropirimine with additives

As expected, a trend is apparent between the temperature of the exotherm on admixture and the activation energy, e.g. hydroxypropyl-β-cyclodexrin/bropirimine admixture yielded an exothermic peak at 215.6°C at a heating rate of 10°/min. The corresponding value for the polyvinyl pyrrolidone/bropirimine mixture was 253.6°C. The activation energy values for the two systems were calculated as 1.59×10^5 J/mol and 1.69×10^5 J/mol respectively. The pre-exponential factors also showed consistency with the former admixture having a higher Z value than the latter.

To check the validity of this method and for comparison, an isothermal experiment was performed. The two components (10%$^w/_w$ PEG 20M and 90%$^w/_w$ bropirimine) were thoroughly mixed and 2.3mg samples accurately weighed into an aluminium pan and isothermally stressed for fixed periods of time. The mixture was then extracted with methanol and injected into the HPLC using 20%$^v/_v$ acetonitrile in the mobile phase (Section 4.3.1) and ABmFPP (50µg/mL in methanol) as the internal standard.

Fig. 4.8 shows plots of ln (mole fraction remaining) against time at various temperatures (190-200°C). The plots are seen to follow first order decomposition in that particular temperature range. For such a decomposition:

$$\ln A_t = \ln A_o - kt \qquad \ldots 4.5$$

where Ao = Concentration at time zero,

At = Concentration at time t,

k = First order decomposition rate constant.

or,
$$k = \frac{\ln (A_o/A_t)}{t} \qquad \ldots 4.6$$

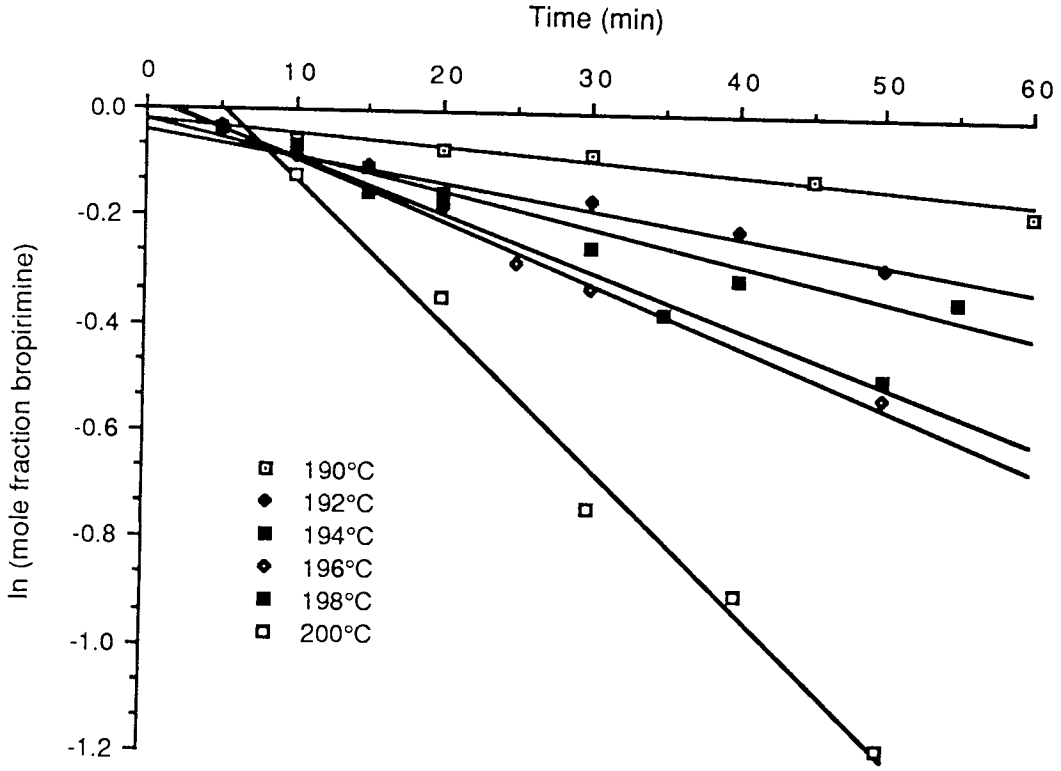

Fig. 4.8: Degradation of bropirimine at various temperatures using the isothermal method

From the Arrhenius equation:

$$k = Z e^{-E/RT}$$

where T = Temperature in K

and Z, E and R have the same meaning as above.

Therefore, $$\frac{\ln (A_o/A_t)}{t} = Z e^{-E/RT}$$

and $$t = \frac{\ln (A_o/A_t)}{Z e^{-E/RT}}$$

Hence it is possible to calculate the time taken for a certain amount of the drug to degrade at a particular temperature if the Z and E values are known.

The variable heating rate experiment provided the rate constants calculated from equation 4.4. The slope of the ln (mole fraction) against time yielded the decomposition rate constant for the isothermal method. The results obtained for the two rate constants are plotted in Fig. 4.9. Variation is seen between the two lines which criss-cross at a coincidental temperature near 468K. On either side of this point, the deviation between the two lines progressively increases. Similar difference between the two methods have also been observed by Torfs *et. al.*[131] using t-butylperpivalate as the model compound and several reasons were given for the difference. Although the variable heating rate method may theoretically appear attractive[128], it is full of experimental variables, e.g. sample mass and particle size are common sources of variation in results[113,130]. Large differences in activation energies were observed when different crucibles were used, possibly due to heat losses[131]. Li Wan Po suggested that errors occuring in instances when

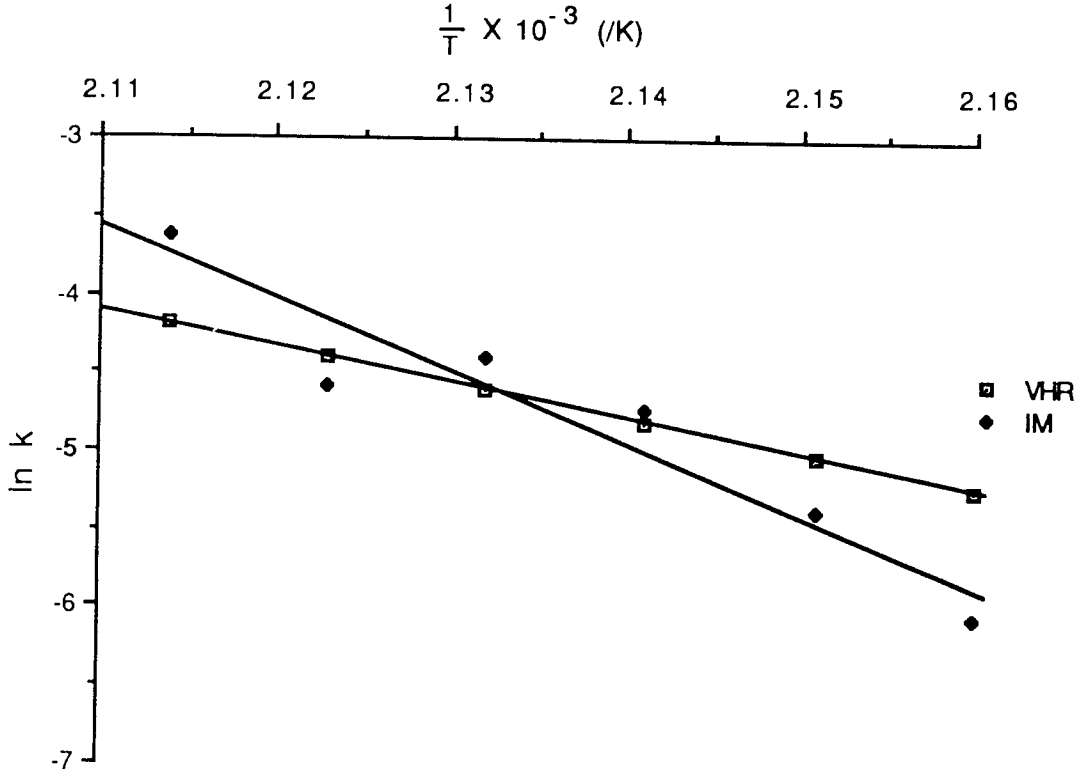

Fig. 4.9: Plots of lnk against 1/T for an admixture of 10% PEG/bropirimine using the variable heating rate (VHR) and isothermal method (IM)

experimental factors were mostly non-conbtributory, external agents such as oxygen or moisture may be responsible[132]. It is also important to determine the peak temperatures accurately as a small change may lead to large errors.

Provided the variables could be identified and accurately controlled, the variable heating rate method may prove to be a powerful addition to an analyst's armoury. This method has the advantages of simplicity of measurements, applicability to many types of reactions and relative insensitivity to secondary reactions[133]. Although considerable differences are seen between the two methods, accuracy of each method can depend on the compound under consideration[133].

4.3.3. The use of DSC in the evaluation of physical changes upon mechanical treatment of compounds.

The physical changes in compounds brought about by mechanical treatment have only been realised in the past 15-20 years and the results made more meaningful with the use of DSC. Experiments usually involved grinding the compound under test with subsequent examination for any polymorphic transitions[134-136]. More important were experiments conducted by Chan and Doelker who subjected over thirty drugs, known to exist in polymorphic forms, to compression and found that tranformations had occured in one-third of them[137]. Addition of certain excipients have been shown to facilitate the rate of transformation from one form to another[138].

The term solvate is a very general definition for the association of the solvent to the solid compound. This association may be by way of physical adsorption, chemisorbed, zeolites, clathrates, pseudosolvates (solvent existing as charged ions) or true solvates (solvate existing in molecular form) and thermal methods can be used to

characterise the type of association[139,140]. Hence crystallisation of a compound from a particular solvent may show marked differences in the DCS thermograms.

Fig. 4.10 shows the acetic acid solvate of bropirimine and the effect of mechanical treatment on the resulting thermogram. Only the portion of the thermogram containing the desolvation is shown since only this part is relevant to the experiment. On grinding the solvate in a pestle and mortar, peak broadening takes place with a subsequent depression of peak maximum temperature. After 5 minutes of grinding the initial peak at 138.9°C is replaced by a broader peak at 118.3°C. These results suggest that desolvation is taking place[141,142], i.e. the bonding force between the acetic acid molecules and bropirimine is weakened by grinding and the amount of acetic acid molecules having a greater freedom of movement in the impaired lattice is increased. The liberated molecules are thus free for any further interactions, and if the parent compound is labile, decomposition may ensue[141,142].

To test the possibility of the liberated acetic acid molecules causing decomposition, the model compound MPAA was used which is known to be highly water-labile[143].

The thermogram of MPAA is displayed in Fig. 4.11 along with those thermograms obtained after the mechanical treatment by way of grinding in a pestle and mortar. No meaningful difference in the thermograms is observed as the size of the sample used will in itself cause minor variations in peak maximum temperatures[113]. However, immediately upon admixture (both components gently mixed in a vial i.e. no grinding) with the acetic acid solvate (25%$^{w}/_{w}$MPAA:75%$^{w}/_{w}$ acetic acid solvate), the individual peaks corresponding to either pure MPAA or the solvate disappear and in their place appears a single shouldered peak at a peak maximum temperature lower than those of

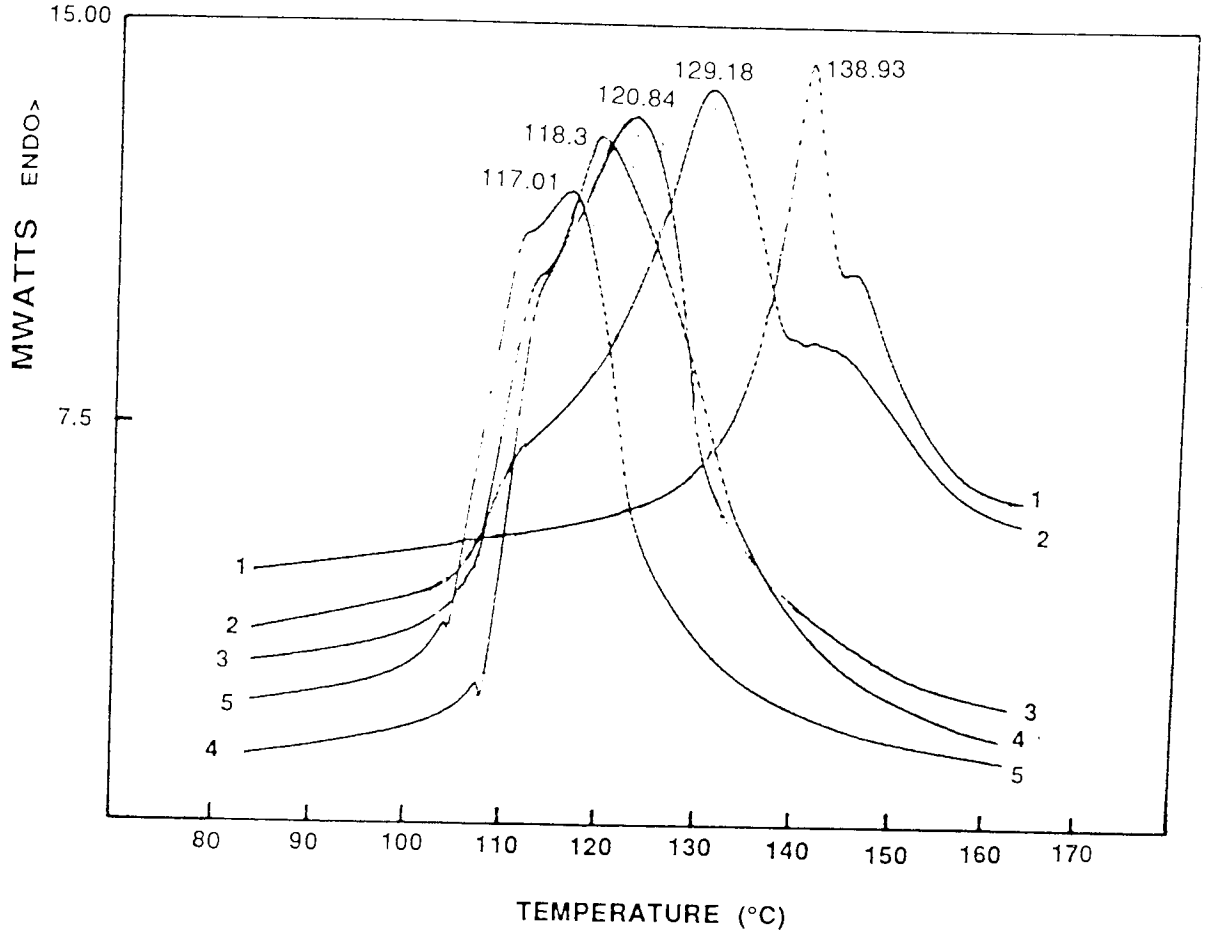

Fig. 4.10: DSC thermograms of acetic acid solvate of bropirimine ground for 1. 0 mins, 2. 1 min, 3. 3 min, 4. 4 min and 5. 5 min

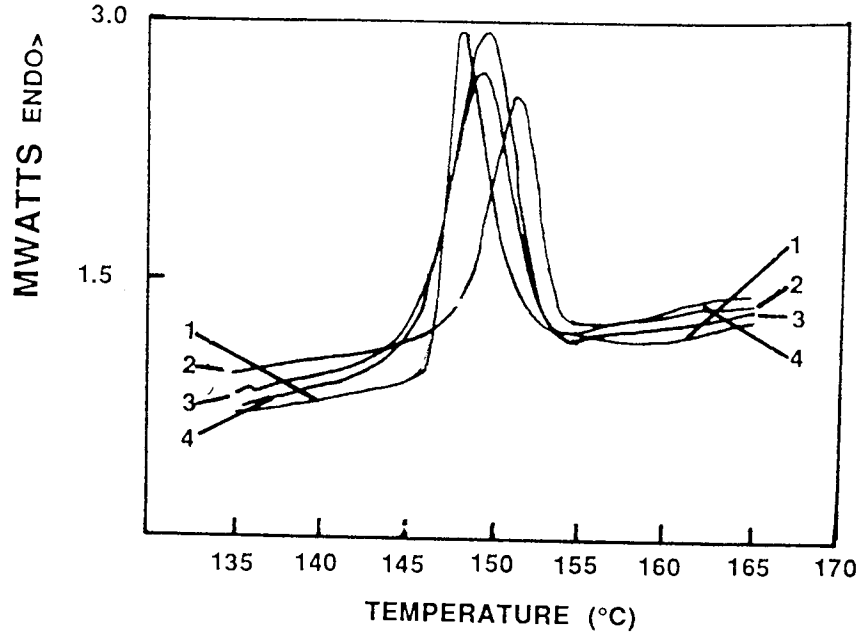

Fig. 4.11: DSC thermograms of 4-Methoxyphenyl aminoacetate hydrochloride (MPAA)
1. No grinding
2. Ground for 5 mins
3. Ground for 15 mins
4. Ground for 20 mins

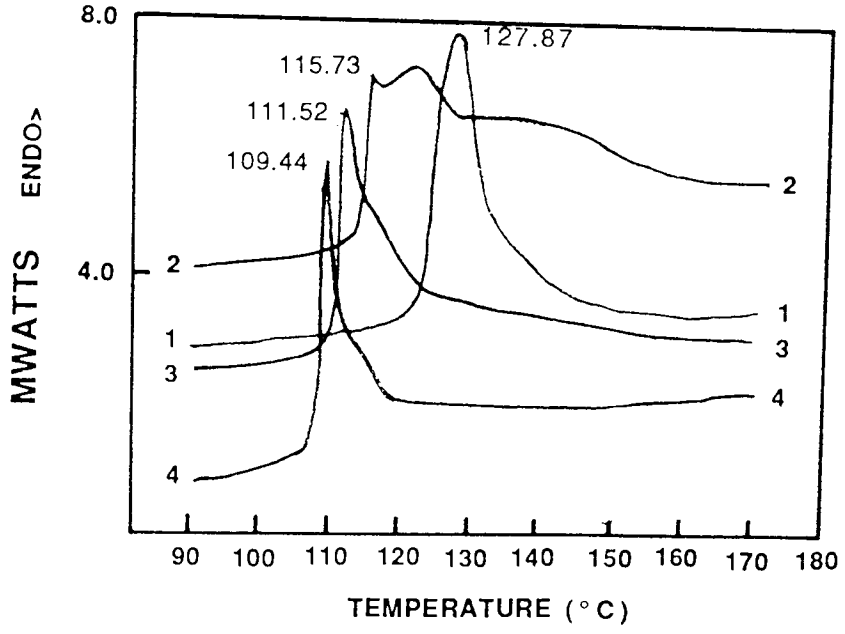

Fig. 4.12: DSC thermograms of 1:1 admixtures of 4-Methoxyphenyl aminoacetate hydrochloride (MPAA) and acetic acid solvate of bropirimine
1. Gently mixed
2. Ground for 1 min
3. Ground for 2 min
4. Ground for 3 min

either pure component (Fig. 4.12). As the length of grinding increases, the peaks progressively appear at a lower temperature and show similarity with the individually ground acetic acid solvate, but at a lower temperature. These events obscured the peaks due to bropirimine in the solvate, and hence no attempt was made to study the possibility of bropirimine peak variation. It is possible that the new peak is due to the depression of desolvation point by MPAA or alternatively a reaction could be taking place.

To test the possibility of decomposition of MPAA, a 50:50 mixture of the acetic acid solvate and the MPAA were ground together as described in Section 4.2.2. The HPLC was effected using the mobile phase described in Section 4.2.2. Typical HPLC traces are shown in Fig. 4.13, using standard solutions along with a mixture of each obtained from partial degradation by grinding MPAA with the acetic acid solvate. Elution times of 5.5 mins and 3.5 mins were recorded for 4-hydroxyanisole and MPAA respectively.

Decomposition in the solid state is a multi-variable phenomenon and two basic models to describe such decompositions (Table 4.4) include:

a. Contracting geometry (or topochemical). It is assumed that the radius of the intact chemical substance decreases linearly with time.

b. Diffusion based. The model assumes that the decomposition is governed by the formation and growth of active nuclei which occur on the surface as well as inside the crystals.

Microscopical examination of the particles showed that MPAA (Fig. 4.14) crystals used in this study existed in irregular slabs. Hence the contracting slab model was used to follow the sold state decomposition of MPAA.

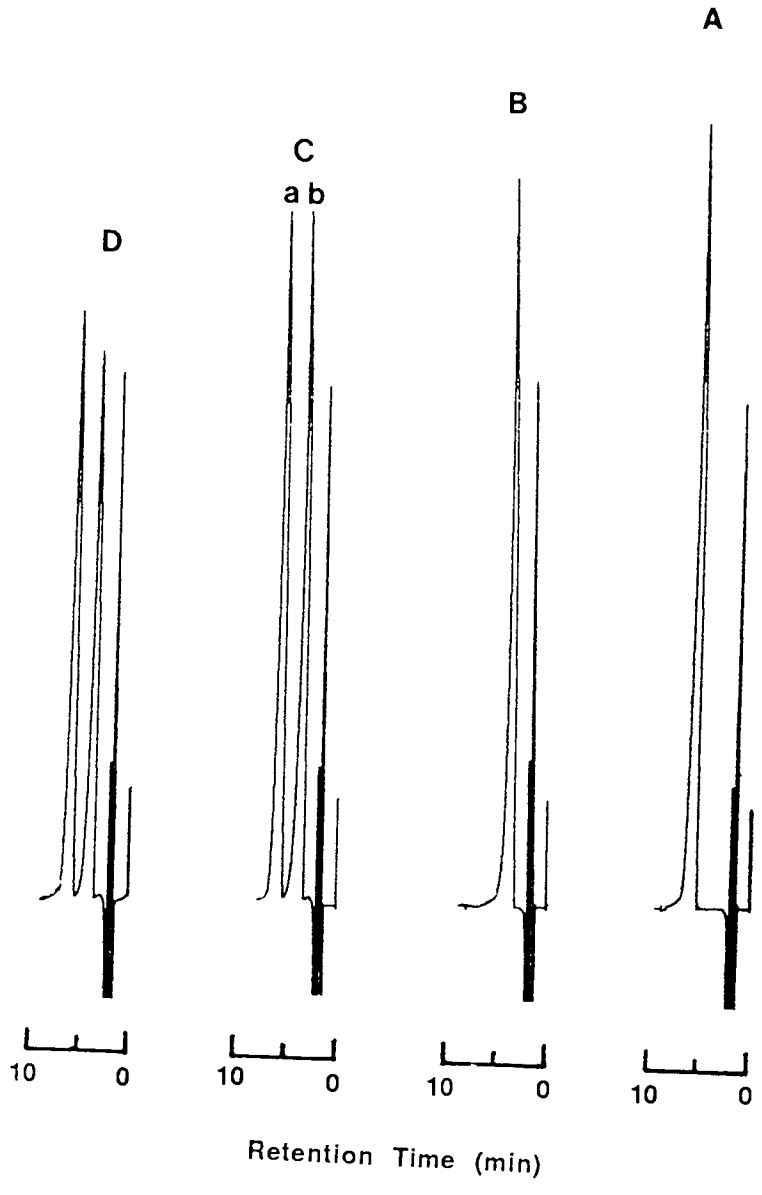

Fig. 4.13: *HPLC traces showing:*
A. 4-hydroxyanisole (a)
B. 4-Methoxyphenyl aminoacetate hydrochloride (MPAA) (b)
C. a mixture of each obtained from partial degradation by grinding with acetic acid solvate of bropirimine (1:1)
D. standard mixture of each component

Fig. 4.14: Photomicrograph of 4-Methoxyphenyl aminoacetate hydrochloride (MPAA) *x10*

1. Contracting Geometry Model

Slab	$(1 - x) = 1 - \left(\frac{kt}{r_o}\right)$
Cylinder	$\sqrt{(1 - x)} = 1 - \left(\frac{kt}{r_o}\right)$
Sphere (cube)	$\sqrt[3]{(1 - x)} = 1 - \left(\frac{kt}{r_o}\right)$

2. Diffusion Model

Cylinder	$\left[1 - \sqrt[2]{(1 - x)}\right]^2 = k't$
Sphere	$\left[1 - \sqrt[3]{(1 - x)}\right]^2 = k't$

where $k' = \frac{2k}{r_o^2}$

x = Mole fraction decomposed
t = time
k = decomposition rate constant
r_o = initial radius of the solid

Table 4.4: Models used for solid state decomposition [adapted from (220)]

Plots of (1-x) against t (Table 4.4) for ground and unground admixture of acetic acid solvate of bropirimine and MPAA are shown in Fig 4.15. Being a prodrug, the MPAA breaks down to yield the active moiety 4-hydroxyanisole (Fig. 4.13). Also shown in Fig. 4.15 are the effects of humidity on the degradation of MPAA. Being water-labile, decomposition follows exposure to moisture and this is clearly seen in Fig. 4.15 and reflected in the decomposition rate constants (Table 4.5). An increase in the rate of degradation is apparent when the relative humidity is increased from 10% to 80%. As already shown above (Fig. 4.10), grinding the acetic acid solvate leads to the liberation of free acetic acid molecules which are in turn available for further reaction. Plots 3 and 4 (Fig 4.15) hence represent decomposition due to acid catalysed hydrolysis of MPAA.

Conditions	k' (=k/r_o)	Correlation coefficient, r
MPAA at 37°C +	5.90×10^{-5}	0.957
MPAA at 37°C + 80% RH	1.16×10^{-4}	0.994
MPAA + solvate (unground) at 37°C + 80% RH	1.83×10^{-4}	0.984
MPAA + solvate (ground for 5 mins) at 37°C + 80% RH	3.10×10^{-4}	0.977

Table 4.5: Rate constants and correlation coefficients for the degradation of MPAA under various conditions

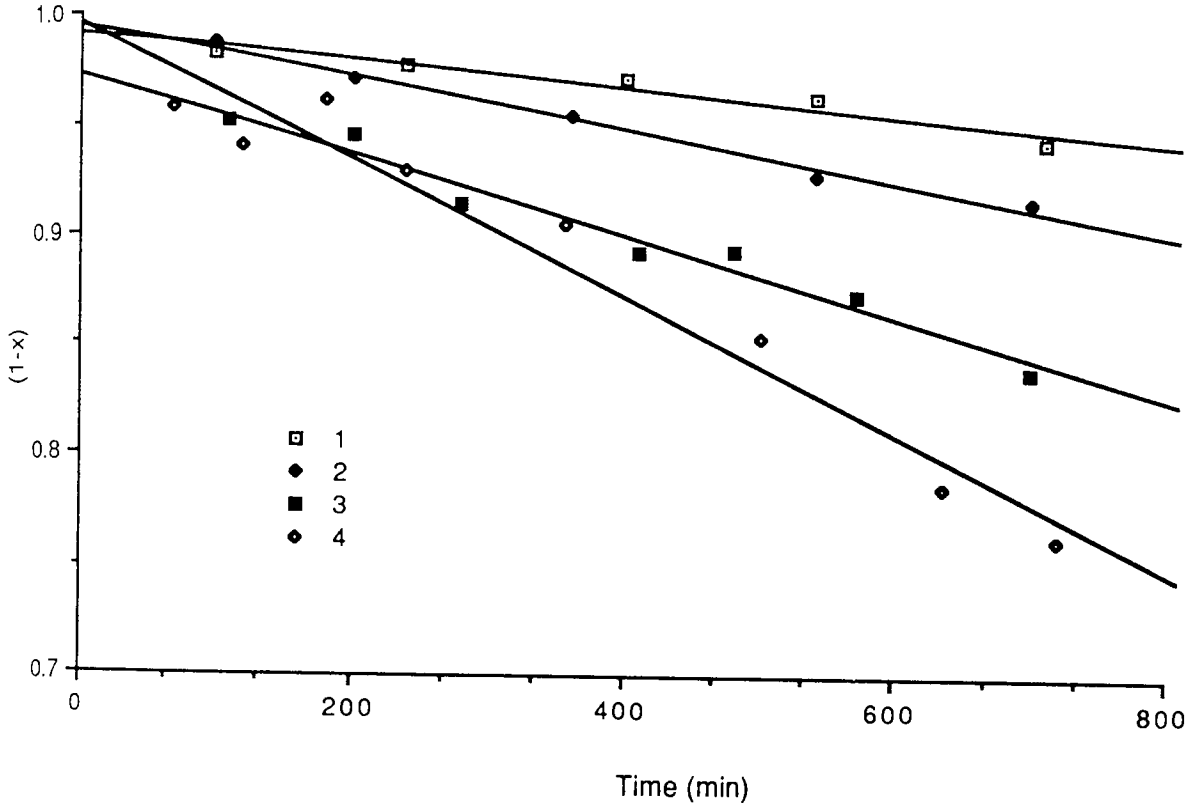

1. MPAA at 37°C +
2. MPAA at 37°C + 80% RH
3. MPAA + solvate (unground) at 37°C + 80% RH
4. MPAA + solvate (ground for 5 minutes) at 37°C + 80% RH

Fig. 4.15: Decomposition of MPAA alone and with admixtures of acetic acid solvate of bropirimine

The above experiments illustrate that the breakdown of a labile drug on admixture may be enhanced when mechanically treated with solvates. Although these types of solvates are uncommon, hydrates are frequently encountered. A very important example is lactose which is widely used as tablet diluent in the pharmaceutical industry.

Thermograms of α-lactose monohydrate run at a heating rate of 10°/min give two peaks (Fig. 4.16). The first endotherm at Ca. 150°C represents the loss of water whereas the second peak at Ca. 217°C represents the melting of the α-lactose monohydrate, followed by irregular peaks indicative of degradation. There are conflicting reports on the temperature at which the α-lactose monohydrate melts. Lerk *et.al.*[145] have reported the melting endotherm at 212°C, whereas Berlin *et.al.*[146] showed it to occur at 223°C, the former using open aluminium pans whereas the latter used crimped pans.

On grinding the α-lactose monohydrate, the dehydration peak begins to develop a shoulder at a lower temperature which becomes progressively bigger and broader upon further mechanical treatment indicating the release of water from the crystal lattice (Fig. 4.16). After 10 minutes of grinding the dehydration peak is almost lost and is replaced by a broad peak with a peak maximum temperature of 139.1°C.

A further endothermic peak begins to develop concurrently with the above peak at Ca. 223°C. The size and the peak maximum temperature of this increase upon mechanical treatment and is possible due to conversion of α-lactose monohydrate to the stable anhydrous α-lactose[145]. Even on purification, the stable anhydrous α-lactose contains a relatively high amount of β-lactose (approx 13%)[148] which shows a melting endotherm at 237°C.[145]. However, because of this mixture, depression of melting point may occur and the double endotherm recorded with the stable anhydrous α-lactose may be the melting of the stable

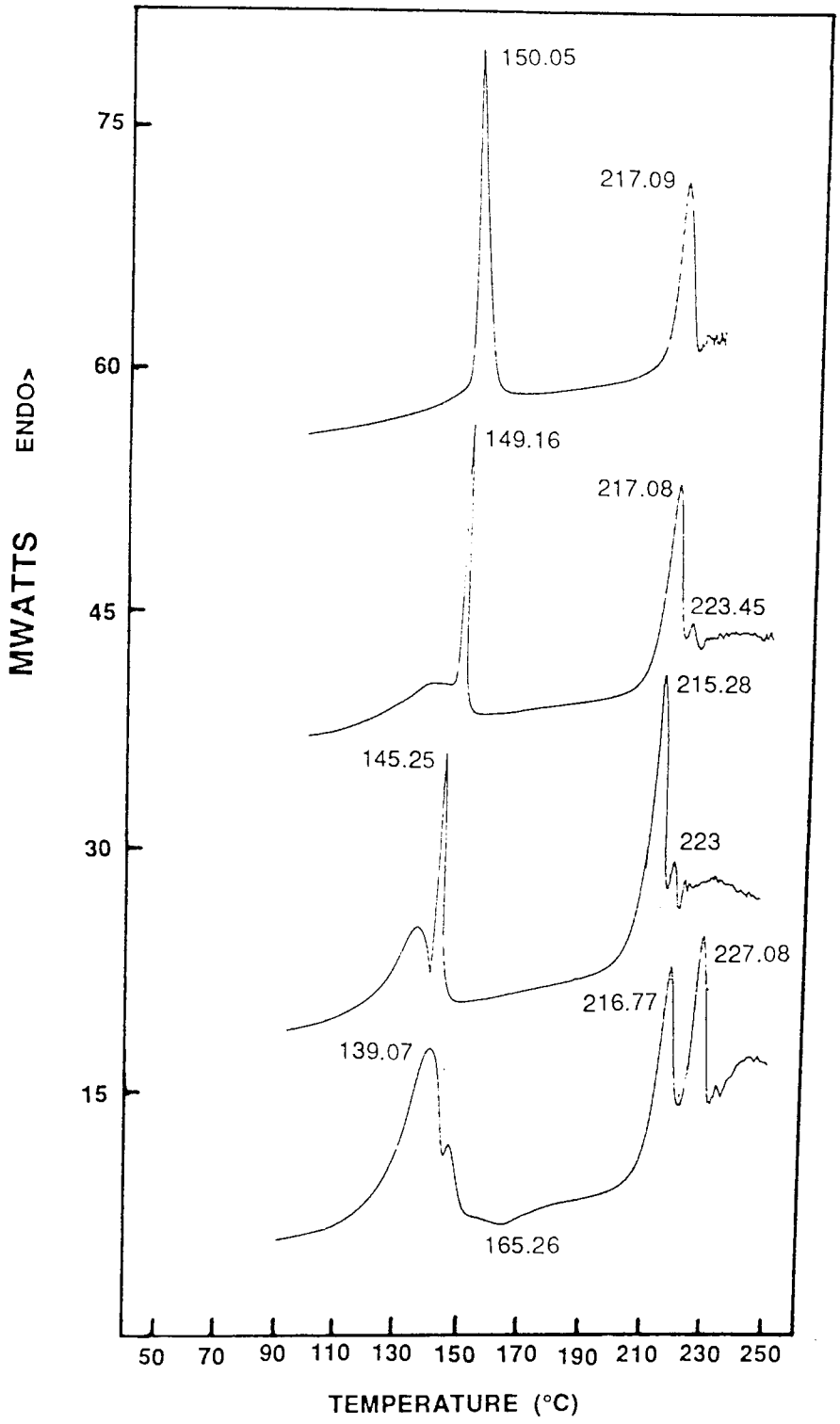

Fig. 4.16: DSC thermograms of
1. α-lactose monohydrate
2. Ground for 2 mins
3. Ground for 5 mins
4. Ground for 10 mins

anhydrous α-lactose followed by the melting of the β-lactose. This may thus explain the progressive decrease in the intensity of the first endotherm and the corresponding increase in the intensity of the second endotherm upon grinding (Fig. 4.19). If increasing the amount of an impurity causes a depression in the melting point then the opposite should also hold. As the size of the second endotherm increases, peak maximum is seen to occur at progressively higher temperature such that from 2 minutes to 10 minutes of grinding, the peak maximum temperature of the endotherm increases from 223°C to 227°C. It is logical to assume, therefore, that mechanical stress leads to the conversion of anhydrous α-lactose to the β-lactose. As the amount of β-lactose increases (and therefore its purity), the peak maximum temperature will tend towards the peak maximum temperature of the pure (98.7%) β-lactose (Ca. 237°C)[143].

A third, exothermic event is seen to occur at a peak maximum temperature of around 165°C after 10 minutes of grinding. This has caused confusion amongst a number of workers[145-147] who recorded the peak at various temperatures, although not always on grinding. Itoh *et.al.*[147] observed that the x-ray diffraction pattern of the anhydrous β-lactose contained a number of peaks which could not be accounted for by α-lactose monohydrate alone. They thus concluded that formation of a new crystal structure has taken place on dehydration but failed to relate this to the exothermic peak they had recorded at 181°C[147]. Although, generally, conversion of one form to another occurs on melting[149], Fernandez-Martin *et.al.*[150] conclusively showed that equilibration between α-form and β-form was taking place in the solid state, albeit at a higher temperature (175-180°C) than the exotherm recorded here.

As with the acetic acid solvate, grinding of lactose monohydrate liberates water which is free to undergo any interactions. Fig. 4.17

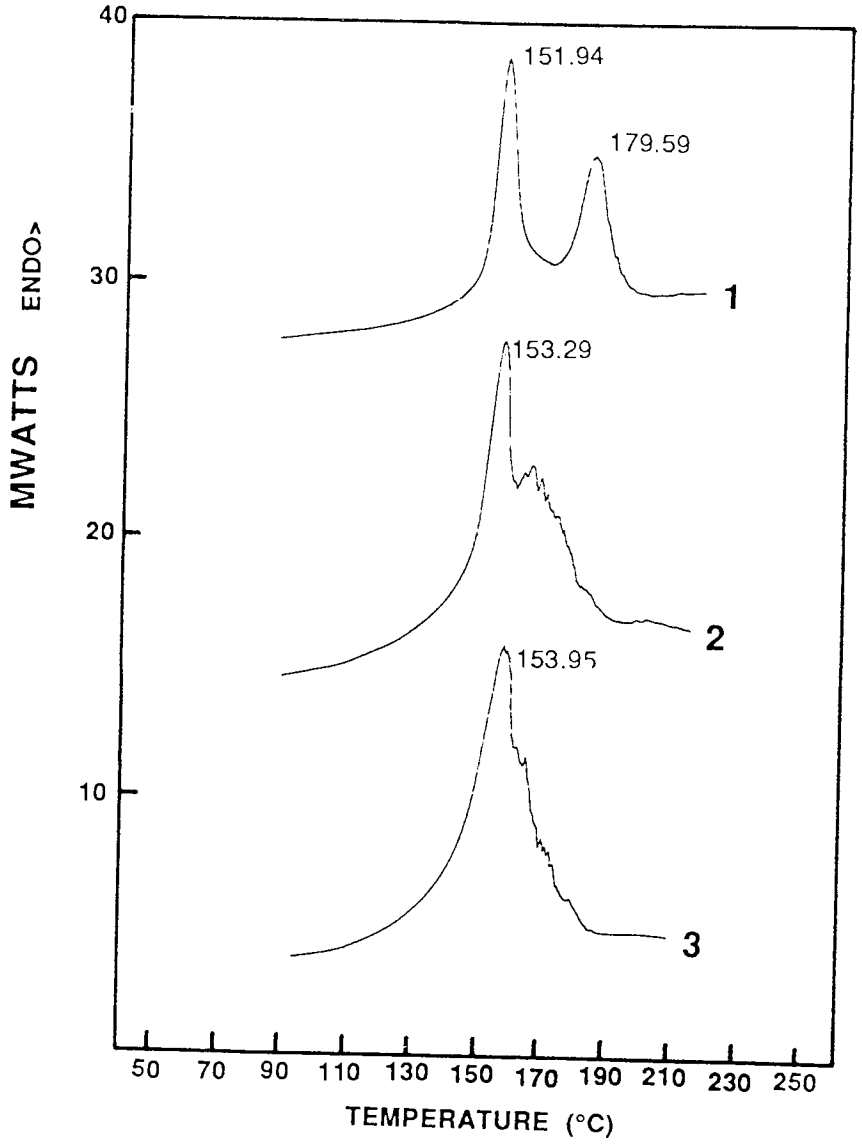

Fig. 4.17: DSC thermograms of 4-Methoxyphenyl aminoacetate hydrochloride (MPAA) and lactose monohydrate admixtures (1:4)
1. Gentle mixing
2. Ground for 1 minute
3. Ground for 2 minutes

shows thermograms obtained for an admixture of MPAA (25%$^{w}/_{w}$) and lactose monohydrate (75%$^{w}/_{w}$) upon grinding. After gentle mixing of the two components in a vial, two endothermic peaks are apparent, the first of which (151.9°C) may be due to dehydration of lactose monohydrate. The second endotherm (179.6°C) cannot be attributed to peaks from either component although a sharp depression in melting point of the lactose may result in such a peak. However, upon grinding, even for periods as short as 1 minute, the peaks coalesce to form one broad peak. Immediately following the peak, the irregular shape of the thermogram signifies degradation.

Fig. 4.18 shows the disappearance of MPAA and the appearance of 4-hydroxyanisole following grinding of the prodrug with lactose monohydrate for 10 minutes and subsequent storage at 37°C and 80%RH. The plots show that degradation of MPAA follows zero order kinetics. After 1500 minutes, all the MPAA has broken down to form 4-hydroxyanisole.

Fig. 4.19 shows the data plotted according to the contracting slab model (Table 4.4) under various conditions. A simple mixture was obtained by sieving the two components individually and then gently mixing them in a vial. A rate constant of 2.55×10^{-4}/min is obtained here (Table 4.6) compared to 1.16×10^{-4}/min for the admixture of acetic acid solvate and MPAA under the same conditions. This suggests that even without grinding there is sufficient interaction to enhance degradation to some extent. The effect is much more pronounced on grinding. There is only a slight difference in the decomposition rates between the samples when only lactose is ground (4.67×10^{-3}/min). In the latter case, the higher decomposition rate constant is probably due to not only a better mix, but also due to an increase in the surface area available for decomposition upon mechanical stressing.

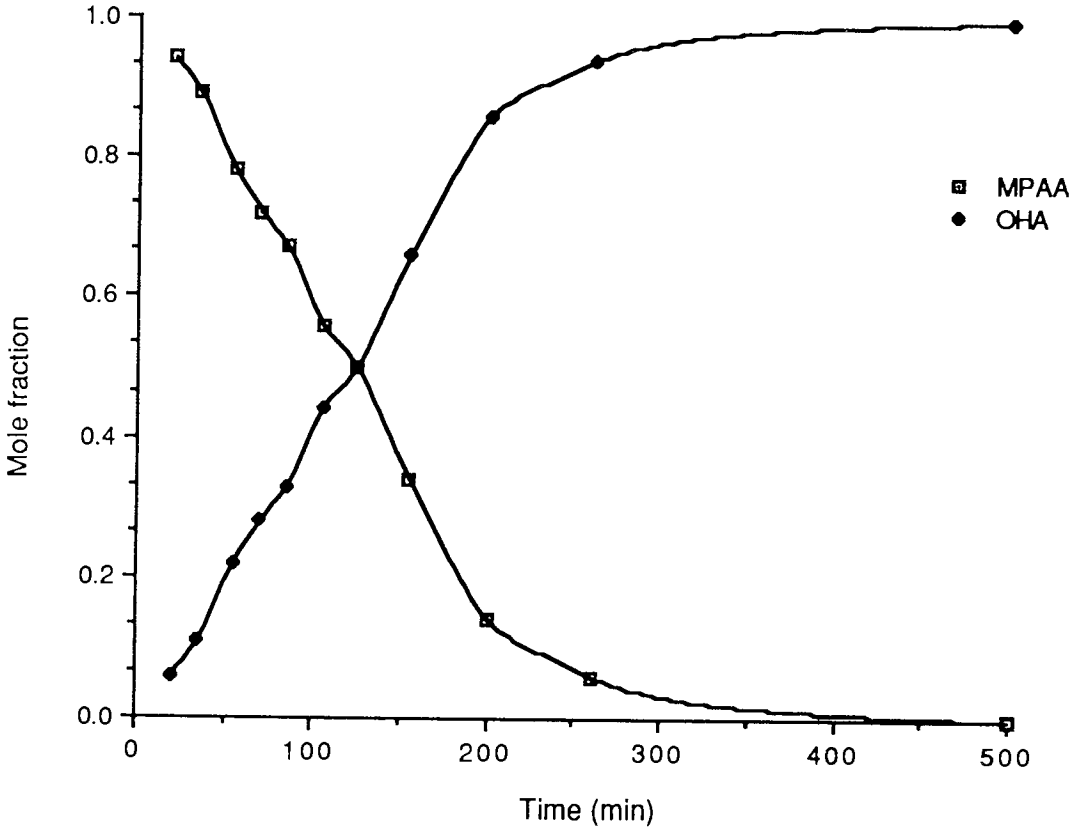

Fig. 4.18: Plots to illustrate the disappearance of MPAA and the appearance of 4-hydroxyanisole (OHA). Both MPAA and lactose ground for 10 min.

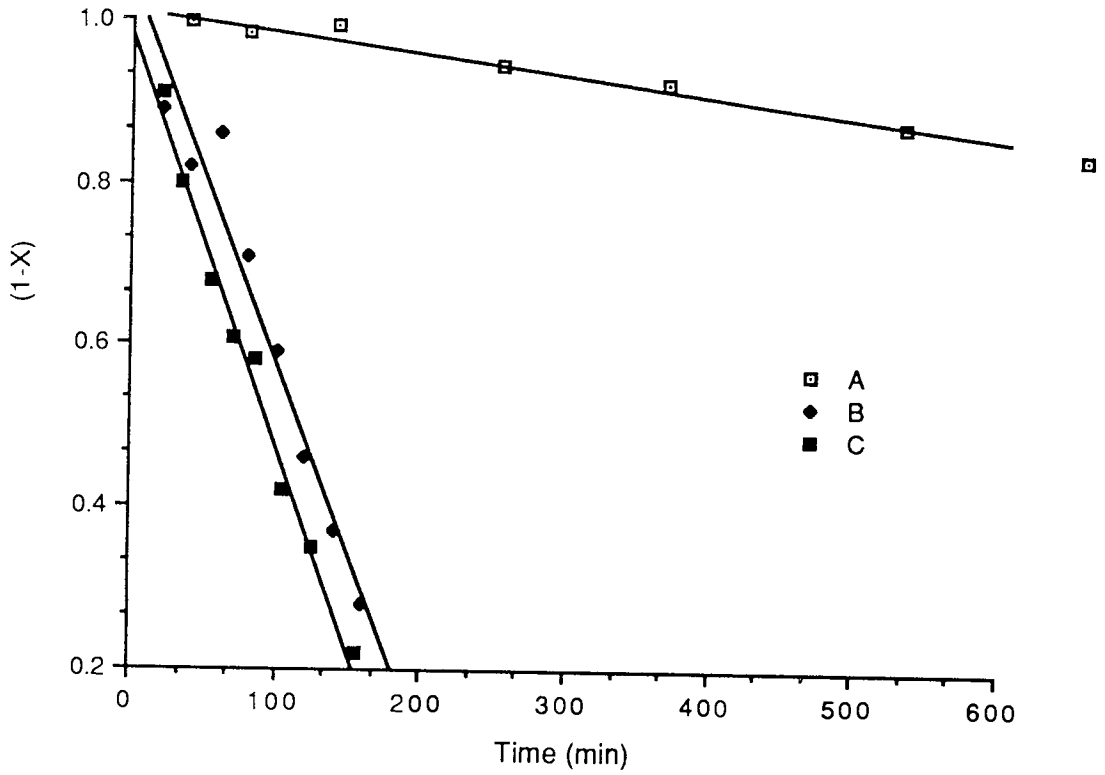

A. Simple mixture
B. Only lactose, ground for 10 minutes
C. Both MPAA and lactose, ground for 10 minutes

Fig. 4.19: Degradation of MPAA on admixture with lactose.

In conclusion, although reports exist on the effect of grinding, these usually tend to relate the mechanical stress to polymorphic changes[134,136-138] or 'in-house' degradation[141,142], i.e. the liberated water causing degradation of the parent compound. Where physical interactions have been observed[116] no attempt had been made to evaluate the cause of interaction. Experiments performed here show conclusively that water labile substances may degrade upon admixture with compounds containing water of crystallisation, even under mild mechanical stress.

Conditions	k' (=k/r_o)	Correlation coefficient, r
Simple mixture	2.55×10^{-4}	0.990
Only lactose, ground for 10 minutes	4.67×10^{-3}	0.977
Lactose and MPAA, ground for 10 minutes	5.04×10^{-3}	0.995

Table 4.6: Rate constants and correlation coefficients for the degradation of MPAA on admixture with lactose

5.0 PHYSICO-CHEMICAL PROPERTIES OF THE IMMUNOMODULARATORY AGENTS

5.1 Introduction

Frequently, the rate determining step in the absorption process of a compound, given orally, is dissolution. A low aqueous solubility may manifest itself in low activity of the drug as a result of low plasma levels. To enhance the solubility, other methods may be considered such as modification of chemical structure[152] or the use of additives, co-solvents and solid state manipulation[153].

Attempts shall be made to determine the physico-chemical properties of the immunomodulatory agents (bropirimine, and its derivatives and pyrimethamine and its derivatives) such as the aqueous solubility and pK_a values. The effects of co-solvents and additives on bropirimine shall be studied in oder to formulate bropirimine for parenteral use.

5.2 Materials and methods

5.2.1 Solubility determination

5.2.1.1 Solubility in Britton-Robinson (B-R) buffers

The buffers (pH 2-11) were prepared as described in Appendix I and the final strength of the buffers adjusted to 0.5M using potassium chloride (Fisons). The acids and bases used in the preparation of the buffers were obtained from different sources and were all of BP standard. Approximately 5mL of each of the buffer was placed in a flat-bottomed vial to which excess (100-200mg) drug (bropirimine, AB, PB, pyrimethamine, MPP, DPP, MDPC, EDPC, PDPC and iPDPC) were added. A small magnetic flea was placed in the vial, the vial was stoppered and mounted on underwater stirrers. The vials and stirrers

were placed in a thermostatically-controlled constant-temperature water bath equilibrated at 25°C. After 90 minutes stirring, the vials were removed from the water bath and the contents filtered through 0.20μm cellulose nitrate Millipore filters, taking care to discard a small portion of the initial filtrate. In order to ascertain that equilibrium had been reached, a control was also run by adding excess of each drug to B-R buffer pH 7.4. Samples were withdrawn at 30, 60, 90 minutes and 24 hours (for bropirimine). In all instances equilibrium appeared to have been reached within 60 minutes (Chapter 6). 2.5mL of each filtrate were then diluted to 5mL with methanol (Fisons) and thoroughly mixed. Any further dilutions were then undertaken with an equimixture of methanol and distilled water. 1mL of the test solution was added to 1mL of internal standard (IS) prepared in equimixture of methanol and distilled water, thoroughly mixed using Whirlmixer (Fisons) and 20μL injected into the HPLC once steady state conditions had been reached i.e. when the same peak heights were obtained for the same concentration of a solution on at least three consecutive occasions. Calibration solutions were prepared in 50%$^{v}/_{v}$ methanol and from this serial dilutions were performed to cover the required range.

Table 5.1 gives details of the composition of the final, injected standard solutions and the internal standards and mobile phases used. Each mobile phase contained 0.1%$^{v}/_{v}$ diethylamine and the pH was adjusted to 2.0 with orthophosphoric acid. The rest of the conditions are shown below:

Loop size	20μL
Flow rate of mobile phase	2mm/min
Wavelength	296nm
Sensitivity	0.16-0.64 AUFS

Compound	Concentration range of standard solutions (μg/mL)	Internal standard and concentration (mg/mL)	Mobile phase
Bropirimine	80 - 400	ABmFPP (0.1)	1
AB	80 - 400	ABmFPP (0.1)	
PB	80 - 400	ABmFPP (0.1)	
MPP	80 - 400	Ethylparaben (10)	2
DPP	80 - 400	Ethylparaben (10)	
MDPC	80 - 400	Ethylparaben (5)	3
EDPC	40 - 200	Methylparaben (10)	
PDPC	40 - 200	Methylparaben (5)	
iPDPC	80 - 400	Methylparaben (5)	

Mobile phases

1. 25%v/v acetonitrile
2. 50%v/v acetonitrile
3. 40%v/v acetonitrile

Table 5.1: Composition of standard solutions and the internal standards and mobile phases used in solubility studies

5.2.1.2 Solubility of bropirimine in sodium carbonate

A stock solution of sodium carbonate (BDH) was prepared by dissolving 21.198g in 1L of distilled water to give a 0.2M solution. This was then serially diluted to give a range of concentrations (0.02M - 0.2M). The solubility study was then carried out as in Section 5.2.1.1.

5.2.1.3 Solubility of bropirimine in acetic acid

Dilutions of 20, 40, 60, and 80% $^{v}/_{v}$ of glacial acetic acid BP (Fisons) were prepared using distilled water. Each concentration was then divided into two 5mL portions and excess bropirimine added. One set was placed in a cold room at 6°C to equilibrate overnight and the other set placed at 60°C for the same length of time. Following the equilibration period, the suspensions were filtered in the usual way into

dry, clean test tubes which were either pre-heated (60°C) or pre-cooled (6°C) and then treated as in Section 5.2.1.1.

5.2.1.4 Solubility of bropirimine in dimethylacetamide (DMA), propylene glycol (PG) and polyethylene glycols (PEGs)

The DMA (Fisons), PG (BDH) and PEGs (nominal molecular weights of 200, 400, 1000, 1500, 4000 and 6000) (BDH) were used as received. Various concentrations (8-40%$^{w}/_{w}$ of each) were prepared in B-R buffer pH 7.4. For higher molecular weight PEGs, gentle heating was needed to melt these in a small amount of the buffer and then made up to volume once cooled. The solutions were then saturated with bropirimine and then treated as in Section 5.2.1.1.

5.2.1.5 Solubility of bropirimine in cyclodextrins

α-, β- and γ- cyclodextrins were purchased from Sigma and used as received. Hydroxypropyl β-cyclodextrin (HPBCD) was prepared as described elsewhere[188,198]. Various concentrations (0.2-15mM) were then prepared in B-R buffer pH 7.2 and treated as in Section 5.2.1.1. The mixture was left stirring for 24 hours.

5.2.1.6 Solubility of bropirimine in N-methyl-D-glucamine

A stock solution of 5%$^{w}/_{v}$ of meglumine was prepared in distilled water. This was then serially diluted to give a range of concentrations (0.1-5%$^{w}/_{v}$). Solubility studies were then carried out as in Section 5.2.1.1.

5.2.2 Partition coefficent (PC) determination

B-R buffers were prepared as described above and in Appendix I. 25mL of each of the buffers were transferred into a 50mL glass flask and 5mL octanol (Fisons) added. The flask was then vigorously shaken

and placed in a shaking constant-temperature water bath, maintained at 25°C, for 10 hours. After this period the two phases were allowed to mutually separate for 24 hours. The octanol layer was then discarded and the pH of the octanol saturated buffer measured. Similarly, 200mL of the octanol were shaken with buffer pH 7.4 for 10 hours at 25°C and then allowed to separate. A stock solution containing 150μg/mL of the drug (bropirimine, AB or PB) was then prepared in this buffer-saturated octanol (A). 5mL of each of the octanol-saturated buffer solutions were transferred into conical glass centrifuge tubes and 5mL of solution A added. The contents were then thoroughly mixed (each tube stirred for 30 seconds continuously and then repeated 10 times) using a Whirlmixer and then placed in a shaking constant-temperature water bath maintained at 25°C, for 90 minutes. The two phases were then separated by centrifugation at 3500 rpm for 10 minutes. The experiment was carried out in quadruplicate. Both phases were analysed.

5.2.2.1 Assay of octanol layer

This was performed by measuring the ultraviolet absorption of the octanol layer. Two matching quartz cells having a path length of 1cm were used, one containing the blank (buffer saturated octanol) and the other containing the test sample. Absorption was then measured on CECIL CE272 digital readout ultraviolet spectrometer at 300nm wavelength. Standard solutions were prepared by serial dilution of solution A with buffer-saturated octanol.

To ensure that equilibrium had been reached, the phases were shaken for a further 5 hours. It was found that equilibrium had been reached in the first instance.

5.2.2.2 Assay of aqueous layer

HPLC was used to carry out assay of the aqueous layer. 1mL of the aqueous phase was diluted with an equal volume of methanol, the mixture thoroughly shaken and 1 mL taken and added to 1mL of internal standard (10μg/mL ABmFPP) prepared in 50%$^{v}/_{v}$ methanol in octanol-saturated buffer. The mixture was thoroughly shaken and 20μL injected into the HPLC. Mobile phase 1 was used at 300nm. The standard solutions were prepared in 50%$^{v}/_{v}$ methanol in octanol-saturated buffer solution which was also used for any dilution.

5.3 Results and discussion

5.3.1 Estimation of dissociation constant (K_a) from solubility data

The knowledge of K_a values has some important clinical applications. Forced alkaline diuresis using sodium lactate increases the pH of the blood and therefore the degree of ionisation resulting in enhanced excretion of aspirin in the event of overdosage[154]. Conversely, forced acid diuresis may be used in the event of amphetamine overdosage[155,156]. Both of these procedures are now routinely performed in clinics.

There are several methods by which the dissociation constant of a compound may be obtained. Such methods include potentiometric titration (which requires the compound to be both stable and soluble), ultraviolet spectroscopy (where the molecular form of the compound must have significantly different absorption from that of the ionic form), and various other methods that require energy calculations[172-175]. Recently, Rosenberg *et. al.* described a useful method by which the solubility of a sparingly soluble and/or labile compound may be determined by difference potentiometry[176], where both the blank (solvent) and solvent-solubilised drug are filtrated against a suitable

titrant. However, this technique also has limitations *viz* that it cannot be used for compounds having more than one dissociation constant. Miyake *et. al.* proposed the use of HPLC for the determination of the dissociation constants but this technique is only valid for compounds which have pH-dependant capacity ratios[177,178]. Direct titration requires the compound to be both soluble and stable and, therefore, may not be appropriate here.

Where the solubility of a compound is pH dependent, the observed solubility, S, can be related to the intrinsic solubility, S_o, and the pH and the pK_a of a compound by equations 5.1 and 5.2.

For basic compounds:

$$S = S_o + \frac{S_o[H_3O^+]}{K_a} \qquad \ldots 5.1$$

For acidic compounds:

$$S = S_o + \frac{S_o K_a}{[H_3O^+]} \qquad \ldots 5.2$$

To test the validity of the two equations 5.1 and 5.2, the observed solubility, S, was plotted against either $[H_3O^+]$ (Fig.5.1) or $\frac{1}{[H_3O^+]}$ (Fig. 5.2). Both plots show good linearity having correlation coefficients of 0.996 and 0.999 respectively, using the value of S_o as 32.0 µg/mL. Most accurate results are obtained when the points chosen for S and $[H_3O^+]$ are as near to the pK_a as possible[173].

The pK_a values for bropirimine calculated here (Table 5.2) compare well with those obtained by Alpar *et.al.*[77] using spectroscopic

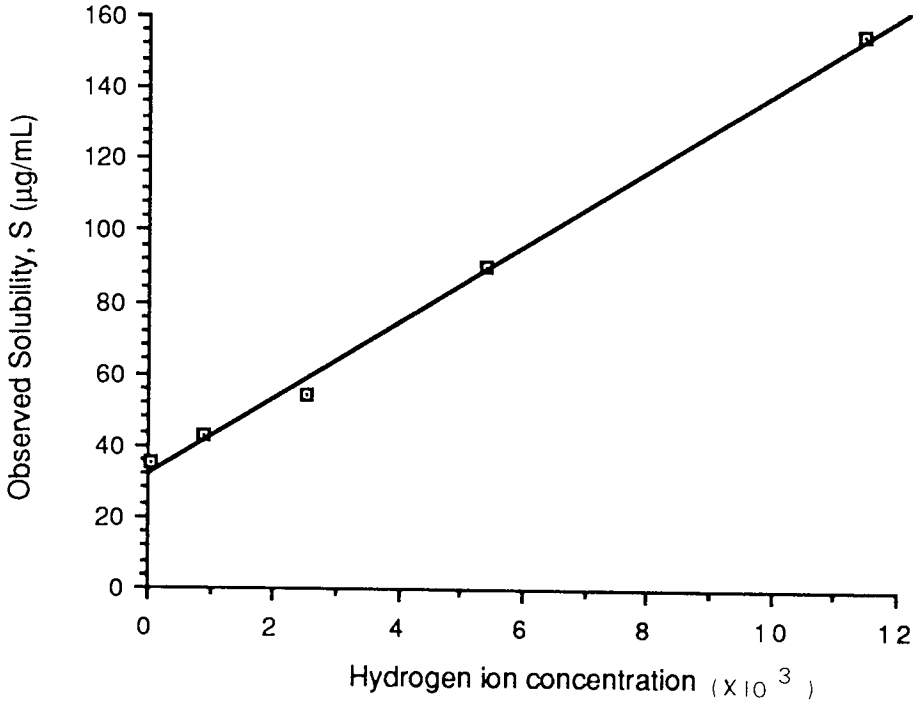

Fig. 5.1: A plot of S against $[H_3O^+]$ for bropirimine to show the validity of equation 5.1

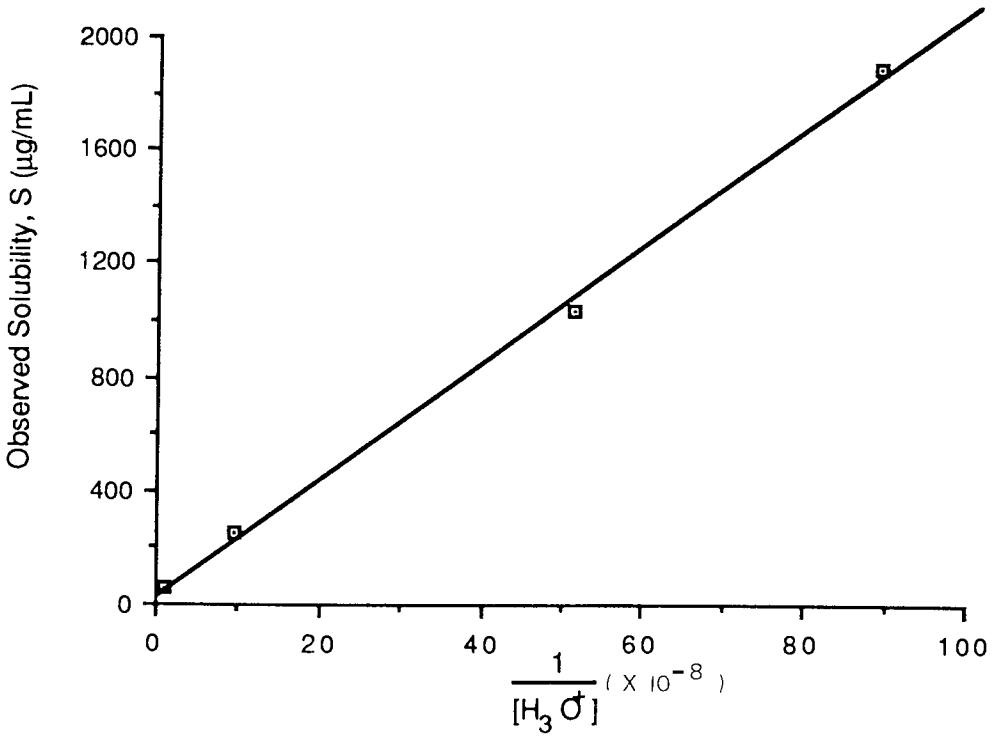

Fig. 5.2: A plot of S against $[H_3O^+]^{-1}$ for bropirimine to show the validity of equation 5.2

method (2.73 and 8.31) and calculations from the solubility data (2.85 and 8.27).

Using equation 5.1 the pK_a values were also calculated for the 2-, 4- and 6- substituted derivatives of pyrimethamine (MPP, DPP, MDPC, EDPC, PDPC and iPDPC). The results are displayed in Table 5.2 along with the aqueous solubilities. It can be seen that as the side chain length of the pyrimethamine derivatives increases, the pK_a values drop correspondingly. Addition of propanoyl group at the 2- position leads to a drop in the pK_a value of approximately 2.5 whereas two propanoyl groups (at the 2- and 4- positions) results in a reduction of approximately 4 pK_a units. A similar trend is followed with the 6-substituted derivatives.

Compound	pK_a	Aqueous solubility, S_w	
		(μg/mL)	(M)
Bropirimine	8.21, 2.52	35.0	1.32×10^{-4}
AB	8.98	13.9	4.51×10^{-5}
PB	10.31	10.0	3.11×10^{-5}
MPP	4.40	88.0	2.89×10^{-4}
DPP	2.89	99.0	2.75×10^{-4}
MDPC	4.62	180.0	6.20×10^{-4}
EDPC	3.86	63.0	2.07×10^{-4}
PDPC	3.53	17.5	5.50×10^{-5}
iPDPC	3.16	4.0	1.15×10^{-5}
Pyrimethamine*	7.00	<10	

* - From the Phamaceutical Codex, 11th Edition, 1979

Table 5.2: List of pK_a values and aqueous solubilities of the immunomodularity agents

5.3.2 Aqueous solubility

Figs. 5.3 - 5.5 show the solubility-pH profiles using B-R buffers for bropirimine, acetyl bropirimine (AB) and propanoyl bropirimine (PB). Fig. 5.3 shows a typical curve of a compound that has two ionisable groups, i.e. both a basic and an acidic function. This behaviour is typical of an amphoteric compound. Ionisation takes place both in acidic and basic environment as shown below:

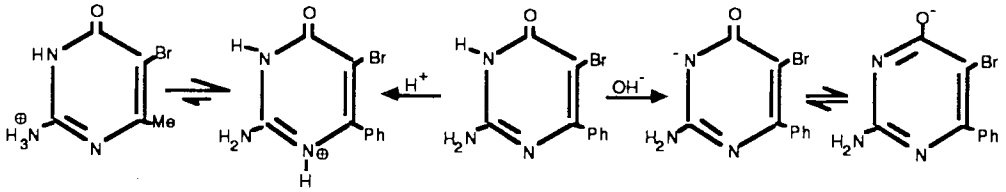

The nitrogen of the 2-amino group can gain a proton and become positively charged, whereas the nitrogen at the 4- position can lose a proton and become negatively charged. The solubility of this class of compound would, therefore, be pH-dependant, passing through a minimum when there is no ionisation.

Since the pK_a of the base is not greater than the pK_a of the acid, bropirimine will not behave as a zwitterion[173]. Blocking the ionisable groups at either position 2- or 4- would result in the loss of the amphoteric character. This can be clearly seen in Fig. 5.4 and 5.5, where solubility-pH profiles are shown for acetyl- and propanoyl bropirimine. Both show profiles characteristic of one acidic centre on the molecule. The increased chain length leads to an increase in the pK_a values (8.98 and 10.31 respectively). Hence the corresponding ionisation takes place at a higher pH.

Figs. 5.6 and 5.7 show plots of MPP and DPP, the 2- substituted pyrimethamine derivatives. These display reverse pH-solubility profiles

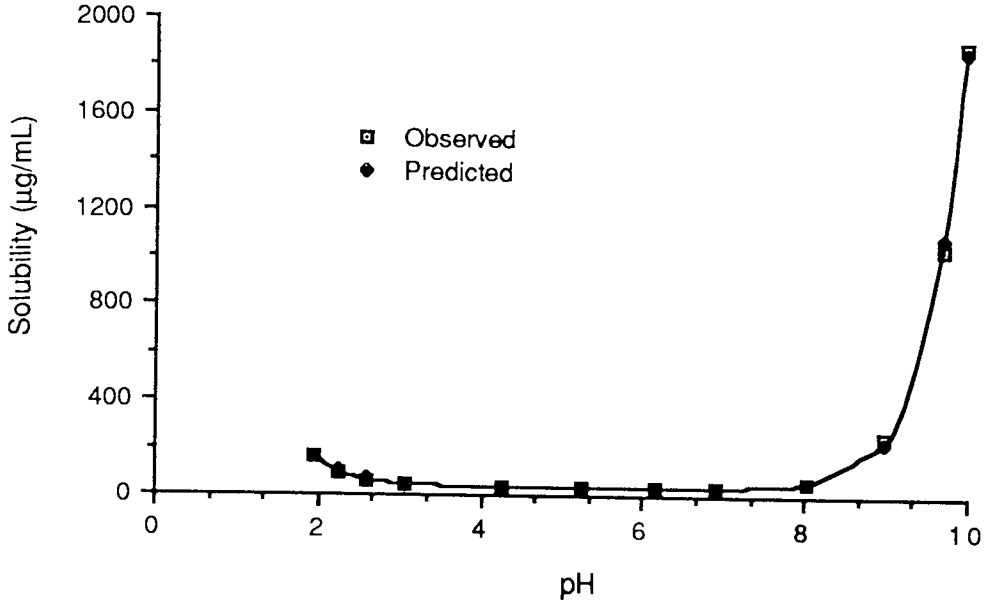

Fig. 5.3: Solubility-pH profile of bropirimine.

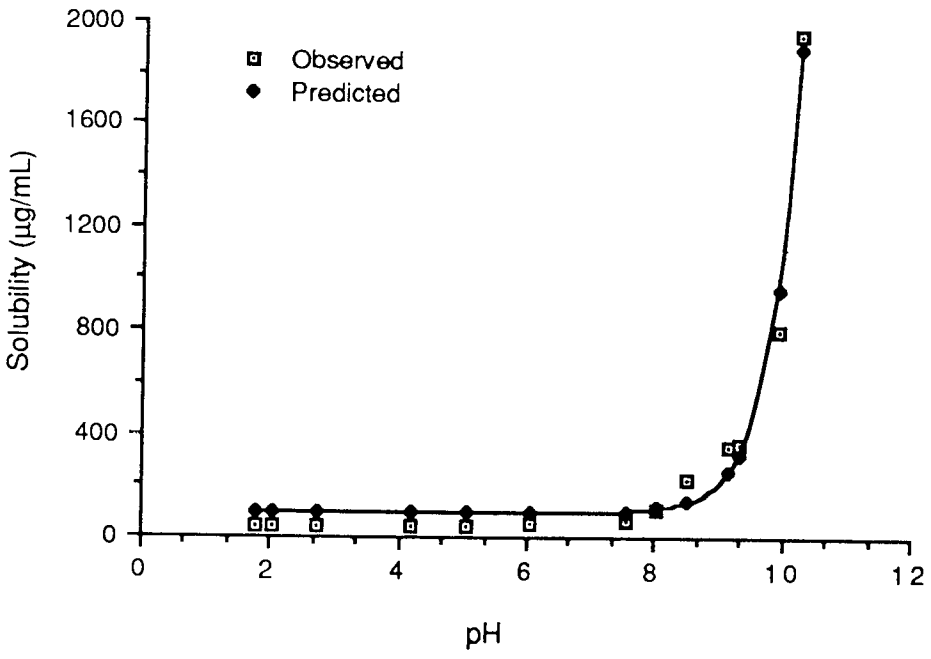

Fig. 5.4: Solubility-pH profile of acetylbropirimine

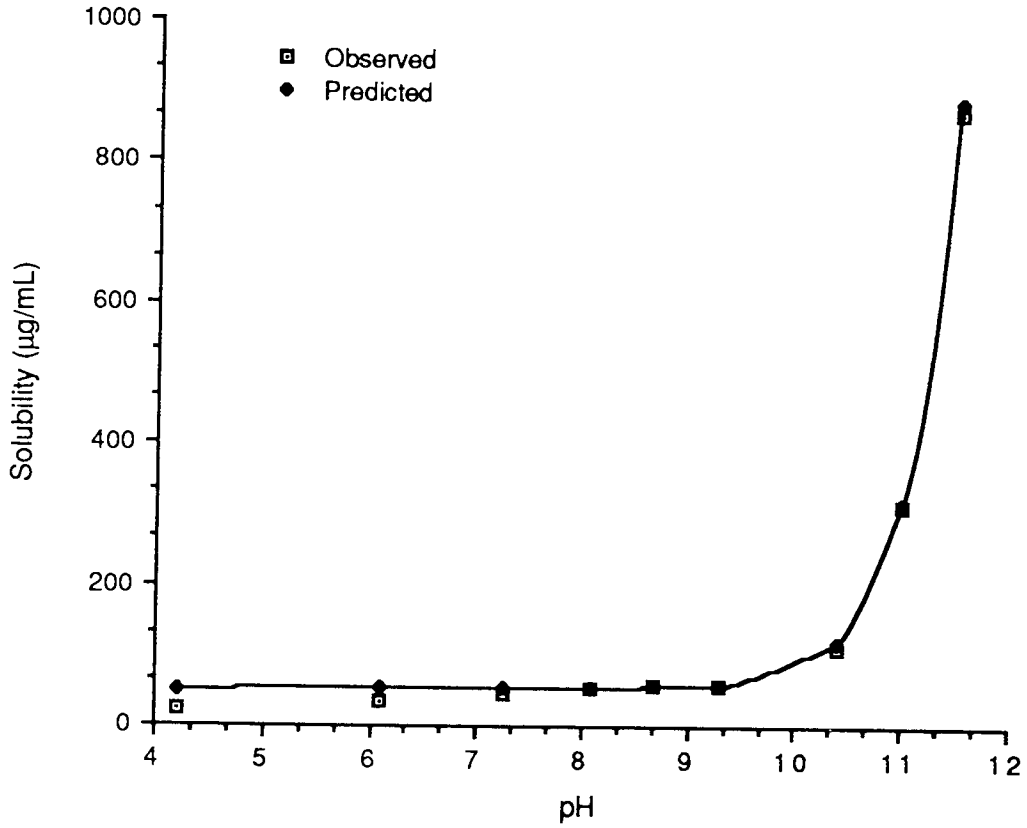

Fig. 5.5. Solubility-pH profile of propanoylbropirimine

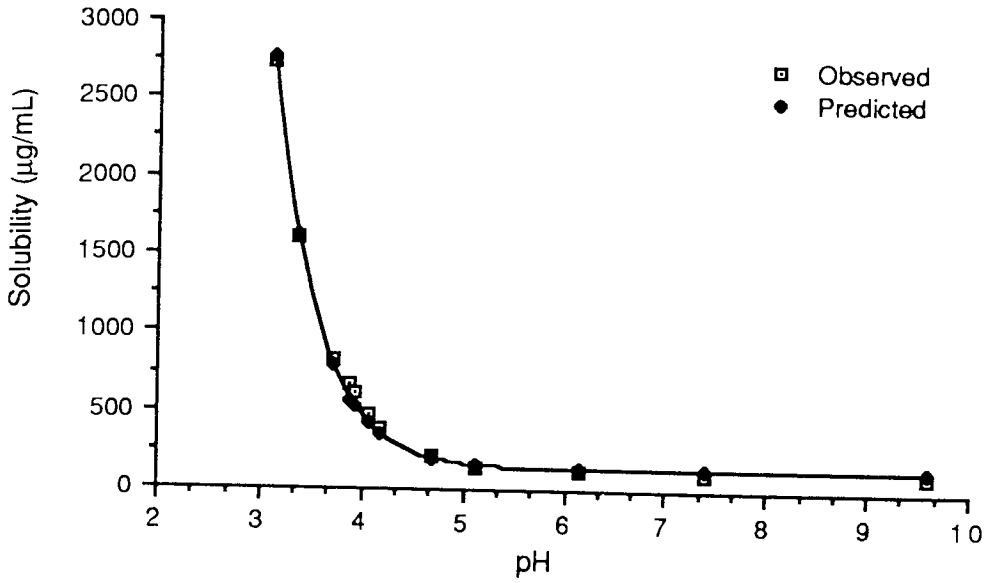

Fig. 5.6: Solubility-pH profile of monopropanoylpyrimethamine

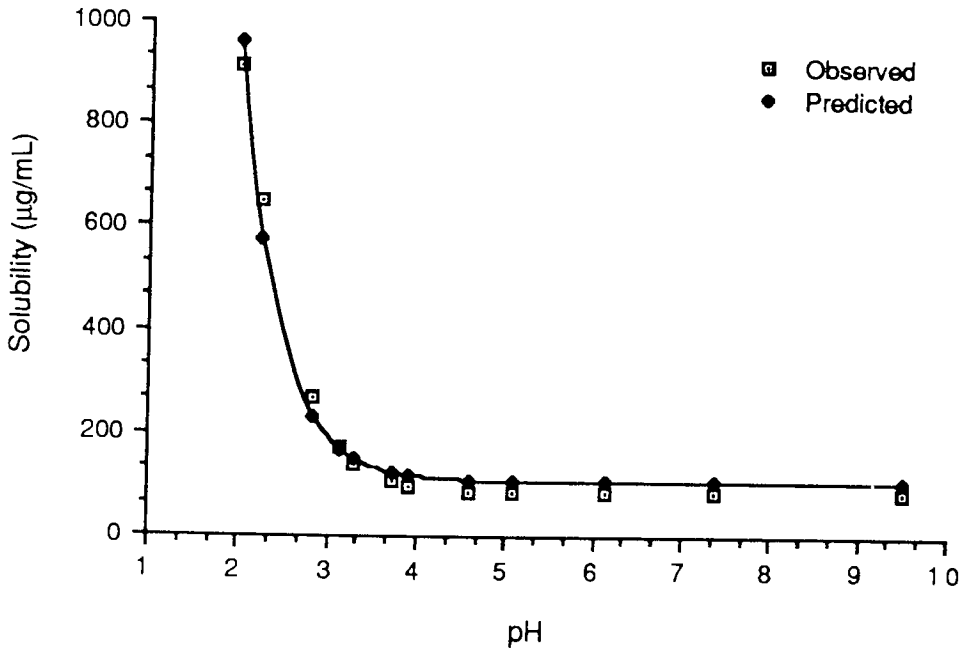

Fig. 5.7: Solubility-pH profile of dipropanoylpyrimethamine

to that seen with AB and PB, indicating a single basic centre. Solubility increases as the pH is reduced with ease of ionisation in the order MPP (pK_a 4.40) > DPP (pK_a 2.89).

The 6-substituted pyrimethamine derivatives (MDPC, EDPC, PDPC and iPDPC) show similar solubility pH profiles as MPP and DPP, again indicating a single basic centre (Figs. 5.8 - 5.11). Aqueous solubility decreases with an increase in the chain length and the pK_a decreases correspondingly.

Once the pK_a is known, equations 5.1 and 5.2 may be used to calculate the solubility at any particular pH. There was generally good agreement between the measured and calculated solubility, as seen in Figs. 5.3 - 5.11.

Using equations 5.1 and 5.2, solubility of each of the compounds was estimated in blood and in the stomach (Table 5.3), assuming pH of 7.4 and 2.0 respectively. Bropirimine, AB and BP being predominantly acidic in nature, show poor solubilities in the stomach (52 - 135μg/mL). These solubilities are related to the degree of ionisation (Section 5.3.3) which are shown in brackets. Although the pH of blood is nearer to the pK_a of bropirimine, it is still not sufficiently close to affect ionisation. For example, the difference between the pK_a of bropirimine (8.21) and the pH of blood (7.4) is only 0.8 units yet only 13.4% of the bropirimine is ionised.

However, the trend is reversed with the pyrimethamine derivatives. These show good solubility in the stomach due to increased ionisation (>90%) and poor solubilities in blood, where they are insufficiently ionised. Hence it is probable (Table 5.3) that pyrimethamine derivatives (MPP, DPP, MDPC, EDPC, and iPDPC) will all have good oral bioavailabilities whereas bropirimine and its

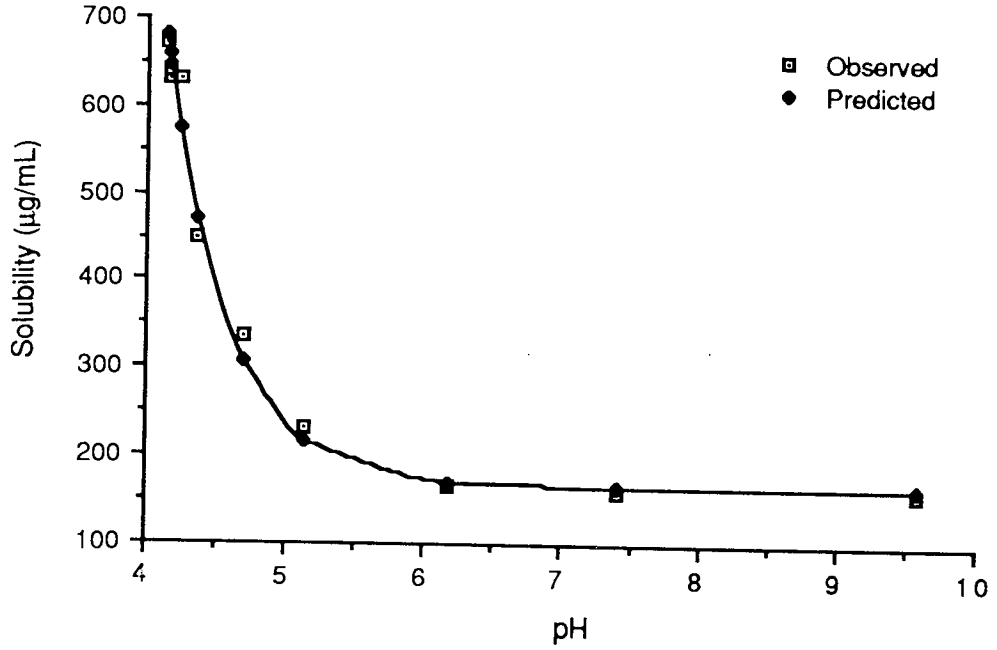

Fig. 5.8: Solubility-pH profile of MDPC.

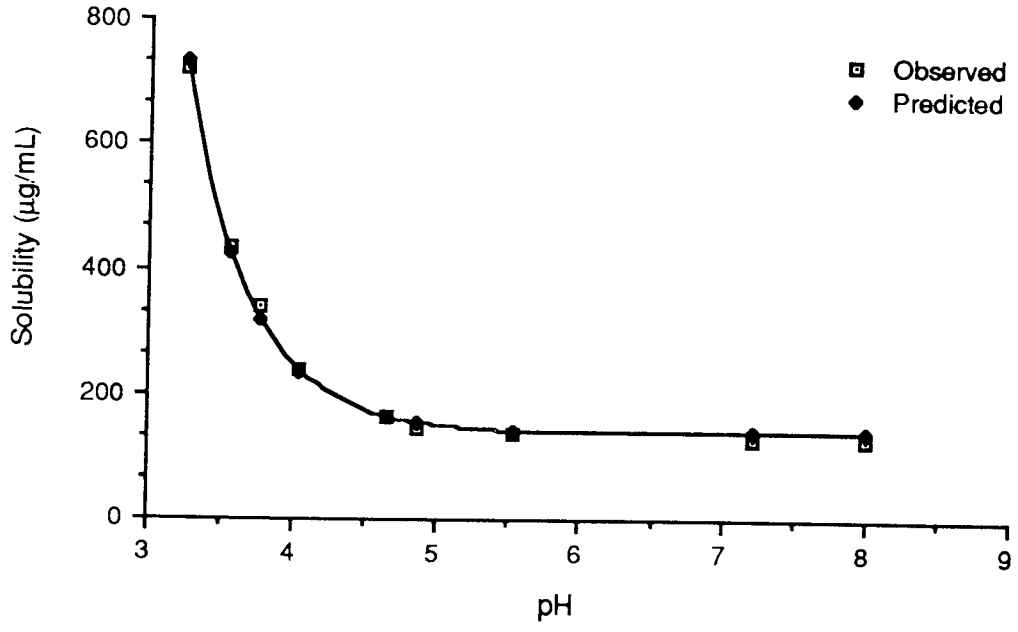

Fig. 5.9: Solubility-pH profile of EDPC

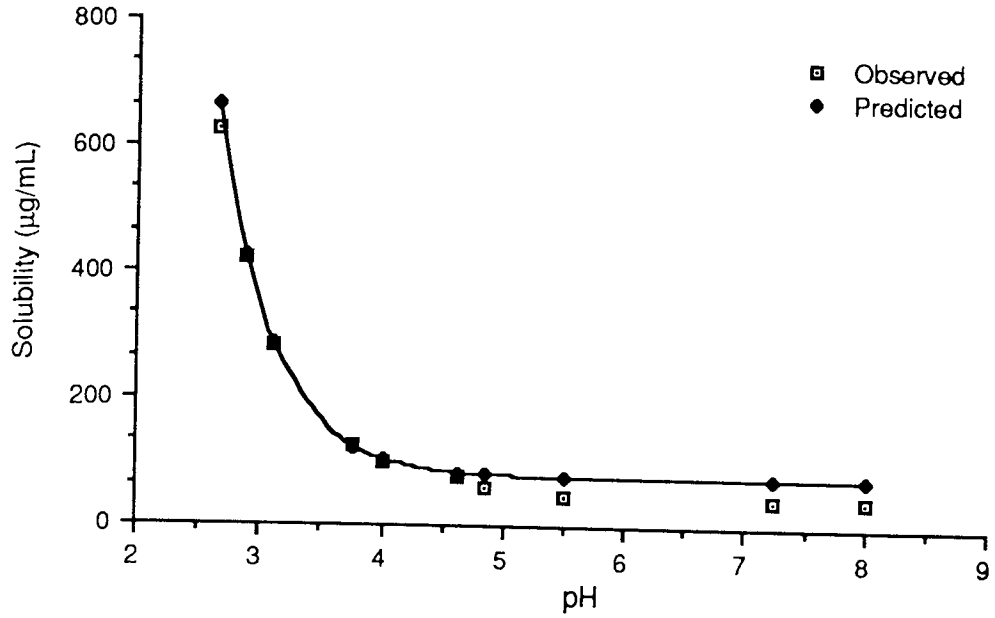

Fig. 5.10: Solubility-pH profile of PDPC

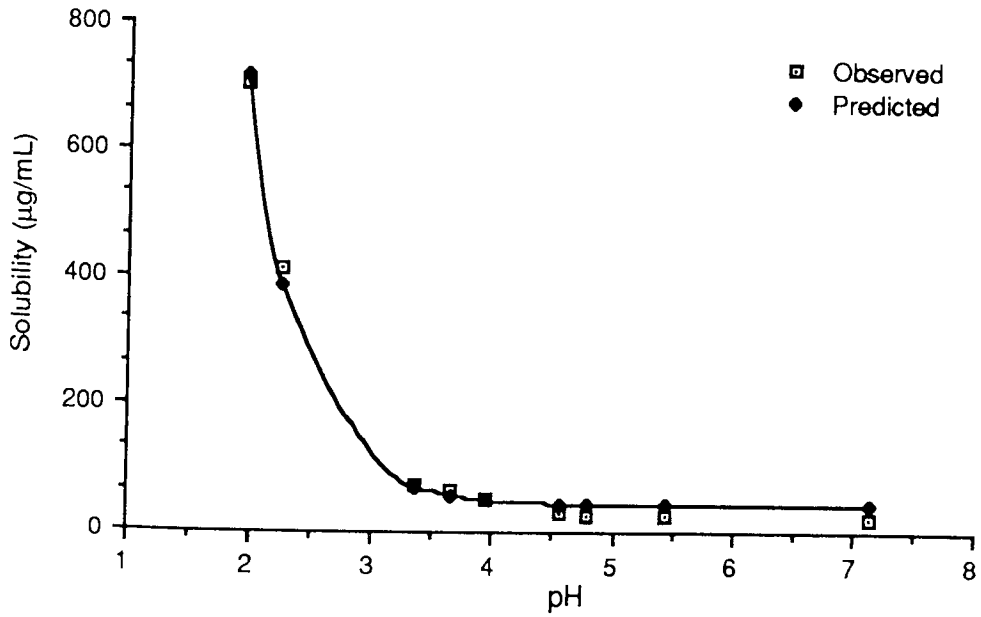

Fig. 5.11: Solubility-pH profile of iPDPC.

derivatives (AB and BP) will have poor bioavailability using the same route of administration.

Compound	Solubility in stomach (μg/mL)	Solubility in blood (μg/mL)
Bropirimine	134.5 (76.8)	38.2 (13.4)
AB	100.4 (0)	103.0 (2.6)
PB	52.1 (0)	52.2 (0.1)
MPP	33390.0 (99.6)	132.4 (0)
DPP	943.0 (88.6)	107.6 (0)
MDPC	69157.0 (99.8)	165.8 (0.2)
EDPC	10297.0 (99.8)	140.2 (0)
PDPC	2721.0 (97.1)	78.0 (0)
iPDPC	663.0 (93.5)	42.9 (0)

Table 5.3: Estimation of solubilities of the immunmodulatory agents in stomach and blood. (Brackets indicate percent ionised)

5.3.3 Partition coefficient (PC)

If two immiscible phases are placed in contact, one containing a solute soluble in both phases, the solute will distribute itself such that, after equilibrium, there is no net transfer of solute from one phase to another. Once this state is reached, then the partition coefficient of a compound, P, may be defined as:

$$P = \frac{C_o}{C_w} \qquad \ldots 5.3$$

Where: C_o is the concentration of solute in the organic layer

C_w is the concentration of solute in the aqueous layer.

The higher the value of P, the greater the lipid solubility of the solute. The parameter P can be used to give an indication of the uptake of a compound by various bodily tissues. The relationship between the biological activity and the partition coefficient was first proposed, independently, by Overton[157] and Meyer[158,159] in order to explain the fact that cellular membranes were more readily penetrated by lipid soluble substances than lipid insoluble substances. Following this, attempts made to relate P to various bioactivities of the drug are legion.

In instances where the measurement of P values is impractical, attempts have been made to calculate these values based on the summation of hydrophobic constants for individual fragments[164-166]. Although good estimates may be obtained for some molecules, the calculations are complex, rely on a number of assumptions, and do not take into consideration the stereochemistry of the molecule and in particular any intramolecular hydrogen bonding.

Although the classical 'shaking flask' method[167] is still the most popular for the experimental determination of P, recently high performance liquid chromatography (HPLC) has been proposed[168-170]. However, the packing material used in the columns was octadecyl silica (ODS) which becomes unstable in the alkaline region[171] and therefore only partition coefficients of neutral forms of acids could be determined. Miyake *et.al.*[177] were able to overcome this problem by using the pH stable porous polymer material. In using the HPLC, the log P_{oct} of the compounds could, thus, be related to the column capacity factor, K', by the general expression:

$$\log P_{oct} = b \log K' + a \qquad \ldots 5.4$$

Where: a and b are constants whose values are dependant on the composition of the mobile phase. The linearity of equation 5.4 appears to depend on the H-bonding ability of the compounds[177]. As the capacity is related to the retention times, low levels of acetonitrile in the mobile phase could give rise to long retention times for hydrophobic compounds representing an inadequacy of this method for such compounds.

Fig. 5.12 shows the variation of apparent partition coefficient, P_{app}, with the pH of the aqueous phase using the method described in Section 5.2.2. P_{app} is obtained if ionisation and its consequences are ignored, and is related to the true partition coefficient as shown below. Bropirimine displays a biphasic curve, having opposite shape to the aqueous solubility-pH profiles.

The degree of ionisation, α, of a basic or acidic compound at a given pH is related to the dissociation constant, K_a, by:

$$\alpha = \frac{[H_3O^+]}{[H_3O^+]+K_a} \qquad \text{for bases} \qquad \ldots 5.5$$

And,

$$\alpha = \frac{K_a}{[H_3O^+]+K_a} \qquad \text{for acids} \qquad \ldots 5.6$$

Using these models, the degree of ionisation at a number of pH values was calculated for bropirimine, AB and PB and displayed in Fig. 5.13. The plots show inverse behaviour to that of Fig. 5.12. As expected, the ionised form of the compound has greater affinity for the aqueous form whereas the molecular form has greater affinity for the organic phase.

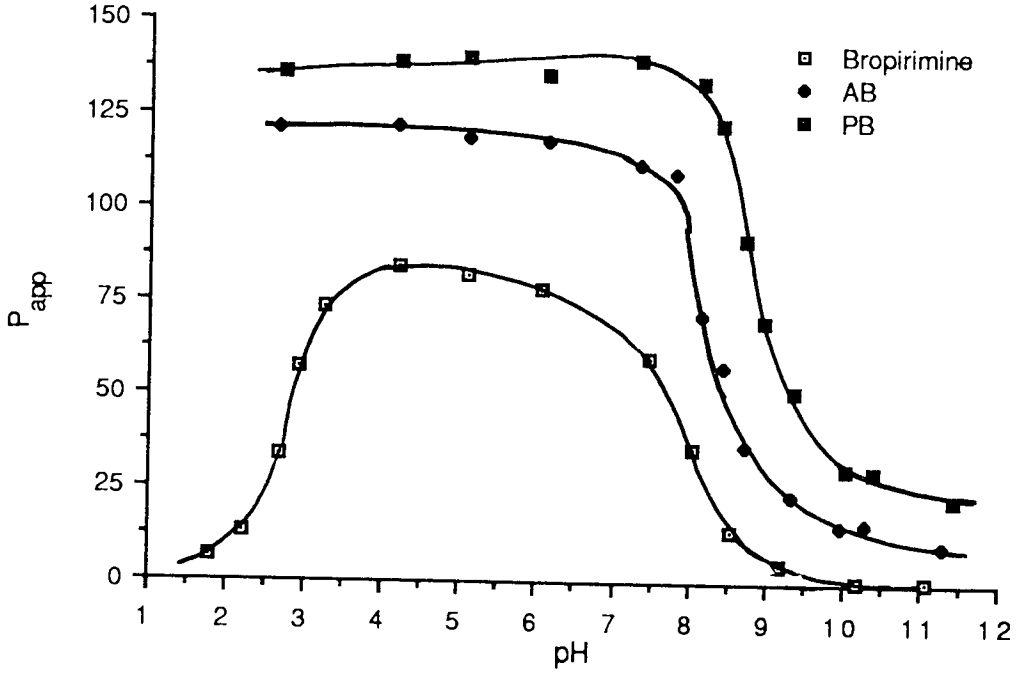

Fig. 5.12. Apparent partition coefficient-pH profiles of bropirimine, AB and PB.

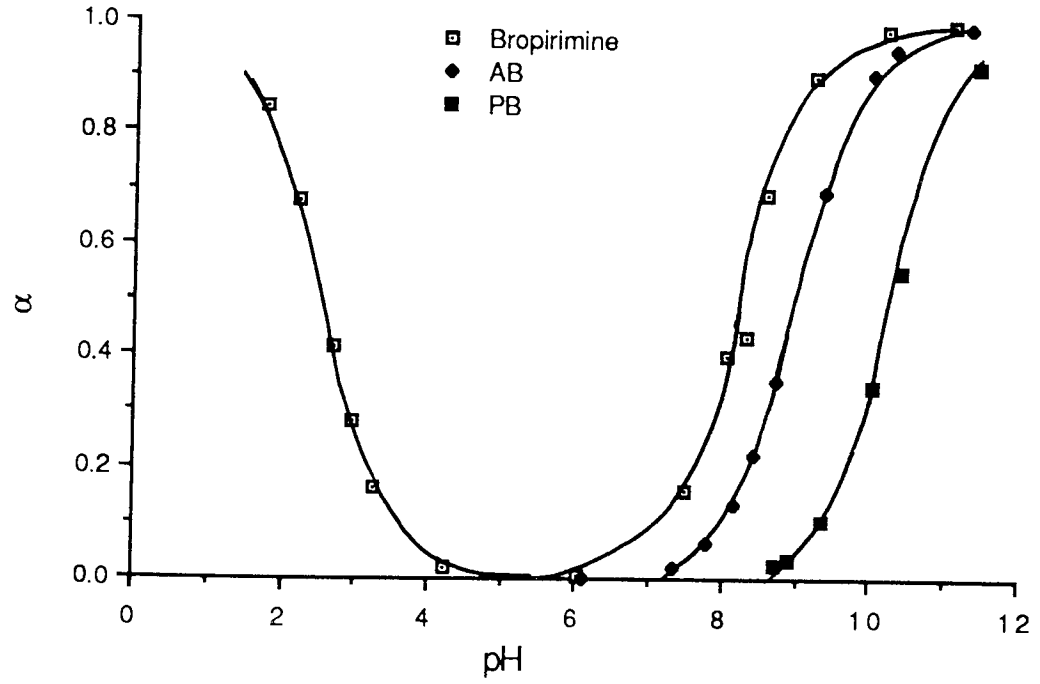

Fig. 5.13. A plot of degree of ionisation, α, against pH for bropirimine, AB and PB.

Irwin and Li Wan Po[179] derived an expression from which the partition coefficient of the unionised fraction, P_u, and the ionised fraction, P_i, may be calculated such that,

$$P_{app} = P_u (1 - \alpha) + P_i\alpha \qquad \ldots 5.7$$

The term $(1-\alpha)$ represents the unionised fraction.

Rearranging equation 5.7 gives

$$\frac{P_{app}}{\alpha} = P_u\left(\frac{1 - \alpha}{\alpha}\right) + P_i \qquad \ldots 5.8$$

Hence a plot of $\frac{P_{app}}{\alpha}$ against $\left(\frac{1 - \alpha}{\alpha}\right)$ should yield a straight line having a gradient of P_u and an intercept P_i. This relationship is clearly seen in Fig. 5.14 for bropirimine. The same model (equation 5.8) was used to calculate the values of P_u and P_i for AB and PB and the results summarised below:

Compound	P_u	P_i	Correlation coefficient, r
Bropirimine	60.6	-1.4	0.997
AB	69.3	4.6	0.988
PB	73.5	5.6	0.998

Table 5.4: A list of P_u, P_i and correlation coefficients for bropirimine AP and PB calculated from equation 5.8

Increasing the side chain length on the bropirimine molecule results in increased lipophilicity of the molecule as reflected in Table 5.4. The

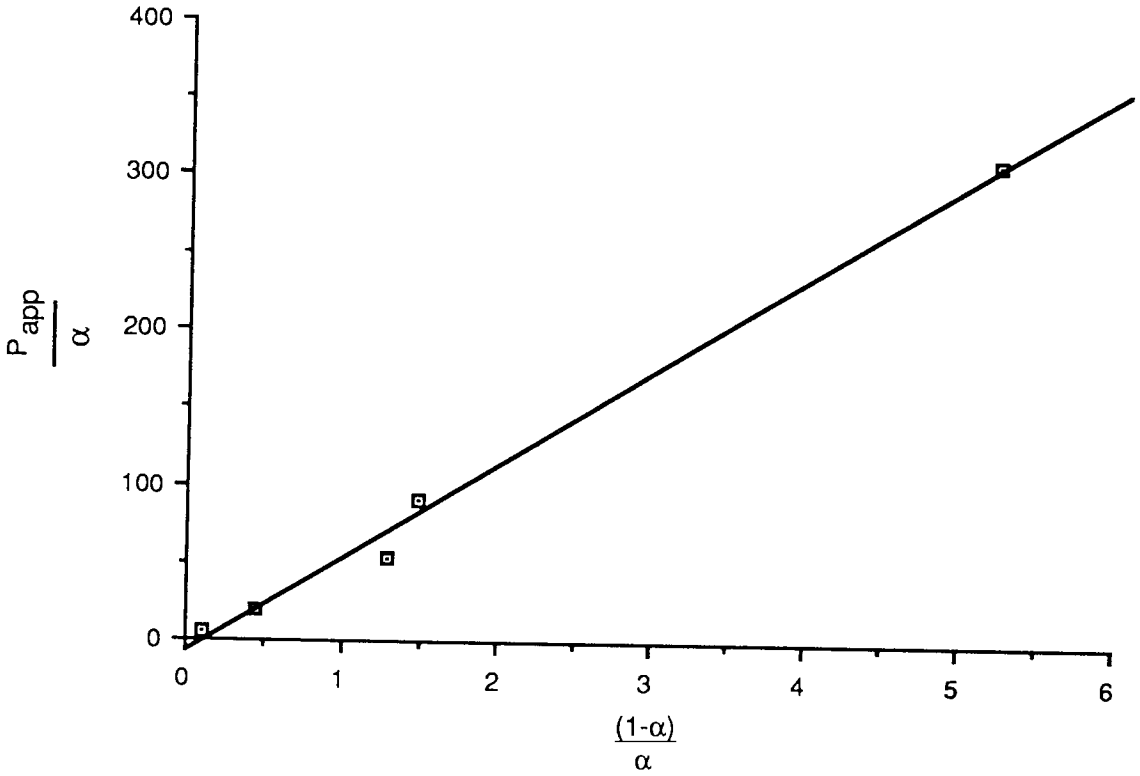

Fig. 5.14: The linear relationship of equation 5.8 for the partition of bropirimine in octanol-buffer at different pH values.

pH-P_{app} profile shows good agreement with that obtained by Alpar *et.al.*[77] using the same method. However, no attempt was made to evaluate P_u or P_i.

Using data obtained by Brodie and Hogan[160,161], Lien derived numerical expressions to correlate the gastric absorption of acidic and basic compounds to their partition coefficients and/or their pK_a values[162] such that:

For acids:

$$\log \% \text{ absorbed} = -6.626 (\log P)^2 + 2.465 \log P - 0.679 \quad \ldots 5.9$$

For bases:

$$\log \% \text{ absorbed} = -0.217 (pK_a - 1) + 1.342 \quad \ldots 5.10$$

Using equation 5.9 and 5.10 the amount absorbed from the stomach was calculated for bropirimine and its derivatives (AB and PB) and for pyrimethamine and its derivatives (MPP, DPP, MDPC, EDPC, PDPC and iPDPC).

Compound	Amount absorbed in the stomach (%)
Bropirimine	10.3
AB	2.6×10^{-19}
PB	7.0×10^{-20}
MPP	4.0
DPP	8.6
Pyrimethamine	1.2
MDPC	3.6
EDPC	5.3
PDPC	6.2
iPDPC	7.5

Table 5.5: Estimation of amounts of bropirimine and its derivatives (AB,PB) and pyrimethamine and its derivatives (MPP, DPP, EDPC, PDPC, and iPDPC) absorbed from the stomach using equations 5.9 and 5.10

The results show that there is poor absorption from the stomach for all the compounds listed in Table 5.5, particularly so for AB and PB. The results are not absolute since a whole range of compounds were used (both aliphatic and aromatic) in deriving the general expressions (equations 5.9 and 5.10). However, Table 5.5 may be used as an approximate indicator for gastric absorption of these compounds.

If it is assumed that the value of $P_i = 0$, then equation 5.7 becomes

$$P_{app} = P_u (1 - \alpha) \qquad \ldots 5.11$$

By incorporating equations 5.5 and 5.6 in equation 5.11, two further expressions are obtained such that,

For acids:

$$\frac{1}{P_{app}} = \frac{1}{P_u} + \frac{K_a}{P_u[H_3O^+]} \qquad \ldots 5.12$$

For bases:

$$\frac{1}{P_{app}} = \frac{1}{P_u} + \frac{[H_3O^+]}{K_a P_u} \qquad \ldots 5.13$$

Hence a second method for obtaining the dissociation constant, K_a, for either acidic or basic compounds is apparent. Fig. 5.15 shows a plot of $\frac{1}{P_{app}}$ against $\frac{1}{[H_3O^+]}$ for bropirimine confirming the linearity of equation 5.12. Hence using the models above (equation 5.12 and 5.13), the pK_a values for bropirimine, AB and PB were calculated and are displayed in Table 5.6. Good agreement is observed between the two methods.

Compound	pK_a from solubility data	pK_a from partition data
Bropirimine	2.52, 8.21	2.73, 8.19
AB	8.98	8.89
PB	10.31	10.38

Table 5.6: Comparison of pK_a values obtained by either using solubility data or by partition data for bropirimine, AB and PB

5.3.4 Solubility of bropirimine in co-solvents and additives

5.3.4.1 Solubility in acids and bases

Figs. 5.16 and 5.17 show the solubility of bropirimine in sodium carbonate and acetic acid respectively. Since bropirimine has both acidic and basic functions, ionisation can occurr in either environment, the extent of which depends on the pH of that environment. Ionisation therefore leads to increased solubility. Fig. 5.16 also shows a plot of bropirimine if pH alone were to dictate solubility. It is possible that the

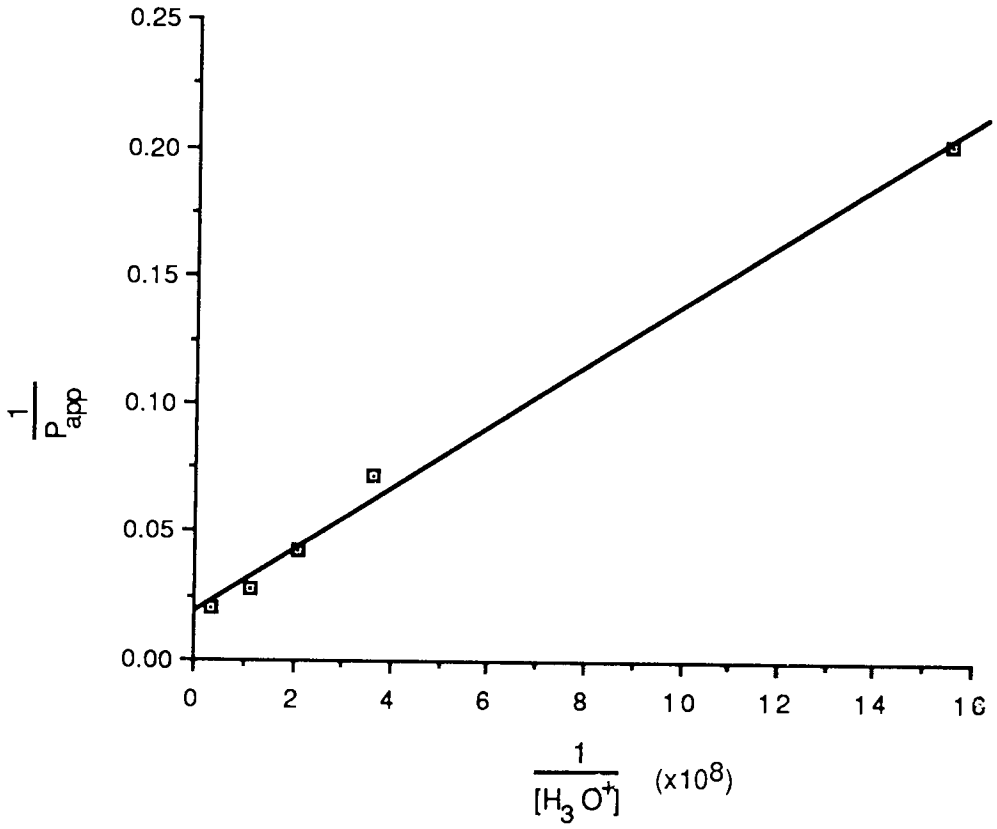

Fig. 5.15: The linear relationship of equation 5.12 for bropirimine.

increased solubility is due to counterion effect as pH alone cannot account for the solubility.

Fig. 5.17 shows the solubility of bropirimine in hot and cold acetic acid (60°C and 6°C respectively). Predictably, the solubility of broprimine is greater in the warm acid than in the cold. This type of information is useful when considering solvate synthesis under controlled conditions.

5.3.4.2 Solubility in co-solvents

Although co-solvent systems are very widely studied and used, how they work is still ill-understood.

There are three major factors that affect the aqueous solubility of a drug[180]. These are:

1. The entropy of mixing which favours complete miscibility of all components.
2. The difference between the sum of the drug-drug (DD) and water-water (WW) interaction on the one hand, and the drug-water(DW) on the other. The difference is related to the activity coefficient of the drug in water, γ_w, by

$$RT \ln \gamma_w = DD + WW - 2\,DW \qquad \ldots 5.14$$

where R = Molar gas constant

T = Thermodynamic temperature.

If DD + WW -2DW > 0, there will be less than complete mixing and the drug will have finite solubility in water. The greater the

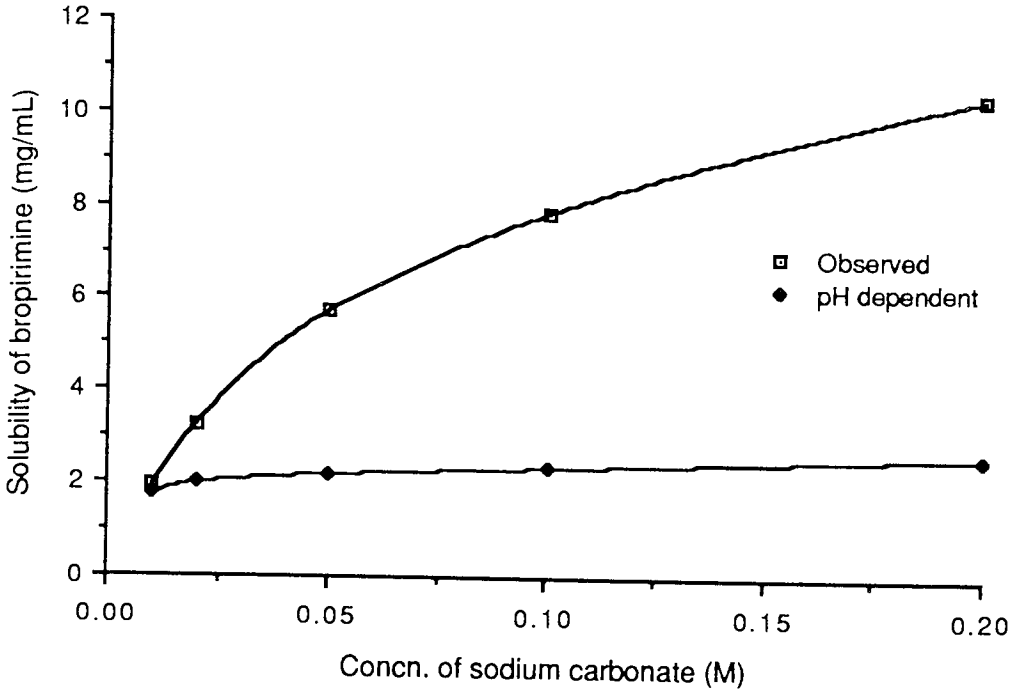

Fig. 5.16: Solubility of bropirimine in sodium carbonate.

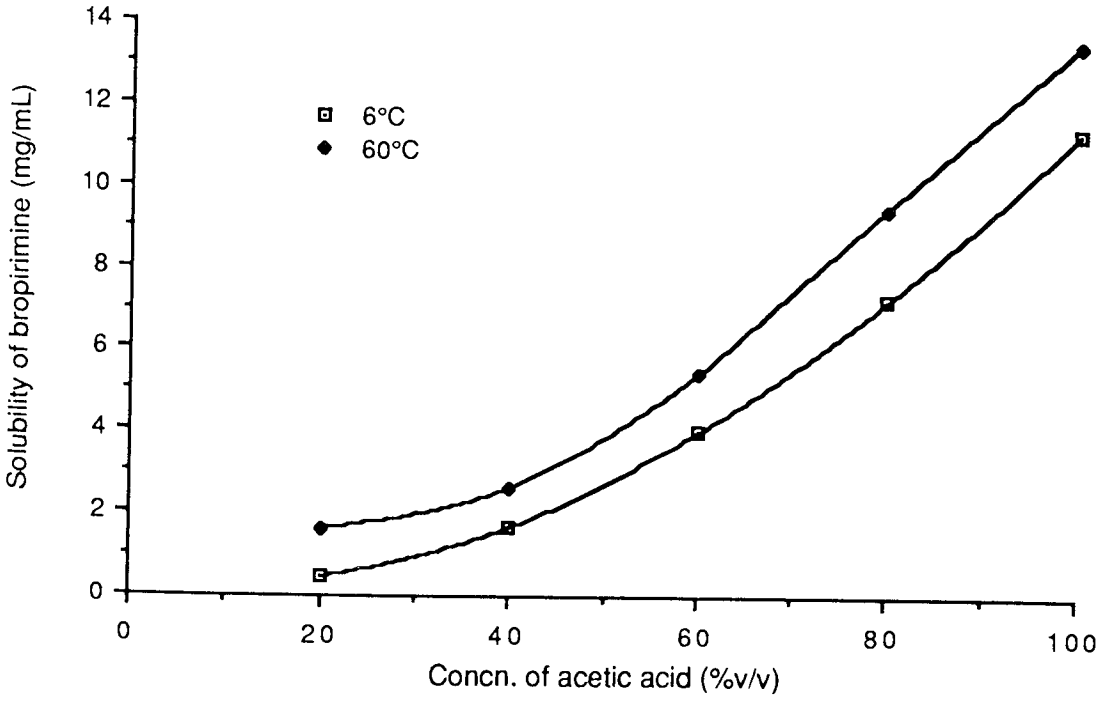

Fig. 5.17: Solubility of bropirimine in acetic acid at 6 °C and 60 °C.

difference between the adhesive and cohesive interactions the lower the solubility.

3. The additional DD interactions that are associated with the lattice energy of the crystalline drugs.

Mathematically, the observed solubility of the drug in water, S_w, is given by

$$\log S_w = \log S_i - \log \gamma_w \qquad \ldots 5.15$$

where S_i = the ideal solubility of the drug in water.

The solubility of a drug may, therefore, be most fruitfully increased by developing a solvent which closely matches the polarity of the drug. Most solutes show an exponential increase in solubility with an increase in co-solvent composition which can be modelled by an equation derived by Yalkowsky and Rubino[187].

$$S_f = S_w e^{S'f} \qquad \ldots 5.16$$

where
- S_f is the solubility in the co-solvent
- S_w is the solubility of the solute in water
- f is the volume fraction of the co-solvent
- S' is a constant characteristic of the system under study and is referred to as the solubilising power of the co-solvent.

Written in logarithmic form, equation 5.16 becomes

$$\log S_f = \log S_w + Sf \qquad \ldots 5.17$$

Where $S = 0.434\ S'$

or,

$$\log \left(\frac{S_f}{S_w}\right) = Sf \qquad \ldots 5.18$$

By dividing the mixed solvent solubility by the aqueous solubility, the curves for different co-solvents may be normalised and comparison made more meaningful. It does not in any way change the shape of the curve.

Fig. 5.18 shows the solubility of bropirimine in dimethylacetamide (DMA). Exponential increase in the solubility of bropirimine is seen up to 50% $^{v}/_{v}$ of DMA at which the solubility of bropirimine is more than 2mg/mL. Application of equation 5.18 and subsequent plot (Fig. 5.19) does not produce a straight line indicating that the system does not conform with equation 5.18.

Fig. 5.20 shows the solubility of bropirimine in a range of polyethylene glycols (PEGs) having nominal molecular weights of 200, 400, 1000, 1500, 4000 and 6000. All show exponential increase in solubility with increases in the concentration of the polymer. Hence, on a molar level, high molecular weight PEGs are better solubilisers of bropirimine than the smaller molecular weight PEGs. However, higher molecular weight PEGs tend to be either semi-solids or solids and difficult to work with in formulation work. Application of equation

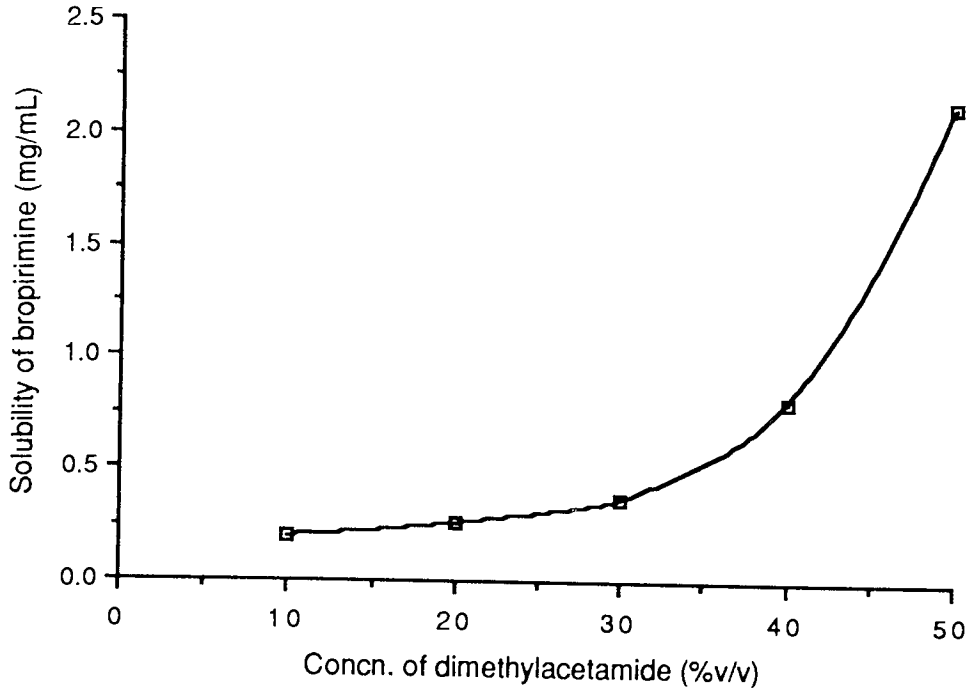

Fig. 5.18: Solubility of bropirimine in dimethylacetamide.

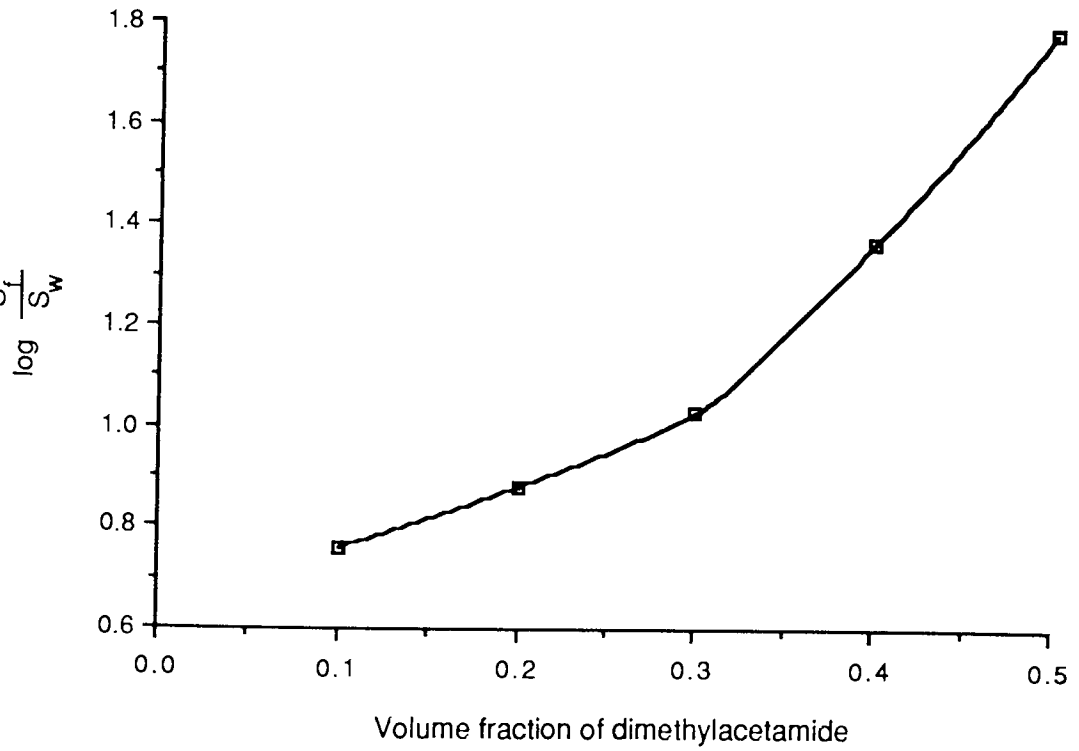

Fig. 5.19: Solubility of bropirimine in dimethylacetamide in accordance with equation 5.18

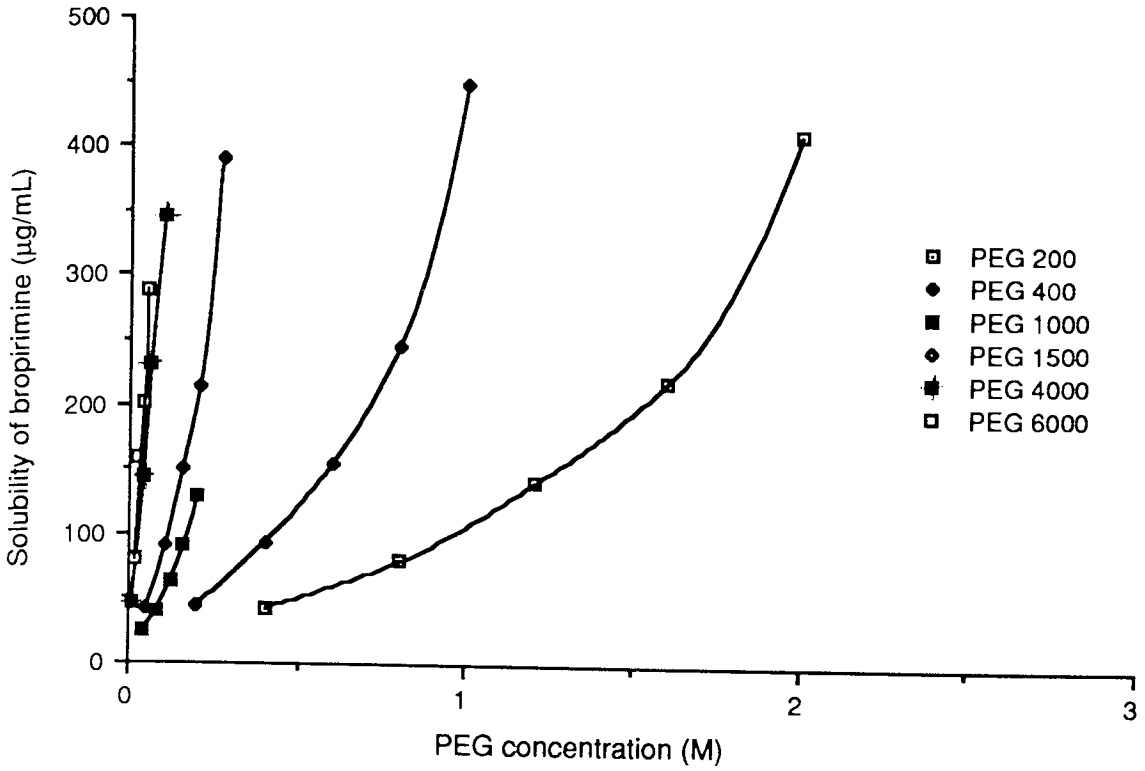

Fig. 5.20: Solubility of bropirimine in polyethylene glycols.

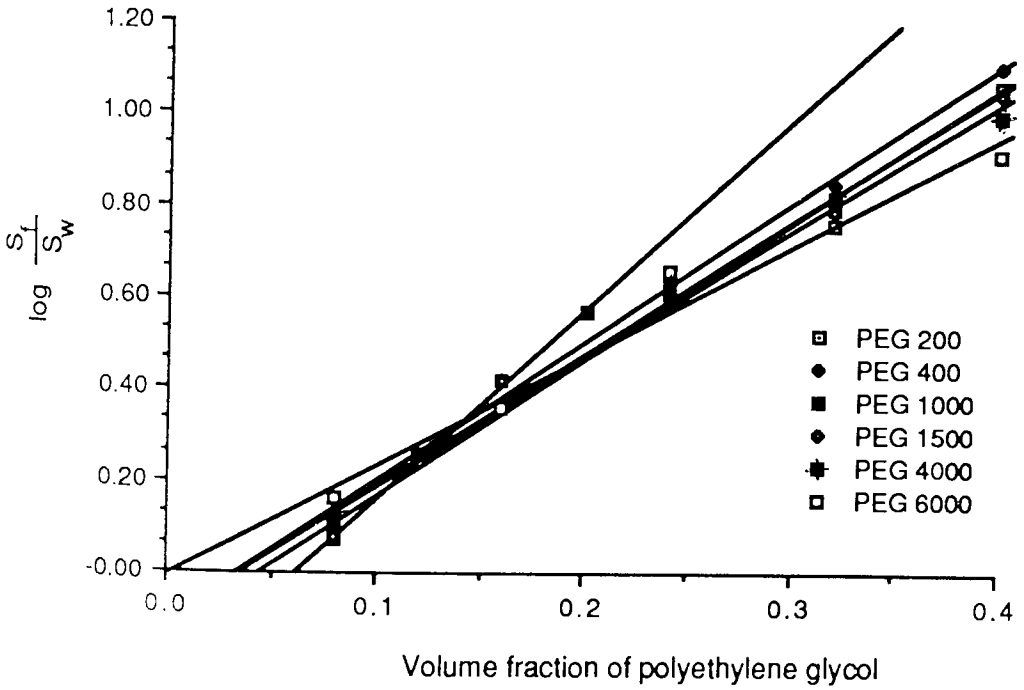

Fig. 5.21: Solubility of bropirimine in polyethylene glycols in accordance with equation 5.18

5.18 gives Fig. 5.21. It is immediately obvious that the PEG series study conforms to equation 5.18, giving linear plots up to volume fraction of 0.4, Table 5.7.

Of all the co-solvents, propylene glycol (PG) is the most commonly used solvent for parenteral products. It is inexpensive, stable, non-toxic, is usually well tolerated and is a good solvent for most drugs. Fig. 5.22 shows the solubility of bropirimine in PG using equation 5.18 yielding a straight line up to a mole fraction of 0.50. This shows that propylene glycol does conform with equation 5.18 and shows ideal behaviour. The hypnotics and anti-epileptics phenobarbital, secobarbital and phenytoin show similar behaviour to that produced with bropirimine (Fig. 5.23)[187].

Yalkowsky and Rubino[187] in deriving equation 5.18 treated the mixed solvent as a linear combination of its components, i.e. the co-solvent in aqueous system is assumed to behave as pure co-solvent with respect to the solute and the water is treated as pure water. However, this does not account for the non-ideality of the system and as a result a modified form of equation 3.10 was introduced[187] where

$$\log\left(\frac{S_f}{S_w}\right) = (A \log P_{o/w} + G)f - Ef^2 \qquad \ldots 5.19$$

where A, G and E are constants

$P_{o/w}$ is the octanol-water partition coefficient of the solute

Using data for the solubility of more than fifty compounds in propylene glycol, Yalkowsky and Rubino[187] obtained

$$\log\left(\frac{S_f}{S_w}\right) = (0.714 \log P_{o/w} + 0.794)f - 0.103f^2 \qquad \ldots 5.20$$

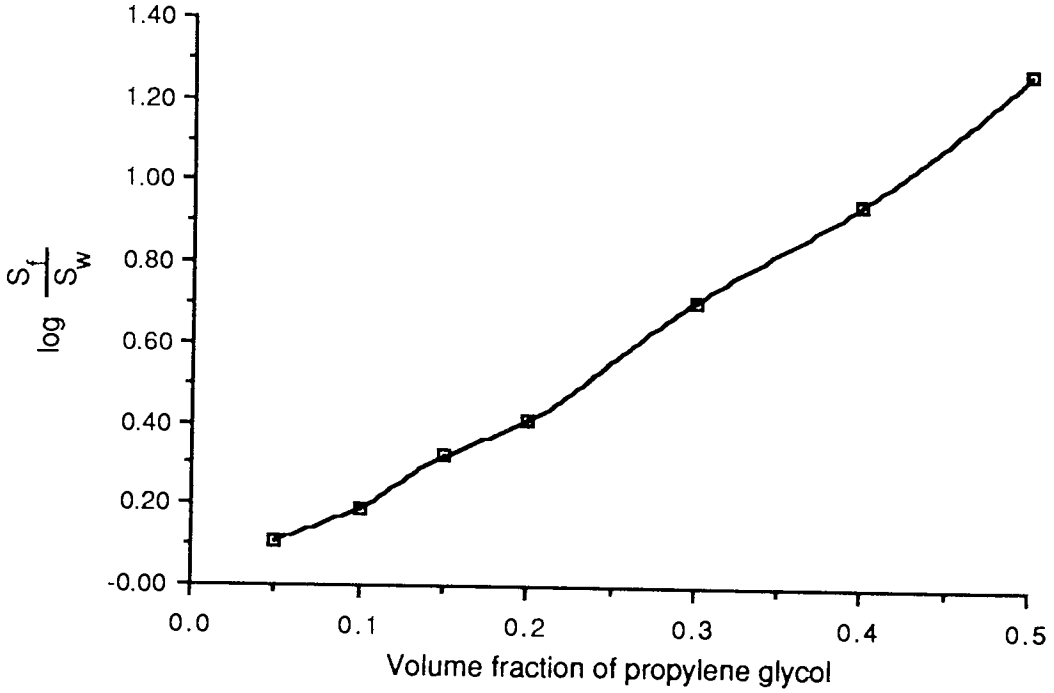

Fig. 5.22: Solubility of bropirimine in propylene glycol in accordance with equation 5.18.

Aston University

Illustration has been removed for copyright restrictions

Fig. 5.23: Reproduced from Ref (187)

Assuming that the value of ($0.103f^2$) is negligible compared to the first term, then the calculation for the slope for bropirimine ($P_{o/w} = 60.6$) is 2.07. In comparison, the observed value from Fig. 5.22 was found to be 2.59. This shows a residual value of 0.52. The residual values for phenobarbital, secobarbital and phenytoin[187] were calculated to be 0.25, 0.39 and 0.46 respectively. Since all of these values are less than unity, it can be concluded that equation 5.19 was successful in predicting the solubility of these components in propylene glycol-water system.

Table 5.7 lists the solubilising power of the co-solvents used here, calculated from the slopes of Figs. 5.19, 5.20 and 5.22.

Co-solvent	Solubilising power, S
DMA	2.544
PEG 200	3.011
400	3.029
1000	4.123
1500	2.884
4000	2.758
6000	2.371
PG	2.59

Table 5.7: Solubilising power, S, of some co-solvents

DMA and PG appear to have identical solubilising power, from Table 5.7. Considerable variation is seen amongst the PEG series. Since these plots use fraction volume instead of a molar scale, results show inconsistency with Fig. 5.20 where higher molecular weight PEGs appear to be better solubilisers. Table 5.7 shows PEG 1000 to have the highest solubilising power.

There have been a number of other attempts at predicting solubility in mixed systems[181-185], but the methods tend to be complicated requiring data (e.g. thermodynamics) that is difficult to obtain.

5.3.4.3 Solubility of bropirimine in cyclodextrins

Cyclodextrins are oligiosaccharides, produced by the enzymatic degradation of starch, containing six (α-cyclodextrin), seven (β-cyclodextrin) or eight (γ-cyclodextrin) glucose units connected by α-(1,4) bonds. Derivatives are prepared by condensation reactions using the parent compounds.

One of the most interesting properties of the cyclodextrins is their ability to form inclusion complexes with a great variety of compounds leading to improved solubility[189-193] or improved dissolution[194]. β-cyclodextrin has also been used to increase the chemical instability of carmofur, a 5-fluorouracil prodrug, in the solid state as a result of hygroscopic nature of the β-cyclodextrin[195].

Fig. 5.24 shows the solubility of bropirimine in α-, β- and γ-cyclodextrin prepared in B-R buffer pH 7.2 at 25°C. As a whole, bropirimine appears to be poorly soluble in these cyclodextrins. Firstly, the cyclodextrin annulus may be too small to incorporate bropirimine as a guest molecule or secondly that there are insufficient interaction sites. A third, and probably the most important, reason may be the poor aqueous solubility of these cyclodextrins. Table 5.8 shows the solubility of α-, β- and γ-cyclodextrin in water. In order to test the third possibility, the solubility of bropirimine in hydroxypropyl β-cyclodextrin, a branched derivative of β-cyclodextrin, which is freely soluble in water, was evaluated. This gives a linear plot (r=0.999) up to a HPβCD concentration of 14.76 mM (2%$^{w}/_{v}$), solubilising almost 250μg/mL of bropirimine. HPβCD also offers increased interactive

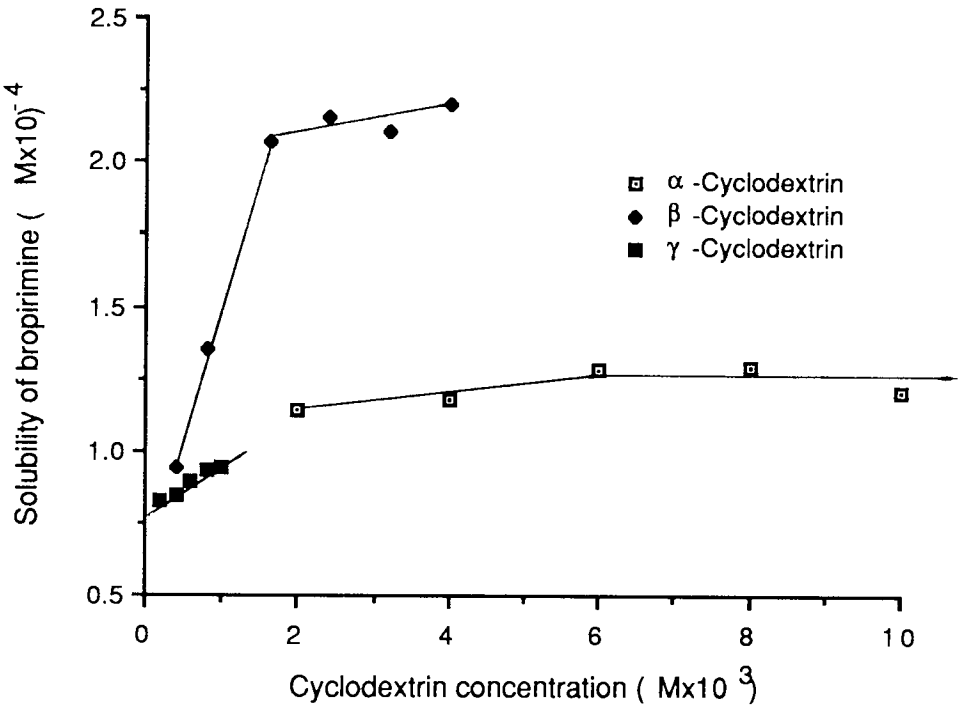

Fig. 5.23: Solubility of bropirimine in α -,β - and γ -cyclodextrins.

sites *viz.* the hydroxy group which can H-bond with bropirimine. The α-, β- and γ-cyclodextrins display a B_s type curve as described by Higuchi and Connors[204]. The initial rising portion is followed by a plateau region which may then descend indicating precipitation of microcrystalline complex[190,192,194]. In contrast, the solubility of bropirimine increased linearly as a function of HPβCD concentration, showing no plateau, and this type of curve is classified as A_L[204].

Cyclodextrin	Aqueous solubility (a) (μg/mL)	Annulus (b) (Å)	Stability constant (/M)
α–	15.00	5.7	25
β–	1.85	7.8	825
γ–	23.00	9.5	71
HP β–	>50.00	(9.5)	365

(a) From ref (198)
(b) From ref (203)

Table 5.8: Some physico-chemical properties of α–, β–, γ– and hydroxypropyl β– cyclodextrin

Stability constants, K, of inclusion complexes were calculated from the initial straight line portion of the phase solubility diagrams (Figs. 5.23 and 5.24) by the following equation[204]

$$K = \frac{\text{slope}}{\text{intercept}(1 - \text{slope})} \qquad \ldots 5.21$$

The results are shown in Table 5.8. The K values could be given a rank order of β->HPβCD>γ->α-cyclodextrin. This indicates that the cavity size of β-cyclodextrin (7.8Å) is the most profitable to bropirimine [size

$\approx$ 8Å[205]]. In each of the instances, the slope was less than unity indicating a possible 1:1 stochiometric complex[192].

In general, however, the stability constants are low. For example prednisolone displayed K values of 298, 3600 and 3240/M with α-, β- and γ-cyclodextrins respectively[190] whereas diazepam showed values of 220 and 170/M in β- and HPβ-cyclodextrins respectively[198], and carmofur gave a value of 530/M[206].

No oral toxicity has been reported with cyclodextrins. However, although haemolysis[196] and local irritation on injection[197] have been reported with the natural cyclodextrins, Yoshida *et.al.*[198] observed that hydroxyalkylation of β-cyclodextrin considerably diminishes these untoward side effects and have suggested the possibility of cyclodextrins for parenteral use.

5.3.4.4 Solubility in meglumine

Meglumine (N-methyl-D-glucamine) is an organic base, a 10% solution in water having a pH between 10 and 12[199]. It has a solubility of 1 in 1 of water and is practically insoluble in organic solvents[199].

Fig. 5.26 shows the solubility of bropirimine in meglumine. At a concentration of 5%$^{w}/_{w}$ meglumine, almost 7mg/mL of bropirimine were solubilised; the pH of the mixture post-saturation being 10.51. It is apparent from Fig. 5.25 that at concentrations of meglumine below 5% the solubility cannot be accounted for as being due to pH alone. It is likely to be hydrophilic counterion enhancing the solubility of bropirimine.

A 5.02%$^{w}/_{v}$ solution of meglumine in water is iso-tonic with serum[199]. It is used for the preparation of salts of iodinated organic acids used in contrast media. Although some haemotological[200] and microcirculatory[201] problems have been observed, they appear to be

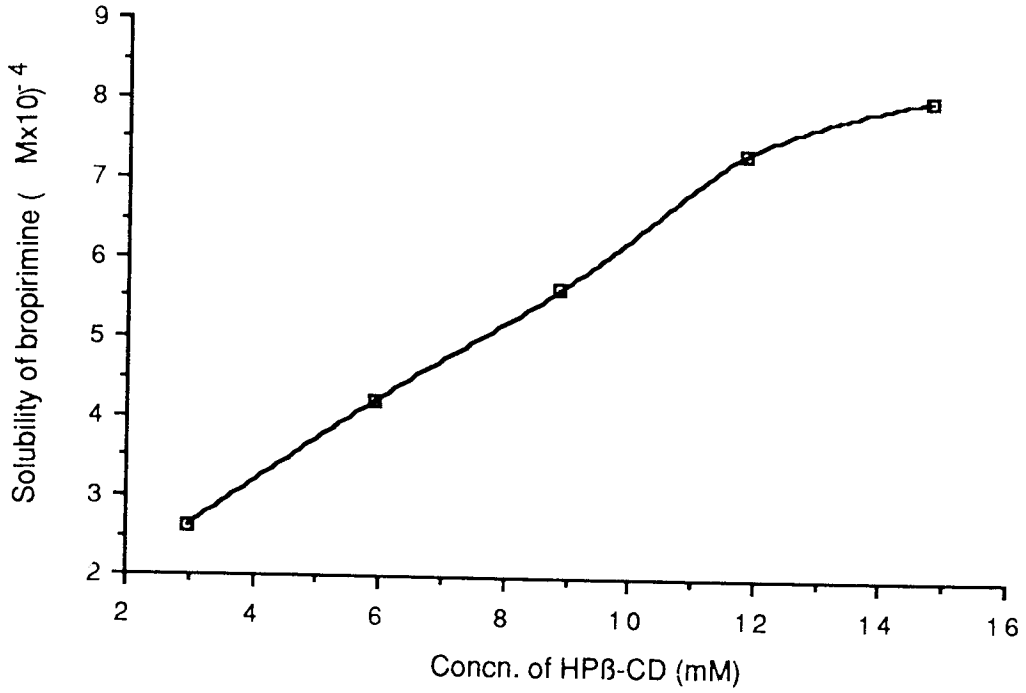

Fig. 5.25: Solubility of bropirimine in hydroxypropyl ß-cyclodextrin.

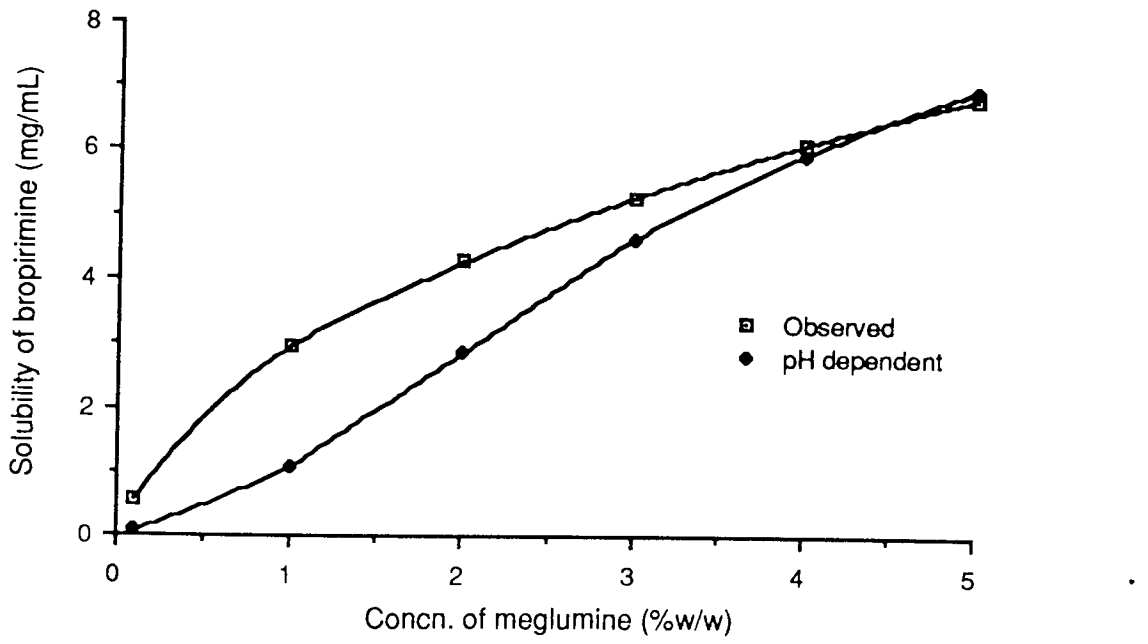

Fig 5.26: Solubility of bropirimine in meglumine.

related to the meglumine salt used[352]. Hence no serious problems should be encountered with meglumine if administered parenterally.

5.3.4.5 Solubility in mixed solvents

Table 5.9 lists various combinations of cosolvents and additives used to solubilise bropirimine. Using the system DMA/meglumine/sodium carbonate, it was possible to solubilise 32mg/mL of bropirimine. This represents an almost 1000 fold increase in solubility over the aqueous solubility. A pH of 10.6 is unlikely to cause severe problems on injection compared with phenytoin injection which has a pH of 12.0[199]. This system appears to be satisfactory for parenteral use.

5.3.4.5.1 Stability of the formulation

A 25mg/mL solution of bropirimine was prepared in vehicle 4 ($10\%^{v}/_{v}$ DMA: $5\%^{w}/_{w}$ meglumine: 0.2M sodium bicarbonate to $100\%^{v}/_{v}$) and sealed in 2mL ampoules. These were then subjected to autoclaving at 121°C and 15lb psi pressure for 20 minutes. Using HPLC as a stability-indicating assay for bropirimine, no degradation was observed. An ultraviolet scan of meglumine before and after autoclaving showed little difference. 3 and 12 months storage of the formulation showed no breakdown of bropirimine although slight yellow discolouration was seen which was identified as being due to DMA.

In conclusion, a study of the physico-chemical properties of bropirimine and subsequent use of co-solvents and additives has produced a formulation that solubilises sufficient bropirimine (>30mg/mL) for any clinical trial work to be undertaken. This represents a 1000-fold increase in solubility over the aqueous solubility of bropirimine.

Solubilising system		pH after saturation with bropirimine	pH alone (mg/mL)	Amount of bropirimine solubilised (mg/mL)
1. DMA	10% v/v			
Distilled water	to 100% v/v	8.15	(0.062)	0.18
2. DMA	10% v/v			
Meglumine	5% w/v			
Distilled water	to 100% v/v	10.33	(4.450)	18.10
3. DMA	10% v/v			
0.2M Sodium carbonate	to 100% v/v	10.40	(5.220)	18.84
4. DMA	10% v/v			
Meglumine	5% w/v			
0.2M Sodium carbonate	to 100% v/v	10.64	(9.040)	32.44

Table 5.9: Solubility of bropirimine in various stabalising systems

6.0 DISSOLUTION STUDIES ON BROPIRIMINE

6.1 Introduction

It is important to note that the dissolution process is not a simple two step process of disintegration of the dosage form followed by dissolution. Scheme 6.1 shows a better representation of the whole process.

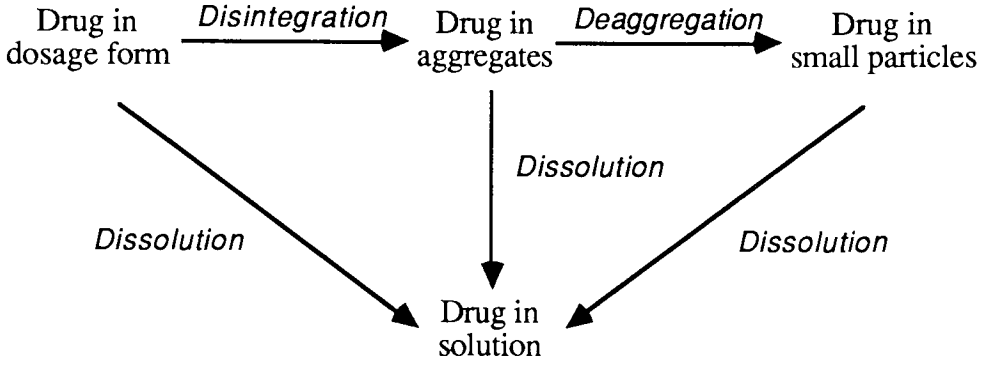

Scheme: 6.1

Because of the complexity of the process, the theoretical equation and models are often incapable of predicting the exact dissolution pattern of the drug formulation. For this reason *in-vitro* dissolution tests are performed and the data obtained is fitted to equations which are either empirical or partly based on the models of dissolution.

There is a general consensus of opinion that the transport across the intestinal wall will only occur if the substance is in a molecularly dispersed form. The physiological availability and the ultimate therapeutic effect will therefore depend on the ability of the compound to undergo sufficient dissolution which in turn is dependent upon the solubility of the compound in that particular environment.

Dissolution may be regarded as occuring in two stages:

1. Surface interaction which loosens the individual molecules from the solid (solvation).

2. The transport of these solvated molecules from the surface into the bulk of the solvent.

The solubility of a solid forming an ideal solution may be described by:

$$\ln x = \frac{-\Delta H_f}{R}\left[\frac{1}{T} - \frac{1}{T_m}\right] \qquad \ldots 6.1$$

where: x = Mole fraction solubility

T_m = Melting point

T = Temperature (Kelvin)

ΔH_f = Heat of fusion

However, surface reaction is usually so rapid that transport of dissolved molecules from the surface to the bulk becomes the rate limiting step in the dissolved process.

The classical diffusion layer model describes dissolution which is based on the assumption that no chemical reaction is involved (Fig. 6.1).

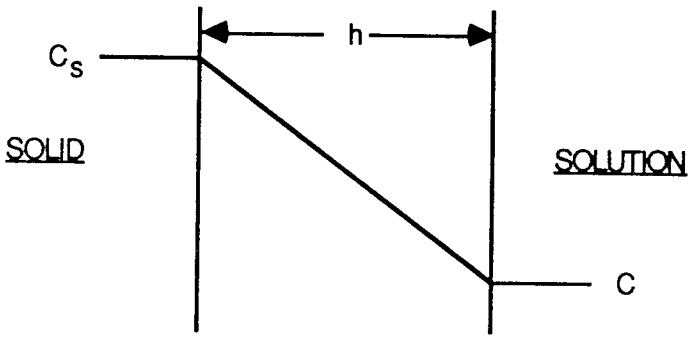

Fig. 6.1: Diagramatic representation of the diffusion layer model

At the solid-liquid interface, there exists an infinitesimally thin film of solution where the concentration of the drug equals its saturation solubility (C_s).

The film is bounded by a stationary diffusion layer of finite but minute thickness, h, across which the concentration of the solute decreases linearly from C_s to C, where C is the uniform concentration found in the bulk of the solution. Fick's first law states that, at steady state, the flux (amount of drug flowing per unit time across a unit area) through a plane perpendicular to the direction of diffusion is directly proportional to the concentration gradient. Thus the movement of solute molecules in a liquid by diffusion is governed by this law. The transport of drugs across biological membranes is also governed by this law. Fick's first law may be expressed as:

$$J = -D \cdot \frac{dc}{dx} \qquad \ldots 6.2$$

Where: J = Flux (in $Mol/m^2/s$)

D = Diffusion coefficient of the solute in the solvent (m^2/s)

$\frac{dc}{dx}$ = Change of concentration as a function of the distance x

(mol/m^4)

The negative sign indicates that the flux is in the direction of decreasing concentration. By definition:

$$J = \frac{\frac{dm}{dt}}{A} \qquad \ldots .6.3$$

Where: $\frac{dm}{dt}$ = Rate of flow of the mass with respect to time

A = Area of plane across which flow occurs

From equations 6.2 and 6.3

$$\frac{dm}{dt} = -DA\left(\frac{dc}{dx}\right) \qquad \ldots 6.4$$

For the diffusion layer model, the concentration gradient across the diffusion layer can be given by:

$$\frac{dc}{dx} = \frac{(C-C_s)}{h} \qquad \ldots 6.5$$

Substituting equation 6.5 in equation 6.4 gives the Noyes-Whitney equation:

$$\frac{dm}{dt} = \frac{DA}{h}(C_s-C) \qquad \ldots 6.6$$

Where: $\frac{dm}{dt}$ is known as the dissolution rate

A is the surface area of the diffusion-layer and is equivalent to the surface area of the solid.

Where the concentration in the bulk (C) approaches zero e.g. under sink conditions, equation 6.6 becomes:

$$\frac{dm}{dt} = \frac{DAC_S}{h} \qquad \ldots 6.7$$

If the surface area is held constant as in a compressed non-disintegrating disc, then equation 6.7 may be integrated to give the amount of drug dissolved at time t, M_t, as:

$$M_t = \frac{D}{h}AC_st \qquad \ldots 6.8$$

or $$\frac{M_t}{A} = kt \qquad \ldots 6.9$$

Where: k = Intrinsic dissolution rate

Hence a plot of M_t/A against t should yield a straight line passing through the origin having a slope of k.

Generally, however, the diffusion layer model is extremely useful to visualize the effect of varying a number of parameters on the dissolution process. From equation 6.6, it may be deducted that:

1. The dissolution rate will increase with an increase in the solubility.
2. The dissolution rate will increase with an increase in the surface area.
3. An increase in the diffusion coefficient or a decrease in the thickness of the diffusion layer (brought about by stirring) will increase the dissolution rate.

Hamlin *et.al.*[209] determined the initial dissolution rates for several classes of compounds, covering five orders of magnitude, and found them to be directly proportional to the solubility of the compounds. In all instances, the experiments were performed under sink conditions. The interval of the initial dissolution period can be somewhat arbitrary and under the discretion of the investigator. Nickalsson *et.al* . observed that dextropropoxyphene napsylate (aqueous solubility = 1.4mg/mL) showed no direct relationship between intrinsic dissolution rate and solubility[210]. This was explained from the fact that this compound exhibited polymorphism and on using data obtained after only one minute dissolution, a better fit for the above relationship was obtained[210].

The aim in this section was to determine the dissolution profiles of bropirimine powder, bropirimine solvates and to estimate the intrinsic dissolution rates from compressed discs. The effects of soluble polymers was also studied.

6.2 Experimental

6.2.1 Particle size analysis

A suspension of bropirimine was prepared by using 10g of the drug in 500mL of distilled water. In order to ensure that no dissolution occured, the distilled water was saturated with bropirimine prior to the experiment. The suspension was thoroughly shaken to ensure good mix. The coulter-counter model ZM-1 was fitted with 140μm diameter size orifice and 0.5mL sampling volume utilised at ambient temperature (21°C) using distilled water as the electrolyte. Various size ranges were then measured and values of 10 readings averaged.

6.2.2. Measurement of intrinsic dissolution

Most of the beaker method apparatus described in the literature basically consists of a beaker containing the dissolution medium maintained at 37°C with a three blade polythene stirrer accurately centred within the beaker. The tablet or disc is gently dropped down the side of the beaker and samples of solution withdrawn for analysis. This method has been modified and used here.

For drugs that are stable, a continuous flow photometric analysis set-up, the first prototype descibed by Kreevoy and Wewerka[213], may be used particularly for slowly dissolving materials. It also has the advantage of minimising sample handling. Several such pieces of apparatus have been described[214], but the basic principle remains the same and the set-up used here is diagrammatically shown in Fig. 6.2.

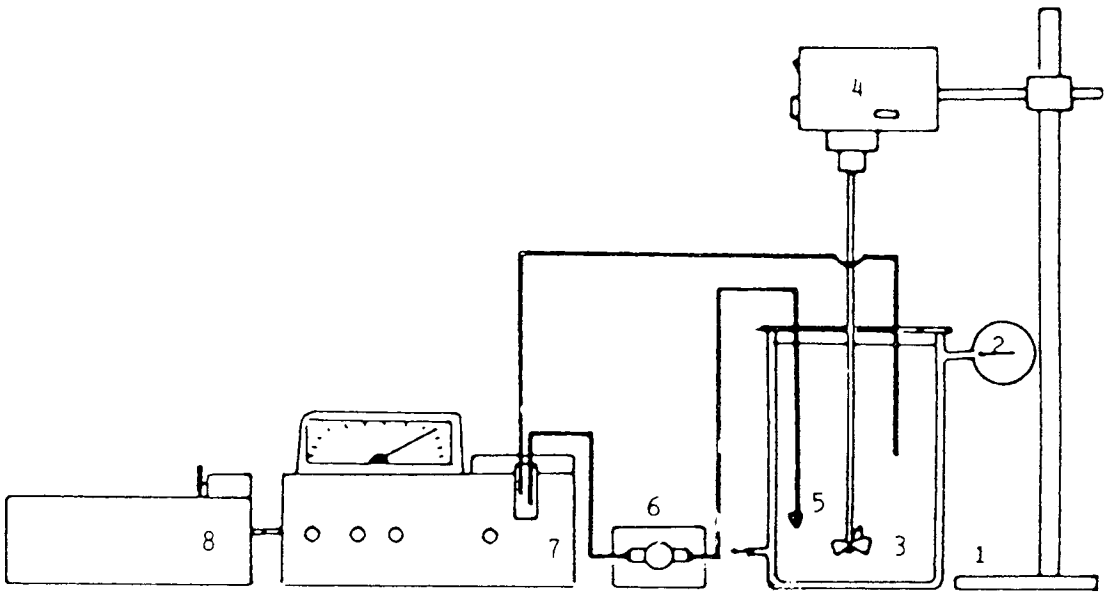

Fig. 6.2: *Block diagram of dissolution equipment.*
The numbered features are:
1. Jacketed cylindrical glass beaker
2. Churchill recirculating thermostatic bath
3. Three bladed stainless steel stirrer
4. Electric motor
5. Sintered glass sparger
6. Electric pump
7. U.V. spectrophotometer
8. Chart recorder

6.2.2.1 Preparation of physical mixes and compressed discs. The soluble polymers polyethylene glycol (PEG, BDH) having a nominal molecular weight of 20,000 (20M) and polyvinyl pyrollidone (PVP, Fisons) having a nominal molecular weight of 44,000 were used. They were size-reduced using a pestle and mortar and sieved such that particles passed through a 500μm sieve but retained on a 300μm sieve were used. The bropirimine was treated likewise. Each of the components was then accurately weighed as required and the two either triturated together on a glass tile or ball-milled for 2 hours using 2mm diameter glass balls. 200mg of the powder (bropirimine or the two component mixture) was accurately weighed and transferred into a stainless steel die, the punches inserted and the contents manually compressed to 8000kg for 2 minutes. The disc was then gently removed from the die and placed in a #10mesh wire basket. This was then clipped on to a stainless steel rotating shaft powered by a Heidolph electric motor. The basket was lowered into a beaker, surrounded by an outer water jacket, containing 1L of dissolution medium (water) maintained at 37°C ± 0.1°C by a Churchill circulating water bath, and the lid placed on the beaker. The arrangement of the apparatus was such that the basket was centrally placed in the beaker and rested 2.5cm from the base. A sintered glass sparger was introduced at one side of the beaker, and was connected to a teflon tube (1mm ID) for sampling. The continuous flow analysis was carried out using a peristaltic electric pump and the ultraviolet absorbance continuously measured on a CECIL CE272 linear readout spectrometer at 305nm, mounted with a 1cm quartz continuous flow cell, at a sensitivity of 0.2 AUFS and recorded on a J J recorder (J J Instruments Ltd). The basket was rotated at 150rpm and the sampling rate kept constant at 5mL/min. The forward

and return lines of the sampling circuit were always placed in the same position on opposite sides of the dissolution chamber. Immediately prior to each run the dissolution medium was circulated through the system and the spectrometer zeroed. The dimensions of each disc before and after dissolution (after drying the tablet) were accurately measured using a micrometer screw guage.

The Britton-Robinson buffers (pH 2.0 and pH 7.4) were prepared in accordance with Appendix I.

6.2.3 Dissolution of powders

200mg of the required sieve size fraction (125-300μm, 300-500μm and 500-650μm) were accurately weighed and triturated with a small quantity of the dissolution medium (2-3mL), pre-heated to 37°C, using a pestle and mortar. The contents were then washed into a 1L flat bottomed beaker surrounded by a water jacket and maintained at 37°C±0.1°C by a Churchill water bath. The remainder of the 1L dissolution medium (37°C) was then added to the dissolution vessel and the contents stirred at 150rpm using a three blade stainless steel stirrer placed 2.5cm from the base of the beaker. The lid was placed on the beaker and analysis carried out as in Section 6.2.2.1.

A stock solution of 1mg/mL was prepared in DMA and diluted with the dissolution media to give the required range of concentrations. These were then circulated through the system in exactly the same way as the test material until a plateau was reached and the process repeated with all the calibration solutions.

6.3 Results and discussion

Fig. 6.3 shows the particle size distribution of the bropirimine powder. It is apparent from the graph that the particles lie within a narrow size range.

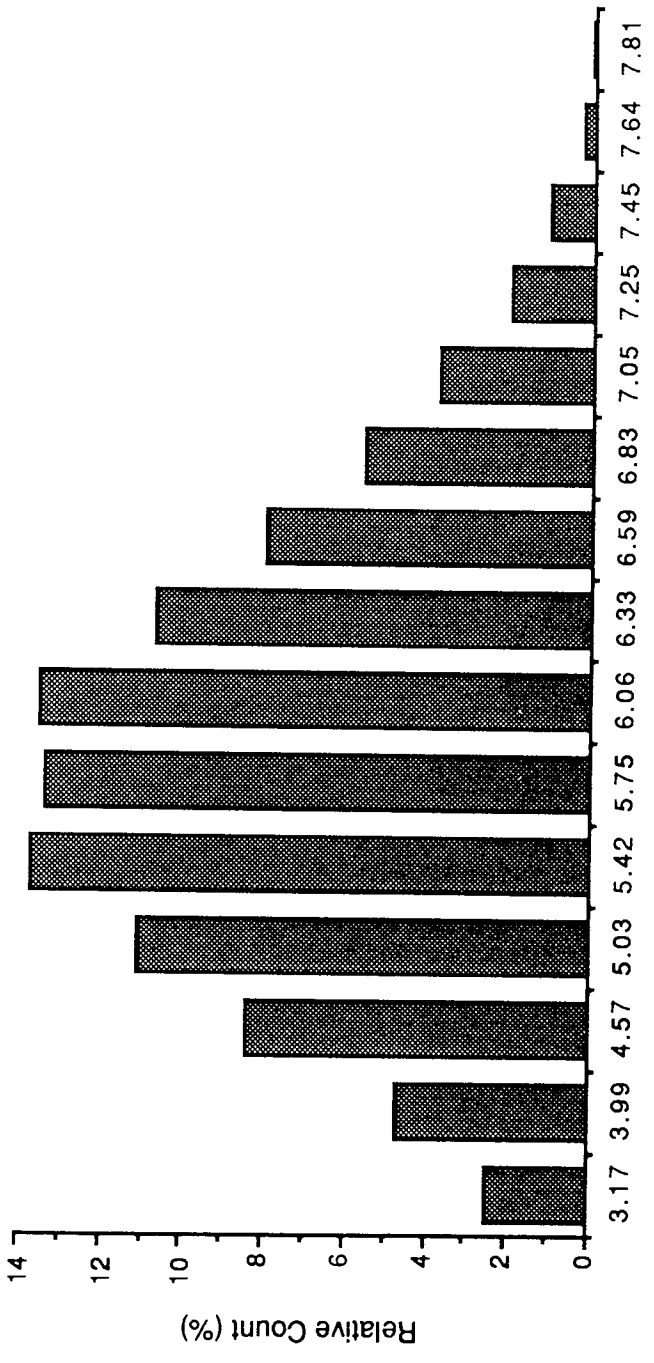

Fig. 6.3: Particle size distribution of bropirimine powder.

Fig. 6.4 and 6.5 show the same data plotted as cumulative count and on a log-normal paper respectively. The arithmetic mean diameter was determined from Fig. 6.5 as 5.70μm.

Particles as small as this usually have high surface energy and invariably form agglomerates which was evident upon sieving. Since it is very difficult to work with particles of such a small size, the following work was peformed on agglomerates.

6.3.1 Dissolution of powders

A number of models have been proposed for the dissolution process of multiparticulate solids[220,221]. For a monodisperse system, the Hixson-Crowell cube root law may be expressed as[220]:

$$\sqrt[3]{M_0} - \sqrt[3]{M_t} = Kt \qquad \ldots 6.10$$

Where: M_0 = Mass of powder used

M_t = Mass of powder dissolved at time t

K = Cube-root dissolution-rate constant

Fig. 6.6 shows the dissolution profiles for three fractions of bropirimine powder *viz*. 125-300μm, 300-500μm and 500-650μm in Britton-Robinson buffer pH 2.0 at 37°C. In all instances indentical profiles were obtained showing high rates of dissolution initially followed by a plateau at approximately 60 minutes.

Because of the low aqueous solubility of bropirimine (35μg/mL) and bropirimine solvates i.e. acetic acid (36μg/mL), N-methylformamide (39μg/mL) and N,N-dimethylformamide (37μg/mL), the amount of powder tested (200mg/1000mL) was either approximately

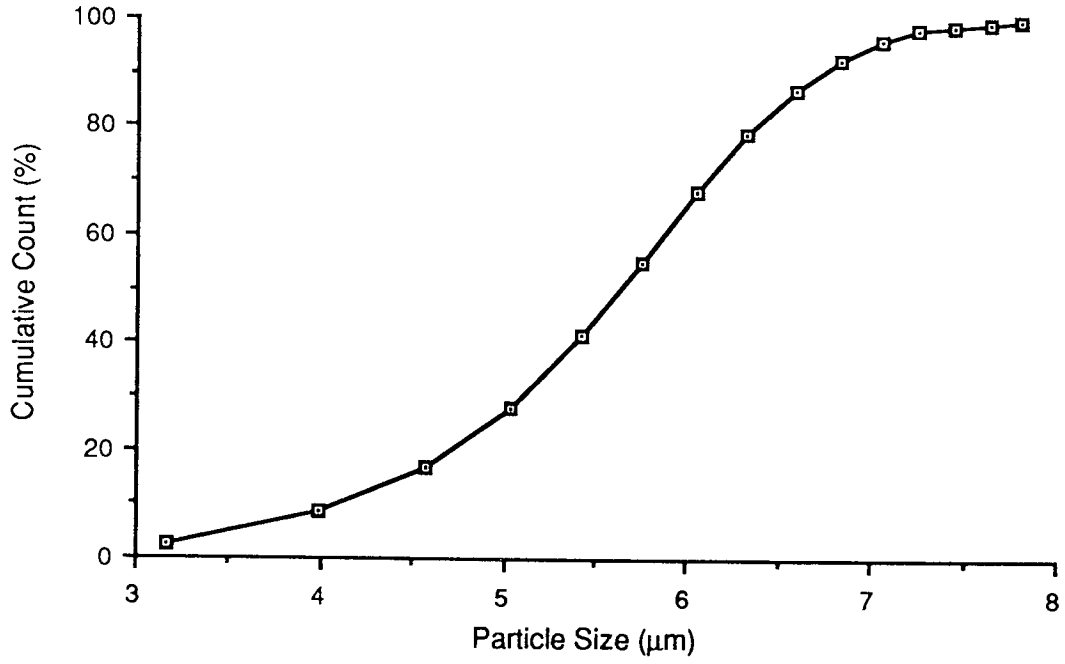

Fig. 6.4: Cumulative undersize distribution curve for bropirimine.

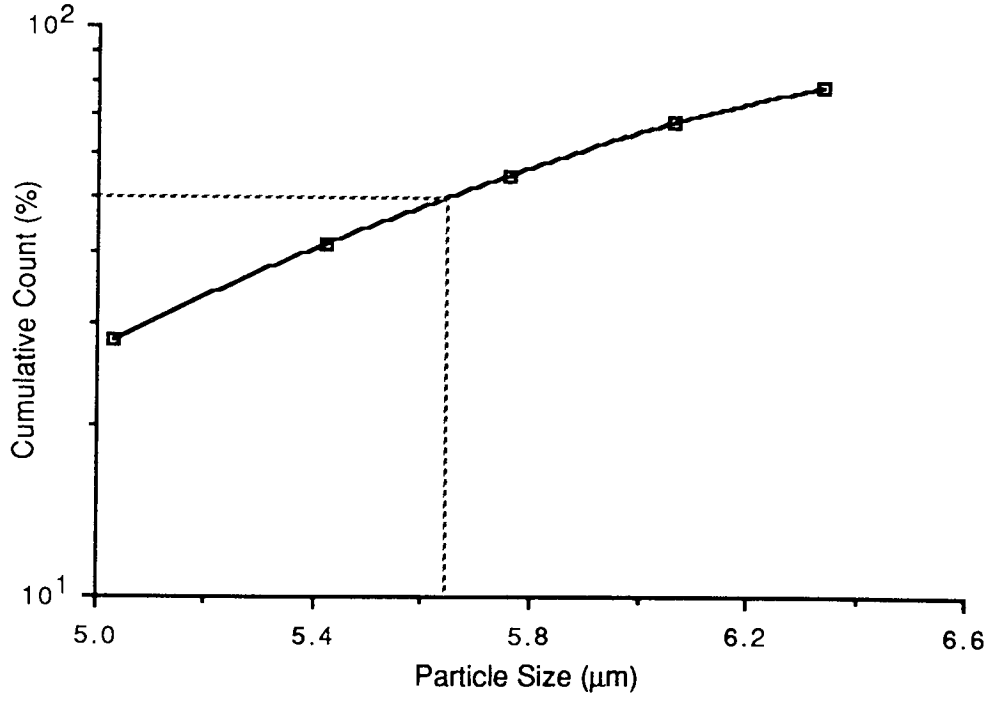

Fig. 6.5: Log-normal plot for bropirimine powder

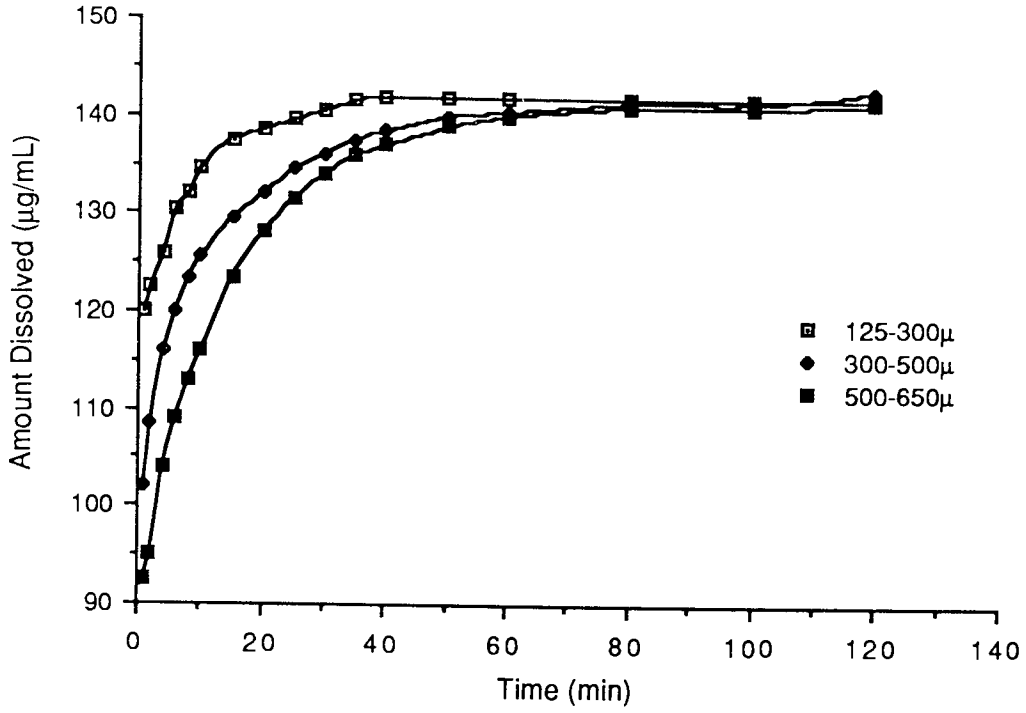

Fig. 6.6: Dissolution profiles of bropirimine in Britton-Robinson buffer pH 2.0 at 37°C.

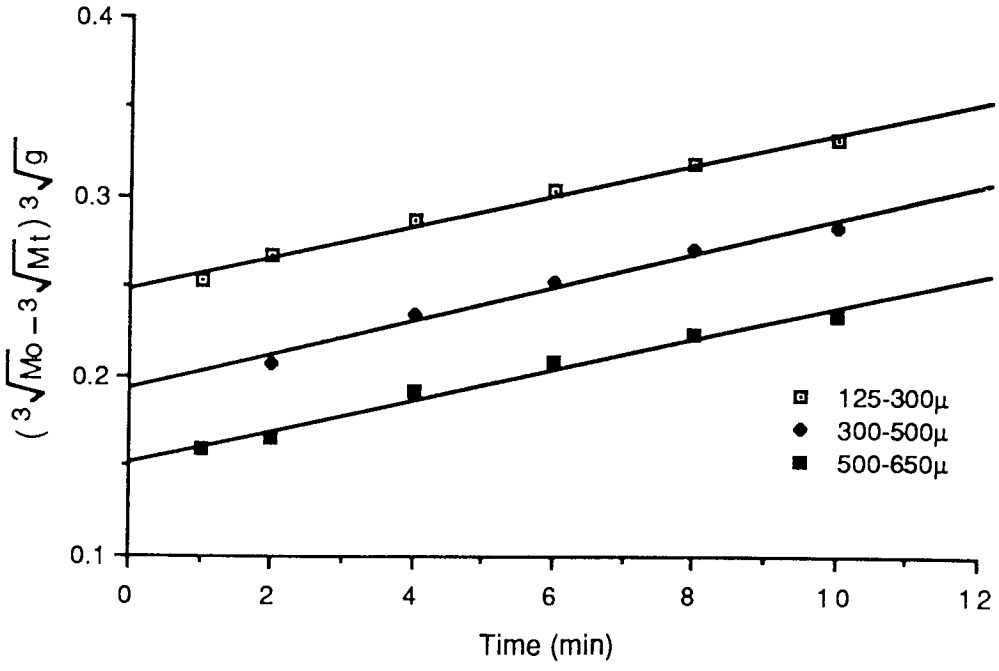

Fig. 6.7: Dissolution of bropirimine powder in accordance with equation 6.10.

1.5 times (pH 2.0) or 5.5 times (pH 7.4) in excess of the solubility and represented non-sink conditions.

Using the data from the early part of the profiles in Fig. 6.6 and substituting into equation 6.10 gives Fig. 6.7 from which the rates (K) were extracted and listed in Table 6.1.

Sieve fraction (μ)	K ($g^{1/3}$/min)	r
125 - 300	8.81×10^{-3}	0.996
300 - 500	9.40×10^{-3}	0.989
500 - 650	8.75×10^{-3}	0.991

Table 6.1: A list of cube-root dissolution-rate constants for three fractions of bropirimine powder

The K values appear identical although the sieve fraction 300-500μm has an apparently higher value than the other two.

Dissolution of bropirimine solvates in Britton-Robinson buffer pH 7.4 (Fig. 6.8) follows a similar pattern as the bropirimine powder. More than 70% dissolution occurs within twenty minutes. Fig. 6.9 shows data plotted according to the Hixson-Crowell cube-root model. All yield linear plots for data taken up to 6 minutes. Using equation 6.10, the rates were calculated from the slope and displayed in Table 6.2. The sieve fraction 125-300μm was used here.

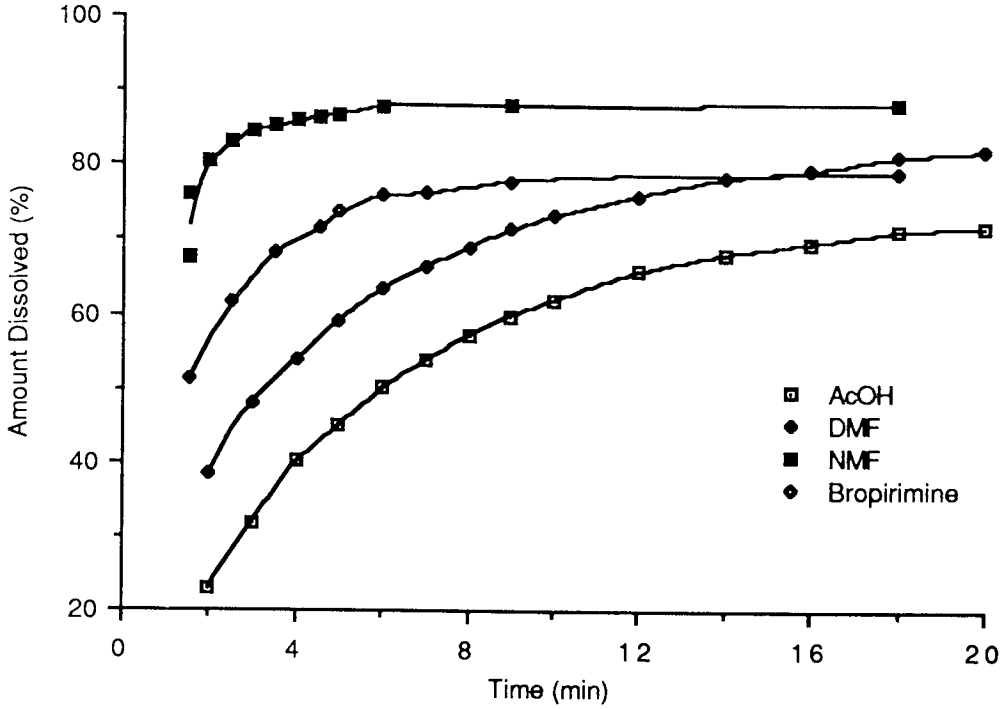

Fig. 6.8: Dissolution profiles of bropirimine and acetic acid (AcOH), N-methylformamide (NMF), N,N-dimethylformamide (DMF) solvates of bropirimine in Britton-Robinson buffer pH 7.4 (sieve fraction 125-300μ).

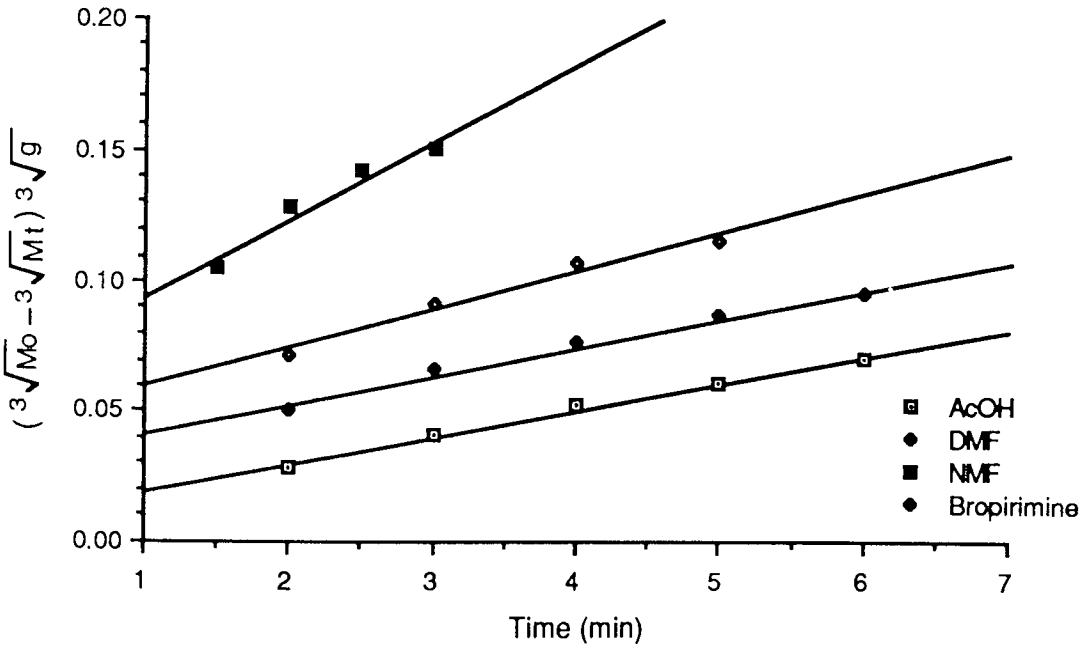

Fig. 6.9: Data from fig. 6.8 plotted in accordance with equation 6.10.

Component	K ($g^{1/3}$/min)
Bropirimine	14.7×10^{-3}
Acetic acid solvate	10.4×10^{-3}
N-methylformamide solvate	29.4×10^{-3}
N, N-dimethylformamide solvate	11.3×10^{-3}

Table 6.2: A list of cube-root dissolution-rate constants for bropirimine and acetic acid, N-methylformamide and N, N-dimethylformamide solvates of bropirimine

Although the rate constant for N-methylformamide solvate is somewhat higher than the other three, possibly due to its solubility, all are in the same order of magnitude. Hence, overall, there is little to be gained by using bropirimine solvates instead of bropirimine in order to increase the dissolution rates.

Gibaldi and Feldman[221] pointed to the fact that unless dissolution was performed under sink conditions, the *in-vitro* results will bear little relationship to *in-vivo* observations. Difficulty would arise in fitting the data to any of the dissolution models and a straight line would not be obtained for log-normal probability plot[222](Fig. 6.10).

The early part of the plot is linear and curvature is only seen on the latter parts of the profiles as a consequence of non-sink conditions. The plots are useful in that parameters such as the extent of dissolution could then be estimated such as the $t_{90\%}$, i.e. the time required for 90% of the drug to be released into solution. For example, the $t_{90\%}$ for 125-300μm, 300-500mm and 500-600μm sieve fractions were estimated to be 5, 12 and 15 minutes respectively. The percentage solubilised is

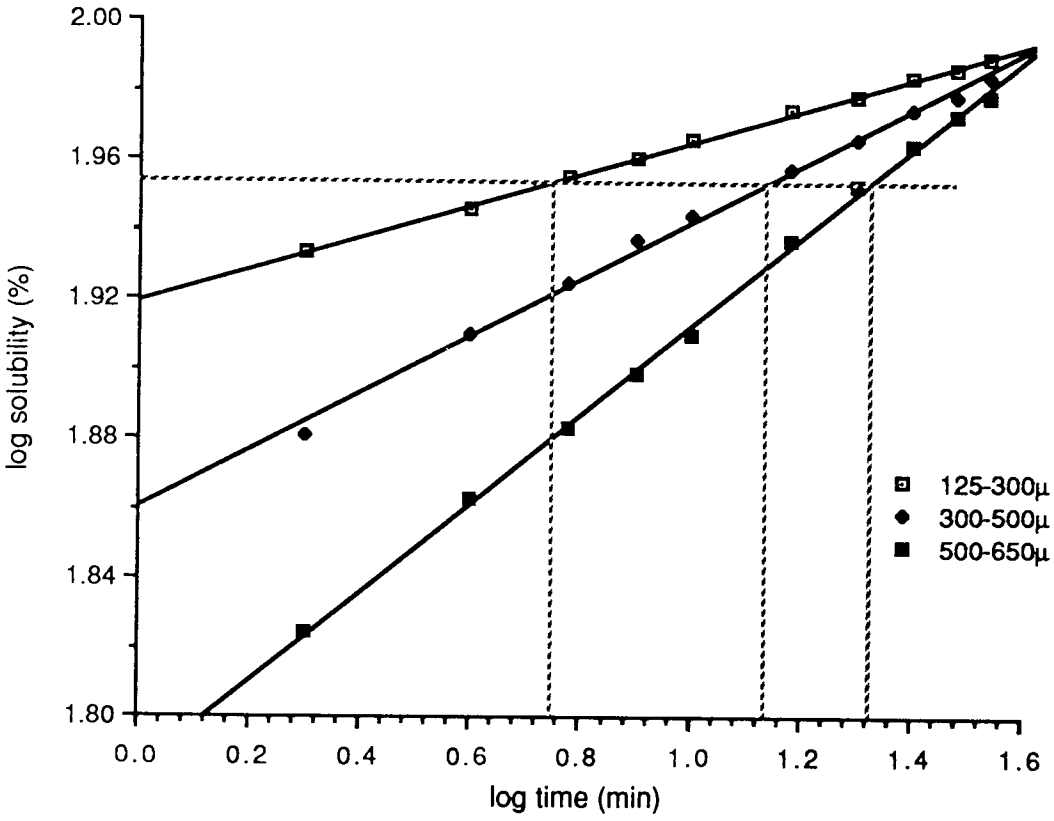

Fig. 6.10: A log-log plot for three sieve fractions of bropirimine.

derived from calculations of the maximum amount that would be soluble at that particular pH (pH 2.0 = 142μg/mL, pH 7.4 = 38.1μg/mL).

6.3.2 Intrinsic dissolution of bropirimine

Most of the methods employed today for intrinsic dissolution testing are modified versions of the apparatus described by Wood *et.al.*[215]. All use a compressed disc held firmly in one place, may it be in the original die or a special holder, with one side exposed to the dissolution medium. A second, less commonly used method is the beaker method, originally used for tablets by Parrott *et.al.*[216] and later adopted by a number of other investigators[217-219] for intrinsic dissolution rate measurements.

Fig. 6.11 shows the intrinsic dissolution of pure bropirimine and on admixture with polyethylene glycol (PEG 20M) using equation 6.9 as the model. In all instances, good linearity is obtained. The slopes of the curves yield the intrinsic dissolution rates which are listed in Table 6.3.

Concentrations of PEG20M (%w/w)	Intrinsic dissolution rate ($mg/cm^2/min$)
0 (Neat bropirimine)	0.24
10	0.27
20	0.30
30	0.37
40	0.46
60	0.98

Table 6.3: Intrinsic dissolution rates for bropirimine and admixtures with PEG20M

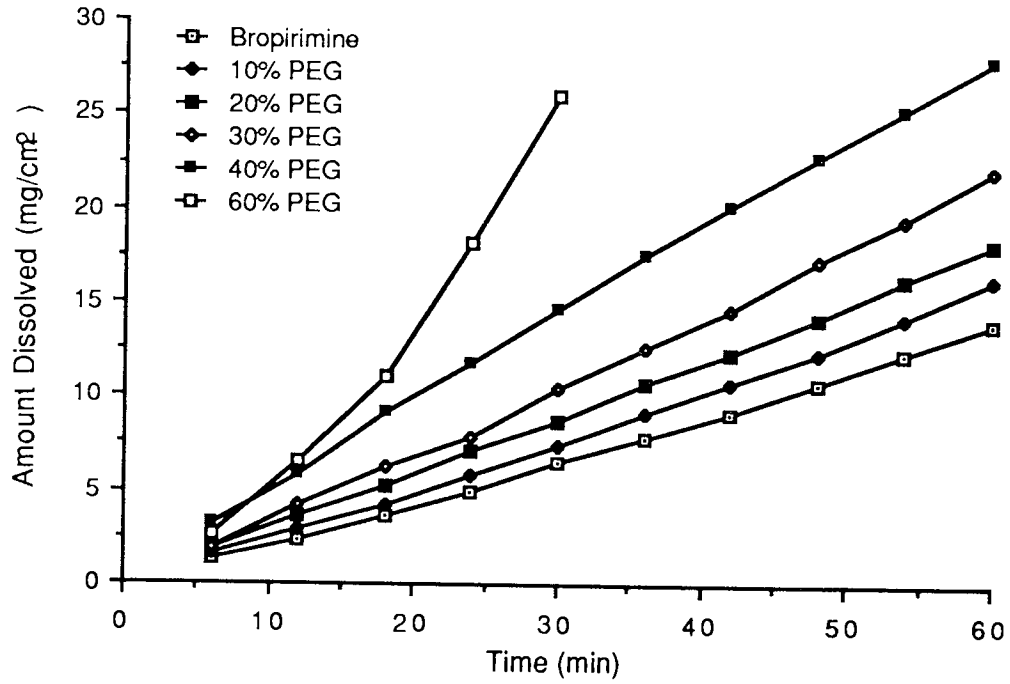

Fig. 6.11: Intrinsic dissolution of bropirimine from compressed discs containing PEG.

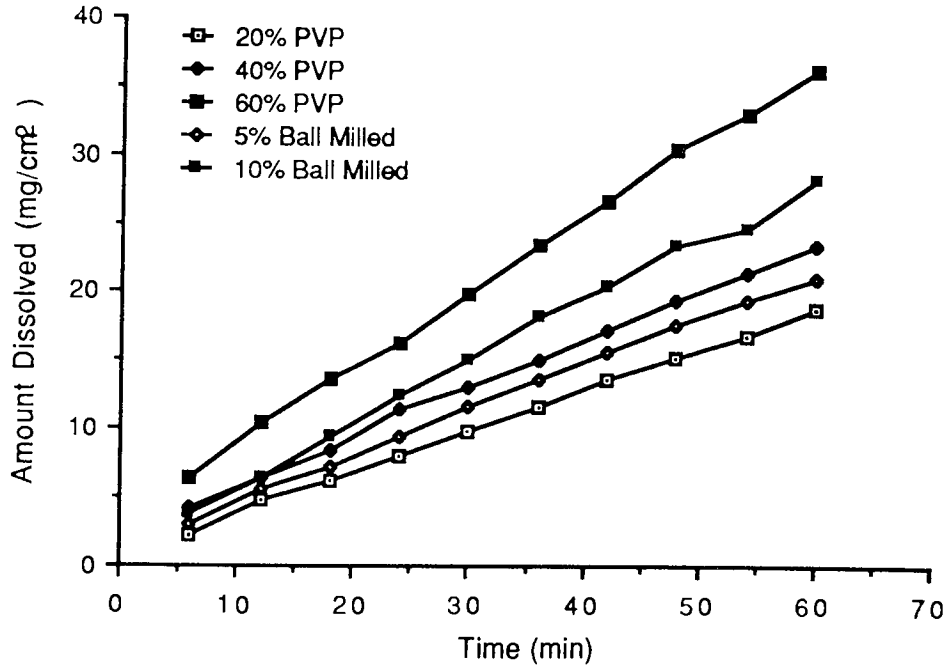

Fig. 6.12: Intrinsic dissolution of bropirimine from compressed discs containing PVP.

Increasing the concentration of PEG 20M in the admixture leads to a corresponding increase in the intrinsic dissolution rates. At concentrations of the polymer >60% $^{w}/_{w}$, the disc disintegrates into small pieces. Using 40%$^{w}/_{w}$ of PEG 20M leads to an almost doubling of the intrinsic dissolution rate.

Fig. 6.12 shows the dissolution from compressed discs made from admixture of bropirimine and polyvinylpyrollidone (PVP) 44M in distilled water at 37°C. Again the intrinsic dissolution rates were calculated from the slopes of the plots and are listed below in Table 6.4.

Concentrations of PVP44M (%w/w)	Intrinsic dissolution rate (mg/cm^2/min)
20	0.31
40	0.36
60	0.55
5 (Ball milled)	0.34
10 (Ball milled)	0.45

Table 6.4: Intrinsic dissolution rates for bropirimine/ PVP44M from compressed discs

Increasing the polymer concentration again leads to increased dissolution rates. Discs containing PVP 44M at a concentration of greater than 60%$^{w}/_{w}$ resulted in disintegration into small particles.
The use of such polymers for increasing the dissolution rates of drugs from either physical mixes or co-precipitates is legion. However, instances have been reported where polymer-drug complex may be so strong as to retard dissolution[224].

The PEG 20M-bropirimine system apparently gives slightly higher intrinsic dissolution rates than the PVP 44M-bropirimine system,

possibly due to differences in the solubility of the two polymers[225,230]. The mechanism of dissolution from such systems has been studied by Doherty *et.al.*[226] whereby mixes of PVP and frusemide were taken and compressed into thin discs. Electron micrographs were then taken before and after the dissolution of the disc. Holes were seen where the polymer had dissolved away leading to increased effective surface area for dissolution. However, no increase in the solubility of the drug was reported. Electron micrographs of a disc containing 40%$^{w}/_{w}$ PEG 20M before and after dissolution were taken and shown in Fig. 6.13. Similar holes to the ones observed by Doherty *et.al.*[226] were seen post dissolution. It is thus plausible to suggest that these polymers increase the dissolution rates by leaving voids within the disc matrix and thus exposing a greater area for dissolution. For diluents having high solubility in the dissolution media, increased dissolution rate is expected[227,228] although the particle size and the homogeneity of the mix can also be equally important[229].

Fig. 6.12 also shows dissolution of compressed discs prepared after ball milling bropirimine and PVP together for 2 hours. The increased rate of dissolution results not only from particle size reduction of the polymer but also the homogeneity of the mix. It is evident from Table 6.4 that this method of preparation gives superior dissolution rates and may be a preferable method of preparation for sparingly soluble drugs[223].

Certain rules have been laid down which give a general idea for *in-vitro* drug absorption. A minimum solubility of 1% is required in the pH 1-7 range to ensure solubility-independant absorption characteristics[211]. However, a compound may have a solubility of the region of 1% but may dissolve so slowly that its dissolution becomes

a

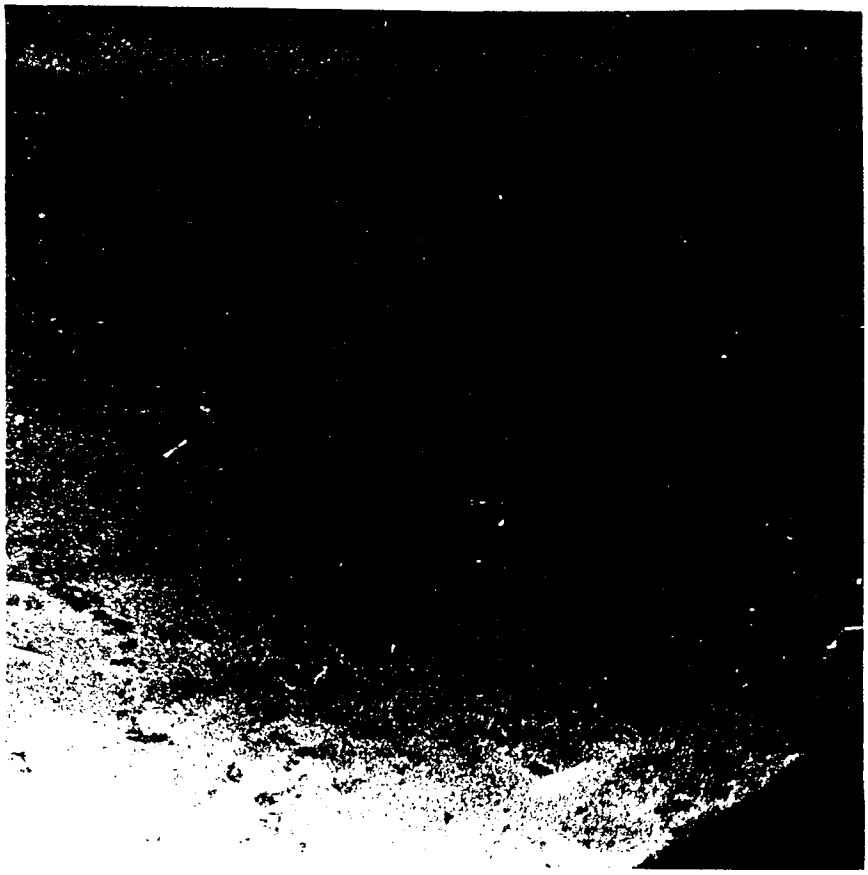

b

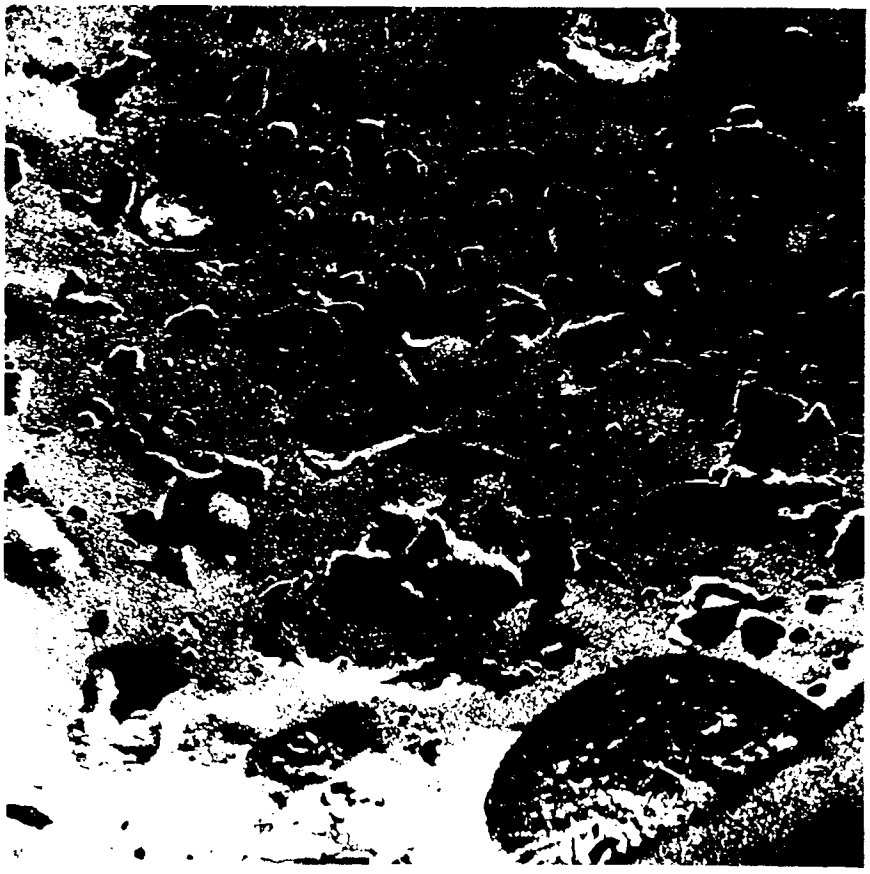

x23

Fig. 6.13: Appearance of a disc containing 60:40 mixture of bropiriminel PEG 20M (a). before and (b). after dissolution

rate-limiting step[211]. Hence both solubility and the rate of dissolution are equally important. In general, if the intrinsic dissolution rate is greater then 1mg/cm^2/min, there is usually no problem in absorption[212]. If it is less than 0.1mg/cm^2/min, there is usually dissolution rate-limited absorption[212]. Between these two values the compound is considered to be borderline and additional information would be required to ascertain the effect of dissolution on the absorption rate[212].

In conclusion, bropirimine does not suffer from dissolution rate problems (K = 0.24mg/cm^2/min) but from its intrinsic solubility (35μg/mL). Solvates (acetic acid, N-methylformamide and N,N-dimethylformamide) neither increased the intrinsic solubility nor had a marked effect on the dissolution rates. Although intrinsic dissolution rates were enhanced using soluble polymers, bropirimine would probably still suffer from bioavailabilty problems.

7.0 STUDIES ON PARENTERAL FORMULATION OF BROPIRIMINE

7.1 Introduction

Although oral dosage forms are the most acceptable and widely used, the parenteral route offers an excellent alternative and is the route of choice for a number of reasons. For example, drugs prone to gastric breakdown (e.g. insulin), poor oral bioavailability, when high systemic levels of the drug are required in a short space of time (e.g. diazepam), to avoid 'first-pass' effect and testing in development of new drugs.

Drugs administered parenterally are considered to be 100% bioavailable and hence dose alterations are readily made to suit each individual. However, the serious drawbacks to this route include patient acceptability, tissue damage, skilled delivery and production problems such as sterility and particulate contamination.

An increasing number of drugs are now formulated as parenterals by the use of co-solvents[236]. It often becomes necessary to administer the drugs parenterally at a concentration which far exceeds its aqueous solubility. As a result precipitation of the drug may occur on injection. Such a problem was identified in the early 1970's when Jusko *et.al*. observed that the high incidence of thrombophlebitis associated with diazepam (aqueous solubility = 48μg/mL) injection was due to the precipitation of the drug at the site of the injection[237]. Phenytoin (aqueous solubility = 16μg/mL) is another example of a drug that has attracted much publicity on this front. Although it is common knowledge that tissue necrosis occurs following injection of an acidic or an alkaline formulation, e.g. phenytoin (pH > 11.5), tissue necrosis due to the phenytoin precipitate has also been identified[238]. Formulation of both of these drugs were in 10% ethanol and 40% propylene having concentrations of 5mg/mL

(diazepam) and 50mg/mL (phenytoin). Plasma concentration data obtained from intramuscular (im) administration of phenytoin could not be fitted into a model involving either first- or zero- order drug absorption[239]. Such an abnormaility could be explained on the assumption that the drug precipitated on delivery and then re-dissolved at the injection site. Phenytoin is often found to be incompatible with common parenteral fluids, such as dextrose and normal saline, resulting in crystal formation[236,240]. Attempts at predicting the solubility of phenytoin in intravenous admixtures by utilising the pK_a of phenytoin (8.3) and the pH of the admixture, were largely unsuccessful due to the unavailability of published data on all of the ingredients encountered[253]. The use of large amounts of co-solvents (e.g. 40% propylene glycol) and extreme pH values (11.5) used to dissolve certain drugs have also been a contributory factor to tissue necrosis and pain on injection[238,241]. Drug precipitation either on injection or co-administration with large volume parenterals has been observed for a number of other drugs[236, 242-244]. These incompatibilites may be as a result of dilution of vehicle containing co-solvents (the composition of which is essential for co-solvent solubilised drugs) or a change in pH or temperature[256].

The potential hazards from such incompatibilities are serious. The precipitate formed can result in erratic or reduced drug availability, tissue necrosis or possible drug embolization leading to amputation of limbs[238]. The co-solvents may themselves have toxicity problems, e.g. propylene glycol and ethanol have been shown to exhibit haematological toxicity[245-247]. The increased viscosity of the vehicle may lead to injection difficulty. The problem of precipitation appears to be related to the rate of delivery of the drugs[237,241,248]. This obviously represents a serious drawback for drugs that need to be administered quickly for life-threatening conditions, e.g. diazepam and phenytoin for *Status epilepticus*.

As yet no fully quantitative method exists to assess precipitation of drugs on injection. Yalkowsky *et.al.* suggested a dynamic method which, if used correctly, could yield semi-quantitative results[249]. A spectrometer was used and absorbance measurements of the dilution of diazepam and alprazolam solutions were recorded above 400nm wavelength. This is above the uv absorbance range of these compounds (220-320nm) and corresponds to dispersion from particles. The peak height of the traces were a measure of the amount of precipitate present.

Bropirimine, like phenytoin and diazepam, also relies on the use of co-solvents for solubilisation (Chapter 5). It is logical to assume, therefore, that problems will also be encountered with bropirimine on injection. In order to assess these problems, a modified version of the method described by Yalkowsky *et.al.*[249] was used and tests carried out on various formulations of bropirimine. For comparison, diazepam and phenytoin injections were also tested.

7.2 Materials and method

Meglumine and N,N-dimethylacetamide were purchased from Sigma and used as received. The diazepam injection was received as 'Valium 10' (10mg/2mL, Roche), the phenytoin as 'Epanutin Ready Mixed Parenteral' (250mg phenytoin sodium in 5mL, Parke Davies) and the 5% dextrose as 'Steriflex' (Boots). Bropirimine was synthesised within the Department of Pharmaceutical Sciences, Aston University, using the method described by Brown and Stevens[250]. All the salts used in the buffers were obtained from various commercial sources and were BP standard. The buffers (Britton-Robinson and Tris) were prepared as described in Appendices I and II[251].

An Imed 960 Volumetric Infusion Pump (Abingdon, Oxon. Infusion rate settings 200-800mL/hr) was connected in series with a uv absorbance spectrometer (Cecil Instruments CE272) which in turn was connected to a chart

recorder (Gallenkamp) run at a chart speed of 2mm/min. The uv spectrometer was mounted with a 10mm path length quartz flow cell (volume 2mL) and operated at a sensitivity of 2.0 AUFS. At a distance 'x' (40-100cm) from the flow cell, an injection port was introduced, having a rubber septum, into a tube of internal diameter 2.5mm. The formulation under test was then injected into this port with a syringe pump (Sage Instruments, Orion Research Inc.) using a 20mL syringe (rate range of 0.1 - 1mL/min) and an 20-gauge needle. The whole set up is displayed in Figure 7.1.

Prior to each experiment, the infusion liquid was flushed through the system until there was no change in the spectrometer reading. The vehicle then acted as the reference and the spectrometer suitably zeroed. The syringe pump was then switched on after setting the desired injection rate. Any subsequent peaks on injection were then attributed to the formation of precipitate. After each experiment, the whole system was flushed through once again with the vehicle to remove any remaining precipitate and the cycle repeated with the next formulation.

7.2.1 Preparation of bropirimine injections

The vehicles/formulations used to prepare the various bropirimine injections were:

Vehicle (A)	DMA	$10\%^{v}/_{v}$
	Meglumine	$5\%^{w}/_{v}$
	0.2M sodium bicarbonate to	$100\%^{v}/_{v}$
Vehicle (B)	DMA	$10\%^{v}/_{v}$
	0.2M sodium bicarbonate to	$100\%^{v}/_{v}$

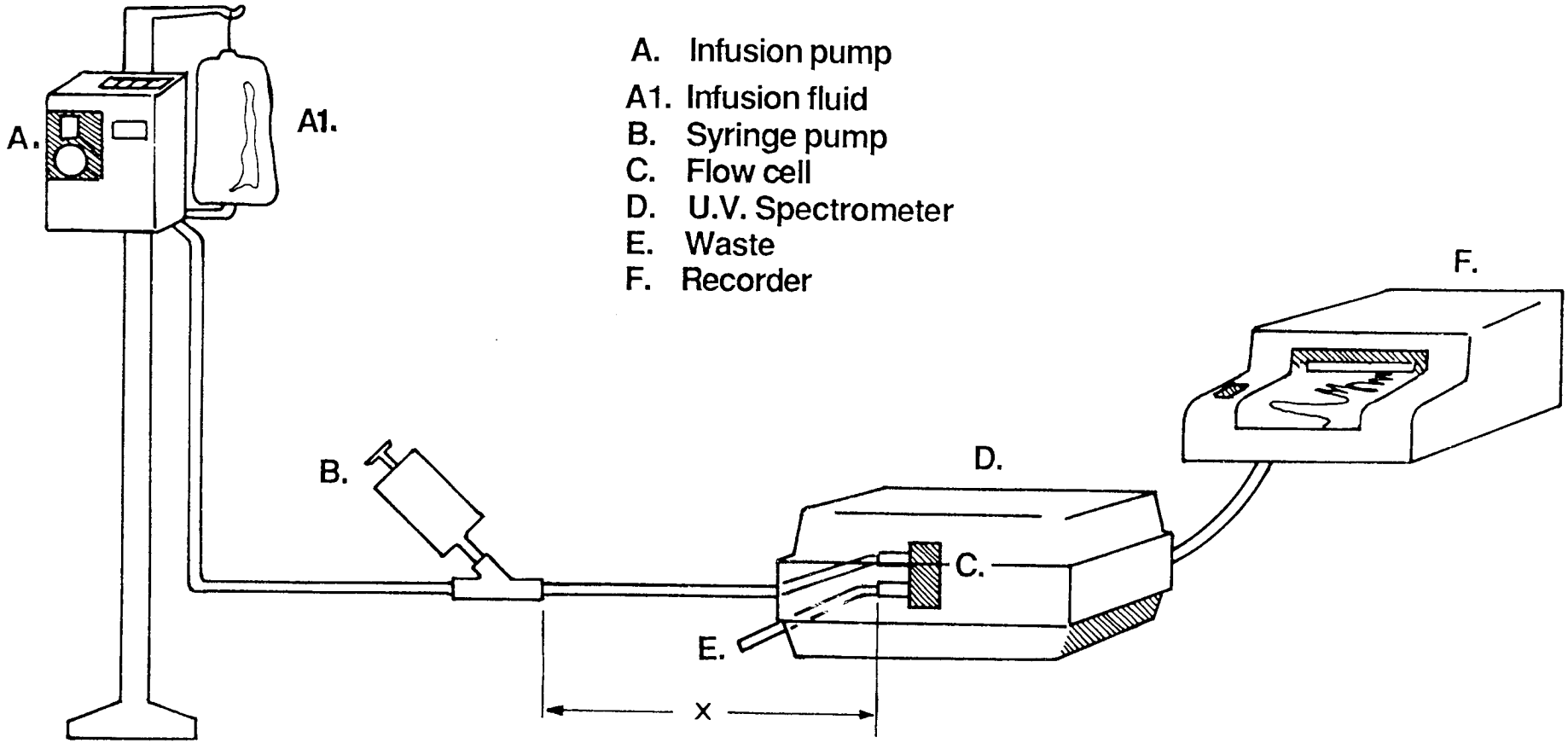

Fig. 7.1: The in-vitro set up for the detection of precipitation on injection

Vehicle (C)	DMA	50%$^{v}/_{v}$
	Meglumine	2.5%$^{w}/_{v}$
	Distilled water to	100%$^{v}/_{v}$
Vehicle (D)	DMA	5%$^{v}/_{v}$
	0.2M sodium bicarbonate to	100%$^{v}/_{v}$

An appropriate amount of bropirimine was added to the vehicle, vigorously shaken, sonicated for 10 minutes and filtered through a 0.2μm Nitrate Millipore filter to remove any extraneous material.

Unless stated otherwise, a 25mg/mL solution of bropirimine was prepared in vehicle (A) and 10mg/mL in vehicles (B), (C) and (D). The approximate limiting solubility in each vehicle was 32mg/mL (A), 20mg/mL (B), 15mg/mL (C) and 14mg/mL (D), such that all concentrations were at least 20% below saturation.

Initially, the effect of wavelength on the noise level was studied with the vehicle flowing through the system. At higher wavelengths (>500nm) any reading of absorbance was principally accounted for as dispersion from the precipitated particles but not with the vehicle alone.

7.2.2 Calculation of buffering capacity

The buffers (25mL) were titrated using 0.1M sodium hydroxide and the pH monitored. The buffering capacity, β, was then calculated from:

$$\beta = \left(\frac{M \times \Delta V}{\Delta pH \times V_1} \right) \times 1000 \ (\text{mEq}/\Delta\text{pH unit}) \qquad \ldots 7.1$$

Where: M = Molar concentration of acid on base

ΔV = Volume of titrant added (mL)

ΔpH = Change in pH corresponding to the addition of ΔV mL of titrant

V_1 = Volume of buffer used (25mL)

7.2.3 Solubility measurements of bropirimine

a. In DMA. The DMA was neutralised by the addition of 0.1M HCl. Concentrations of DMA ranging from 10-50%$^v/_v$ were then prepared in Britton-Robinson buffers of the required pH (6.5 - 10). Excess bropirimine was added and the mixture stirred for 6 hours. Once equilibrated, the pH values of the suspensions were measured and re-adjusted to the pre-saturation values with 0.1M HCl. The suspensions were then stirred for a further 18 hours, filtered through a 0.2µm Nitrate Millipore filter and the pH measured. Any subsequent dilutions were then carried out using the appropriate buffer. 20µL of the filtrate were then injected into the HPLC using 25%$^v/_v$ acetonitrile at pH 2.0 as the mobile phase (Chapter 2) and ABmFPP as the internal standard.

b. In formulation (A). The pH of vehicle (A) was adjusted using 0.1M HCl. Again, this was saturated with bropirimine, the pH re-adjusted and equilibrated for a further 18 hours. One set of experiments was left at room temperature (21°C) and the other in a cold room (6.4°C). The mixtures were then treated as described above.

7.3 Results and discussions

Fig. 7.2 shows the effect of wavelength on the trace produced when 5% dextrose was passed through the system at an arbitrary flow rate of 200mL/hr, using the same liquid for injection at a rate of 0.51mL/min. At wavelengths below 650nm, the noise level, possibly due to absorbance, is high; whereas

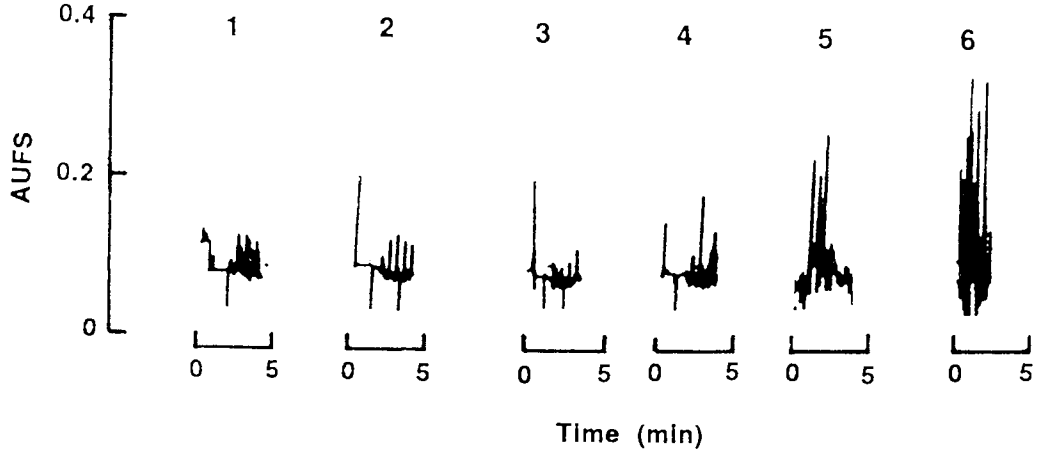

Fig. 7.2: *The effect of wavelength on the noise level of the vehicle*
(1) 800 nm *(2)750 nm* *(3) 700 nm*
(4) 650 nm *(5) 590 nm* *(6) 500 nm*
Conditions: *flow rate:* *400 mL/hr*
Injection rate: *0.51mL/min*
chart speed: *2 mm/min*

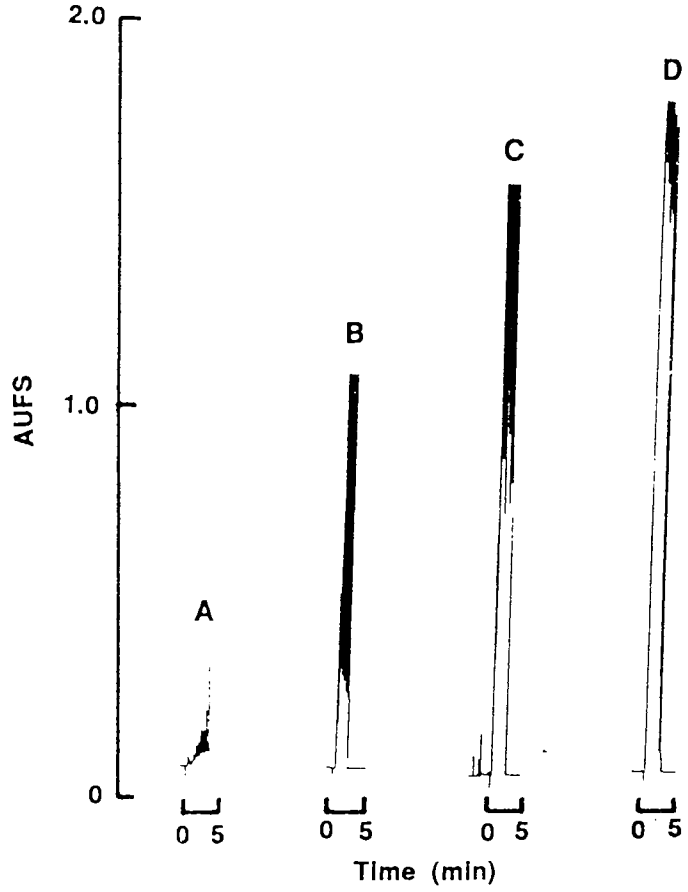

Fig. 7.3: *The effect of injection rate on precipitation*
(A) 0.10 *(B) 0.24* *(C) 0.51 and (D) 1.00 mL/hr.*
Conditions: *flow rate:* *200 mL/mhr*
chart speed: *2 mm/min*
λ: *700 nm*

wavelengths above this show appreciably reduced and acceptable noise levels. Similar results were shown by all the formulation vehicles. A working wavelength of 700nm was then chosen for subsequent experiments.

With dextrose flowing through the system, an injection of 25mg/mL of bropirimine, formulated in vehicle (A), at an injection rate of 0.51mL/min showed no precipitate. Reducing or increasing the infusion flow rate and increasing injection rate up to 1mL/min had no effect. Because the bropirimine solubility is co-solvent dependent, a precipitate was expected on dilution of the formulation in the dextrose (25%). However, the solubility of bropirimine is also greatly enhanced at high pH values and measurement of the pH of the end mixture (dextrose + bropirimine formulation) showed that the pH had increased from 5.3 to 10.0, that is, the buffering capacity had been exceeded and the final pH was sufficiently high to keep the bropirimine in solution. Replacement of dextrose with Tris buffer (0.2M) pH 7.4 also resulted in lack of of buffering capacity (final pH = 9.5) with no bropirimine precipitate evident. Further Tris buffers of one-and-a-half (0.3M) and double strength (0.4M) were prepared and titrated against 0.1N sodium hydroxide to calculate the buffering capacity over the range pH 7.3 to 7.5. The results are shown in Table 7.1

	TRIS BUFFER			BLOOD *
	0.2 M	0.3 M	0.4 M	
Buffering capacity ($mEq/_{\Delta}pH$)	15	21	25	18

* Obtained from literature (251). This figure is for 1kg of tissue.

Table 7.1: Buffering capacities of Tris buffer

It can be seen that 0.3M Tris buffer has a similar buffering capacity to blood. When this buffer was substituted for dextrose, immediate precipitation of bropirimine resulted. However, to ensure that buffering capacity is maintained, Tris double strength (0.4M) buffer was used for the remainder of experiments.

Fig. 7.3 shows the effect of varying the injection rate of a 25mg/mL solution of bropirimine in Vehicle (A), at an infusion flow rate of 200mL/hr, on the resultant trace. As the precipitate forms, a peak is recorded which has an irregular appearance (pH of final solution = 7.44 c.f. the original of 7.40). This is indicative of the inhomogeneity of a suspension passing through the flow cell. Little precipitation was detected at lower injection rates (<0.24mL/min). However, increasing the injection rate to 0.51mL/min produced so much precipitate that the tubing was blocked, that is, occlusion occured within the system. Taking average peak height as an indicator of the precipitate when steady state conditions have been reached, a graph of injection rate against peak height may be plotted (Fig. 7.4). It can be seen that when the injection rate is increased from 0.24mL/min to 0.51mL/min, there is a sharp increase in the rate of formation of the precipitate. Above injection rates of 0.51mL/min, there is no change in peak height as occlusion occurs and the flow stops leading to a plateau.

The effect of varying the infusion rate can be seen in Fig. 7.5 and 7.6. Increased infusion rate leads to increased dilution such that at very high infusion flow rates (> 600mL/hr) negligible precipitate is detected. This flow rate represents a dilution factor of 41.7. Semilogarithmic plot of peak height against the infusion rates shows good straight line relationship in the range 100mL/hr to 600mL/hr (Fig. 7.7). Although infusion rates vary accordingly to the requirements (typical range 200-600μL/hr), Fig. 7.7 suggests that in order to minimise precipitation at an injection rate of 0.24mL/min, the infusion rate should be in excess of 600mL/hr.

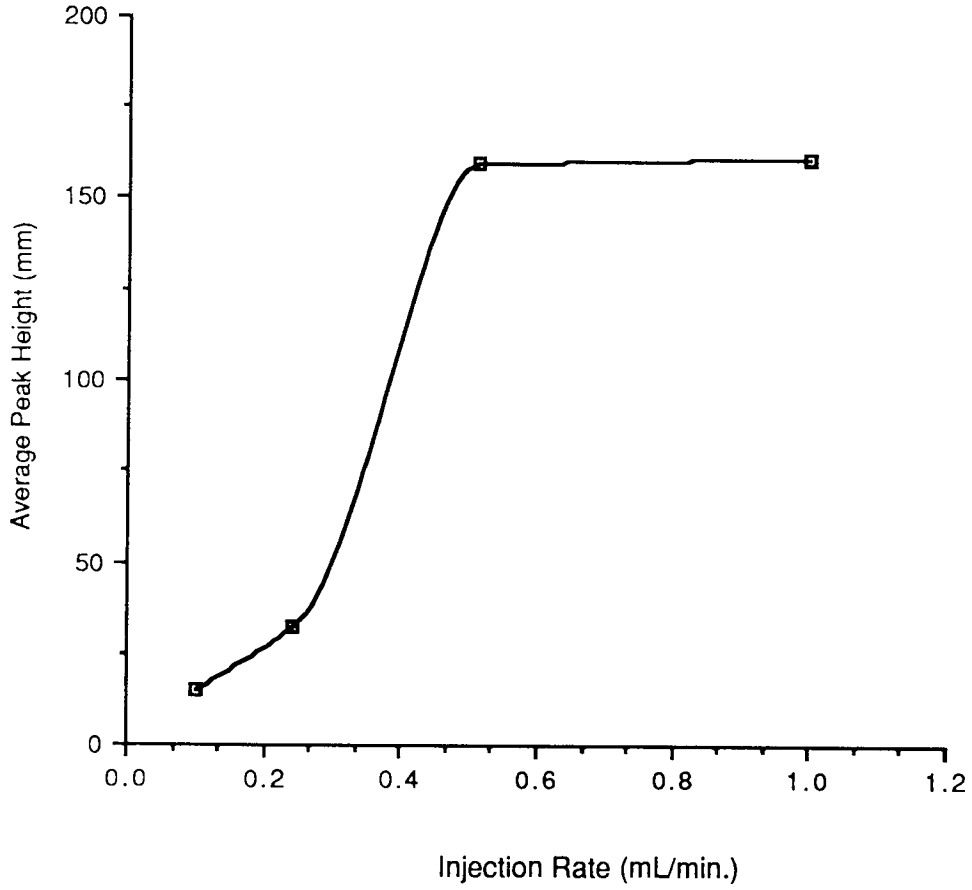

Fig. 7.4: Effect of injection rate on precipitation

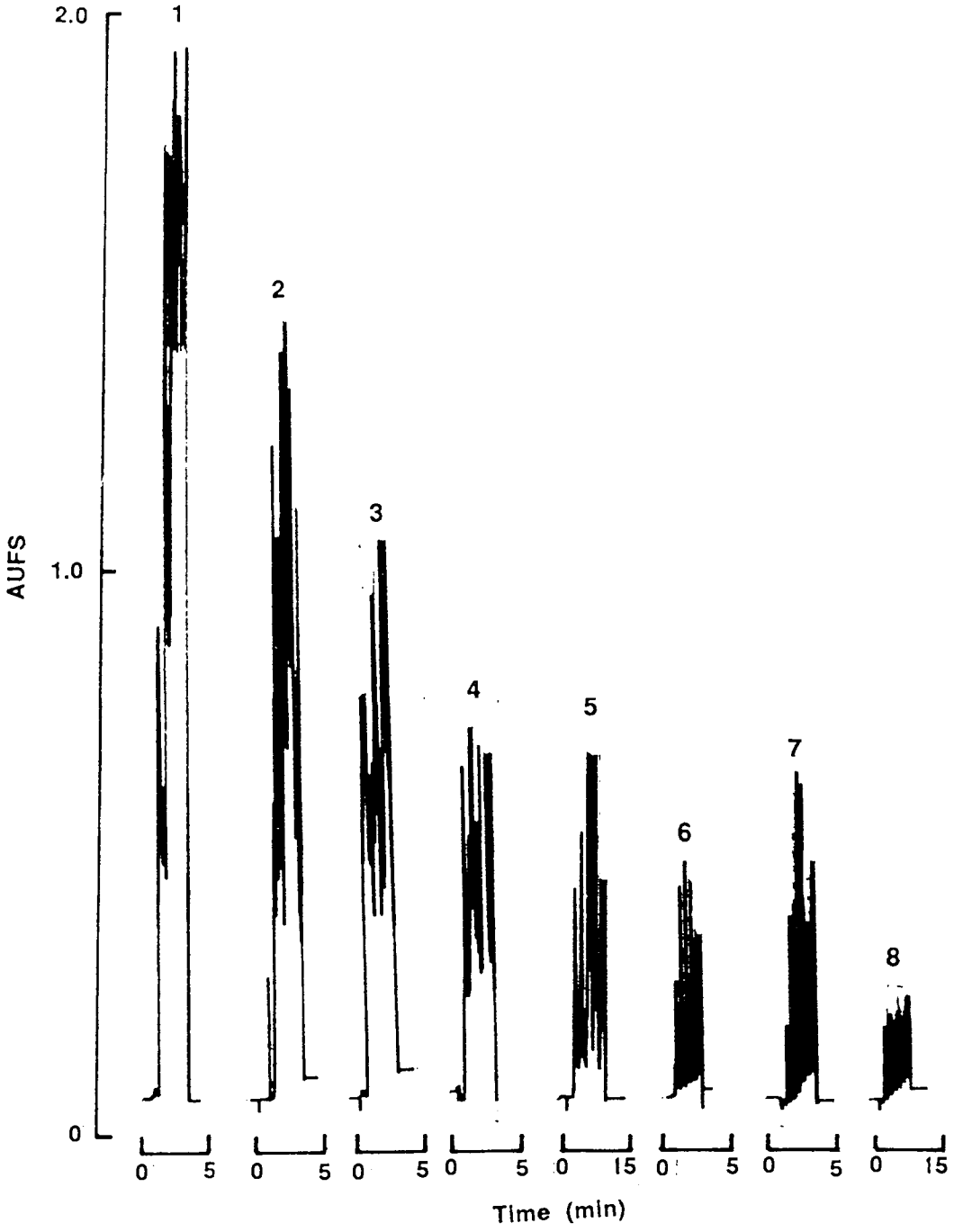

Fig. 7.5: The effect of infusion rate on precipitation
(1) 100 (2) 200 (3) 300
(4) 400 (5) 500 (6) 600
(7) 700 (8) 800 mL/hr
Conditions: Injection rate: 0.24 mL/min
chart speed: 2 mm/min
λ: 700 nm

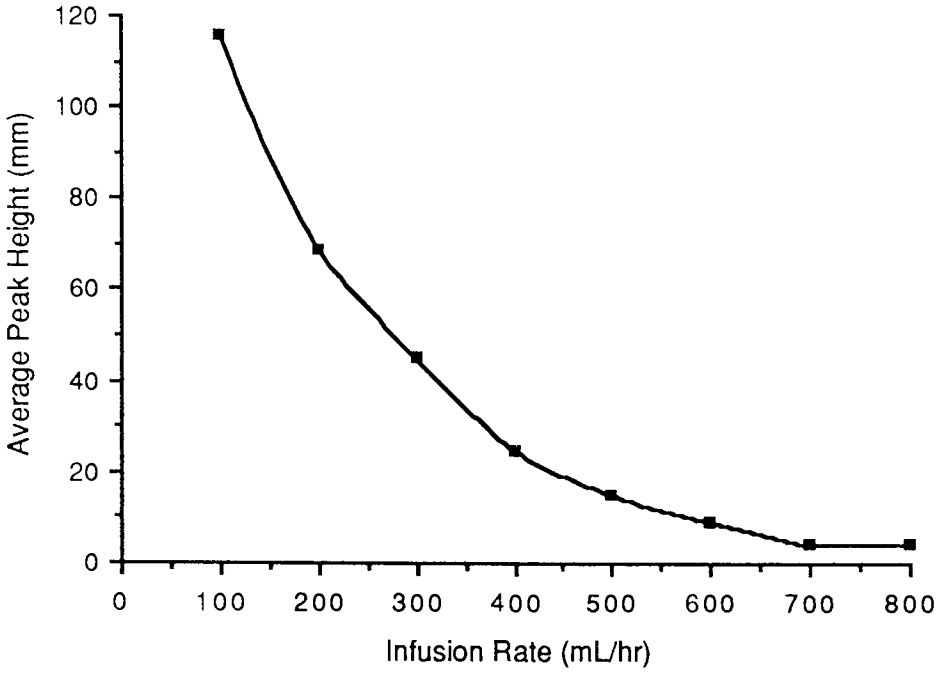

Fig. 7.6: Effect of infusion rate on precipitation.

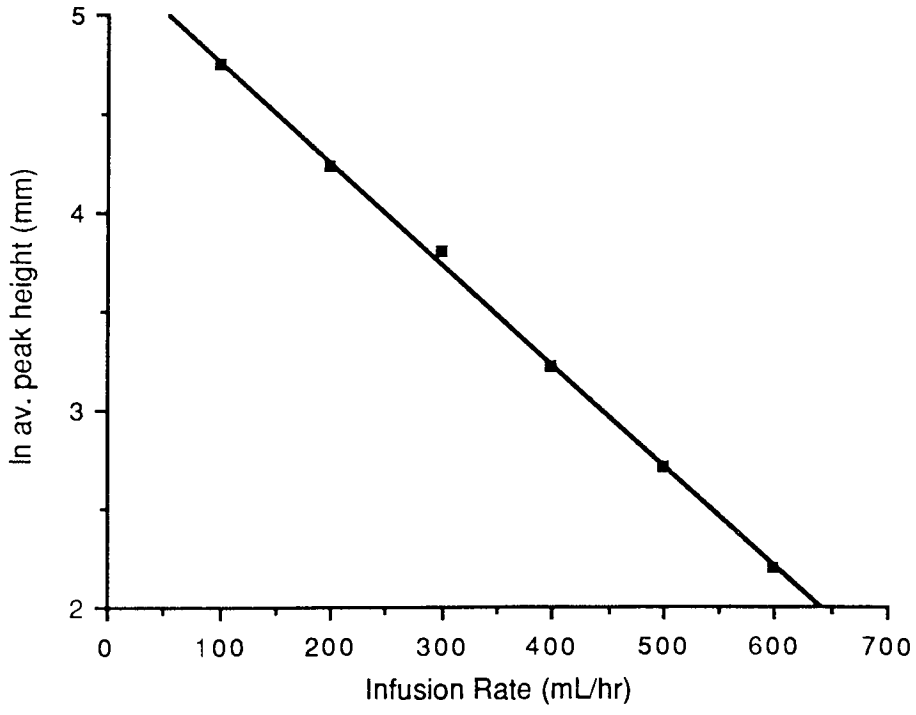

Fig. 7.7: Effect of infusion rate on precipitation.

The concentration of the drug in the formulation plays a significant role if precipitation is to be avoided. Fig. 7.8 shows five different concentrations of bropirimine in vehicle (A) and their effect on precipitation. Injection of concentrations below 20mg/mL into mobile phase flow rate of 400mL/hr show very little precipitate, whereas concentrations at and above this precipitate out rapidly. It may therefore be preferable to administer low concentrations of bropirimine at high injection rates rather than high concentrations over a long period of time.

Changing the distance between the injection port and the flow cell (x) did not significantly affect the result and no apparent trend was seen (Fig. 7.9). If the distance 'x' is short (<15cm) then, occassionally, peaks may be seen which are due to a phenomenon called Schleiren patterns[249]. Such patterns form when there are differences in the refractive indices of the two liquids flowing though the flow cell only partially mixed. Longer distances provide sufficient time for the two components to mix and hence no extra peaks are observed.

Fig. 7.10 shows the effect of co-solvent composition and its pH on the solubility of bropirimine. As expected, an increase in the pH of the solvent results in an enhanced solubility of bropirimine. At these higher pH values, the enhanced solubility is likely to be due to ionisation whereas at lower pH values the solubility is likely to be due to the co-solvent alone.

Using vehicle (A) at a number of different pH values, the solubility profile obtained for bropirimine is displayed in Figs. 7.11 and 7.12. Since the co-solvent composition stays constant, the exponential increase in the solubility of bropirimine is due to ionisation. Figs. 7.11 and 7.12 also show results of experiments conducted at 6.4°C, a typical temperature frequently encountered during warehouse storage. Semi-logarithmic plots give straight lines which can consequently be used to give an indication of the concentration of bropirimine that would not result in a precipitation of the drug. Formulations containing

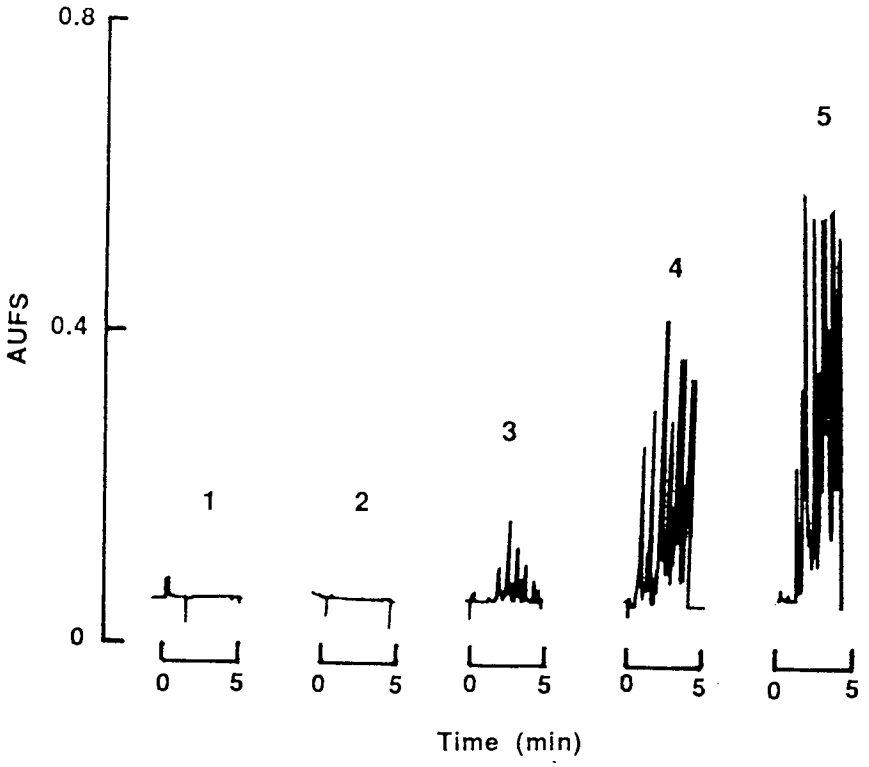

Fig. 7.8: *Effect of bropirimine concentration on precipitation*
(1) 5 *(2) 10* *(3) 15*
(4) 20 *(5) 25 mg/mL.*
Conditions: *flow rate:* *400 mL/hr*
Injection rate: *0.24 mL/min*
chart speed: *2 mm/min*
λ: *700 nm*

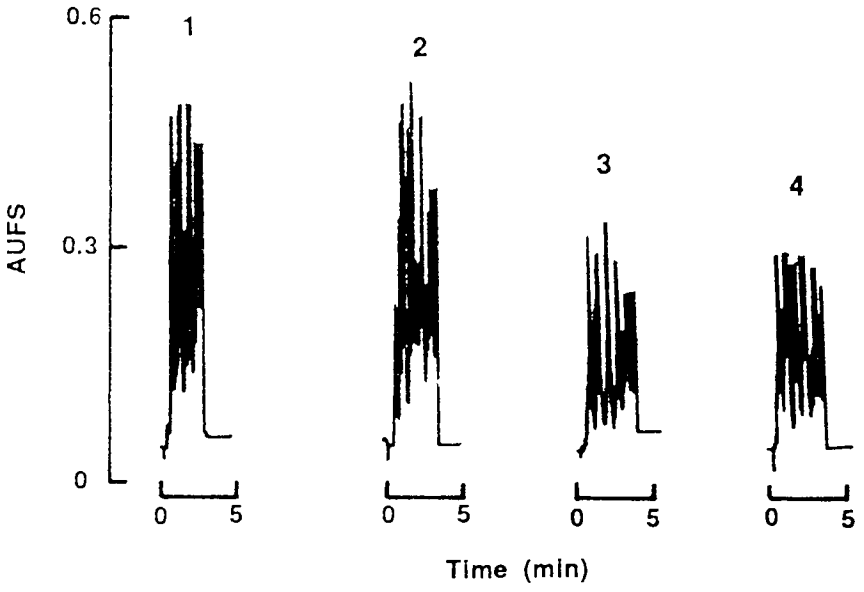

Fig. 7.9: *Effect of tube length (x) on precipitation*
(1) 100 *(2) 80* *(3) 60 and (4) 40 cm.*
Conditions: *flow rate:* *400 mL/hr*
Injection rate: *0.24 mL/min*
chart speed: *2 mm/min*
λ: *700 nm*

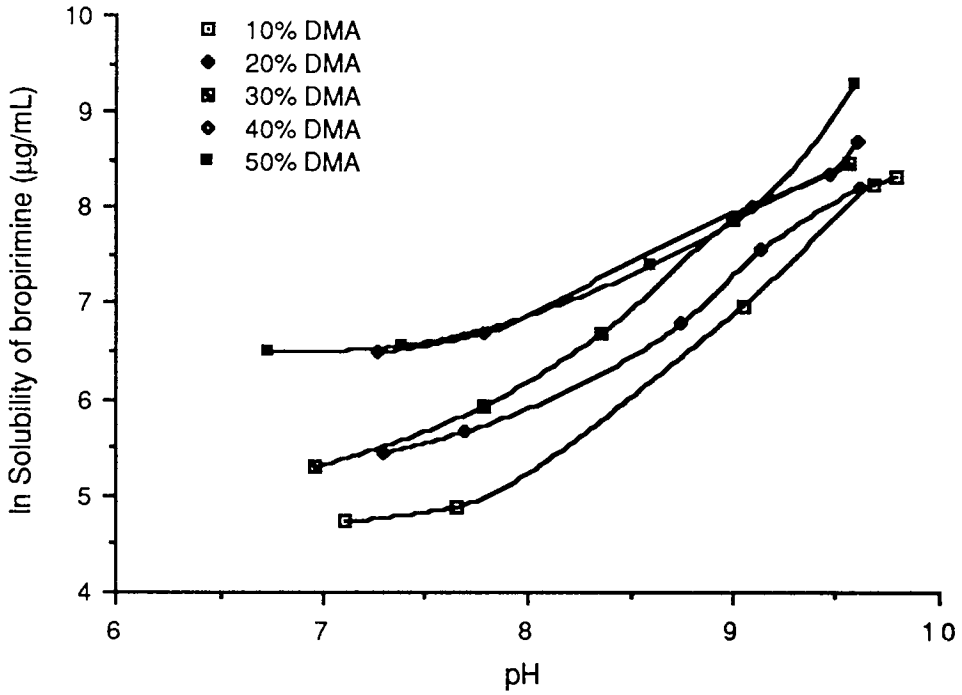

Fig. 7.10: The effect of DMA composition and pH on the solubility of bropirimine

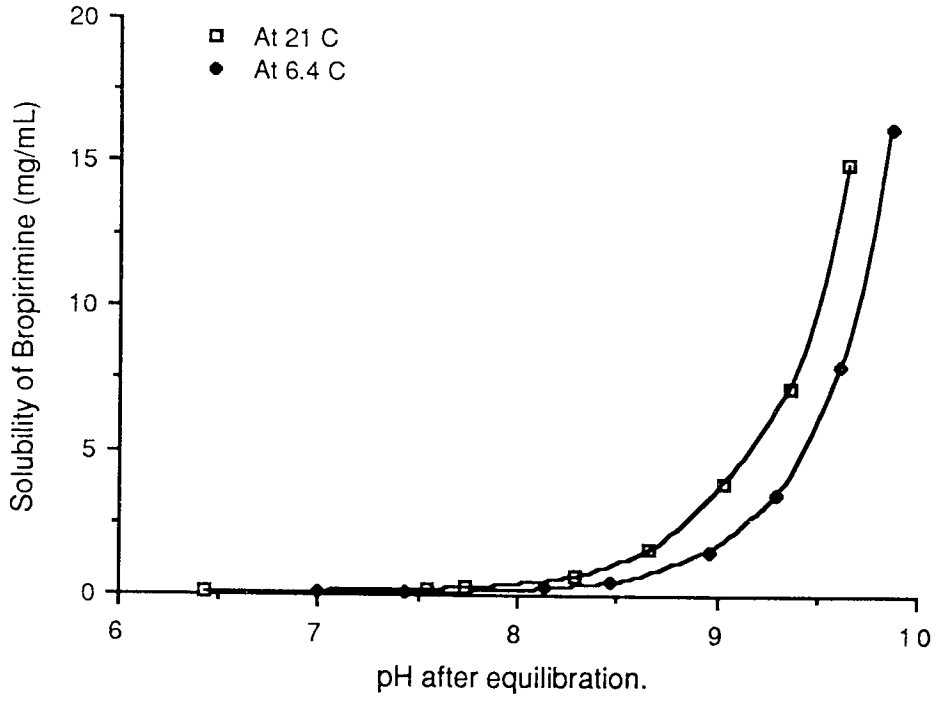

Fig. 7.11: Effect of formulation pH (vehicle A) on the solubility of bropirimine at two temperatures

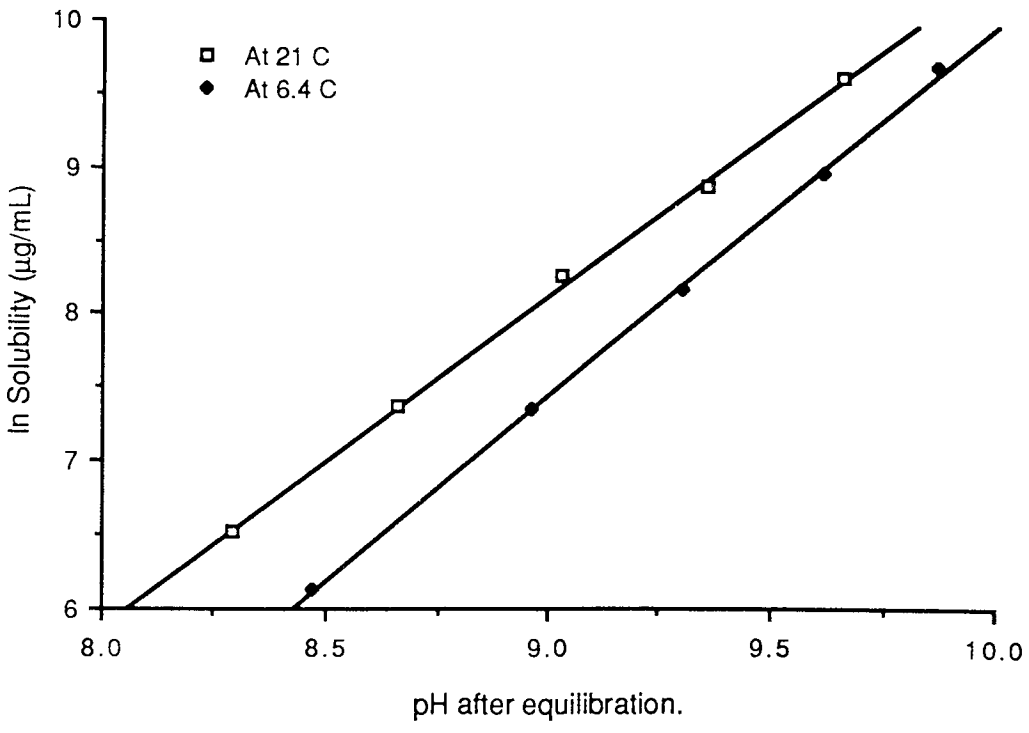

Fig.7.12: Effect of formulation pH (vehicle A) on the solubility of bropirimine at different temperatures

concentrations of bropirimine below the straight line should always stay in solution above that temperature. It is suggested that for co-solvent dependent formulations, the concentration should be at least 20% below saturation (in that particular formulation) to account for either a drop in temperature or dilution of the formulation[256].

Using an infusion flow rate of 30mL/min, Yalkowsky demonstrated that when diazepam was injected into a flow of either 5% dextrose or normal saline, precipitation of the drug occurred at an injection rate of 2mL/min (dilution factor of 15)[249]. This is because formulation of diazepam is co-solvent dependent and no pH control is necessary. Fig. 7.13(c and d) shows precipitation of diazepam on injection at an injection rate of 400mL/min using a 5% dextrose solution. Similar behaviour is observed when Tris buffer was used. Phenytoin injection is formulated using the same co-solvent compositions as diazepam injection (10% ethanol, 40% propylene glycol) but in addition phenytoin also requires strict pH control (≥11.5). It has an aqueous solubility of approximately 16μg/mL based on a solution pH of 4.9 or less at which the drug is calculated to be ≤0.04% ionised and 99.6% ionised at pH≥11.7[253]. Bropirimine having a pK_a of 8.21 (Chapter 5) will behave similarly to phenytoin (pK_a 8.3) with regards to ionisation. Phenytoin appears to be much more sensitive to pH changes than bropirimine and rapid precipitation results when the pH is reduced to below 11.7[236]. Fig. 7.13(B) shows phenytoin precipitation in dextrose solution when injected at a rate of ≥0.24 mL/min at an infusion rate of 400mL/min (dilution factor of 27.8). The resultant solution had a pH of 10.2. Extreme care must therefore be exercised in injecting phenytoin very slowly.

Where a formulation is co-solvent dependent, then precipitation on injection may be explained from the following:

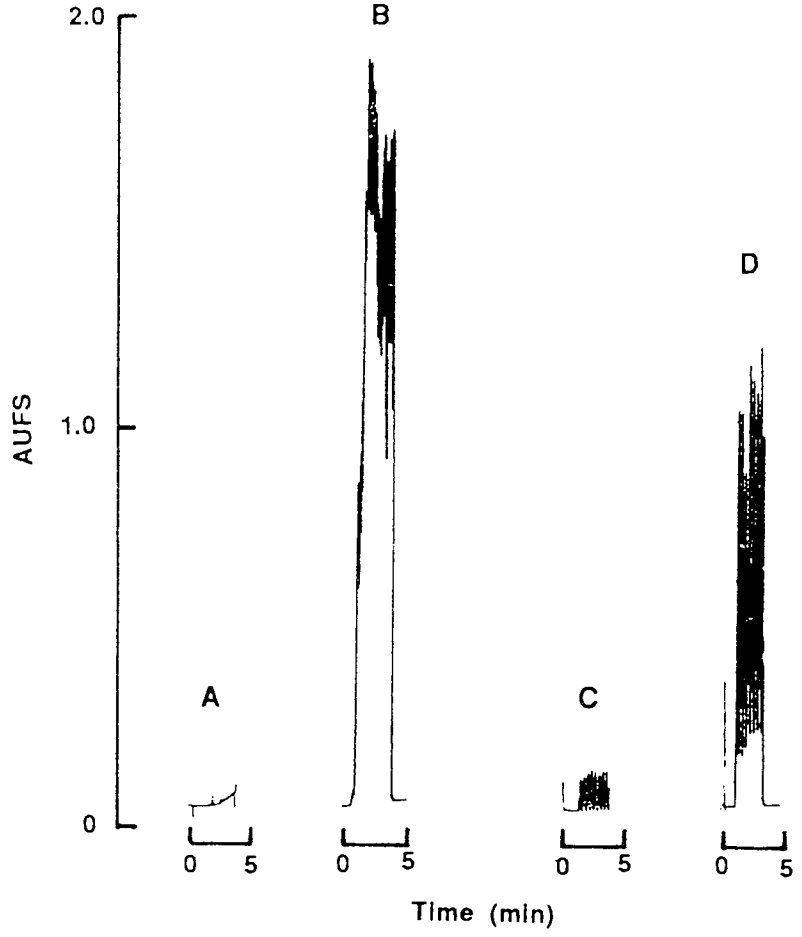

Fig. 7.13: The effect of phenytoin and diazepam injections on precipitation
(A) 0.1 mL/min phenytoin *(B) 0.24 mL/min phenytoin*
(C) 0.51 mL/min diazepam *(D) 1.0 mL/min diazepam*
Conditions: flow rate: 400 mL/hr
chart speed: 2 mm/min
λ: 700 nm

1. On injection of such a formulation, dilution takes place, may it be infusion fluid or blood. The concentration of the drug and the co-solvent decrease proportionally to one another[254].
2. The solubility of the drug in the mixed solvent decreases exponentially as the concentration of the co-solvent is decreased linearly (Chapter 5)[245].

As mentioned above, in order to demonstrate precipitation on injection, buffering capacity must be maintained during each experiment. In order to simulate injection into the blood stream, the buffering capacity of the mobile phase (infusion fluid) must be at least 18mEq/ΔpH at pH 7.4. Fig. 7.14 shows the effect of an injection rate of various solutions containing 10mg/mL bropirimine on the pH change of Tris double strength buffer (0.4M) at an infusion flow rate of 400mL/hr. Also shown are the diazepam and phenytoin formulations.

Formulation 1	'Valium 10"	
Formulation 2	DMA	50%$^{v}/_{v}$
	0.2M sodium carbonate to	100&$^{v}/_{v}$
Formulation 3	DMA	50%$^{v}/_{v}$
	Meglumine	2.5%$^{v}/_{v}$
	Distilled water to	100%$^{v}/_{v}$
Formulation 4	"Epanutin Ready Mixed Parenteral"	
Formulation 5	Meglumine	5%$^{v}/_{v}$
	0.2M sodium carbonate to	100%$^{v}/_{v}$

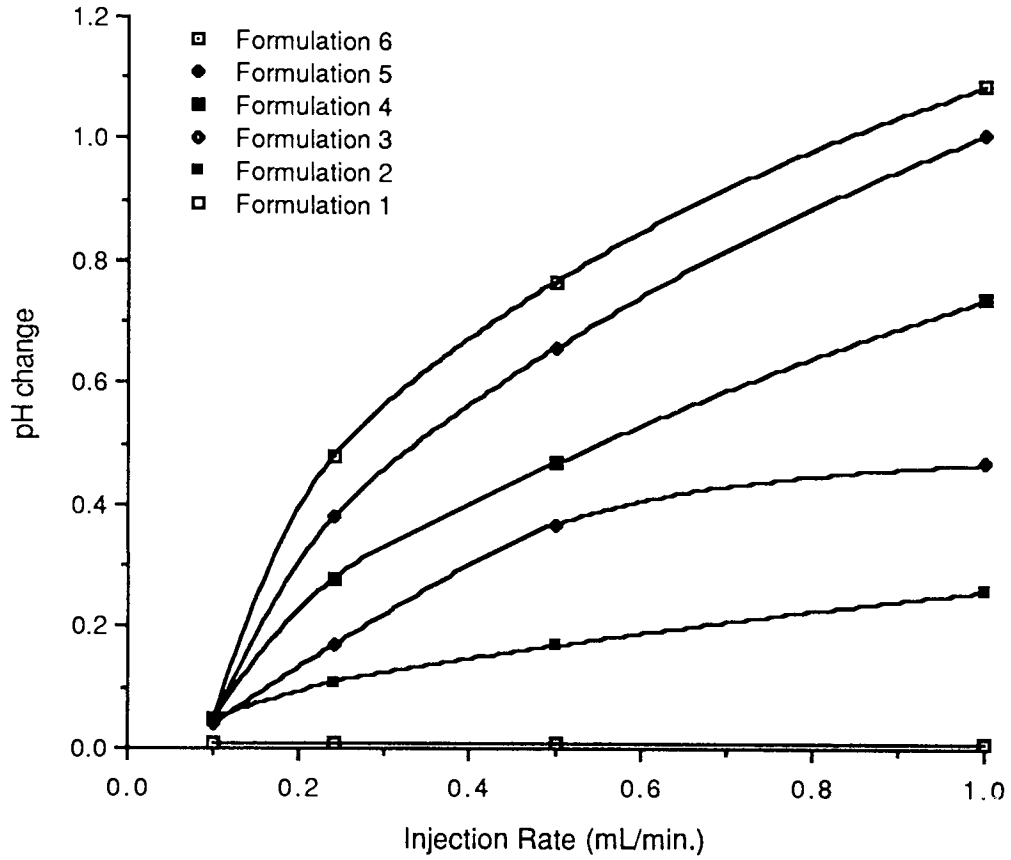

Fig. 7.14: The effect of injection rate on the pH change of Tris double strength buffer by several formulations

Formulation 6	DMA	10%$^{v}/_{v}$
	Meglumine	5%$^{v}/_{v}$
	0.2M sodium carbonate to	100%$^{v}/_{v}$

This experiment gives an indication of the strength of the buffer needed to maintain the desired pH. In all instances, except for formulation 6 at an injection rate of 1mL/min, buffering capacity was maintained with Tris double strength buffer.

In conclusion, *in-vitro* testing of formulations is possible provided the experimental conditions are well controlled, e.g. buffering capacity. By using slow injection rates (<0.24mL/min) or high infusion rates (>400mL/hr), precipitation of bropirimine can be minimised. Furthermore, as an added precaution, it is advisable to maintain the dose of a co-solvent dependent drug to at least 20% below the saturation limit[256].

8.0 THE SUPPOSITORY AS A DOSAGE FORM FOR BROPIRIMINE

8.1 Introduction

Suppositories are medicated solid dosage forms generally used in the rectum, vagina and, to a lesser extent, the urethra[257]. They can either exert a direct action on the rectum (e.g. for the relief of haemorrhoids), to produce evacuation of the bowel (e.g. glycerine suppositories) or to provide systemic effect[258]. They have a number of advantages over the oral route:

1. By-passing portal circulation and thus reducing possible 'first-pass effect' degradation[259-261].

2. Drugs that cause irritation to the gastric mucosa may be given via this route e.g. aminophylline.

3. They may be administered to subjects who will not or cannot swallow, e.g. infants.

4. Useful for patients who are unconcious or mentally disturbed.

5. In certain instances, the duration of action via the rectal route may be prolonged[260].

Disadvantages include the limited knowledge of mechanism(s) of absorption from the rectum and poor patient acceptability/compliance, especially in Britain[262]. The bioavailability and the problems associated with the retention of the suppository in the correct position may also be contributory factors.

8.1.1 Rectal Anatomy

Fig. 8.1 shows a section of the human rectum with emphasis on the venous drainage. The upper part of the rectal submucosa is fed by the superior haemorrhoidal vein which empties into the portal vein, whereas the lower part is fed by veins which lead to the inferior vena cava. Hence drugs given in enemas will be subject to possible microsomal metabolism whereas careful insertion of suppositories may either prevent or reduce 'first-pass' metabolism[260,263].

The rectal epitheluim is predominantly columnar or cuboidal with numerous globlet cells, and because villi are absent the surface area of the rectum is only 200-400cm^2. This contrasts with the absorbing area of the small intestine which is approximately 2,000,000cm^2[263]. The water content of the rectum is low and in the region of 2 to 3mL in adults, present as mucous of relatively high viscosity[263]. The high viscosity will, to some extent, retard the diffusion of drug molecules.

8.1.2 Factors affecting rectal absorption

The suppository is a complex dosage form. The absorption process is not only affected by the pharamaceutical properties of the suppository and the drug substance, but also on the physiological nature of the rectal environment. It is not the aim of this work to discuss each step involved in the rectal delivery of drugs. However, in order to appreciate the complexity of the whole process and to simplify matters, a list of factors that are involved are given in Table 8.1.

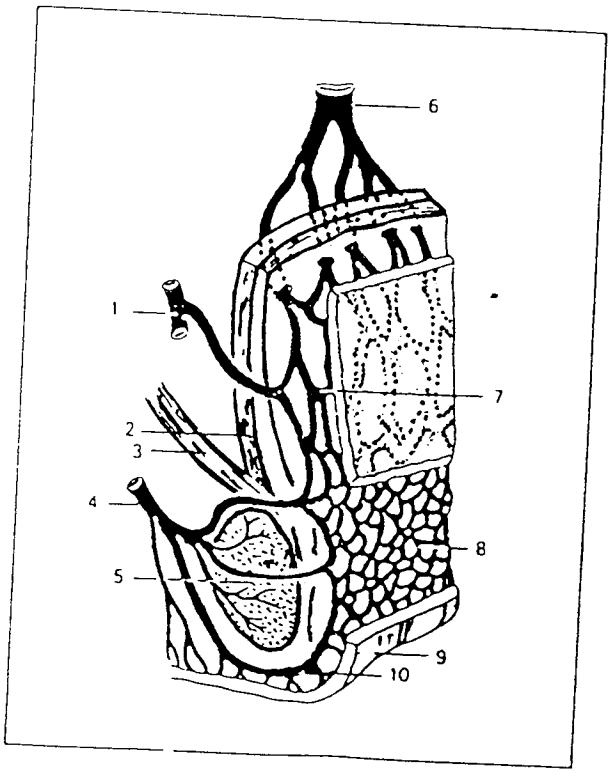

Fig. 8.1: *Detailed diagram of the venous drainage of the human rectum.*
1. Middle rectum vein
2. Tunica musculanis, stratum longitudinale
3. M. Levator ani
4. Inferior rectal vein
5. M. sphincter ani externus
6. Superior rectal vein
7. and 8. Plexus venosus rectalis (submucosus)
9. Skin
10. V. margianlis with Plexus subcutanous

Rectal fluid	Drug substance	Vehicle
Amount	Solubility	Composition
pH	pk_a	Fusion behaviour
Buffer capacity	Drug concentration	Rheological behaviour
Surface tension	Particle size	
Viscosity	Surface properties	
Luminal pressure		

Table 8.1: Factors influencing drug availability from suppositories [Adapted from (264,265)]

8.1.3 Aim

The aim of the work here was to establish whether it is possible to administer bropirimine rectally in the form of a suppository. The bases (Suppocire L, Witepsol H15 and polyethylene glycol) were chosen because of their common use. Since there are complex processes occuring in the rectum (Table 8.1), it is extremely important to establish the viability of the dosage form *in-vitro*. Hence considerable emphasis will be placed on *in-vitro* study. Some *in-vivo* work was carried out to complement the *in-vitro* experiments.

8.2 Materials and methods

The excipients PEG 1000 (BDH), PEG 4000 (BDH), Witepsol H15 (Brome and Schimmer), Suppocire L (Gattefosse), N,N-dimethylacetamide (Fisons), meglumine (Sigma), sodium lauryl sulphate (BDH) (0.01%$^{w}/_{w}$,

1.0%$^{w}/_{w}$), Tween 80 (BDH) (0.2%$^{w}/_{w}$, 0.4%$^{w}/_{w}$) were used as received. The Britton-Robinson buffers (2.0, 7.0, and 11.2) were prepared as described in Appendix I.

8.2.1 Preparation of suppositories

All the suppositories were prepared by the fusion method[258]. The displacement values were calculated as shown below[258]:

1. Six suppositories containing the base only were prepared and weighed (= a mg).

2. Six suppositories containing the medicament were prepared and weighed (= b mg).

3. Amount of the base used in Step 2 (= c mg).

Hence a - c mg = the amount of base displaced by d mg of medicament.

$$\text{Displacement value, DV} = \frac{d}{a - c}$$

Hence using bropirimine, the DV for PEG (96%$^{w}/_{w}$ PEG 1000 : 4%$^{w}/_{w}$ PEG 4000), Witepsol H15 and Suppocire L were calculated as 1.7544, 1.2500 and 0.6849 respectively. In each instance, to account for wastage, the amount of the drug and the base were calculated and weighed for two extra suppositories.

By using the DV values, sufficient amount of the base was accurately weighed and placed in a small stainless steel evaporating basin. This was gently heated using a water bath so that the base just melted. A small amount of this melt was then added to the powdered

bropirimine (particles passing through a 180μm sieve but retained on a 90μm sieve were used) on a porcelain tile, quickly levigated with a spatula to form a homogeneous dispersion and transferred back to the basin. The whole content was then mixed using sufficient heat to melt the mass whenever necessary. The mixture was continuously stirred in order to minimise sedimentation of the powdered drug particles and poured into a stainless steel mould (6x1g size) once it began to congeal. Each of the mould cavities was overfilled, to take into consideration contraction of the base on cooling, and then left to congeal further.

Once cool, the excess mass was removed using a warm spatula. These were then left for a further 10-15 minutes and then finally removed by unscrewing the two halves of the mould and gently pushing the suppositories out one at a time.

8.2.2 *In-vitro* dissolution testing of suppositories

A Caleva Model 7ST continuous flow dissolution apparatus was used in conjunction with a LKB Ultraspec II ultraviolet spectrometer mounted with eight 1cm path length flow cells, enabling continuous monitoring of the dissolution media in all the six dissolution vessels. This was interfaced with an IBM personal computer, using the software provided by LKB, and the output recorded on an Epson LX-800 printer. The liquid was pumped through the system using a Watson-Marlow peristaltic pump (10mL/min). The paddles were set in accordance with the USP II assembly using the plastic pieces provided to set the distances from the base of the dissolution vessels.

For each set of dissolution tests, the suppositories were gently dropped into 1L of the dissolution media pre-heated to 37°C ± 0.5°C and the system switched on at a pre-set rotational speed (50 rpm). The computer was appropriately programmed to start recording, by taking

into account the lag-time (the time for the test dissolution media to reach the flow cells), at fixed time intervals. Prior to each set of experiments, the system was equilibrated and suitably zeroed by circulating only the dissolution media. Using a 1 point calibration, a 100% solution (3μg/mL) was placed in one of the flow cells along with the dissolution media in a second cell. The computer then compared the values obtained from the dissolution test to the blank and the standard and displayed percent released against time plots as either individual curves or an average.

After each experiment, the system was thoroughly cleaned by flushing with warm water to remove any remaining residues from the fatty bases.

Unless otherwise stated, all the dissolution studies were performed using distilled water as the dissolution medium at 37°C ± 0.5°C.

Conditions	
Wavelength	: 300nm
Rotational speed	: 50rpm
Pump speed setting	: 7.0 (10mL/min)
Temperature	: 37°C ± 0.5°C
Suppository size	: 1g
Capacity of dissolution medium	: 1L

3 mg of bropirimine were incorporated into each suppository in order to achieve sink conditions (aqueous solubility = 35μg/mL).

8.2.3 *In-vivo* Testing of bropirimine suppositories

Male Dutch rabbits, weighing between 1.6kg to 4.1kg, were used for the *in-vivo* experiments. They were fasted overnight prior to all experiments but given free access to water.

Before the insertion of the suppository, blood was withdrawn from the anaesthetised (Halothane) rabbits by cardiac puncture to act as the blank and for the preparation of standards.

The suppository was inserted into the rectum at a distance of approximately 1cm from the anus and the anus firmly stitched to prevent any leakage of medicament. 1mL blood samples were withdrawn by puncturing the marginal ear vein, into heparinised [1000 units/mL mucous heparin sodium ("Multiparin"); Weddel] plastic vials at various time intervals. The samples were then spun down using a microfuge (10,000 rpm for 2 minutes) to obtain a clear, straw coloured plasma.

0.4mL of the plasma was transferred into a small glass centrifuge tube using a 1mL Gilson pipette. To this was added 0.5mL of methanol (Fisons), which was sufficient to denature any proteins in the plasma (apparent from the formation of precipitate upon the addition of methanol), and 0.1mL of a 10µg/mL solution of internal standard (ABmFPP) prepared in methanol. The content of the tube was thoroughly mixed using a Whirlmixer (Fisons) and centrifuged at 3500 rpm for 10 minutes (Starstedt LC1 centrifuge).

HPLC Conditions

Mobile phase	:	25%v/v acetonitrile
		0.1%v/v diethylamine
		adjusted to pH 2.0 using orthophosphoric acid
Flow rate	:	1mL/min
Chart speed	:	2mm/min
Wavelength	:	300nm
Sensitivity	:	0.01 - 0.02 AUFS

The calibration curve was prepared by fortifying plasma from rabbits with bropirimine to give concentration range between 1-5μg/mL using 0.1mL of a 10μg/mL solution of ABmFPP in 1 mL as the internal standard.

8.3 Results and discussion

Although the USP basket method (Method I) is the common and accepted method for suppository dissolution, one serious drawback was observed here which prevented its further use. When the fatty bases were used, less than 10% bropirimine release was observed after 1 hour. Closer inspection of the basket showed clogging of the mesh by the fatty bases which thus formed a physical barrier to the drug. No clogging was apparent with the water-soluble PEG bases. McElnay and Nicol[266], and to a lesser extent Zuber *et.al.*[267] observed similar behaviour and cautioned users of this method against the possibility of large variations in results due to clogging. Hence the basket method was replaced with the USP paddle method (Method II) in order to achieve a better comparison between the fatty and water-soluble bases.

The complexity of the dissolution process for a suppository may be appreciated by considering the various stages of dissolution. Table 8.1 lists

factors influencing availability of the drug from fatty suspension suppositories. Fig. 8.2 shows schematically the events following the insertion of a suppository and leading to dissolution[265].

Although the diagram is an oversimplification of the whole process, it highlights possible hurdles that may be encountered. It is important to bear in mind that suppository dissolution does not occur in individual steps but several processes may be involved simultaneously, e.g. it is possible for melting and absorption to take place at once. The same scheme may by used to explain events occuring *in-vitro*.

8.3.1 *In-vitro* dissolution testing of bropirimine suppositories

8.3.1.1 Effect of suppository base on the release of bropirimine

Fig. 8.3 shows the dissolution curves for suppositories prepared from either fatty bases (Witepsol H15, Suppocire L), or the water-soluble PEG base. A series of PEG bases exist having different nominal molecular weights such that the physical characteristics of the PEG suppositories may be varied by varying the amount of each in the mixture[258]. A mixture containing 96%$^{w}/_{w}$ PEG 1000 and 4%$^{w}/_{w}$ PEG 4000 has been shown to be a suitable combination, giving good release profiles[268,269] whilst having desirable rheological properties, in particular a linear relationship between the elastic moduli and the breaking strength[270,271]. This was then used as the water-soluble base for bropirimine suppositories.

The dissolution plots show percentage released against time under sink conditions. There is a striking difference between the three bases with Suppocire L and Witepsol H15 showing poor release of bropirimine compared to the rapid release from the PEG base. After 50 minutes the total amount released from the three bases was 35%, 43% and 87% for Suppocire L, Witepsol H15 and PEG 1M:4M respectively.

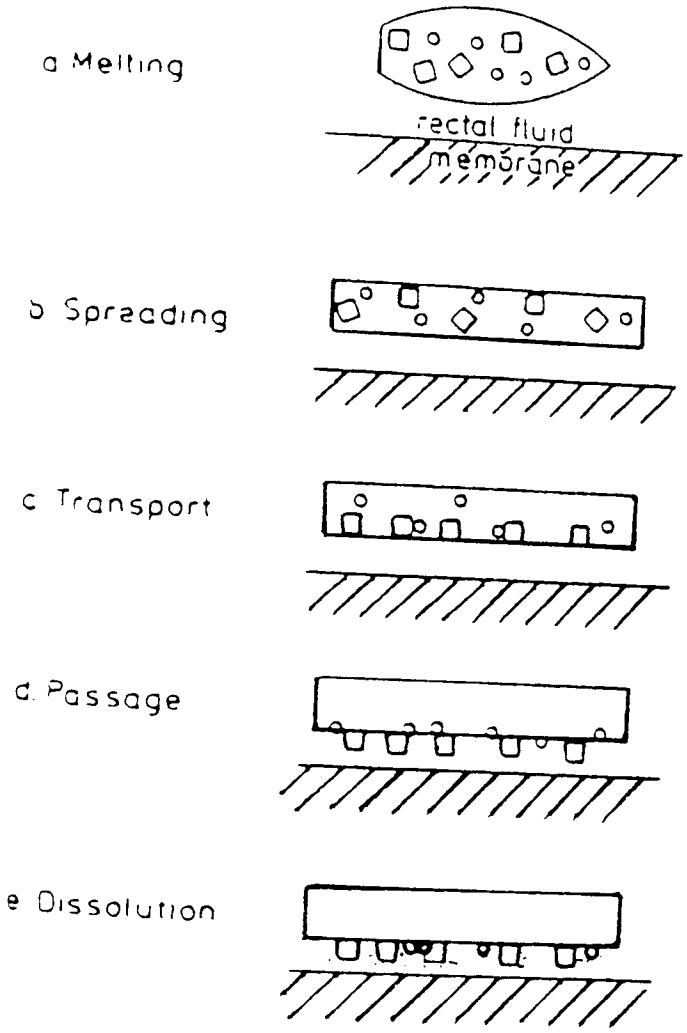

Fig. S 2: Processes involved in the release from fatty suspension suppositories [adapted from (265)]

The release rates, calculated from the linear portion of the graphs, were 0.78%/min (Suppocire L), 0.94%/min (Witepsol H15) and 7.98%/min (PEG 1M:4M).

After the initial non-linearity, zero order release of the drug is observed with the three bases, especially for the PEG 1M:4M base, consistent with observations made by other workers[272,273].

The PEG bases dissolve rapidly in water and therefore release the contents quickly by exposing more of the bropirimine particles to the dissolution medium. However, PEG bases have also been known to form soluble complexes, as observed by Higuchi and Lach[274] and Corrigon and Timoney[225], but no evidence was found that supported this theory with regard to bropirimine (Chapter 5).

The fatty bases do not dissolve but melt and form a ball. The incorporated drug will not, therefore, be exposed to the dissolution medium as rapidly as the PEG bases. Increased partition coefficient of bropirimine between the fatty bases and water may also contribute to the low release rate[273,275], although this parameter was not measured. As an example, Iwaoku *et.al*. showed that phenobarbital (partition coefficient of 4.44 in chloroform:water), structurally similar to bropirimine, had higher release rates in Witepsol H15 than with a base consiting of a 3:1 mixture of PEG 1M:4M[276]. No attempt was made to estimate the partition coefficient of phenobarbital between the base and the dissolution medium (normal saline).

Because the PEG 1M:4M base gave very high dissolution rates, Witepsol H15 was used in the proceeding experiments to assess if various additives or hydrodynamics of the system have any influence over the release rate of bropirimine.

8.3.1.2 The effect of stirring speed on the release of bropirimine

Fig. 8.4 shows the plots of percentage released against time by varying stirring speeds (W). Any type of agitation promotes dissolution by reducing the thickness of the boundary layer around the dissolving solid and thus facilitating greater diffusion of the dissolved solute into the bulk of the dissolution medium.

For any relationship to exist between the stirring speed and rate of release of a solute, it is important to have a good control of the hydrodynamics of the experiment[277]. Obtaining the rate constants from the linear portion of the graphs (Fig. 8.4), a plot of square root of stirring speed against release rate yields a straight line ($r = 0.951$) indicating a linear relationship (Fig. 8.5) for speeds up to 150rpm. When the total amount released after 50 minutes was plotted against stirring speed, a 'tailing off' effect is observed showing that total amount released (at $t = 50$ minutes) becomes independant of agitation at higher speeds (Fig. 8.6). The release rate at zero agitation may be estimated by extrapolation of the straight line in Fig. 8.5. For suppositories containing 3mg per suppository of bropirimine using Witepsol H15 as the base, this value was equal to 0.61%/min.

8.3.1.3 The effect of surfactants on the release of bropirimine

Fig. 8.7 shows the effect of an anionic surfactant (sodium lauryl sulphate, SLS) and a non-ionic surfactant [Tween 80 : polysorbate 80 : polyoxyethylene(20) sorbitan monooleate] on the release of bropirimine from suppositories prepared using Witepsol H15 as the base.

Surfactants exert their solubilising effect by wetting and by forming aggregates called micelles, the shape of which are dictated by the type of surfactant used and its concentration[278].

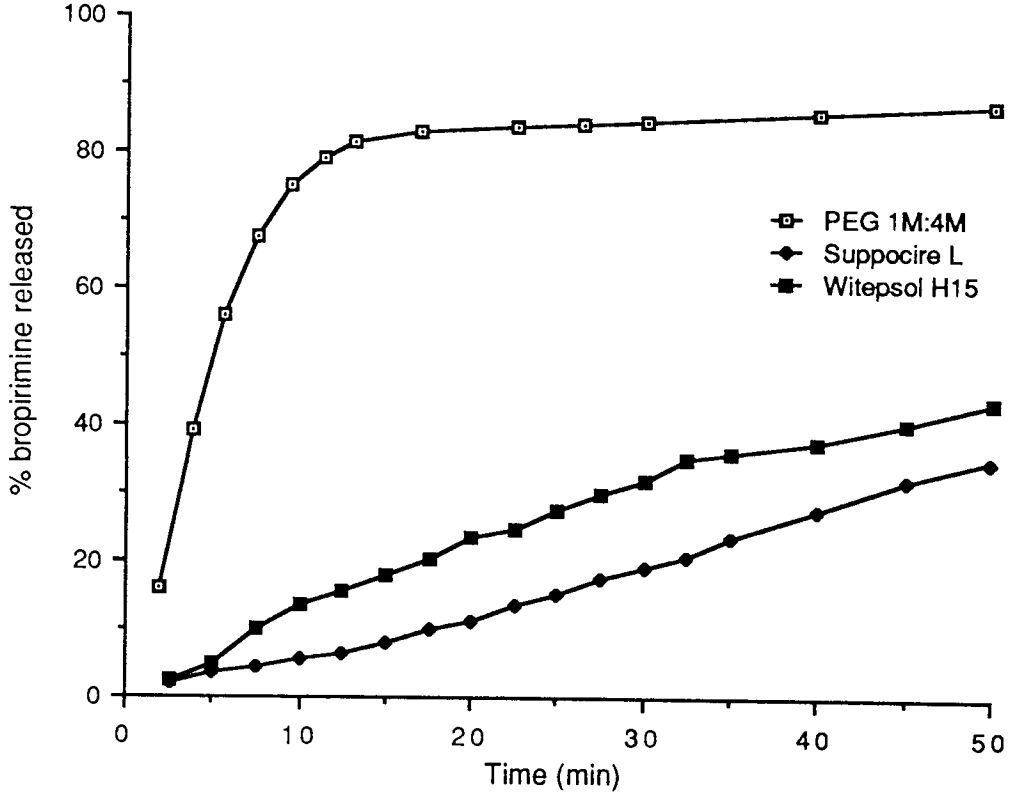

Fig. 8.3: Release of bropirimine from different suppository bases in distilled water at 37°C

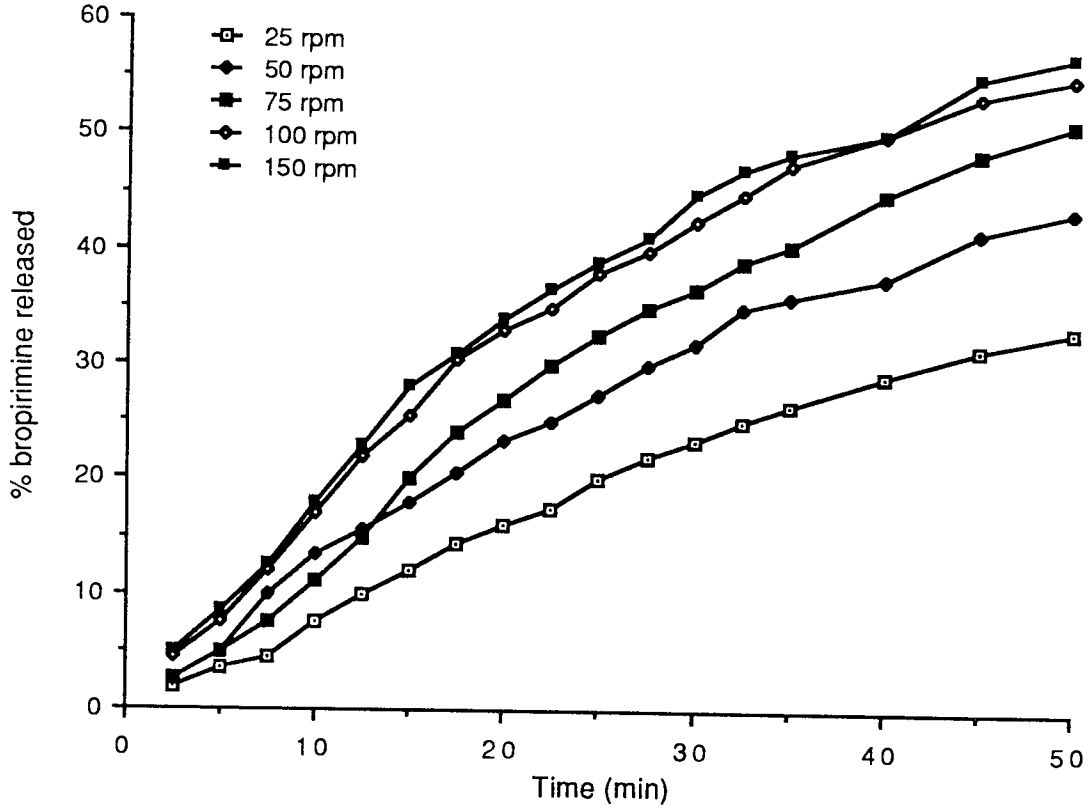

Fig. 8.4: The effect of stirring speed on the release of bropirimine in distilled water at 37°C using Witepsol H15 as the base

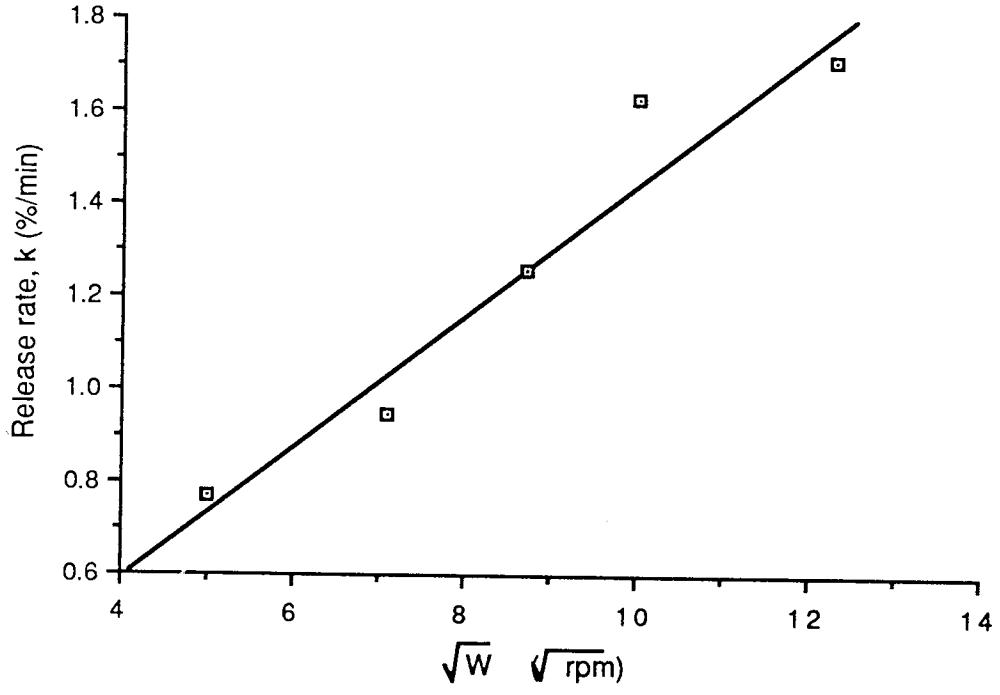

Fig. 8.5: A plot to show the linear relationship between the release rate and the stirring speed

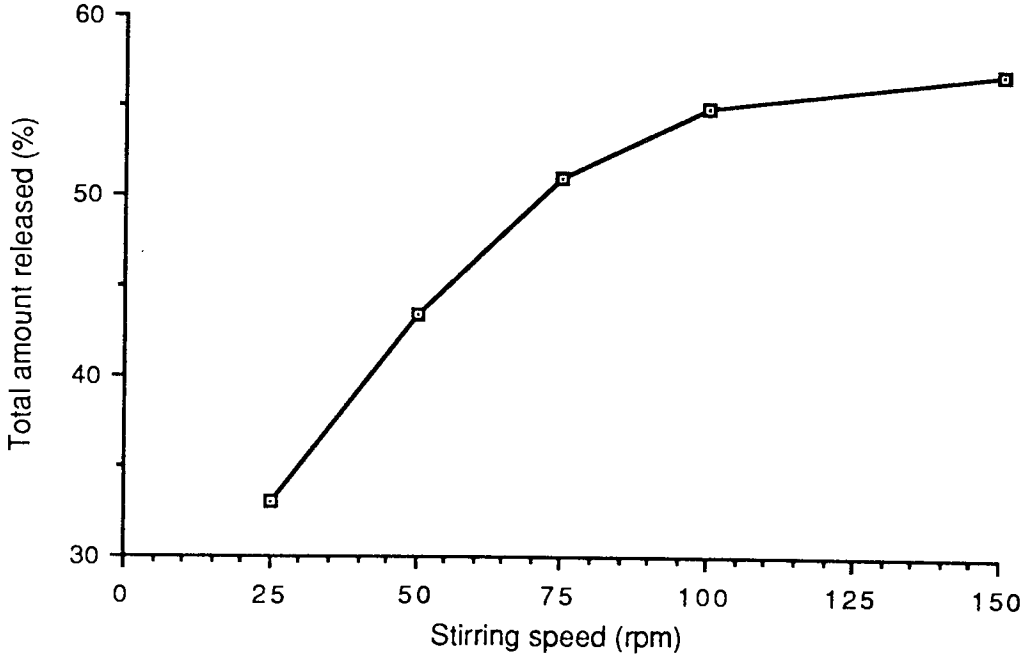

Fig. 8.6: A plot of total amount of bropirimine released after 50 minutes against stirring speed

SLS consists of a mixture of sodium alkylsulphate with predominantly sodium dodecyl sulphate [$C_{12}H_{25}SO_4^-N_a^+$] which has a critical micelle concentration (CMC) of 0.23%$^w/_v$ at 25°C. At concentrations either below or above the CMC, SLS shows slight enhancement of the initial dissolution rate although no great increase in the total amount released after 50 minutes was observed over Witepsol H15 alone. This increase in the initial dissolution rate may be as a result of increased wetting which can bring about earlier peak maxima for certain compounds *in-vivo*[279].

Increasing the concentration of the non-ionic surfactant Tween 80 (HLB = 15.0) leads to a decreased release of bropirimine from the suppositories. This behaviour is not altogether uncommon and has been observed both *in-vivo* and *in-vitro*. Riegelman and Crowell[280] described in their report that the rectal absorption of triiodophenol was retarded by surfactants *viz* SLS and Tween 20, but failed to elucidate the cause of this retardation. Kakemi *et.al.*[281], using Tween 80, also showed that there was poor rectal absorption of sulphonamides and suggested that this may be due to the poor absorption of micelles due to their range size. A more plausible explanation for bropirimine is that the surfactant may affect the hydrophobic-hydrophilic character of the base[273] leading to a change in the partition coefficient of the drug between the base and the dissolution media. An increased suppository base/water partition coefficient would therefore result in low release and poor subsequent bioavailability[273].

8.3.1.4 Effect of pH of the dissolution media on the release of bropirimine

In order to establish the release profiles at different pH values, the distilled water was replaced with Britton-Robinson buffers pH 2.0,

7.0 and 11.2 (Appendix I) having a molar strength of 0.5M. The results are shown in Fig. 8.8. A rank order for the dissolution rates is obtained and is in the order pH 11.2 (3.33%/min) > pH 2.0 (2.8%/min) > pH 7.0 (1.04%/min) > distilled water (0.95%/min).

Bropirimine, being an amphoteric compound, can ionise in both acidic and basic media. The acidic portion of the molecule has a greater effect on the solubility than the basic part and hence the rates show a consistency with the pH-solubility plot (Chapter 5) i.e. the rate of release of bropirimine at different pH values will follow the same shape as the pH-solubility profile passing through a minimum in the neutral region. Solubility of bropirimine in these buffers was calculated as 134.50μg/mL (pH 2.0), 35.14μg/mL (pH 7.0) and 3.24mg/mL (pH 11.4) from Chapter 5. The P_{app} values were estimated as 11.2, 68.6 and 0.4 respectively.

8.3.1.5 Effect of meglumine on the release of bropirimine

Fig. 8.9 shows the release of bropirimine with variation in meglumine concentration in the suppository using Witepsol H15 as the base at 37°C in distilled water at a stirring speed of 50rpm. As the concentration of meglumine increases, both the rate of release and the total amount released after 50 minutes are seen to increase. At approximately 5%$^{w}/_{w}$ meglumine in the suppository, saturation appears to have been reached as reflected in Fig. 8.10 where 'tailing-off' effect is observed for a semi-logarithmic plot of release rate against meglumine concentration. More than 95% of bropirimine is released at a concentration of 5%$^{w}/_{w}$ of meglumine (k = 7.5%/min) compared to 0.1%$^{w}/_{w}$ meglumine where 49% of bropirimine is released (k = 1.63%/min) and Witepsol H15 alone with approximately 42% release (k = 0.95%/min) in the same time (t = 50 minutes). Although the increase

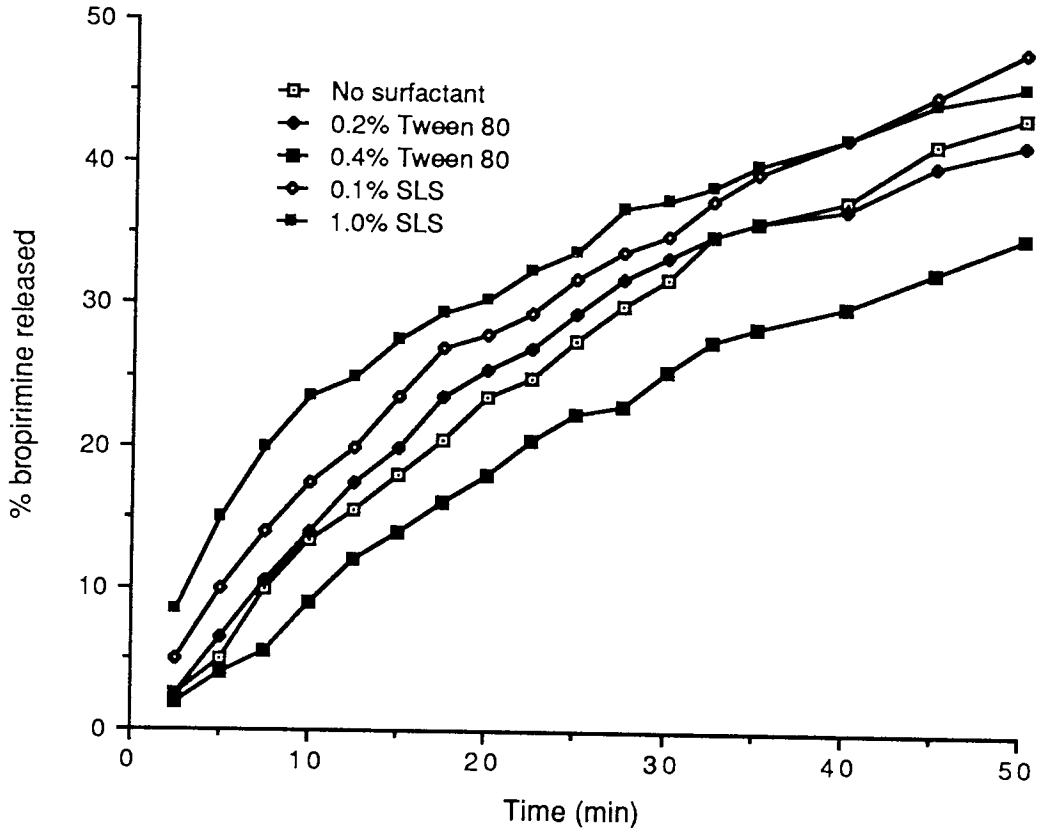

Fig. 8.7: The effect of surfactants on the release of bropirimine in distilled water at 37°C (50 rpm)

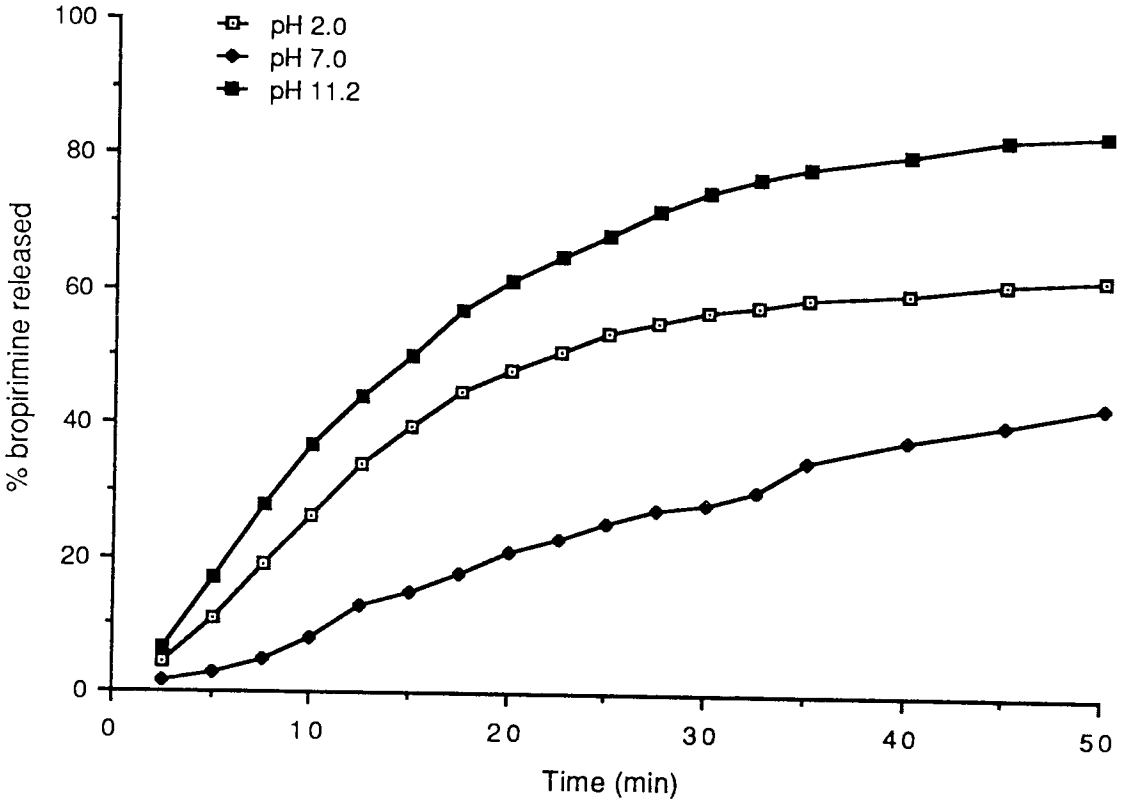

Fig. 8.8: The effect of pH on the release of bropirimine in Britton-Robinson buffers at 37°C (50 rpm)

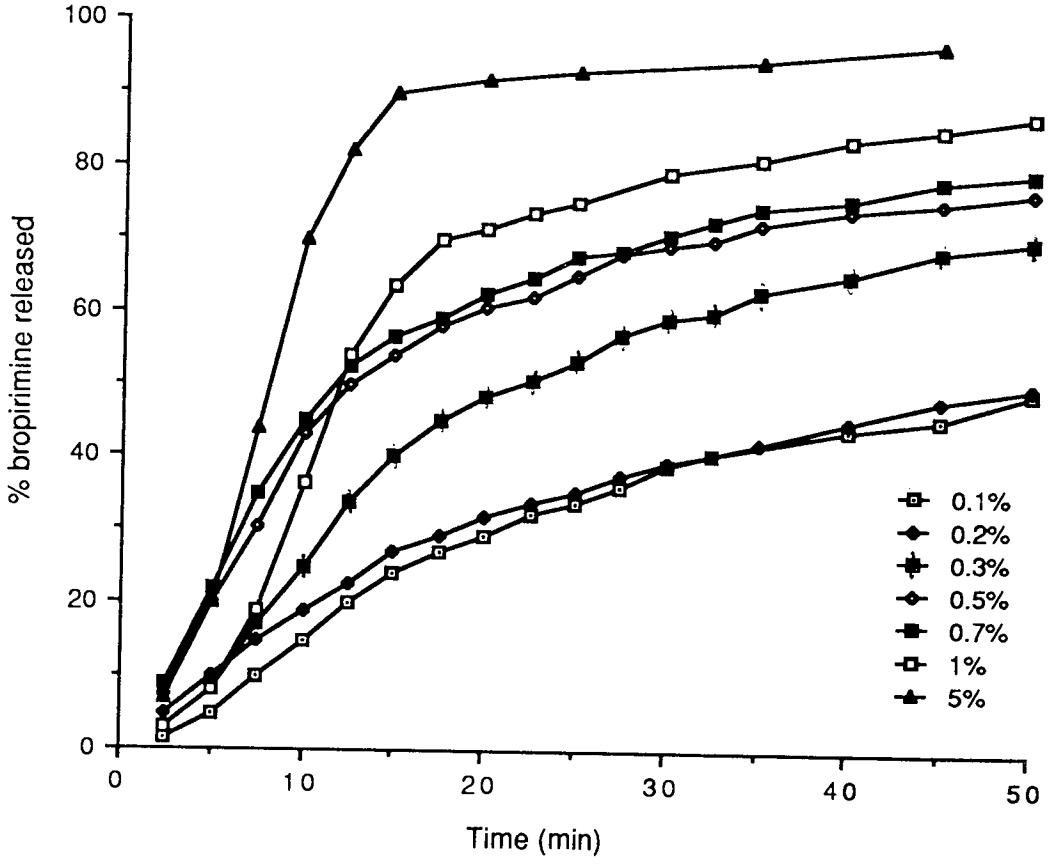

Fig. 8.9: The effect of meglumine in the suppository on the release of bropirimine in distilled water at 37°C (50 rpm)

in the release rate may be due to counter ion effect, pH will also have an effect since meglumine dissolved in water forms a basic solution.

Suppositories containing 0.2%$^{w}/_{w}$ meglumine increased the pH of the dissolution medium (distilled water) from 5.6 (0.25% ionised) to 6.3 (1.2% ionised) in 50 minutes, whereas the 5%$^{w}/_{w}$ meglumine formulation increased the pH to 9.30 (92.5% ionised). Hence the increase in pH leads to increased ionisation of bropirimine and therefore a subsequent increase in solubility in that particular medium.

8.3.2 *In-Vivo* testing of bropirimine suppositories.

The *in-vivo* testing procedures, carried out on male Dutch rabbits, were described in Section 8.2.3. Reproducibility studies were carried out using six replicate analyses of plasma samples which had been spiked such that the concentrations were 2μg/mL and 10μg/mL. The coefficient of variations for recovery of bropirimine were calculated as 6.1% and 3.1% respectively.

Using the conditions and mobile phase described in Section 8.2.3, levels of bropirimine as low as 0.5μg/mL could be detected.

Tables 8.2, 8.3 and 8.4 show the pharmacokinetic data for four rabbits using PEG 1M:4M, Suppocire L and Witepsol H15 respectively at a dose of 90mg/kg of rabbit.

The substantial variation amongst the data for each rabbit means that the three formulations, incorporating three different bases, cannot be readily compared. Several reasons exist for the discrepancies. The rabbits used varied in weight from 1.6kg to 4.1kg and so the biological variation is expected to be high. 1g suppositories were used in each instance and insertion into the same space in the rectum would be impossible. Uptake of bropirimine into the lymphatic system may also play a role.

Since the *in-vitro* experiments show that drug delivery via a suppository is viable, it is plausible to suggest that with careful design of *in-vivo* experiments, this route of administration may be better utilized and the results made more meaningful. Due to the lack of time and resources, this part of the work could not be brought to conclusion.

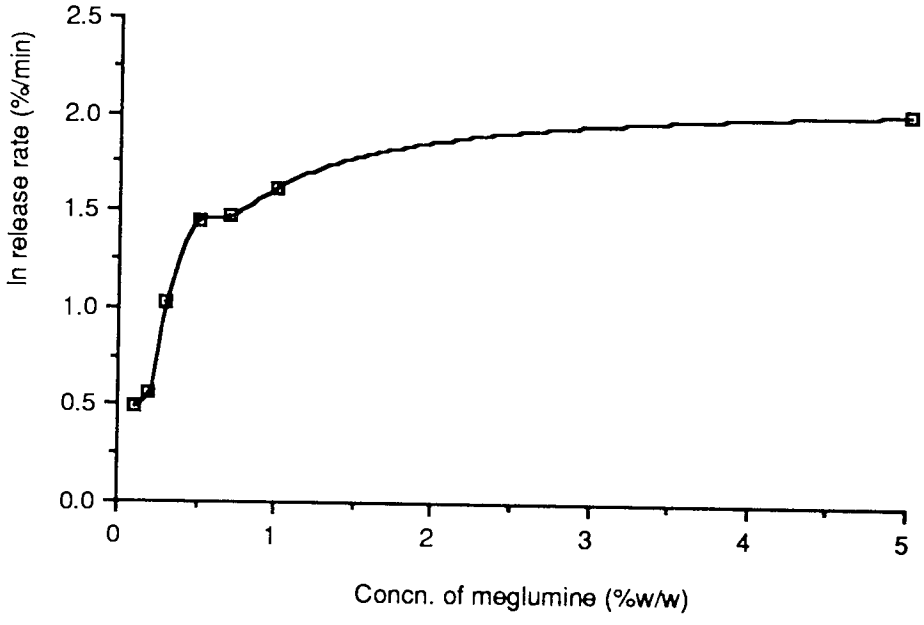

Fig. 8.10: A plot of release rate against concentration of meglumine in the suppository

R	k_{abs}	k_{el}	V	AUC	$t^{ab}_{1/2}$	$t^{el}_{1/2}$	t_{max}	C_{max}	r
1	0.00049	0.04624	0.4408	4416.0	1414.7	14.99	99.4	2.06	0.557
2	0.001228	0.005706	3.447	4576.0	564.3	121.50	343.0	3.69	0.765
3	0.000818	0.3914	0.1671	1376.3	846.9	1.77	15.8	1.11	0.595
4	0.008038	0.008106	4.615	2406.0	86.2	85.50	123.9	7.14	0.833

R - Rabbit

k_{el} - Elimination rate constant

AUC - Area under the curve

$t^{el}_{1/2}$ - Elimination half-life

C_{max} - Maximum concentration

k_{abs} - Absorption rate constant

V - Volume of distribution

$t^{ab}_{1/2}$ - Elimination half-life

t_{max} - Time to reach maximum concentration

r - Correlation coefficient

Table 8.2: Pharmacokinetic parameters of rabbits 1, 2, 3 and 4 using 90 mg/kg bropirimine and PEG 1M:4M as the suppository base

R	k_{abs}	k_{el}	V	AUC	$t^{ab}_{1/2}$	$t^{el}_{1/2}$	t_{max}	C_{max}	r
1	0.003766	0.3001	0.7527	398.40	184.00	2.310	14.77	1.419	0.853
2	0.01976	0.4024	1.0539	212.23	35.08	1.723	7.88	3.590	0.830
3	0.003031	0.05336	3.615	466.56	228.70	12.990	56.99	1.190	0.934
4	0.007791	0.02278	8.1518	484.60	88.97	30.420	71.57	2.160	0.822

R - Rabbit

k_{el} - Elimination rate constant

AUC - Area under the curve

$t^{el}_{1/2}$ - Elimination half-life

C_{max} - Maximum concentration

k_{abs} - Absorption rate constant

V - Volume of distribution

$t^{ab}_{1/2}$ - Elimination half-life

t_{max} - Time to reach maximum concentration

r - Correlation coefficient

Table 8.3: Pharmacokinetic parameters of rabbits 1, 2, 3 and 4 using 90 mg/kg bropirimine and Suppocire L as the suppository base

R	k_{abs}	k_{el}	V	AUC	$t^{ab}_{1/2}$	$t^{el}_{1/2}$	t_{max}	C_{max}	r
1	0.000627	0.4997	0.1213	1485.08	1104.67	1.387	13.39	0.924	0.312
2	0.000489	0.1042	0.8294	1041.37	1416.94	6.652	51.70	0.497	0.195
3	0.007093	0.01152	42.7150	182.92	97.73	60.180	109.56	0.596	0.874
4	0.004279	0.005244	14.2900	1201.34	162.00	132.170	210.74	2.090	0.766

R - Rabbit

k_{el} - Elimination rate constant

AUC - Area under the curve

$t^{el}_{1/2}$ - Elimination half-life

C_{max} - Maximum concentration

k_{abs} - Absorption rate constant

V - Volume of distribution

$t^{ab}_{1/2}$ - Elimination half-life

t_{max} - Time to reach maximum concentration

r - Correlation coefficient

Table 8.4: Pharmacokinetic parameters of rabbits 1, 2, 3 and 4 using 90 mg/kg bropirimine and Witepsol H15 as the suppository base

9.0 CONCLUSION

A study of the stability and the physico-chemical properties of the pyrimidine based immunomodulatory drugs bropirimine and its 2-N-acetyl- and 2,N-propanoyl-derivatives and the 2/4- (2-N-propanoyl- and 2,4-N,N-dipropanoyl pyrimethamine) and 6-carboxylate analogues (methyl-, ethyl-, propyl- and isopropyl esters) of pyrimethamine was presented.

Reversed-phase high-performance liquid chromatography (HPLC) was used as the method of assay for all the drugs. The mobile phase consisted of mixtures of acetonitrile/0.1%$^{v}/_{v}$ diethylamine adjusted to pH 2.0 with orthophosphoric acid. By varying the composition of the acetonitrile only (25%$^{v}/_{v}$ - 55%$^{v}/_{v}$) adequate separation of each class of compounds was affected.

Stability studies indicated that bropirimine is a very stable entity. The derivatives of both bropirimine and pyrimethamine were not sufficiently thermo- or pH-labile to be considered as potential prodrugs. In each case the derivatives became increasingly stable as the series progressed.

Differential scanning calorimetry (DSC) of bropirimine indicated incompatibility, namely debromination, with a number of excipients commonly used in formulation work, although the temperature at which this occurs (>200°C) is unlikely to cause formulation or manufacturing problems. Also described here is a method for accelerated stability testing of drugs by variable heating rates using the DSC. Provided the experimental variables, e.g sample weight, particle size, etc., are well controlled then there is a good possibility of obtaining accurate results from this method.

Poor aqueous solubility was exhibited by both bropirimine and the pyrimethamine derivatives. The values of the dissociation constants (K_a) were calculated from the solubility-pH profiles. Bropirimine was found to have a biphasic solubility-pH profile and hence two pK_a values (2.52 and 8.21).

The poor aqueous solubility of bropirimine (~35μg/mL) meant that formulation problems would arise. The approach of prodrug synthesis and solvate formation [acetic acid, N,N-dimethylacetamide (DMA) and N-methylformamide (NMF) solvates] proved fruitless. However, by using co-solvents and additives, the aqueous solubility was considerably increased such that using a system consisting of 10%$^{v}/_{v}$DMA/5%$^{w}/_{v}$ meglumine in 0.2M sodium carbonate, 32mg/mL of bropirimine were solubilised which represented an almost 1000-fold increase in solubility. This formulation, hence, incorporates sufficient bropirimine for any clinical work to be undertaken. One year stability study of this formulation showed no evidence of degradation. Intrinsic dissolution testing of bropirimine indicated the possibility of serious oral bioavailability problems, caused by low intrinsic dissolution rates.

Since the bropirimine formulation is heavily co-solvent/additive dependent, an *in-vitro* method was devised to test the possibility of precipitation on injection. When a buffer of sufficient buffering capacity (0.4M Tris) was used, precipitation resulted on injection. By utilising low injection rates and high mobile phase flow rates, precipitation was minimised.

The possibility of rectal delivery of bropirimine, using suppositories as the dosage form, was considered. *In-vitro* dissolution studies indicated that, using a mixture of 96%$^{w}/_{w}$ polyethylene glycol 1000 and 4%$^{w}/_{w}$ polyethylene glycol 4000 as the base, this method of drug delivery is viable, giving quick release of bropirimine (>80% in 15 minutes). Furthermore when 5%$^{w}/_{w}$ meglumine was added to the suppository base Witepsol H15, the total amount of bropirimine released after 50

minutes was doubled. However, *in-vivo* work on male Dutch rabbits gave inconclusive results with wide variation in data. By comparison with the *in-vitro* study, the results could be explained on the basis of inadequate technique rather than poor route of administration. Due to lack of time the *in-vivo* technique could not be perfected.

APPENDIX I

TABLE 2 (*)

pH	Britton Robinson Buffer *					KCl added per liter of buffer to produce an ionic strength of		
	Composition (g/l)				Ionic strength (M)			
	NaOH	CH_3CO_2H	H_3PO_4	H_3BO_3		0.1 M	0.5 M	1 M
1.81	0.000	2.402	3.920	2.473	0.0134	6.389	36.211	73.439
1.89	0.195	2.343	3.824	2.413	0.0161	6.255	36.077	73.355
1.98	0.381	2.288	3.733	2.355	0.0180	6.113	35.935	73.213
2.09	0.556	2.234	3.647	2.301	0.0200	5.964	35.786	73.064
2.21	0.772	2.184	3.564	2.248	0.0225	5.755	35.577	72.855
2.36	0.889	2.135	3.484	2.198	0.0245	5.621	35.443	72.721
2.56	1.043	2.089	3.409	2.151	0.0273	5.430	35.242	72.520
2.87	1.191	2.044	3.336	2.105	0.0302	5.203	35.025	72.303
3.29	1.333	2.002	3.267	2.061	0.0331	4.987	34.809	72.087
3.78	1.469	1.961	3.200	2.019	0.0360	4.771	34.593	71.871
4.10	1.600	1.922	3.136	1.979	0.0388	4.562	34.384	71.662
4.35	1.725	1.884	3.075	1.940	0.0417	4.346	34.163	71.445
4.56	1.846	1.848	3.015	1.902	0.0445	4.137	33.959	71.237
4.78	1.962	1.813	2.958	1.867	0.0475	3.914	33.736	71.014
5.02	2.074	1.779	2.904	1.832	0.0506	3.683	33.505	70.783
5.33	2.182	1.747	2.851	1.799	0.0539	3.436	33.258	70.536
5.72	2.286	1.716	2.800	1.767	0.0571	3.198	33.020	70.298
6.09	2.386	1.686	2.751	1.736	0.0603	2.959	32.781	70.059
6.37	2.483	1.657	2.703	1.706	0.0636	2.713	32.535	69.813
6.59	2.575	1.628	2.658	1.677	0.0671	2.452	32.274	69.552
6.80	2.667	1.601	2.613	1.649	0.0712	2.147	31.969	69.247
7.00	2.754	1.575	2.570	1.622	0.0758	1.804	31.626	68.904
7.24	2.839	1.550	2.529	1.596	0.0815	1.379	31.201	68.479
7.54	2.921	1.525	2.489	1.570	0.0882	0.879	30.701	67.979
7.96	3.000	1.501	2.450	1.546	0.0952	0.357	30.179	67.457
8.36	3.077	1.478	2.412	1.522	0.0993	0.052	29.874	67.152
8.69	3.152	1.456	2.376	1.499	0.102	—	29.672	66.950
8.95	3.224	1.434	2.340	1.477	0.104	—	29.523	66.801
9.15	3.294	1.413	2.306	1.455	0.106	—	29.374	66.652
9.37	3.362	1.392	2.272	1.434	0.107	—	29.300	66.578
9.62	3.429	1.373	2.240	1.413	0.109	—	29.151	66.429
9.91	3.493	1.353	2.208	1.393	0.110	—	29.076	66.354
10.38	3.556	1.334	2.178	1.374	0.111	—	29.001	66.279
10.83	3.616	1.316	2.148	1.355	0.112	—	28.927	66.205
11.20	3.676	1.298	2.119	1.337	0.114	—	28.778	66.056
11.40	3.733	1.281	2.091	1.319	0.116	—	28.629	65.907
11.58	3.789	1.264	2.063	1.302	0.118	—	28.480	65.758
11.70	3.844	1.248	2.036	1.285	0.121	—	28.256	65.534
11.82	3.897	1.232	2.010	1.268	0.123	—	28.107	65.385
11.92	3.949	1.216	1.985	1.252	0.126	—	27.883	65.161
11.98	4.000	1.201	1.960	1.237	0.128		27.734	65.012

(*) Since pH values depend on ionic strength (2), the actual pH of each solution must be checked experimentally. The values reported are the Britton-Robinson original ones (without potassium chloride)

* Anali di Chemica , 64-1974

APPENDIX II

Tris buffer [251]

Contains tris (hydroxymethyl) aminoethane 6.06g per litre (50.0mM per litre) and the specified amount of hydrochloric acid.

	Hydrochloric acid	
pH	mM/L	g/L
7.2	44.7	1.63
7.4	42.0	1.53
7.6	39.3	1.43
7.8	33.7	1.23
8.0	27.9	1.02
8.2	22.9	0.83
8.4	17.3	0.63
8.6	13.0	0.47
8.8	8.8	0.32
9.0	5.3	0.19

APPENDIX III

I	2-amino-5-bromo-6-methyl pyrimidin-4(3H)-one (ABMP).
II	2-amino-5-iodo-6-phenyl pyrimidin-4(3H)-one (AIPP).
III	2-amino-5-bromo-6-phenyl pyrimidin-4(3H)-one (ABPP).
IV	Acetyl bropirimine (AB).
V	Propanoylbropirimine (PB).
VI	Pyrimethamine (Py).
VII	2-N-propanoyl pyrimethamine (MPP).
VIII	2,4-N,N-dipropanoyl pyrimethamine.
IX	Methyl 5-(p-chlorophenyl)-2,4-diaminopyrimidine-6-carboxylate (MDPC).
X	Ethyl 5-(p-chlorophenyl)-2,4-diaminopyrimidine-6-carboxylate (EDPC).
XI	Propyl 5-(p-chlorophenyl)-2,4-diaminopyrimidine-6-carboxylate (PDPC).
XII	Iso-propyl 5-(p-chlorophenyl)-2,4-diaminopyrimidine-6-carboxylate (iPDPC).
XIII	4-methoxyphenyl aminoacetate hydrochloride (MPAA)
XIV	2-amino-5-(4-chlorophenyl)-6-ethylpyrimidin-4(3H)-one.
XV	4-amino-5-(4-chlorophenyl)-6-ethylpyrimidin-2(1H)-one.
XVI	Dimer of XIV and XV.
XVII	Bropirimine dimer.
α-CD	α-cyclodextrin.
Å	Angstrom.
AUFS	Absorbance units full scale.
β-CD	β-cyclodextrin.
BP	British Pharmacopoeia.
DMA	N,N-dimethylacetamide.
DMF	N,N-dimethylformamide.
γ-	γ-cyclodextrin.
HPLC	High performance liquid-chromatography.
im	Intramuscular.
in	Intranasal.
ip	Intraperitoneal.
iv	Intravenous.
ivag	Intravaginal.
μ	Micro/ionic strength
NMF	N-methylformamide.
ODS	Octadecylsilane.
PEG	Polyethylene glycol.
po	Post oral.
PVP	Polyvinylpyrolidone.
rpm	Revolutions per minute.
sc	Subcutaneous.
SDS	Sodium dodecyl sulphate.
t1/2	Half-life.
UV	Ultraviolet.
$^{v}/_{v}$	Volume per volume.
$^{v}/_{w}$	Volume per weight.
$^{w}/_{w}$	Weight per weight.

U-54,461: Toxicology

Repeated Dose Studies

Type of Study	Compound	Species	Number of Animals	Route of Administration	Dose	Period of Administration	Observations, Results and Conclusions	Ref.
Urinary Tract Study	U-54,461	Rat	5/sex/level	Oral	0, 300, 300 mg/kg/day	Ten or 20 days	There were no characteristable changes produced as determined by gross and microscopic examination of the urinary tract	7205/78/ 72631004
Tolerance	U-54,461	Rat	10/sex/level	Oral	0, 100, 300, 600 mg/kg/day	14 days	Body weights were slightly depressed at 100 and 300 mg/kg/day dose levels, and moderately depressed at 600 mg/kg/day. A dose-related increase in atypical lymphocytes in the peripheral blood and decrease in serum cholesterol were noted. Splenomegaly, hyperplasia of the lymph nodes and mononuclear cell inflammation about the medium sized blood vessels in the liver and lungs were also noted	7205/80/ 72631004
Tolerance	U-54,461	Dog	1/sex/level	Oral	0, 50, 100, 150 mg/kg b.i.d	9 1/2 days	Decreased food consumption with resulting body weight loss, and a severe decrease in the number of circulating platelets were noted for all treated dogs. The platelet numbers recovered upon cessation of drug treatment.	7205/80/ 72631007
Tolerance	U-54,461	Dog	4 females	Oral	300 mg/kg/day then 100 mg/kg/day in divided doses	9 days 16 days	At 300 mg/kg/day, vomiting, weight loss, poor appetites and markedly depressed platelet counts were produced. After a 12 day rest period then reinitiation of drug treatment at 100 mg/kg/day, this level was tolerated. Very little vomiting occurred. The platelet counts were slightly to moderately depressed after 1 week of treatment, but recovered to normal range while drug administration was continued. Tissue pathology was not evident and very scant evidence of drug effect was noted in bone marrow sections	7205/79/ 72631005

PATHOLOGY & TOXICOLOGY RESEARCH

Tabular Summary of Animal Toxicology Studies on U-54,461

U-54,461: Toxicology

Other Animal Studies

Type of Study	Compound	Species	Number of Animals	Route of Administration	Dose	Period of Administration	Observations, Results and Conclusions	Ref.
Toxicity and Sensitization Test	U-54,461 Positive control = DNCB	Guinea Pig	5/sex Positive controls 9 males and 10 females treated	Dermal	Sufficient amount of 20% concentration to cover preclipped patch of skin Positive controls received equal amount of DNCB	Clipped intra-scapular area exposed for 6 hours on sensitizing days 1, 8 and 15 and challenge dose on day 29 Three male and 3 female U-54,461 treated animals sacrificed 24 hours after the 3rd sensitizing dose	No observable effects, such as irritation, were recorded at 24 hours following the three sensitizing doses in any guinea pigs of the three treated groups. Following the challenge dose, very slight erythema was observed in 11/13 guinea pigs treated with U-54,461. In the DNCB Group, 6/10 showed very slight erythema and 1/10 showed well defined erythema; very slight edema was recorded in 2/10. Very slight to slight infiltrations of mononuclear cells were observed in the dermis of microscopic sections of skin of 14/19 guinea pigs treated with U-54,461. The treatment-induced effects appeared to be minimal in all aspects of evaluation. On the basis of the results, although DNCB treated guinea pigs did not afford a good positive control, U-54,461 was not regarded as an inducer of delayed-type cutaneous sensitization	7263/83/027
Irritation	U-54,461	Rabbit	6 male	Dermal	500 mg/site	Single dose on each of abraded and unabraded skin sites	No irritation was noted at any intact skin site. Minimal irritation was noted along the scratch marks of the abraded sites of 2 rabbits. Thus, U-54,461 would not be considered to be a primary dermal irritant	7277/83/001

APPENDIX VI

PATHOLOGY & TOXICOLOGY RESEARCH — Tabular Summary of Animal Toxicology Studies on U-54,461

U-54,461: Toxicology — Mutagenicity Studies

Type of Study	Compound	Species	Number of Animals	Route of Administration	Dose	Period of Administration	Observations, Results and Conclusions	Ref.
Mammalian Cell Mutation Assay	U-54,461 ENU positive control	Chinese Hamster V-79 cells		*In Vitro*	25, 50, 100 µg/ml 40 µg/ml	2 hour exposure	U-54,461 did not produce a significant increase in the number of mutant Chinese hamster V-79 cells resistant to 6-thioguanine whereas the positive control (ENU) did produce a significant increase. Thus, in this assay, U-54,461 would not be considered to be mutagenic	7268/84/004
Micronucleus	U-54,461	Rat	10 male/level	Intraperitoneal	0, 275, 550 and 1100 mg/kg	One-half dose given at 0 and 24 hours	U-54,461 did not significantly increase the incidence of micronucleated polychromatophilic erythrocytes (PCEs) above the control level. The positive control, cyclophamide, did significantly increase the incidence of micronucleated PCEs. Therefore, U-54,461 did not act as a clastogen or chromosomal mutagen	7268/83/027

U-54,461: Toxicology

Single Dose Studies

Type of Study	Compound	Species	Number of Animals	Route of Administration	Dose	Period of Administration	Observations, Results and Conclusions	Ref.
LD_{50}	U-54,461	Mouse	10/sex/level	Intraperitoneal	0 (vehicle), 630, 1250, 2500, 5000 mg/kg	Single Dose	LD_{50}: 2471 (1349-3417) mg/kg At 1250 mg/kg: Depression	7263/83/012
LD_{50}	U-54,461	Rat	10/sex/level	Intraperitoneal	0 (vehicle), 630, 1250, 2500, 5000 mg/kg	Single Dose	LD_{50}: 1845 (1577-2135) mg/kg Treated rats gained less body weight than controls and majority of surviving rats had slight peritoneal adhesions at terminal sacrifice.	7263/83/015
LD_{50}	U-54,461	Mouse	10/sex/level	Oral	0 (vehicle), 630, 1250, 2500, 5000 mg/kg	Single Dose	LD_{50}: >5000 mg/kg	7263/83/013
LD_{50}	U-54,461	Rat	5 M/level	Oral	0, 3200 mg/kg	Single dose	LD_{50}: 3200 mg/kg	7205/79/ 7263/006
LD_{50}	U-54,461	Rat	10/sex/level	Oral	0 (vehicle), 630, 1250, 2500, 5000 mg/kg	Single dose	LD_{50}: >5000 mg/kg At 2500 mg/kg: feces lighter in color. At 5000 mg/kg: 1 rat depressed, emaciated, cold to touch, and red material around nose and/or forepaws.	7263/83/020

REFERENCES

1. Isaacs, A. and Lindenmann, J.; "Virus Interference. I. The Interferon" Proc. R. Soc. Ser. B., 147, 258 (1957).

2. Dorner, F., Scriba, M. and Weil, R.; "Interferon: Evidence for its glycoprotein nature" Proc. Nat. Acad. Sci., U.S.A., 70, 1981 (1973).

3. Mogensen, K.E. and Cantell, K.; "Human leukocyte Interferon: A role for disulphide bonds" J. Gen. Vir., 22, 95 (1974).

4. Tyrell, D.A.J.; "Interferon produced by cultures of calf kidney cells" Nature, 184, 452 (1959).

5. Youngner, J.S. and Salvin, S.B.; "Production and properties of Migration Inhibitory Factor and Interferon in the Circulation of Mice with Delayed Hypersensitivity" J. Immunology, III, 1914 (1973).

6. Stewart, E.W., in The Interferon System (2nd Ed.). Springen-Verlag/Wein, NY (1981).

7. Data Sheet Compendium (1989).

8. Kajander, A., Essen, R., Isomaki, H. and Cantell, K.; "Interferon Treatment of Rheumatoid Arthritis" Lancet, 1, 984 (1970).

9. Cantell, K., Pulkkinen, E., Elosuo, R. and Suominen, J.; "Effect of Interferon on Severe Psychiatric Disease" Annals of Clin. Res., 12, 131 (1980).

10. Editorial, New England Journal of Medicine, 318, 1409 (1988).

11. "Alpha Interferons - are they all the same?" The Pharm. J., 240, 750 (1988).

12. Scott, G.M.; "Interferon: Pharmacokinetics and toxicity" Philosphical Transactions of the Royal Society of London, B299, 91 (1982).

13. Emodi, G., Just, M., Hernandez, R. and Hirt, H.; "Circulating interferon in man after administration of exogeneous human leukocyte interferon" Journal of National Cancer Institute, 54, 1054 (1975).

14. Strander, H., Cantell, K., Coulström, G. and Jakobsson, P.; "Clinical and laboratory investigations on man: Systemic administration of potent interferon to man", Ibid 51, 733 (1973).

15. Sethi, K.K. and Brandis, H.; "Interferon enhances T-cell mediated cytotoxicity of H-2 compatible target cells infected with UV-inactivated herpes simplex virus", Archives of Virology, 57, 117 (1978).

16. Zarling, J.M., Sosman, J., Eskra, L., Borden, E.C., Horoszewicz, J.S. and Carter, W.; "Enhancement of T-cell cytotoxic responses by purified human fibroblast interferon", Journal of Immunology, 121, 2002 (1978).

17. Minato, N., Bloom, B.R., Jones, C., Holland and J., Reid, L.M.; "Mechanism of rejection of virus persistently infected tumour cells by athymic nude mice", Journal of Experimental Medicine, 149, 1117 (1979).

18. Reid, L.M., Minato, N., Gresser, I., Holland, J., Kadish, A. and Bloom, B.R.; "Influence of anti-mouse interferon serum on the growth and metastasis of tumour cells persistently infected with virus and of human prostatic tumours in athymic nude mice", Proceedings of National Acadamy of Sciences (USA), 78, 1171 (1981).

19. Vignaux, F., Gresser, I., and Fridman, W.H.; "Effect of virus-induced interferon on the antibody response of suckling and adult mice", European Journal of Immunology, 10, 767 (1980).

20. Rabinovitch, N., Manejias, R.E., Russo, M. and Abbey, E.F.; "Increased spreading of macrophages from mice treated with interferon inducers", Cell Immunology, 29, 86 (1977).

21. Mantovani, A., Dean, J.H., Jessels, T.R. and Heberman, R.B.,; "Augmentation of tumourcidal activity of human monocytes and macrophages by lymphokines", International Journal of Cancer, 25, 691 (1980).

22. Youngner, J.S. and Stinebring, W.R.; "Interferon production in chickens injected with *Brucella abortus* " Science, 144, 1022 (1964).

23. Stinebring, W.R. and Youngner, J.S.; "Patterns of interferon appearance in mice injected with bacteria or bacterial endotoxin", Nature, London, 204, 712 (1964).

24. Merigan, T.C.; "Induction of circulating interferon by synthetic anionic polymers of known composition", Ibid, 214, 416 (1967).

25. Wheelock, E.F.; "Interferon-like virus-inhibitor induced in human leukocytes by phytohemagglutinin", Science, 149, 310 (1965).

26. Green, J.A., Cooperband, S.R. and Kibrick, S.; "Immune specific induction of interferon production in cultures of human blood lymphocytes", Science, 164, 1415 (1969).

27. Krueger, R.F. and Mayer, G.D.; "Tilorone hydrochloride: an orally active antiviral agent", Science, 169, 1213 (1970).

28. Mayer, G.D. and Krueger, R.F.; "Tilorone hydrochloride: Mode of action", Science, 169, 1214 (1970).

29. Lampson, G.P., Tytell, A.A., Field, A.K., Nemes, M.M. and Hilleman, M.R.; "Inducers of interferon and host resistance. I. Double-stranded RNA from extracts of *Penicillium funiculosum.*", Proceedings of National Acadamy of Sciences, USA, 58, 782 (1967).

30. Field, A.K., Lampson, G.P., Tytell, A.A., Nemes, M.M. and Hilleman, M.R.; "Inducers of interferon and host resistance. IV. Double stranded replicative form RNA (MS2-RF-RNA). from *E. Coli* infected with MS 2 Coliphage", Ibid, 58, 2102 (1967).

31. Field, A.K., Tytell, A.A., Lampson, G.P. and Hilleman, M.R.; "Inducers of interferon and host resistance. II.Multi-stranded synthetic polynucleotide complexes", Ibid, 58, 1004 (1967).

32. Tytell, A.A., Lampson, G.P., Field, A.K. and Hilleman, M.R.; "Inducers of interferon and host resistance. III. Double-stranded RNA from reovirus type 3 virions (reo.3-RNA)", Ibid, 58, 1719 (1967).

33. De Clerq, E.; "Interferon Inducers", Antibiotics Chemotherapy, 27, 251 (1980).

34. Stringfellow, D.A; in "Interferon and Interferon Inducers: Clinical applications", Marcel Dekker Inc., NY, 145 (1980).

35. Stringfellow, D.A.; "Induction of Interferon with Low Molecular Weight Compounds: Fluorenone esters, Ethers (Tilorone) and Pyrimidinones", Methods in Enzymology, 78(A), 262 (1981).

36. Nichol, F.R., Weed, S.D. and Underwood, G.E.; "Stimulation of Murine Interferon by a Substituted Pyrimidinone", Antimicrobial Agents and Chemotherapy, 9(3), 433 (1976).

37. Stringfellow, D.A.; "Comparative Interferon Inducing and antiviral properties of 2-amino-5-bromo-6-methyl-4-pyrimidinol (U-25,166), tilorone hydrochloride and polyinosinic acid", Ibid, 11, 984 (1977).

38. Larsen, E.R., Hamilton, R.D., Gray, J.E. and Clark, J.J.; "Histological Predictiveness of Renal Tolerance in the Rat in a series of Substituted Pyrimidinones", Current Chemotherapy and Infectious Disease, ed. J.D. Nelson, C. Grassi, ASM, 1413 (1980).

39. Stringfellow, D.A., Vandenberg, H.C. and Weed, S.D.; "Interferon induction by 5-halo-6-phenyl pyrimidines", Ibid 1406 (1980).

40. Stringfellow, D.A.; "Interferon Inducers as Antiviral and Antineoplastic Agents", Current Chemotherapy and Immunotherapy, Proceedings of the 12th International Conference of Chemotherapy, 1118 (1981).

41. Stringfellow, D.A. and Weed, S.D.; "5-halo-6-phenyl pyrimidinones: A new series of interferon inducing agents", in Interferon: Properties and Clinical Uses, Ed. A. Khan, N.O. Hill, Wadley Press, 315 (1980).

42. Stringfellow, D.A.; "Antineoplastic Properties of Interferon Inducers", in Advances in Enzyme Regulation, Ed. G. Weber, Pergamon Press, 19, 335 (1981).

43. Stringfellow, D.A.; "6-aryl pyrimidinones: Interferon Inducers - Immunomodulators - Antiviral and Antineoplastic Agents", Augmenting Agents in Cancer Therapy, Ed. E.M. Hersh, 215 (1981).

44. Hamilton, R.D., Wynalda, M.A., Fitzpatrick, F.A., Teagarden, D.L., Hamdy, A.H., Snider, B.G., Weed, J.D. and Stringfellow, D.A.; "Comparison between circulating interferon and drug levels following administration of 2-amino-5-bromo-6-phenyl-4(3H)-pyrimidinone (ABPP) to different animal species", Journal of Interferon Research, 2, 317 (1982).

45. Weed, S.D., Kramer, G.D. and Stringfellow, D.A.; "Antiviral properties of 6-aryl pyrimidinones", in Current Chemotherapy of Infectious Disease, Proceedings of International Congress of Chemotherapy, Ed. J.D.Nelson and C. Grassi, ASM, Washington DC, 11(23), 1408

46. Hamdy, A.H. and Stringfellow, D.A.; "Interferon induction by 6-aryl pyrimidinones". Ibid, 2, 1404 (1980).

447. Renis, H.E. and Eidson, E.E; "Protection of female mice from genital herpes simplex virus type 2 (HSV-2) infection by 2-amino-5-halo-6-phenylpyrimidinones", Proceedings of the 81st Annual Meeting of American Society of Microbiology, March 1-6 (1981).

448. Renis, H.E. and Eidson, E.E; "Protection of mice from genital herpes virus tinfection by 2-amino-5-halo-6-arylisocytosines", in The Human Herpes Virus, eds. A. Nahmias, W.R. Dowdle and R.F. Schinazi, Elsevier, NY, March 17-21 (1980).

449. Brideau, R.J. and Wolcott, J.A.; "Effect of pyrimidinone treatment on lethal and immunosupressive murine cytomeglovirus infections", Antimicrobial Agents and Chemotherapy, 28, 485, (1985).

50. Milas, L., Hersh, E.M., Stringfellow, D.A. and Hunter, N.; "Studies on the antitumour activities of pyrimidinone-interferon inducers. I Effect against artificial and spontaneous lung metastases of murine tumours", Journal of National Cancer Institute, 68(1), 139 (1982).

51. Li, H.L., Wallace, T.L., Richard, K.A. and Tracey, E.D.; "Mechanism of Antitumour Action of Pyrimidinones in the Treatment of B16 melanoma and P388 Leukaemia", Cancer Research, 45, 532 (1985).

52. Sidky, Y.A., Borden, E.C., Wierenga, W. and Bryan, T.G.; "Inhibitory Effects of Interferon inducing Pyrimidinones on the Growth of Transplantable Mouse Bladder Tumours", Cancer Research, 46, 3798 (1986).

53. Chang, A.Y.C., Pandya, K.J., Stringfellow, D.A. and Chuang, C.; "Treatment of 7,12-dimethylbenz(α).anthrocine (DMBA) - induced rat mammary cancer by 2-amino-5-bromo-6-phenyl-4(3H)-pyrimidinone (ABPP) and tamoxifen", Journal Infectious Research, 3(3), 299 (1983).

54. Li, H.K., Johnson, M.A., Moeller, R.B. and Wallace, T.L.; "Chemoimmunotherapy of B16 melanoma and B386 leukaemia with cyclophosphamide and pyrimidinones", Cancer Research, 44(7), 2841 (1984).

55. Li, H.L., Wallace, T.L., Wierenga, W., Skulnick, H.I. and DeKoning, T.F.; "Antitumour activity of Pyrimidinones, a Class of Small-Molecule Biological Response Modifiers", Journal of Biological Response Modifiers, 6, 44 (1987).

56. Li, H.L, Wallace, T.L., Hamilton, R.D. and DeKoning, T.F.; "Pharmacological evaluation of combination therapy of P388 leukeamia with cyclophosphamide and pyrimidinones", International J. Immunopharmacology, 9(1), 31 (1987).

57. Eggermont, A.M.M., DeBruin, R.W.F., Marquet, R.L. and Jeekel, J.; "Efficacy of treatment with ABPP and recombinant γ-interferon on colon cancer in rats depends on tumour site, tumour load and treatment schedule", Surgical Forum, 37, 342 (1986).

58. Loughman, B.E., Gibbons, A.J., Taggart, M.T. and Renis, H.E.; "Modulation of Mouse Natural Killer Cell activity by Interferon and Two Antiviral Isocytosines", Current Chemotherapy and Infectious Diseases, Proceedings of 11th ICC, ed, J.D. Nelson, C. Grassi, ASM, NY, 1398 (1980).

59. Fast, P.E. and Stringfellow, D.A.; "Immune modulation by two Antiviral Isocytosines with different abilities to Induce Interferon", Ibid, 1396 (1980).

60. Fast, P.E., Hatfield, C.A., Sun, E.L. and Stringfellow, D.A.; "Polyclonal ß-cell activation and Stimulation of Specific Antibody Responses by 5-Halopyrimidinones with Antiviral and Antineoplastic Activity", Journal of Biological Response Modifiers, Raven Press, NY, 1, 199 (1982).

61. Taggart, M.T., Loughman, B.E., Gibbons, A.J. and Stringfellow, D.A.; "Immunomodulatory Effects of 2-amino-5-bromo-6-methyl-4-pyrmidinol and its isocytosine anaolgs", Current Chemo. Infect, Dis., Proc. 11th ICC, ed. J.D.Nelson and C. Grassi, ASM, NY, 1400 (1980).

62. Lotzova, E., Savary. C.A., Khan, A. and Stringfellow, D.A.; "Stimulation of natural killer cells in two random bred strains of athymic rats by interferon-inducing pyrimidinones". J. Immunol., 132(5), 2566 (1984).

63. Lotzova, E., Savary. C.A., Lowlachi, M and Murasko, D.M.; "Cytotoxic and morphologic profile of endogeneous and pyrimidinone-activated murine NK cells". J. Immunol., 136(2), 732 (1986).

64. Kuo, P.T., Wilson, A.C., Goldstein, R.C. and Schaub, R.B.; "Suppression of experimental atherosclerosis in rabbits by interferon-inducing agents". J. of American College of Cardiology., 3(1), 129 (1984).

65. Crowe, D., Nerland, D.E., Stringfellow, D.A. and Sonnenfeld, G.; "Effects of 5-halopyrimidinones with antiviral and antineoplastic activity on murine cytochrome P-450". J. Biol. Resp. Modif., 3, 15(1984).

66. Skulnick, H.I., Ludens, J.H., Wendling, M.G., Glenn, E.M., Rohloff, N.A., Smith, R.J. and Wierenga, W.; "Pyrimidinones **3**. N-substituted 6-phenylpyrimidinones and pyrimidinediones with diuretic/hypotensive and anti-inflammatory activity" J. Med. Chem., 29, 1499 (1986).

67. Torrence, P.F. and Declerq, E.; "Inducers and Induction of Interferons". Pharmacol, Ther., 2, 1(1977).

68. Declerq, E.; "Interferon induction by synthetic polynucleotides: recent development", in Chandra, Antiviral Mechanisms in the Control of Neoplasia, Plenum Press, NY, 641 (1979).

69. Stringfellow, D.A.; "Nonpolynucleotide inducers of interferon" in Interferons and Their Applications, eds. P.E. Came and W.A. Carter, Springer-Verlag, Berlin, 371 (1984).

70. Stringfellow, D.A., Weed S.D., and Underwood, G.E.; "Antiviral and interferon-inducing properties of 1,5-diaminoanthraquinones". Antimicrob. Agents Chemother., 15, 111 (1979).

71. Stringfellow, D.A.; "Prostaglandin restoration of interferon response of hyporeactive animals". Science, 201, 376 (1978).

72. Oku, M., Imanishi and Kishida, T.; "Interferon counteracts pyrimidinone-induced hyporeactivity and the combined treatment has antitumour effect in mice". Gann, 75. 631 (1984).

73. Stringfellow, D.A.; "Hyporeactivity and interferon induction: Characterisation of a hyporeactive factor in the serum of encephalomyocarditis virus-infected mice". Infect. Immunity, II, 294 (1975).

74. Skulnick, H.I., Weed, S.D., Eidson, E.E., Renis, H.E., Wierenga, W., and Stringfellow, D.A.; "Pyrimidinones. **1**. 2-amino-5-halo-6-aryl-4(3H)-pyrimidinones. Interferon-inducing antiviral agents". J. Med. Chem., 28, 1864 (1985).

75. Eriksson, S.O. and Meresaar, V., "Hydrolysis of anilides". Acta Chem. Scand., 25(7), 27 (1971).

76. Stringfellow, D.A., Vandeberg, H.C. and Weed, S.D.; "Interferon induction by 5-halo-6-phenylpyrimidinones". J. Int. Res., 1(1), 1 (1980).

77. Alpar, H.O., Whitmarsh, S.J., Ismail, H., Irwin, W.J., Slack, J.A., Belaid, K.A. and Stevens, M.F.G.; "Formulation studies on [2-amino-5-bromo-6-phenyl-4(3H)-pyrimidinone] (ABPP), an interferon inducer and anti-tumour agent". Drug Dev. Ind. Pharm., 12(11-13), 1795 (1986).

78. Rios, A.A., Stringfellow, D.A. Fitzpatrick, F.A., Reela, S.B., Guehteneck, G.O. and Hersh, E.M., "Phase I Study of 2-amino-5-bromo-6-phenyl-4(3H)-pyrimidinone (ABPP) and oral interferon inducers in cancer patients". J. Biol. Response Modif., 4, 123 (1986).

79. Earnhart, R.H., Hamilton, R.D., Henry, C.S., Hanover, C.K., Maite, M.H., Agrawal, B.L., and Todd, W.M.; "Phase I trial, pharmacokinetics of interferon (IFN) induction of an oral divided-dose schedule of 2-amino-5-bromo-6-phenyl-4(3H)-pyrimidinone (ABPP) in cancer patients". (Abstract), Proceeding AACR, 26, 159 (1985).

80. Farber, E.M., and Nall, L.; "An appraisal of measures to prevent and control psoriasis", J. Am. Acad. Dermat, 10(3), 512 (1984).

81. Faber, E.M., and Nall, L.; "Epidimiology in psoriasis research" Hawaii Med. Journal, 41, 430, (1983).

82. Farber, E.M., and Nall, L.; "Psoriasis. A review of recent advances in treatment", Drugs, 28, 324 (1984).

83. Faber, E.M., and Nall, L.; "The natural history of psoriasis in 5600 patients", Dermatologica, 148, 1 (1974).

84. Epstein, J.H.; "Risks and benefits of the treatment of psoriasis", N. Eng. J. Med., 300, 852 (1979).

85. Halvey, S., Halney, J., Boney, G., Rosenfeld, J.B. and Feverman, E.J.; "Dialysis therapy for psoriasis. Report of three cases and review of the literature". Archives of Dermatology, 117, 69 (1987).

86. Orenberg, E.K., Deneau, D.G., and Pounds, D.; "Treatment of chronic psoriatic plaque with hyperthermia induced by ultrasound". In Farber and Cox (Eds) Psoriasis: Proceedings of the Third International Synposium, Grune and Stratton, NY, 345, (1982).

87. Tackett, L.L., and Anderson, S.G.; "Interferon Standards". Symp. Series Immunobiol. Standard". (Kanger, Basel), 14, 277, (1970).

88. Cantrell, K. and Pyhala, L.; "Circulating interferon in rabbits after administration of human interferon by different routes". J. Gen.Vir., 20, 97 (1973).

89. Ng, M.N. and Vilcek, J.; In: Advances in Protein Chemistry. Eds. C.B. Anfinsen, J.J. Edsall and F.M.R. Chards. Academic Press, NY and London (1972).

90. Carter, W.A.; "Interferon : Evidence for subunit structure". Proc. Nat. Acad. Sci., 67(2), 620 (1970).

91. Vileck, J.; In: 'Interferons' Virology Monographs, Vol. 6. Springer-Verlag, Wein and NY (1969).

92. Maeyer-Guignard, J.D., Maeyer, E.D. and Jullien, P.; "Interferon synthesis in rat-to-mouse radiation chimeras injected with Newcastle Disease Virus", Proc. Nat. Acad. Sci., 63, 732 (1969).

93. Heller, E.; "Enhancement of Chikungunya Virus replication and inhibition of interferon production by Actinomycin-D". Virology, 21, 652 (1963).

94. Tan. Y.H., Creagan, R.P. and Ruddle, F.H.; "The somatic cell genetics of human interferon. Assignments of human interferon loci to chromosomes 2 and 5". Proc. Nat. Acad. Sci., 71(6) 2251 (1974).

95. Colby, P., and Chamberlain, M.J.; "The Specificity of interferon induction in chick embroyo cells by helical RNA". Proc. Nat. Acad. Sci., 63, 160 (1969).

96. Jameson, P., and Grossberg, S.E.; "Interferon induction in mice by complexes of polynucleotides of varying sizes". Bacterial. Proc., L55 (1970).

97. Nickoloff, B.J.; "New Strategies for psoriasis therapy", Cutis, 37(6), 421 (1986).

98. Champion, R.H., "Psoriasis", BMJ, 292, 1693 (1986).

99. Blaney, J.M., Hansch, C., Silipo, C., and Vittoria, A.; "Structure-activity relationships of dihydrofolate reductase inhibitors". Chem. Rev., 84, 333 (1984).

100. McCormack, J.J.; "Dihydrofolate reductase inhibitors as potential drugs". Med. Res. Rev., 1(3), 303 (1981).

101. Dibella, N.J., Nan, D.D., Aeling, J.L. and Andreozzi, R.J.; "Treatment of severe psoriasis with pyrimethamine". Arch. Dermat., 113, 172, (1977).

102. Roth, B., and Cheng, C.C.; "Recent progress in medicinal chemistry of 2,4-diamino pyrimidines". In : Progress in Medicinal Chemistry (Vol. 19). Eds. G.P. Ellis and G.B. West. Elsevier Biomedical Press (1982).

103. Li Wan Po, A. and Irwin, W.J.; "High Performance Liquid Chromatography. Techniques and Applications". J. Clin. Hosp. Pharmacy, 5, 107 (1980).

104. Engelhart, H.; "The Role of Moderators in Liquid-Solid Chromatogrpahy". J. Chromatographic Science, 15, 380 (1977).

105. Wynalda, M.A. and Fitzpatrick, F.A.; "High Performance Liquid Chromatography Determination of 5-halopyrimidinones Interferon Inducers", Anal. Chem., 52, 1931 (1980).

106. Snyder, L.R.; "A rapid approach to selecting the best experimental conditions for high-speed liquid chromatography. Part I - estimating inital sample resolution and the final resolution required by a given problem". J. Chromat. Sci., 10, 200 (1972).

107. Cassel, B. and Ohnishi, T.; "DSC. New developments in clinical analysis by physicochemical research" in Analytical Calorimetry, Vol 3., R.S. Porter and J.F. Johnson (Eds.). Plenum Press (1974).

108. Cassel, R.A.; "A high sensitivity DSC study in biochemistry: Protein denaturation in dilute aqueous solution". Perkin-Elmer Thermal Analysis Application Study No. 5, (1973).

109. Van Dazee, B.F.; "Thermal analysis of human stratum corneum", J. Investigative Dematology, 65, 404 (1975).

110. Carter, B.R., Chapman, D., Hawes, S.M. and Saville, J.; "Lipid phase transitions and drug interactions". J. Biochem. Biophys. Acta., 363, 54 (1974).

111. Giron, D.; "Applications of thermal analysis in the pharmaceutical industry". J. Pharm. Biomed. Analysis, 4(6), 755 (1986).

112. Fairbrother, J.E.; "Pharmaceutical application of thermal analysis". Therm. Anal. Abs., 15(3), 109 (1986).

113. Pope, M.I. and Judd, M.D.; In "Differential Thermal Analysis". Heydn, London, (1977).

114. Daniels, T., In "Thermal Analysis", The Anchor Press, Tiptree (UK) (1973).

115. Botha, S.A., DuPreez, J.L. and Lotter, A.P.; "DSC screening for drug-drug and drug-excipient interaction in polypharmaceuticals intended for the alleviation of the symptoms of colds and flu I.". Drug Dev. Ind. Pharm., 12(6), 811 (1986).

116. Botha, S.A., DuPreez, J.L., and Lotter, A.P.; "DSC Screening for drug-drug and drug-excipient interaction in polypharmaceuticals intended for the alleviation of the symptons of colds and flu, II.". Drug Dev. Ind. Pharm., 13(7), 1197 (1987).

117. Schwalbe, C.H. and Bryant, P.; unpublished data.

118. Whitmarsh, S.J.; "The Formulation of Insoluble Drugs for Parenteral Administration for Clinical Trials". MSc Thesis, Aston University (1985).

119. Griffin, R.J., Schwalbe, C.H., Stevens, M.F.G., and Wong, K.P.; "Structural studies on bio-active compounds. Part 3. Re-examination of the hydrolysis of the antimalarial drug pyrimethamine and related derivatives and crystal structure of a hydolysis product". J. Chem. Soc. Perkin Trans., I, 2267 (1985).

120. Kerr, J.A. and Trotman-Dickenson, A.F.; In West, R.C. (Ed) Handbook of Chemistry and Physics, 59th Edn., CRC Press Inc., Boca Raton, FL, 1978-79, P.F-247.

121. Olafson, P.G. and Bryan, A.M.; "Thermal analysis of 5-halo-2'-deoxynucleosides". J. Thermal Anal., II, 359 (1977).

122. Olafsson, P.G. Bryan, A.M. and Lau, K.; "A DSC-TLC analysis of thermolysis reaction involving 2'-deoxynucleosides". J. Thermal Analysis, II, 377 (1977).

123. Ford, J.L., Stewart, A.F., and Rubinstein, M.H.; "The assay and stability of chlorpropamide in solid dispersion with urea". J. Pharm. Pharmacol., 31, 726 (1977).

124. Brown, W.E., Dollimore, D. and Galway, A.K.; "Reactions in the solid state". In Bamford, C.H. and Tipper, C.H.F., (Eds.), Comprehensive Chemical Kinetics, Vol. 22, Elsevier, Amsterdam, 1980.

125. Carstensen, J.T.; In "Pharmaceutics of Solids and Solid Dosage Forms", Wiley, NY, (1977).

126. Carstensen, J.T.; In "Solid Pharmaceutics : Mechanical Properties and Rate Phenomena", Academic, NY (1980).

127. Mroso, P.V., Li Wan Po, A. and Irwin, W.J.; "Solid state stability of aspirin in the presence of excipients : Kinetic interpretation, modelling and prediction". J. Pharm. Sci., 71, 1096 (1982).

128. Ozawa, T.; "Kinetic analysis of derivative curves in thermal analysis". J. Therm. Anal., 2, 301 (1970).

129. ANSI/ASTM E 698-79, "Standard Test Method for Arrhenius Kinetic Constants for Thermally Unstable Materials". American Society for Testing and Materials, Washington DC.

130. Van Dooren, A.A. and Weesp, D.B.V.; "Effects of operational factors on kinetic parameters determined with DSC". In Thermal Analysis, Vol. I, B. Miller (Ed)., Wiley, Chichester, p80 (1982).

131. Torfs, J.C.M., Dejj, L., Dorrepaal, A.J. and Heijens, J.C.; "Determination of Arrhenius Kinetic Constants by differential scanning calorimetry". Anal. Chem, 56, 2863 (1984).

132. Li Wan Po, A.; "Application of Differential Scanning Calorimetry in Pharmacy : Prediction of Solid State Stability of Drugs". Anal. Proc., 23, 391 (1986).

133. Duswalt, A.A.; "The practice of obtaining kinetic data by differential scanning calorimetry". Thermochim. Acta., 8, 57 (1974).

134. Otsuka, M., Matsumoto, T., and Kaneniwa, N.; "Effect of environmental temperature on polymorphic solid-state transformation of indomethacin during grinding". Chem. Pharm. Bull., 34(4), 1784 (1986).

135. Lefebvre, C., and Guyot-Hermann, A.M.; "Polymorphic transitions of carbamazepine during grinding and compression". Drug Dev. Ind. Pharm., 12(11-13), 1913 (1986).

136. Kaneniwa, N. and Otsuka, M.; "Effect of grinding on the transformation of polymorphs of chloramphenicol palmitate". Chem. Pharm. Bull., 33(4) 1668 (1985).

137. Chan, H.K. and Doelker, E.; "Polymorphic transformation of some drugs under compression". Drug Dev. Ind. Pharm., 11 (1 and 2) 315 (1985).

138. Takahashi, Y., Nakashima, K., Ishihara, T., Nakagawa, H. and Sugimolo, I.; "Polymorphisms of fostedil : Characterisation and polymorphic change by mechanical treatments". Drug. Dev. Ind. Pharm., 11(8), 1543 (1985).

139. Brown, D.E. and Hardy, M.J.; "Characterisation of organic and inorganic hydrates and solvates by thermal methods". Thermochimica Acta, 90, 149 (1985).

140. Brown, D.E., and Hardy, M.J.; "Pharmaceutical applications of thermal methods : the use of DSC and TG in the characterisation of organic and inorganic solvates". Thermochimica Acta, 85, 521 (1985).

141. Otsuka, M., and Kaneniwa, N.; "Effects of grinding on the physicochemical properties of cephalexin powder". Chem. Pharm. Bull., 32(3), 1071 (1984).

142. Takahashi, Y., Nakashima., Nakagawa, H. and Sugimoto, I.; "Effects of grinding and drying on the solid-state stability of ampicillin trihydrate". Chem. Pharm. Bull, 32(12), 4963 (1984).

143. Griffin, R.J.; Aston University (Unpublished data).

144. "The Pharmaceutical Handbook". Nineteenth Edition, Pharamaceutical Press (London), 1980.

145. Lerk, C.F., Buma, T.J., and Andreal, A.C.; "The effect of mechanical treatment on the properties of lactose as observed by differential scanning calorimetry". Neth. Milk Dairy J., 34, 69 (1980).

146. Berlin, E., Kliman, P.G., Anderson, B.A. and Pallansch, M.J.; "Calorimetric measurement of the heat of desorption of water vapor from amorphous and crystalline lactose". Thermochima Acta, 2, 143 (1971).

147. Itoh, T., Satoh, M. and Adachi, S., "Differential Thermal Analysis of α-lactose hydrate". J. Dairy Science, 60(8)., 1230 (1977).

148. Buma, T.G. and Van der Veen, H.K.C.; "Accurate specific optical rotations of lactose and their dependence on temperature", Neth. Milk Dairy J., 28, 175 (1974).

149. Houminer, Y.; "Thermal degradation of carbohydrates". In Molecular Structure and function of good carbohydrates, G.E. Birch and L.F. Green (ed.), Applied Science Publ., London, 133 (1973).

150. Fernandez-Martin, F., Morais, F. and Ohano, A.; "Thermal behaviour of lactose", Proc 2nd Int. Cong. Eng. and Food (Helsinki), Vol. 1 and 2, 523 (1980).

151. Wierenga, W.; "Antiviral and other bioactivities of pyrimidinones", Pharm. Therm., 30, 67 (1985).

152. Martin, Y.C.; In "Quantitative Drug Design, a Critical Introduction", Marcel Dekker, N.Y., 49 (1978).

153. Yalkowsky, S.H. (Ed.); "Techniques of solubilisation of Drugs", Marcel Dekker, Volume 12, (1981).

154. Lawson, A.A. and Proudfoot, A.T.; "Acute salicylate poisoning', Lancet, 1, 1038 (1969).

155. Peters, L.; "Renal tubular excretion of organic bases", Pharm. Rev., 12, 1 (1960).

156. Ritschel, W.A.; In "Perspectives in clinical pharmacy", 1st ed., Franke, D.E. and Whitneys, H.A.K. (Eds.), Drug Intelligence Publication, Hamilton, 325 (1972).

157. Overton, E.; "Studen Über Narkose", Jena: Fischer (1901).

158. Meyer, H.; "Zur Theorie der Alkoholnarkose", Arch. Pathol. Pharmakol., 46, 338 (1899).

159. Meyer, H.; "Zur Theorie der Alkoholnarkose", Ibid., 46, 338 (1901).

160. Brodie, B.B. and Hogben, C.A.M.; "Some physicochemical factors in drug action", J. Pharm. Pharmacol., 9, 345 (1957).

161. Brodie, B.B.; In "Animal and Clinical Pharmacology Technique and Drug Evaluation", Ed. J.H. Nodine and P.E. Seigler, Chicago, Yearbook Publications, 69 (1964).

162. Lien, E.J.; "Physicochemical Properties and Gastrointestinal Absorption of Drugs", Drug Intell., 4, 7 (1970).

163. Lien, E.J.; "Structure activity relationships and drug disposition", Ann. Rev. Pharmacol. Toxicol., 21, 31 (1981).

164. Nys, G.G and Rekker, R.F.; "Statistical analysis of series partition coefficients with special reference to the predictability of folding drug molecules. Introduction in hydrophobic fragmental constants (f-values)", Chim. Ther., 8(5), 521 (1973).

165. Nys, G.G. and Rekker, R.F.; "Statistical analysis of series partition coefficients with special reference to the predictability of folding drug molecules, introduction in hydrophobic fragmental constants (f-values)", Ibid, 361 (1974).

166. Chou, J.T. and Jurs, P.C.; In "Physical-chemical properties of drugs", Yalkowsky, S.H., Sinkula, A.A. and Valvani, S.C. (Eds.), Marcel Dekker, N.Y., 165 (1980).

167. Hanch, C.; :A quantitative approach to biochemical structure activity relationships", Acc. Chem. Res., 2, 232 (1969).

168. Unger, S.H., Cooke, J.R. and Halenberg, J.S.; "Simple procedure for determining octanol-aqueous partition coefficient distribution and ionisation coefficients by reversed phase HPLC", J. Pharm. Sci., 67, 1304 (1978).

169. Unger, S.H. and Fenerman, T.F.; "Octanol-aqueous partition, distribution and ionisation coefficients by reversed phase HPLC", J. Chromat., 107, 219 (1979).

170. Thus, J.L.G. and Kraak, J.L.; "Comparison of phenyl- and octadecyl-modified silica gel stationary phase for the prediction of n-octanol-water partition coefficients by high-performance liquid-chromatography", J. Chromat., 320, 271 (1985).

171. Unger, K.K., Becker, N. and Roumeliotis, P.; "Recent development in the evaluation of chemically bonded silica packings for liquid chromatography". J. Chromat., 125, 115 (1976).

172. Perrin, D.J.; In"Physical Chemical Properties of Drugs". Yalkowsky, S.H., Sinkula, A.A. and Valvani, S.C. (Eds). Marcel Dekker, NY, 1 (1980).

173. Albert, A, and Serjeant, E.P.; In "The determination of ionisation constants". Chapman and Hall Ltd., London (1971).

174. Cookson, R.F.; "The determination of acidity constants". Chem. Rev. 74, 5 (1974).

175. Connors, K.A.; In "A textbook of Pharmaceutical Analysis". 2nd Edition, John Wiley and Sons, NY (1975).

176. Rosenberg, L.S. and Wagenkuecht, D.M.; "pK_a determination of sparingly soluble compounds by difference potentiometry". Drug. Dev. Ind. Pharm., 12(10), 1449 (1986).

177. Miyake, K., Kitaura, F., Mizuno, N., and Terada, H.; "Determination of partition coefficient and acid dissociation constant by high performance liquid chromatography in porous polymer gel as stationary phase". Chem. Pharm. Bull., 35(1), 377 (1987).

178. Miyake, K. Okumura, K and Terada, H.; "Determination of acid-dissociation constant by high-performance liquid chromatography". Chem. Pharm. Bull., 33(2), 769 (1985).

179. Irwin, W.J. and Li Wan Po, A.; "The dependence of amitriptyline partition coefficients on lipid phase", Int. J. Pharm., 4, 47 (1979).

180. Yalkowsky, S.H.; In 'Techniques of solubilisation of drugs". Marcel Dekker, Vol. 12, p1 (1981).

181. Hildebrand, J.H. and Scott, R.L.; In 'The solubility of non-electrolytes", Reinhold Publishing Co., N.Y. (1950).

182. Martin, A., Newbinger, J. and Adjei, A.; "Extended Hildebrand solubility approach: solubility of theophylline in polar binary solvents", J. Pharm. Sci., 69(5), 1487 (1980).

183. Martin, A., Paruta, A.N. and Adjei, A.; "Extended Hildebrand solubility approach: Methylxanthines in mixed solvents", J. Pharm. Sci., 70(10), 1115 (1981).

184. Wu, P.L. and Martin, A.; "Extended Hildebrand solubility approach: p-hydroxybenzoic acid in mixtures of dioxane and water", J. Pharm. Sci., 72(6), 587 (1983).

185. Martin, A., Wu, P.L., Liron, Z. and Cohen, S.; "Dependence of solute solubility parameters on solvent polarity", J. Pharm. Sci., 74(6), 638 (1985).

186. Ochsner, A.B. and Sokolski, T.D.; "Predicting solubility in non-ideal multicomponent systems using UNIFAC group contribution model", J. Pharm. Sci., 74(6), 634 (1985).

187. Yalkowsky, S.H. and Rubino, J.T.; "Solubilisation by co-solvents.1. organic solutes in propylene glycol-water mixtures". J. Pharm. Sci. 74(4), (1985).

188. Muller, B.W. and Brauns, U.; "Hydroxypropyl-ß-cyclodextrin derivatives : Influence of average degree of complexing ability and surface activity". J. Pharm. Sci., 75(16), p571 (1986).

189. Ramachandra, P.H. and Rhodes, C.T., "Preparation of a phenytoin ß-cyclodextrin complex and evaluation of a suspension and tablet dosage form prepared from the complex". Pharm. Acta. Helv. 60(2), 53 (1985).

190. Uekama, K., Sakai, A., Arimori, K., Otagiri, M. and Saito, H.; "Different mode of prednisilone within α-, ß- and γ- cyclodextrins in aqueous solutions and in solid state". Pharm. Acta. Helv., 60(4), 117 (1985).

191. Si-Nang, L., Simond, V., Schiff, V., Trottier, D. and Pouvrat, A.; "Formation of a complex between the analgesic, 6-benzoyl-benzoxazolidinone (CERM 10194), and ß- cyclodextrin". Pharm. Acta. Helv. 60(4), 112 (1985).

192. Chow, D.D., and Karara, A.H.; "Characterisation, dissolution and bioavailability in rats of ibuprofen - ß-cyclodextrin complex system". Int. J. Pharm., 28, 95 (1986).

193. Miyajima, K., Ikuto, M., and Nakagaki, M.; "Interaction of short chain alkylammonium salts with cyclodextrins in aqueous solutions". Chem. Pharm. Bull., 35(1), 389 (1987).

194. Uekama, K., Imai, T., Maeda, T., Irie, T., Hirayama, F. and Otagiri, M.; "Improvement of dissolution and suppository release characteristics of fluorbiprofen by inclusion complexation with heptakis (2,6-di-o-methyl)-ß-cyclodextrin". J. Pharm. Sci., 74(8), 841 (1985).

195. Kikuchi, M., Hirayama, F. and Uekama, K.; "Improvement of chemical instability of carmofur in ß-cyclodextrin solid complex by utilising some organic acids". Chem. Pharm. Bull., 35(1), 315 (1987).

196. Irie, T., Otagiri, M., Sunada, M., Uekama, K., Ohtani, Y., Yamada, Y. and Sugiyama, Y.; "Cyclodextrin induced hemolysis and shape change of human erythrocytes *in-vitro*". J. Pharmacobio-Dyn., 5, 741 (1982).

197. Uekama, K. and Otagiri, M.; "Cyclodextrins in Drug Carrier Systems". In CRC Critical Reviews in Therapeutic Drug Carrier Systems. Vol. 3. CRC, FL, 1 (1987).

198. Yoshida, A., Arima, H., Uekama, K. and Pitha, J., "Pharmaceutical evaluation of hydroxyalkyl ethers of ß- cyclodextrins". Int. J. Pharm., 46, 217 (1988).

199. Martindale, 28th Edition, Pharmaceutical Press, 1982.

200. Aspelin, P., "Effect of ionic and non-ionic contrast media on morphology of human erythrocytes". Acta. Radiologica Diag., 19(20), 675 (1987).

201. Ekeland, A. and Uflacker, R.; "Effect of meglumine metrizoate and metrizamide on the microcirculation" Acta Radiol. Diag., 19, 969 (1978).

202. Laniado, M., Wienmann, H.J., Schorner, W., Flexis, R. and Speck, U.; "First use of GdDTPA/dimeglumine in man" Physiol. Chemistry and Physics and Medical NMR, 16, 157 (1984).

203. Szetli, J.; In "Cyclodextrins and Inclusion Complexes" Akademiai Kiado, Budapest, p 25 (1982).

204. Higuchi, T and Connors, K.A.; "Phase solubility techniques". In C.N. Reilley (Ed), Advances in Analytical Chemistry and Instrumentation, Interscience, N.Y. 132 (1965).

205. Schawlbe, C. and Bryant, P.; Aston University (Unpublished date).

206. Kikuchi, M., Hirayama, F. and Uekama, K.; "Improvement of oral and rectal bioavailabilities of carmofur by methylated ß-cyclodextrin complexations' Int. J. Pharm., 38, 191 (1987).

207. Harned, H.S. and Hamer, W.J.;"The ionisation constant of water in potassium chloride solutions from electromotive forces of cells without liquid junction." J. Am. Chem. Soc., 55, 2194 (1933).

208. Bruile, P.Y. and Mautner, H.G.; "Intramolecular catalysis and the involvement of tetrahedral intermediate partitioning in the hydrolysis of benzoylcholine, benzoylthiomocholine and their dimethylamino analogs." J. Am. Chem. Soc., 95, 1582 (1973).

209. Hamlin, W.E., Northam, J.I. and Wagner, J.G.; "Relationship between *in-vitro* dissolution rates and solubility of numerous compounds representative of various chemical species" J. Pharm. Sci., 54(11), 1651 (1965).

210. Nickalson, M. and Brodin, A.; "The relationship between intrinsic dissolution rates and solubilities in the water-ethanol binary solvent system' Int. J. Pharm., 18, 149 (1984).

211. Smyth, R.D. and Hottendorf, G.H.; "Application of Pharmacokinetics and biopharmaceutics in the design of toxicological studies" Toxicol. App. Pharmaçol., 53, 19 (1980).

212. Kaplan, S.A.; "Biopharmaceutical considerations in drug formulation design and evaluation" Drug Metab. Revs., 1(1), 15 (1972).

213. Kreevoy, M.M. and Wewerka, E.M.; "A filter paper diaphragm technique for diffusion coefficients" J. Phys. Chem., 71, 4159 (1967).

214. Lathia, C.D. and Bernakar, U.V.; "Advances in dissolution technology: Design, pros and cons" Drug Dev. Ind. Pharm., 12(1+2), 71 (1986).

215. Wood, J.H., Syarto, J.E. and Letterman, H.; "Improved holder for intrinsic dissolution rate studies" J. Pharm. Sci., 54, 1068(1965).

216. Parrott, E.L., Wurster, D.E. and Higuchi, T.; "Investigation of drug release from solids. I. Some factors influencing the dissolution rate" J. Pharm. Sci., 44, 269 (1955).

217. Nelson, E.; "Solution rate of the theophylline salts and effects from oral administration" J. Pharm. Sci., 46, 607 (1957).

218. Nelson, E.; "Dissolution rate of mixtures of weak acids and tribasic sodium phosphate" J. Pharm. Sci., 47, 300(1958).

219. Mitchell, A.D. and Saville, D.J.; "The dissolution of aspirin and aspirin tablets" J. Pharm. Pharmacol., 19, 729 (1967).

220. Carstensen, J.T., In "Pharmaceutics of Solids and Solid Dosage Forms", Wiley, N.Y., 1977.

221. Gibaldi, M. and Feldman, S.; "Establishment of sink conditions in dissolution rate determinations. Theoretical considerations and applications to non-disintegrating dosage forms" J. Pharm. Sci., 56(10), 1238 (1967).

222. Wagner, J.G.; " Interpretation of percent dissolved-time plots derived from *in-vitro* testing of conventional tablets and capsules" J. Pharm. Sci., 58(10), 1253 (1969).

223. Nozawa, Y., Mizumoto, T. and Higashide, F.; "Improving dissolution rates of practically insoluble drug phenytoin by roll mixing with polyvinylpyrollidone" Pharm. Acta. Helv., 60(5), 175 (1985).

224. Corrigan, O.I.; "Retardation of polymeric carrier dissolution by dispersed drugs: factors influencing the dissolution of solid dispersions containing polyethylene glycols" 5th Pharmaceutical Technology Conference, April 8th - April 10th, 1986, Harrogate, England.

225. Corrigan, O.I. and Timoney, R.F.; "The influence of polyethylene glycols on the dissolution properties of hydroflumethiazide" Pharm. Acta. Helv., 51, 268 (1976).

226. Doherty, C., York, P. and Davidson, R.; "Mechanisms of dissolution of frusemide/PVP solid dispersions" 5th Pharmaceutical Technology Conference, April 8th - April 10th, p29, 1986, Harrogate, England.

227. Westerberg, M., Jousson, B. and Nystrom, C.; "Physico-chemical aspects of drug release. **IV**. The effect of carrier particle properties on the dissolution rate from ordered mixtures" Int. J. Pharm., 28, 23 (1986).

228. Nystrom, C. and Westerberg, M.; "The use of ordered mixtures for improving the dissolution rate of low solubility compounds" J. Pharm. Pharmacol., 38, 161 (1986).

229. Sjökvist, E. and Nystrom, C.; "Physico-chemical aspects of drug release. **VI**. Drug dissolution rate from solid particulate dispersions and the importance of carrier and drug particle properties: Int. J. Pharm., 47, 51 (1988).

230. Rahman, A., Cradock, J.C. and Davignon, J.P.; "Dissolution and absorption of the antineoplastic agent Ellipticine" J. Pharm. Sci., 67(5), 613 (1978).

231. Larsen, J.J. and Bundgaard, H., "Prodrug forms for the Sulphonamide group. **III**. Chemical and enzymatic hydrolysis of various N-sulfonyl imidates - a novel prodrug form for a sulphonamide group or an ester function". Int. J. Pharm., 51, 27 (1989).

232. Mayersohn, M., "Physiological factors that modify system drug availability and pharmacological response in clinical practice". In Blanchard, J., Sawchuk, R.J. and Brodie, B.B. (Eds), Principles and Perspectives in Drug Bioavailability, S. Karger, Basel, p211 (1972).

233. Digenis, G.A., Beihn, R.M., Theodorakis, M.C. and Shmabhu, M.B., "Use of ^{99m}Tc-labelled triethyleneteramine - polystyrene resin for measuring the gastric emptying rate in humans". J. Pharm. Sci., 66, 442 (1977).

234. Bundgaard, H. and Buur, A., "Prodrugs as drug delivery systems. **65**. Hydrolysis of α--hydroxy- and α-acyloxy-N-benzoylglycine derivatives and implications for the desighn of prodrugs of NH- acidic compounds". Int. J. Pharm., 37, 185 (1987).

234. Bundgaard, H. and Buur, A., "Prodrugs as drug delivery systems. 65. Hydrolysis of α-hydroxy- and α-acyloxy-N-benzoylglycine derivatives and implications for the design of prodrugs of NH-acidic compounds". Int. J. Pharm., 37, p185 (1987).

235. Larsen, J. and Bundgaard, H., "Prodrug forms for the sulphonamide group. **I**. Evaluation of N-acyl deriviatives, N-sulphonylamidines, N-sulphonylfilimines and sulphonyl ureas as possible prodrug derivatives". Int. J. Pharm., 37, 87 (1987).

236. Trissle, L.A., In "Handbook on Injectable Drugs". Washington DC, Am. Soc. Hosp. Pharmacists, 1983.

237. Jusko, W.J. Gretch, M. and Gassett, R., "Precipitation of Diazepam from Intravenous Preparations". J. Am. Med. Assoc., 225(2), 176 (1973).

238. Kilarski, D.J. Buchanan, C. and Behren, L.V., "Soft tissue damage associated with intravenous phenytoin". The New England Journal of Medicine, 311 (18), 1186 (1984).

239. Kostenbauder, H.B., Rapp, R.P., McGovren, J.P., Foster, T.S., Perrier, D.G., Blacker, H.M. , Hulon, W.C. and Kinkel, A.W., "Bioavailability and single dose pharmacokinetics of intramuscular phenytoin". Clinical Pharmacology and Therapeutics, 18(4), 449 (1975).

240. Pfeifle, C.E., Adler, D.S. and Gannaway, W.L., "Phenytoin Sodium Solubility in Three Intraveneous Solutions". American J. of Hosp. Pharmacy, 38(3), 358 (1981).

241. Korttila, K., Sothman, A. and Andersson, P., "Polyethylene glycol as a solvent for diazepan : Bioavailability and clinical effects after intramuscular administration, comparison of oral, intramuscular and rectal administration, and precipitation from intraveneous solutions". Acta Pharmcol et toxicol., 39, 104 (1976).

242. Jargens, R.W., Deluca, P.P. and Papachimitrious, D., "Compatability of Amphotericin B with certain large volume parenterals" Am. J. of Hosp. Pharm., 38(3), p377 (1981).

243. Allen. L.V. and Stiles, M.L., "Compatability of various admixtures with secondary additives at Y-injection sites of intraveneous administration sets". Part 2a. Ibid 38(3), 380 (1981).

244. Cohen, M.H., Johnston-Early, A., Hood, M.A., McKenzie, M., Citron, M.L., Jaffe, N. and Krasnow, S.H., "Drug precipitation within i.v. tubing: A potential hazard of chemotherapy administration". Cancer Treatment Reports, 69(11), 1325 (1985).

245. Smith, B.L. and Cadwallader, D.E., "Behaviour of erythrocytes in various solvent systems, **III**. Water-polyethylene glycols". J. Pharm. Sci., 56, 351 (1967).

246. Cadwallader, D.E., Wickcliffe, B.W. and Smith, B.L., "Behaviour of Erythrocytes in various solvent systems, **II**. Effect of temperature and various substances on water-glycerin and water-polyethylene glycol solutions". J. Pharm. Sci., 53, 927 (1964).

247. Cadwallader, D.E., "Erythrocyte stability in ethanol-saline solutions". Br. J. Anaesth., 50, 81 (1978).

248. Gannaway, W.L., Wilding, D.C. Siepler, J.K., King, J.H. and Lee-Ow, A., "Clinical use of intravenous phenytoin sodium infusions". Clinical Pharmacy, 2, 135 (1983).

249. Yalkowsky, S.H., Valvani, S.C., and Johnson, B.W., "*In-vitro* method for detecting precipitation of parenteral formulations after injection". J. Pharm. Sci., 72(9), 1014 (1983).

250. Brown, T.B. and Stevens, M.F.G., "Triazines and related products, **XV**. 2,4-diamino pyrimidines and 2-aminopyrimidinine- 4(3H)-ones bearing 1,2,3-benzotriazinyl groups as potential dihydrofolic reductase inhibitors.". J. Chem. Soc., Perkin Trans., 1(11), 1023 (1975).

251. Diem, K. and Lentner, C. (Eds), In "Documenta Geigy. Scientific Tables". (7th Ed.). Geigy Pharmaceuticals, Macclesfield (1975).

252. Basu, K., Kildsig, D.O. and Mitra, A.K.; "Synthesis ond kinetic stability studies of progesterone derivatives." Int. J. Pharm., 47, 195 (1988).

253. Newton, D.W. and Kluza, R.B., "Prediction of phenytoin solubility in intraveneous admixtures : Physicochemical theory". Am. J. Hosp. Pharm., 37(12), 1647(1980).

254. Yalkowsky, S.H. and Valvani, S.C., "Precipitation of solubilised drugs due to injection on dilution". Drug Intell. Clin.. Pharm., 11, 417 (1977).

255. Yalkowsky, S.H., Valvani, S.C. and Amidon, G.L., "Solubility of nonelectrolytes in polar solvents **IV**, Nonpolar drugs in mixed solvents". J. Pharm. Sci., 65(10), 1489 (1976).

256. Howard, J.R. and Gould, P.L., "The use of co-solvents in parenteral formulations of low-solubility drugs". Int. J. Pharm., 25, 359 (1985).

257. Anschel, J. and Lieberman, H.A., "Suppositories". In the Theory and Practice of Industrial Pharmacy. Lachman et.al. (Eds), 2nd Ed., p245 (1976).

258. Carter, S.J. (ED)., "Suppositories and Pessaries". In: Dispensing for Pharmaceutical Students. 12th Ed. Pitman Books Ltd. (London), p232(1975).

259. Gray, H., In "Anatomy of the Human Body". 24th Ed., Lewis, W.H., (ed), Lea & Febiger, Philadelphia, p1317 (1942).

260. De Boer, A.G., Briemer, D.D., Mattie, H., Pronk, J. and Gubbens-Stobe, J.M., "Rectal bioavailabilty of lidocaine in man: Partial avoidance of 'first pass' metabolism". Clin. Pharmacol. Therap., 26, 701 (1979).

261. Bowman, W.C. and Rand, M.J. (Eds). In "Textbook of Pharmacology" 2nd Edition, Blackwell Scientific Publication, Oxford (UK), p40.15 (1980).

262. Editorial. "Suppositories for systemic medication: An underused approach". Drug. Ther. Bull, 21(14), 53 (1983).

263. De Boer, A.G., Moolenaar, F., de Leede, L.G.J. and Briemer, D.D., "Rectal drug administration. Clinical pharmacokinetic considerations". Clin. Pharm. 7, 285 (1982).

264. De Blaey, C.J. and Polderman, J., "Rationals in the design of rectal and vaginal delivery forms of drugs", in Aviens (Ed), Drug Design, Vol. 9, Academic Press, London, 1980.

265. De Blaey, C.J. and Fokkens, J.G., "Drug release from suppositories". Pharm. Res., 2, 61 (1985).

266. McElnay, J.C. and Nicol, A.C., "The comparison of a novel continuous flow dissolution apparatus for suppositories with the rotating basket technique". Int. J. Pharm., 19, 89 (1984).

267. Zuber, M., Pellion, B., Arnaud, P and Chaumeil, J.C., "Kinetics of theophyltive release from suppositories *in vitro*: influence of physicochemical parameters". Int. J. Pharm, 47, 31 (1988).

268. Palmieri, A., Danson, T., Groben, W., Jukka, R. and Dummer, C., "Dissolution of suppositories. III. Effect of insoluble polyvinyl-pyrollidone on acetaminophen release". Drug. Dev. Ind. Pharm., 9(3), 421 (1983).

269. Palmieri, A., "Suppository dissolution testing. Application design and release of aspirin". Drug. Dev. Ind. Pharm. 7(2), 247 (1981).

270. Marriott, C and Kellway, I.W., "The relationship between physical and drug release properties of PEG bases". J. Pharm. Phamacol, 26, Suppl. 132p (1974).

271. Kellaway, I.W. and Marriott, C., "Correlation between physical and drug release characteristics of polyethylene glycol suppositories". J. Pharm. Sci., 64(7), 1163 (1975).

272. Puffer, H.W. and Cromwell, W.J., "Salicylate release characteristics of selected polyethylene glycol suppositories". J. Pharm. Sci., 62(2), 242 (1973).

273. Ibrahim, S.A., Abd Elbary, A., Elsorady, H. and Abd Elmonem, H., "Release characteristics of oxyphenbutazone from different suppository bases". Pharmazie, 35(3), 170 (1980).

274. Higuchi. T. and Lach, J.L., "Study of possible complex formation between macromolecules and certain pharmaceuticals". J. Am. Pharm. Assoc., Sci. Ed., 43, 465 (1953).

275. Kassem, A.A., Nouvel-Din, E., Adb Elbary, A. and Fadel, H.M., "*In-vitro* release of chloramphenicol from different suppository bases". Pharmazie, 30(7), 472 (1975).

276. Iwaoku, R., Okomatsu, Y., Kino, S., Arimori, K. and Nakano, M., "Enhanced absorption of phenobarbitone from suppositories containing phenobarbital povidone co-precipitate". Chem. Pham. Bull., 32(3), 1091 (1984).

277. Nicklasson, M. and Brodin, A., "On the determination of true intrinsic rates of dissolution by means of generalised rotating disk method". Acta. Pharm. Suec., 19, 109 (1982).

278. Florence, A.T. and Attwood, D., In "Physicochemical Priciples of Pharmacy", Macmillan Education Ltd., London, 1981.

279. Ulrich, K. and Wiese, C.F., "Absorption of aprobarbital and sodium aprobarbital from different suppositories bases". Archiv. for Pharma. Og. Chemi., 22, 921 (1967).

280. Riegelman, S and Crowell, W., "The Kinetics of Rectal Absorption. **II.** The absorption of anions". J. Am. Pharm. Assoc., Sci. Ed., 47, 127 (1958).

281. Kakemi, K., Takaichi, A. and Muranishi, S., "Absorption and excretion of drugs. **XXVII.** Effect of non-ionic surface active agents on rectal absorption of sulphonamides". Chem. Pharm. Bull., 13(8), 976 (1965).

282. Bundgaard, H. and Johnsen, M.; "Hydrolysis of N-(a-hydroxybenzoyl) benzamide and other N-(α-hydroxyalkyl) amide derivatives: Implications for the design of N-acyloxyalkyl-type prodrugs". Int. J. Pharm., 22, 45 (1984).

283. Bundgaard, H., Buur, A., Chang, S.C., and Lee, V.H.L., "Prodrugs of timolol for improved ocular delivery: Synthesis, hydrolysis kinetics and lipophilicity of various timolol esters". Int. J. Pharm., 33, 15 (1986).

284. Budgaard, H. Ed., "Design of Prodrugs". Elsevier, Amsterdam, 1985.